Development of a Sediment Yield Model for South East Ghana in the Regions around Lake Volta

Mark Christopher Bambury

Doctor of Philosophy

Aston University

February 2007

Aston University

Development of a Sediment Yield Model for South East Ghana in the Regions around Lake Volta

Mark Christopher Bambury

Doctor of Philosophy, 2007

Summary

Soil erosion is one of the most pressing issues facing developing countries. The need for soil erosion assessment is paramount as a successful and productive agricultural base is necessary for economic growth and stability. In Ghana, a country with an expanding population and high potential for economic growth, agriculture is an important resource; however, most of the crop production is restricted to low technology shifting cultivation agriculture. The high intensity seasonal rainfall coincides with the early growing period of many of the crops meaning that plots are very susceptible to erosion, especially on steep sided valleys in the region south of Lake Volta.

This research investigated the processes of soil erosion by rainfall with the aim of producing a sediment yield model for a small semi-agricultural catchment in rural Ghana. Various types of modelling techniques were considered to discover those most applicable to the sub-tropical environment of Southern Ghana. Once an appropriate model had been developed and calibrated, the aim was to look at how to enable the scaling up of the model using sub-catchments to calculate sedimentation rates of Lake Volta.

An experimental catchment was located in Ghana, south west of Lake Volta, where data on rainstorms and the associated streamflow, sediment loads and soil data (moisture content, classification and particle size distribution) was collected to calibrate the model. Additional data was obtained from the Soil Research Institute in Ghana to explore calibration of the Universal Soil Loss Equation (USLE, Wischmeier and Smith, 1978) for Ghanaian soils and environment.

It was shown that the USLE could be successfully converted to provide meaningful soil loss estimates in the Ghanaian environment. However, due to experimental difficulties, the proposed theory and methodology of the sediment yield model could only be tested in principle. Future work may include validation of the model and subsequent scaling up to estimate sedimentation rates in Lake Volta.

Keywords: USLE, soil erosion, GIS, annual estimates, single-storm modelling

Acknowledgements

The author wishes to thank a number of people for their support and encouragement over the years.

Firstly, to Dr. John Elgy, who supervised and advised on the work in this thesis and to Dr. Peter Hedges for his assistance whenever John was unavailable. Within the department, thanks should also go to Robert Poole for his assistance in all matters technical when faced with a computing predicament and to all the other staff who have assisted over the years with whatever problem that may have occurred.

Special thanks go to the staff at the Soil Research Institute in Ghana, the offices at both Accra and Kumasi. At Accra for there assistance with the field work providing labour, transport, equipment and expert knowledge. In particular, thanks go to Mr Enoch Boateng (as external supervisor, guide and host) and Mr Timothy Ayamga (who provided invaluable expertise in the field). At Kumasi, thanks go to those who prepared and acquired the plot data that was provided for use within the thesis.

To the EPSRC for the funding and support provided.

Also to Dr. John Purkiss and Dr. Neil Short for the organisation of the social events for the current and ex-postgraduate students of the department. And to all those who attended the social events, advised, listened, encouraged and were generally supportive throughout the time of the PhD.

To all those who have contributed time and assistance, whether it was technical expertise or just simply moral support, to my family, friends and colleagues and finally to Bex for all her support and encouragement as the project neared its conclusion.

Contents

List of Tables

List of Figures

List of Plates

Chapter 1

Introduction

1.1 Soil Erosion

Degradation of agricultural land is a major problem worldwide, but is especially detrimental in developing countries. According to Stocking (1995), 50% of agricultural land in developing countries is degraded which constitutes 56% of the world's total degraded agricultural land. Table 1.1 shows the relative percentages of degraded land in each of the continents. The problem of degradation on agricultural land is particularly acute when the land is subject to land-use changes, especially in the initial creation of agricultural land and at the beginning of growing seasons when the crops have not reached maturity. The crops grown will generally not be able to afford the same protection to the soil from erosive elements as the natural vegetation.

	Agricultural Land			Permanent Pasture			Forest and Woodland		
	Total	Degraded	%	Total	Degraded	%	Total	Degraded	%
Africa	187	121	65	793	243	31	683	130	19
Asia	536	206	38	978	197	20	1273	344	27
S America	142	64	45	478	68	14	896	112	13
C America	38	28	74	94	10	11	66	25	38
N America	236	63	26	274	29	11	621	4	1
Europe	287	72	25	156	54	35	353	92	26
Oceania	49	8	16	439	84	19	156	12	8
World	1475	562	38	3212	685	21	4048	719	18

Table 1.1 Extent of Major Productive Land Uses Affected by Soil Degradation (millions ha) (from Stocking, 1995)

Soil erosion is one of the processes of land degradation and is defined as the removal of surface material by wind or water (Kirkby, 1980). Other forms of degradation include extreme salinisation, formation of large gullies and land slips and landslides (Stocking, 1995). Erosion by wind and water is the most common form of land degradation and providing it is recognised early enough, is fortunately a

reversible process. The process is considered reversible for two reasons. Firstly, the soil is able to regenerate through the decomposition of bedrock and leaf litter adding to the depth of the soil matrix. Providing that the problems are recognised before a significant amount of soil is lost then preventative methods can be employed so that the rate of regeneration exceeds the rate of erosion allowing the eroded soil to be recovered. Secondly, the solutions can be employed at relative small costs. Other land degradation processes such as extreme salinisation are much more costly and harder to restore.

The two main measures of soil erosion are soil loss and sediment yield. Soil loss is defined as the amount of soil lost in a specified time period over an area of land which has experienced net soil loss. Sediment yield is defined as the amount of sediment that leaves a specified area of land in a given time period (both from Nearing et al., 1994).

Both measures are important to modern soil conservationists and land management planners quantifying different aspects of the environmental impacts of soil erosion. Soil loss measurements provide information to agricultural planners about the change in productivity levels of cultivated land due to the soil loss, allowing planners to formulate management schemes to control rates of erosion. Sediment yields, however, provide information for conservation planners about the environmental consequences of the transported eroded soil. These consequences include the siltation of reservoirs and large rivers and the transport of pollutants attached to the soil particles.

1.2 Erosion in Ghana

In Ghana, a country with an exponentially expanding population and high potential for economic growth, agriculture is a vital resource. In some areas most of the crop production is low technology and restricted to shifting cultivation with most units effectively being self-sufficient smallholdings, which trade the surplus in the large urban areas and towns. Small-scale cash crop production, such as cocoa beans, is also undertaken. High intensity seasonal rainfall coincides with the early growing period for many of the crops such as maize, cassava and yam. This means that the plots are very susceptible to high erosion rates especially when combined with farming areas on steep-sided valleys in the regions around the southern half of Lake Volta. According to Hens and Boon (1999), the environmental situation in Ghana is characterized by desertification, land degradation, soil erosion and inadequate water supply.

Many of the key environmental issues facing Ghana can be summarized from Hens and Boon (1999) as follows. Annual loss of forest cover over the whole of the country is estimated at 22 000 ha. The clearing of forests using bushfires leads to low agricultural yields, which in turn put more pressure on the land to be used for cultivation. The need for high quality agricultural land is important in a country where the agricultural sector accounts for more than 40% of the GNP and from which 75% of the population earns its living. In addition, soil erosion caused by poor agricultural management is causing increased sediment loads in rivers and suspended particles in water bodies. In Ghana where Lake Volta is a major reservoir and power generator (through the hydroelectric plant at the Akosombo Dam) such information is potentially very economically important. This is because of the damage that would be inflicted by increased sedimentation rates. The increased sediment load would

decrease the capacity of the reservoir and therefore its generating capabilities and there would be an increased cost of dredging to clear the extra sediment. A simple, easily validated sediment yield model can provide useful indications to both areas at risk from a high net soil loss and identify areas susceptible to high sedimentation rates.

Although some work has been done in Ghana in modelling soil erosion, most of the research comprises of either general studies of possible erosion (FAO, 2003) or simple empirical models and estimations such as Amisigo and Akrasi (2000), Oduro-Afriyie (1996) and Folly (1995).

A further project to have been undertaken in Ghana in recent years was the GERMP (Ghana Environmental Resource Management Project) (Boateng et al., 1998). The project aimed to produce land use suitability maps for Ghana so that land resources could be effectively used without adverse environmental consequences. The project mainly used the principal of Agro-Ecological Zoning (AEZ) adapted from the system developed for Kenya (Kassam et al., 1991). It was from this project that the basis for this thesis was derived. The GERMP made limited analyses of potential soil erosion due to land-use changes within its crop suitability investigations, but only took soil loss into account indirectly through the parameters that are taken into consideration when applying the AEZ method for land-use utilisation suitability. Hence, this project undertakes to quantify soil losses and sediment yields as an additional environmental planning and management tool to the GERMP. The current state of soil erosion and land degradation in Ghana is summarised from a 2003 FAO report as follows.

Soil degradation is widespread in Ghana to the extent that areas that are not degraded at present are being threatened. Soil erosion was noticed in Ghana nearly

six decades ago and over the past three decades, the phenomenon has become an important form of land degradation in Ghana. Soil erosion occurs in the form of:

- Sheet erosion through surface runoff
- Rill erosion in impermanent and shifting micro-channels
- Gully erosion in permanent channels
- The soil Research Institute has interpreted the major soils in terms of their severity and type of erosion hazard, which showed that:
- Slight to very slight sheet erosion affects less than 1 percent of Ghana
- Slight to moderate sheet and gully erosion affects 31 percent of Ghana
- Moderate to severe sheet erosion and gully erosion, but more of the latter, affects 44 percent of the total area of Ghana.
- Moderate to very severe sheet and gully erosion, but more of the former, affects 25 percent of the total area of Ghana.

Thus, almost 70 percent of the country is subject to moderate to severe sheet or gully erosion and about 40 percent of this land is in the savannah area.

The FAO research concentrated on the areas in the south east of Ghana in the region around Lake Volta. This was mainly because it had been identified that this region was where the majority of agricultural growth was occurring, in the regions of the country where higher rainfall occurs. Erosion rates often increase as a direct result of land-use change especially when this involves forested areas being turned over to agricultural use. Forests generally afford ample protection to soil from the erosive forces of rain; however, crops that are smaller and less densely planted do not afford the same defence and often in the early growing periods expose large areas of bare soil in the spaces into which they will grow. The areas identified also share the other

key property for enhanced erosion rates, that they exist where the terrain is moderately to steeply sloped.

Simple modelling techniques were applied to assess potential erosion rates across the regions identified for analysis. This enabled a single small catchment to be identified in which to carry out fieldwork experiments to assess rates of erosion that was originally intended for validation of the model that was to be developed.

Wind erosion although a dominant cause of erosion in parts of the world and may possibly be a significant factor in the semi-arid regions of the north of Ghana, in the region where the study was carried out in the south of the country it does not have any significant effect.

Most of the study area in the south is looking at the effect of the removal of rainforest land, often steep-sided valleys, for the use of cropland. In these areas, wind is not a predominant meteorological force and the plots that the farmers are creating are in sheltered valleys surrounded by trees that act as a windbreak. This prevents wind erosion playing any great part in the erosion process and so it is not included in the study.

1.3 Modelling Soil Erosion and Techniques

Soil erosion modelling began in the early 20th century in the mid-west US because of the dust bowl crisis. As a result of intensive farming methods developed in the US combined with several years of extended droughts and low rainfalls, the soils in the mid-west became very dry and especially vulnerable to erosion. This triggered the US government to begin heavy investments in research into the relationships between rainfall and erosion in both natural and agricultural environments. The first soil erosion models were simplistic, empirical and attempted

only to quantify soil loss in terms of slope and rainfall. As research progressed and simulation techniques became more sophisticated, the soil erosion models developed to represent many more of the processes that influence erosion and most recently have been adapted to quantify sediment yield as well as soil loss.

Many soil erosion models have been developed by many researchers for many environments. Table 1.2 shows examples of some of the common soil erosion models.

Soil Loss Models:	
USLE (Universal Soil Loss Equation)	(Wischmeier and Smith, 1978)
RUSLE (Revised Universal Soil Loss Equation)	(Renard et al., 1991)
Sediment Yield Models:	
ANSWERS (Areal Non-point Source Watershed Environment Response Simulation)	(Beasley et al., 1982)
AGNPS (Agricultural Non-Point Source Pollution)	(Young et al., 1987)
CALSITE (Calibrated Simulation of Transport Erosion)	(Bradbury et al., 1993)

Table 1.2 Common Soil Erosion Models

All soil erosion models can be described in a basic format as a function of four environmental factors, such that:

$$SE = f(\text{topography, soil, landuse, climate}) \qquad \text{equation 1.1.}$$

where SE is the quantity of soil erosion in t/ha/yr. Equation 1.1 applies more appropriately to the soil loss models. Sediment yield models use the same basic function as soil loss models, but contain a further function using more complex attributes of each of the factors to calculate the sediment yield from a catchment such that:

$$SY = f(\text{SE, topography, hydrology}) \qquad \text{equation 1.2}$$

where SY is the sediment yield and SE is from equation 1.1.

1.4 Aims and Objectives

The main aim of the research was to establish and test a sediment yield model on a small rural catchment that according to soil loss estimates experienced net soil loss erosion that was more than a pre-established acceptable limit. Previous research undertaken in Ghana (GERMP, Boateng et al, 1998) had established the need for agricultural management, but had not taken into consideration soil loss potential and sediment yields accrued from the agricultural land. The objectives of the research can thus be broken down into the following stages:

1. Establish through background research the process of soil erosion and principles of soil loss and sediment yield modelling.
2. Establish basic data requirements and format to consistent types (much of the data collected in Ghana is in old imperial measures).
3. Using basic data create soil loss potential maps for designated area.
4. Highlight at risk areas within the designated area.
5. Investigate and model sediment yields within a selected high risk area.
6. Investigate soil loss problems due to land use change.
7. Investigate sedimentation rates in Lake Volta due to current and increased sediment loads.

1.4.1 Potential of GIS

Modelling soil erosion and sediment yield across an entire catchment, especially when considering the high levels of spatial resolution required to create the discrete areas needed for accurate distributed parameter modelling, requires a large amount of processing power.

With the recent advances in modern computing, the processing power is now readily available and with the development of GIS software, two and three dimensional distributed modelling can be easily performed.

To undertake such modelling the computing requirements become fairly great especially when considering the flow routing aspects of the model. The development of comprehensive user-programmable GIS has made such modelling much easier.

1.4.2 Assessment of Rates of Erosion

Rates of erosion resulting from changes in land use are important indicators of the environmental consequences of turning land over to agricultural use. They can also be used to provide the following information: rates of decline of productivity to agricultural land, sustainability information for defined land use types and, when combined with streamflow and transport data, can provide sediment yield values for agricultural areas for assessment of sediment pollution.

1.4.3 Development and Testing of a Sediment Yield Model

Development of a simple conceptual sediment yield model can provide many challenges especially when considering the limited data available from developing countries. The model needs to have as few calibrated parameters as possible to reduce the errors that will accrue when modelling a limited data set.

1.5 Data Acquisition

To calibrate and validate any soil erosion model, data is required about many different catchment characteristics, including transported sediment, rainfall and flow rates, soil types and land-use. Modelling can be undertaken on either an annual basis

or a daily basis, but due to limited funding and thus a limited time available acquiring data in Ghana, data for this research project was collected for single storm modelling on a daily basis. In total five weeks were spent in Ghana, of which two weeks were spent collecting data from an experimental catchment south-west of Lake Volta. Further calibration data for other parameters within the model were acquired from the Soil Research Institute at Kumasi.

1.6 Outline of Thesis

Chapter 2 discusses the general principles relating to the theory and processes of land degradation in the form of soil erosion, its management and consequences. Due to the complex nature and interactions of the process of soil erosion, it can be studied from many viewpoints in different disciplines. These disciplines include hydrology, ecology, socio-economics, geography, geomorphology and meteorology. Thus, chapter 2 reflects on all these different viewpoints, demonstrating the reasoning on which the final emphasis of the thesis was based. Chapter 3 then goes on to discuss in detail the various approaches used when modelling soil erosion. Some of the main erosion models that have been developed over the past few decades are analysed in detail. Particular focus is given to Universal Soil Loss Equation (USLE, Wischmeier and Smith, 1978), the theory behind its development and its relevance to modern day erosion studies. The USLE is an empirical soil loss equation for calculating potential soil loss from plots of land based on land-use, topography, rainfall and soil properties. The USLE despite its age and limitations can still be used to provide useful estimates of areas of potentially damaging soil loss and was therefore used to identify possible catchments for the experimental studies to be used for verification of the model to be developed.

Chapter 4 covers some of the modelling issues that had to be resolved before modelling work commenced, (i.e. scale and resolution and the calculation of topographic attributes from a digital elevation model, DEM). The correct calculation of topographic attributes is one of the most important aspects of the model as this allows the flow path network to be correctly established.

Chapter 5 looks at the GIS environment. GIS are geographical information systems, it is the technology of using computers to digitally store, display and analyse geographic information. It also discusses the selection of the GRASS (Geographical Resources Analysis Support System) GIS software suite, its operation and programming capabilities and its suitability for erosion modelling.

As funding was very limited, before commencing any experimental work in Ghana, initial estimates were made to assess the potential for the occurrence of extreme soil erosion within the larger area that had been selected for analysis. These initial assessments were essential to ensure that the most productive use of time and money could be made during the short field trip to Ghana. Chapter 6 outlines the preliminary studies that were undertaken, and the use of the USLE to identify the catchments that were potential field sites.

The field trip to Ghana is described in chapter 7. The chapter covers the location and description of the experimental catchment, and the methodologies and procedures used for collecting the experimental data. The results and analysis of the data collected in Ghana are reported in Chapter 8. This chapter includes the experimental data collected from the selected catchment and additional data acquired from the Soil Research Institute (Kumasi). The data obtained from the experimental catchment was assessed for its accuracy and applicability; it was not used until later, after the model was developed. The data from Kumasi, however, was used to verify

the assumptions made about the USLE factors used in the initial calculations (chapter 6) and for subsequent use in the model.

Chapter 9 discusses the development of the model. The details of the programming environment and difficulties encountered are dealt with as well as the decision making processes to develop a simple model capable of operating with the limited data available from developing countries. Chapter 10 then covers the application of the model. The parameters that are required to calibrate and validate the model, the procedures involved for collecting the data those parameters and a critical analysis of the appropriateness of the data that was collected during the fieldwork exercises in Ghana.

The last two chapters, 11 and 12, give a critical appraisal of the research that was undertaken, discuss the outcomes and conclusions that can be drawn from the modelling that has been undertaken, the reliability of the results and the future applications and improvements of the study.

1.7 Summary

Within developing countries there is a need to know both the net soil loss from agricultural land so that agricultural productivity can remain high and also to quantify the sediment yield from agricultural catchments to determine the potential for pollutant transport and sedimentation rates of key reservoirs and lakes.

Chapter 2

Literature Review and Principles of Soil Erosion Modelling

2.1 Introduction

With the global population ever increasing and the need to sustain the populous becoming increasingly important, land degradation has become one of the single most imperative issues to affect modern society. However, it is also one of the most complicated problems to have to assess, quantify and prioritise. There are several diverse issues involved in the processes and effects of land degradation, but first it is important to define the various terminology used to prevent confusion and to explain the importance of each aspect of the process.

Land degradation is a generic expression defined by Stocking (1995) as a composite term signifying the temporary or permanent decline in the productive capacity of the land. It is the aggregate diminution of the productive potential of the land, including its major uses (rain-fed arable, irrigated, rangeland and forestry), its farming systems (e.g. smallholder subsistence) and its value as an economic resource. Land degradation has many forms; most have irreversible effects such as landslips and landslides, creation of large gullies, extreme salinisation, etc. Soil degradation is defined by Stocking (1995) as a decrease in soil quality as measured by changes in soil properties and processes, and the consequent decline in productivity in terms of immediate and future production.

Stocking (1995), further defines six processes of soil degradation: water erosion, wind erosion, excess of salts, chemical degradation, physical degradation (of physical properties, e.g. porosity and permeability) and biological degradation. Of these six processes, this thesis focuses on soil erosion, specifically erosion by water.

Whilst, as already stated, most of these processes are irreversible; soil degradation by water is however reversible by the addition of nutrients or soil amendments, and re-establishing vegetation and other management practices.

2.2 What is soil erosion?

2.2.1 Definitions of soil loss and sediment yield

It is important to start out by defining what is meant by soil erosion and defining the relevant terms that are used in the context of soil erosion modelling. According to Stocking (1995), soil erosion is defined as one of the main processes of degradation and consists of physical detachment of soil particles by wind and water, and their subsequent transport to other parts of the landscape, to rivers and the sea. However, out of this definition two main points arise that need clarifying. Firstly, there is the issue of at what point does the rate of soil erosion become significant? Secondly, there is the consideration of what happens to the eroded soil particles? The first issue is discussed in more detail in the next section, but in brief, covers the philosophies of what are the natural and acceptable rates of soil erosion. This is because to some extent there is the question of definition and perspective.

The second issue deals with the more fundamental levels of soil erosion and the individual physical processes involved. Two common phrases in soil erosion modelling are soil loss and sediment yield; both are important measures of soil erosion depending upon the type of study being undertaken. Nearing et al (1994) defined soil loss as the amount of soil lost in a specified time period over an area of land which has experienced net soil loss, and sediment yield as the amount of sediment which leaves a specified area of land in a given time period. These are

important concepts that play a crucial part in calculating the on-site and off-site effects of soil erosion.

A simplistic but effective explanation for this can be demonstrated using figure 2.1. When considering the diagram, soil loss is the quantity of soil eroded from an area at point A, but where that soil ends up is not defined. The eroded soil could end up at either point B or point C. Sediment yield is the quantity of soil eroded from point A that is transported to point C in the permanent stream network and is then

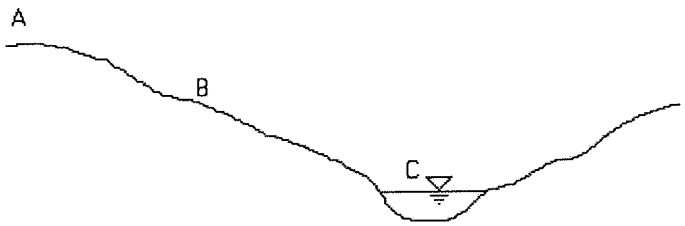

Figure 2.1 - Schematic diagram demonstrating differences between sediment yield and soil loss

possibly carried to the catchment outlet. Soil particles are not guaranteed to be carried to the catchment outlet either immediately or at all. Some particles may be kept in storage for a period. However, the distinction of loss and yield has important considerations when taking into account the different effects of soil erosion. Particles that end up at C will potentially have a greater negative environmental effect than those that end up at B. Although there will be significant negative effects in terms of net soil loss at A, wherever the particles are re-deposited. Those particles that enter the permanent stream network carry additional effects of potentially polluting the water supply and causing siltation of reservoirs.

Further, on the definitions of erosion terminology, according to Yiatyew et al (1999), it is important to note that sediment yield and erosion are two different terms that are not interchangeable. Sediment yield for a watershed includes the erosion from slopes, channels, and mass wasting, minus the sediment that is deposited after it is eroded, but before it reaches the point of interest. Soil erosion is more applicable as

a generic term for the overall process with terms like sediment yield and soil loss dealing with specific aspects of erosion.

2.2.2 Definitions and explanations of other terminology and processes of soil erosion

To discuss the individual processes involved in soil erosion another definition of soil erosion can be considered. According to Morgan (1986) soil erosion is a two-phase process consisting of the detachment of individual particles from the soil mass and their transport by erosive agents such as running water and wind. This, as a basic definition is adequate, however, there are many other sub-processes in soil erosion that need to be taken into account when modelling soil erosion. For example, as Kusumandari and Mitchell (1997) extended Morgan's definition with a third phase – when sufficient energy is no longer available to transport particles, deposition of the soil particles occurs.

According to Lal and Elliot (1994), the predominant processes that determine erosion are infiltration, run-off, detachment and transport by raindrops and overland flow (interrill erosion), detachment and transport by concentrated flow (rill erosion), and deposition.

It can be seen from just these two statements that there are many processes, factors and properties involved in soil erosion. There are also many sub-processes involved in the detachment and transport phases. Within detachment, there are the properties of erodibility and erosivity. Within transport, there is overland flow in the forms of sheet flow and rill/gully flow, the formation of rills and gullies, and full stream flow. There are two more sub-processes to be considered: the erosion of material from streambeds in rills, gullies, streams and rivers; and the re-entrainment

of deposited sediment back into the flow from the streambed. These are both separate sub-processes, but are often lumped together for simplification when modelling soil erosion.

Thus, when considering all the processes and influences a tree diagram can be constructed to how each of the processes and properties relate to each other, see figure 2.2.

2.2.3 Physical properties and factors influencing soil erosion

The physical properties are those that are predetermined by the natural conditions of the environment. The processes of soil erosion are governed by the physical properties and are concepts of the factors that influence soil erosion.

Soil erodibility and rainfall erosivity are very important physical factors that affect the magnitude and rate of soil erosion. Erodibility and erosivity are arguably two of the most important measures in the whole process of soil erosion. These two properties are the only ones that have a direct effect on the rate of soil erosion yet cannot be affected by remedial measures; thus they are fixed constants that need to be overcome in any soil conservation practices by changing the effects the property has rather than trying to alter the quantitative value of the property itself.

2.2.3.1 Erodibility

Erodibility is a property of the soil, defined by Lal and Elliot (1994) as a measure of the soil's susceptibility to detachment and transport by the agents of erosion. This definition is only accurate in certain circumstances depending upon the way in which modelling is undertaken. In the case of the Universal Soil Loss

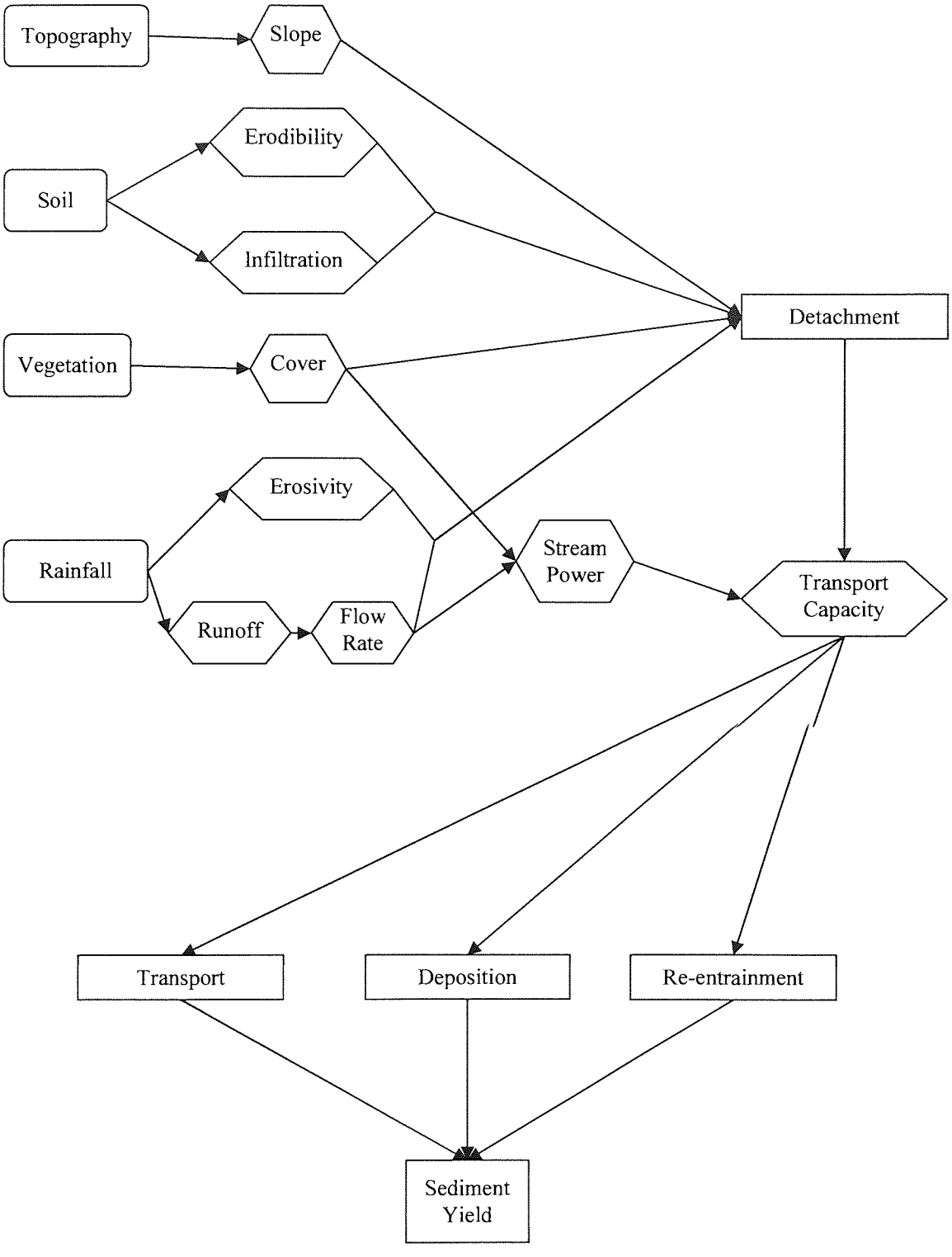

Figure 2.2 Flow Chart to demonstrate the links between the processes and properties involved with soil erosion

Equation (USLE) (Wischmeier and Smith, 1978), (see section 3.3), in its original usage, the soil erodibility factor K was based on soil loss from a unit plot. This definition includes the transport of the soil from the plot. However, more recent soil erosion models use the USLE simply as a measure of the soil loss from a certain point, with other sections of the model dealing with the transport of the soil particles. In this instance, only the detachment of soil particles is appropriate in the definition. The K factor is therefore an empirical quantity based upon the composition of the soil, i.e. the particle size distribution (soil grading) and organic matter content.

The composition and texture of the soil are very important in determining the erodibility of a soil. Sandy soils have a higher infiltration rate and thus lower rates of runoff; particles are more easily detached due to a lower cohesiveness, but are less easily transported, as they are larger. Clay soils are highly cohesive and so are not easily detached, but smaller particles are easily transported and low infiltration rates may lead to greater runoff and increased erosion rates. Silt soils are the most easily eroded as particles are more easily detached and almost as easily transported as clay particles. Subsoils of silts are often consolidated or have high clay contents, which leads to greater runoff through decreased infiltration rates.

2.2.3.2 Erosivity

Erosivity is an expression of the ability of erosive agents, like water, to cause soil detachment and its transport (Lal and Elliot, 1994). The erosivity of rainfall is largely defined by the intensity of the rainfall, although other factors such as the quantity of rainfall, the drop size, the runoff rates and the quantity of runoff also affect erosivity. A similar problem arises with erosivity as did with erodibility. The rainfall erosivity is represented within the USLE by the R factor; in this instance, runoff is a

factor that is taken into consideration, which under these circumstances is applicable. However, when considering rainfall erosivity within the context of a sediment yield model, it is only appropriate to consider the ability of rainfall to detach soil particles not to transport them.

2.2.3.3 Vegetation cover

The vegetation cover across the land surface determines the amount of protection afforded to the soil from the erosive power of the rainfall. There are two ways in which the vegetation can protect the soil, the plant itself and the leaf litter on the soil surface. The plant growth intercepts some of the raindrops absorbing the energy from the raindrop so that it has less erosive power when it impacts on the ground surface. There are two determining factors in this process. Firstly, there is the leaf area (parametrically known as the LAI, leaf area index). The LAI is a relatively simple concept; the larger the LAI the more raindrops can be intercepted and thus the more protection is afforded to the soil. The second factor, and the more important, is the height of leaves above the ground surface. According to Kusumandari and Mitchell (1997), raindrops reach over 95% of their terminal velocity over a height of 8m. Therefore, the lower the vegetational cover is to the ground the greater the reduction of the impact energy and hence the erosive power of the raindrops. They also note that drop size may be increased through accumulation on the leaf surface. Thus, the shape of leaves also can play a crucial part. A cup-shaped leaf with the tip as the lowest point to the ground will greatly enhance this effect.

The leaf litter also plays a crucial part in absorbing raindrop energy and reducing erosion of the soil matrix. The mulch created from the decomposing organic matter is more cohesive than the soil matrix but also still has relatively high

infiltration rates. This helps to reduce the rate of erosion by reducing the erosive energy of the raindrops.

There is, however, one major disadvantage when considering the reduction of raindrop energy by the leaf litter with regard to its effects on agricultural land. On agricultural land, because of ploughing and other such activities the organic layer is mixed in to the soil and becomes a significantly reduced layer that affords less protection than a natural organic layer.

The effects of vegetational cover are defined as the C factor within the USLE. The C factor takes into account the affects of leaf litter; natural vegetation has significantly lower values due to the inclusion of an undisturbed organic layer.

There is also the consideration that once the upper layers of soil have started to be eroded, the erosive power of raindrops will have a more enhanced effect on the soil as lower layers will be more susceptible to erosion than the organic layer on top. However, this is also dependent upon the make up of the soil itself and the depth and properties of each layer, which change as each horizon is passed whilst traversing vertically down through the soil.

2.2.3.4 Topography

The topography of an area is, like the vegetation cover, one of the more easily adjustable factors influencing erosion. The two main topographic features that effect soil erosion are the slope steepness and the slope length, although there is still much discussion on the extent of the influence of the latter on erosion rates. Slope steepness is self-explanatory; it is the average gradient of the slope between two specified points, usually expressed as a percentage. Slope length is a less explicit term. Smith and Wischmeier (1957) defined slope length as the distance from the point of origin

of overland flow to the point where either the slope gradient decreases enough that deposition begins, or the runoff water enters a well-defined channel that may be part of a drainage network or a constructed channel (usually irrigation works in the case of agricultural land). Whilst the final part of the definition is easy to identify, the point at which gradient decreases enough for deposition to occur is more ambiguous. This point is very hard to define; for example, it can depend on the quantity of runoff that is flowing, the greater the runoff the less likely it is that deposition will occur. There may also be more than one point at which deposition occurs between the origin and the permanent stream network.

In soil erosion modelling the two topographic measures of slope (length and steepness) are often combined into one modelling parameter, e.g. the LS factor in the USLE (see section 3.4.3).

2.2.3.5 Detachment by rainfall

The detachment of soil particles by rainfall is the first stage in the process of soil erosion. The detachment of soil particles from the soil matrix is dependent upon a number of factors; the impact force of the raindrops, the cohesive forces within the soil and the angle of slope of the soil surface. The first two factors are the more important; the raindrop impact force needs to be sufficiently high to dislodge the soil particle by overcoming the cohesive forces that are holding the particle in place. The slope angle also affects the force required to dislodge the soil particle from the soil matrix but to a much lesser extent. The steeper the slope angle the greater the resultant force from the raindrop along the direction in which the soil particle will be dislodged and thus less force will be required to remove the soil particle.

However, this is only a simple model of the detachment of soil particles. Nearing (1997a) proposed a series of equations to represent the detachment of soil particles by both raindrops and runoff. He describes the impact of raindrops as creating transient vertical pressures on soils in the order of hundreds of kPa, which are transformed into high-velocity lateral jets of water that eject soil particles into the air. However, the penetration of these stresses into the soil is only very shallow; thus, raindrops are able to erode only a very thin layer of the soil surface at any point in time.

To describe the forces (interaction) of raindrop impact, Nearing (1997a) uses the principle that in a homogeneous solid, the pressures induced by an impacting fluid, P_w, are a function of the densities and compressional wave velocities of the two materials (i.e. the soil and the raindrop) (taken from work by Adler, 1979 and Springer, 1976). The equation is:

$$P_w = \rho_w C_w v / (1 + \rho_w C_w / \rho_t U_t) \qquad \text{Equation 2.1}$$

where C_w is the velocity of a compression wave water, v is the relative velocity of the two materials at the time of impact, ρ_w is the density of water, ρ_t is the density of the solid, and U_t is the velocity of the compression wave in the solid.

2.2.3.6 Detachment by flow

The detachment of soil particles by flow occurs when the flow has sufficient energy to overcome the friction and cohesive forces holding the particle into the soil matrix. There are however, more than one instance and type of detachment.

Traditionally the mechanics of detachment by flow has been explained by the use of flow parameters such as shear stress and stream power.

Chadwick and Morfett (1993), describe the simple forces acting on a particle on the streambed that can potentially be dislodged. Figure 2.3 shows the forces involved; figure 2.3a shows the change in velocity of the fluid to the interface resulting in a shear stress force at the interface, where τ_0 is the shear stress at the interface and u is the velocity of the fluid. Figure 2.3b shows the forces applied to a particle susceptible to detachment, where F_L is the lift force, F_D is the drag force, and W' is the immersed weight of the particle.

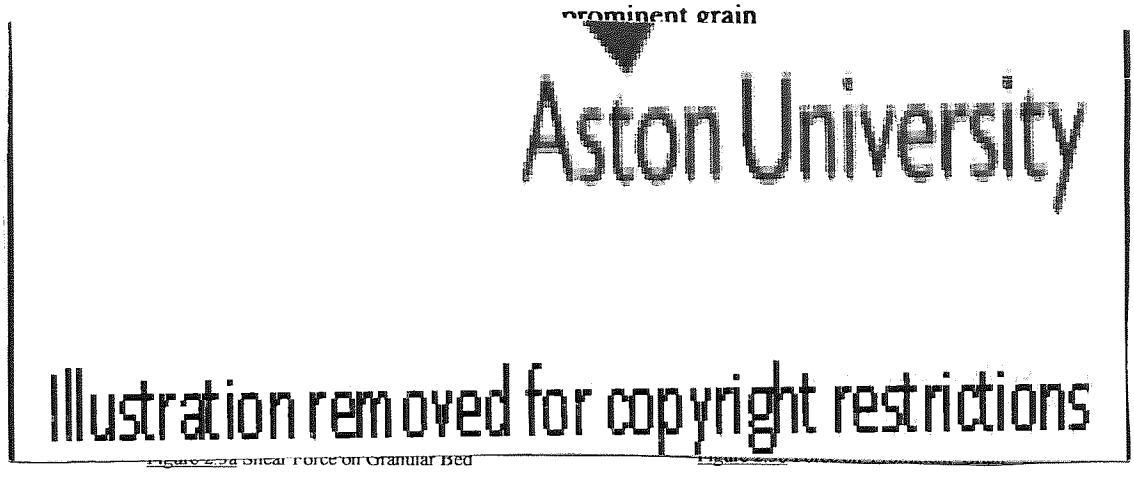

Figure 2.3 Forces Involved in the Detachment of Sediment from the Stream Bed (from Chadwick and Morfett, 1993)

As mentioned in section 2.2.3.5, Nearing (1997a) also discusses the mechanics of soil detachment by runoff. He states that it has been recognised that the mechanics of detachment of particles by flow is not a simple function of averages of flow parameters such as shear stress or stream power. Nearing instead considers the mechanics of soil detachment from probability functions. This work derives from Grass (1970) who showed that the initiation of movement of particles from a fine sand bed could be described as the overlap of two probability distributions, one that describes the distribution of instantaneous bed shear stresses and one that describes

the resistance of the individual sand grains on the bed. Thus, the probabilistic model derived for soil detachment takes the form:

$$e = FPM \qquad \text{Equation 2.2}$$

where F ($s^{-1}m^{-2}$) is the temporal and spatial frequency of turbulent 'bursting events', P is the probability that the shear stress of the burst event exceeds the local resistance to detachment and induces tensile failure, M (kg) is the average mass of soil detached per failure event, and e (kg $s^{-1}m^{-2}$) is the detachment rate per unit area of soil surface. After multiplying the spatial and temporal frequency estimates (provided by Raudkivi and Tan, 1984 and Gordon, 1975), the functional form of F is given by:

$$F = 4\times10^{8} Cg(hI)^{3/2}/\sigma \qquad \text{Equation 2.3}$$

where C is the Chezy roughness coefficient, I is the inclination of the slope, h is the thickness of the flow, and σ the thickness of the turbulent boundary layer. For the shallow flows under consideration it is assumed that the boundary layer thickness, σ, can only be as thick as the depth of flow h; therefore, F is approximated as:

$$F = K_1 Ch^{1/2} I^{3/2} \qquad \text{Equation 2.4}$$

where K_1 is a linear coefficient. The probability of failure P, is given by:

$$P = 1/2 - \varphi(T-\tau_b)/\left(\left[s(T)\right]^2 - \left[s(\tau)\right]^2\right) \qquad \text{Equation 2.5}$$

where .φ is the cumulative probability function of the standard normal variate, T is the mean value of the capacity term, which is either soil resistance or tensile strength, τ_b is the mean value of the demand, i.e. burst-event shear stress, s(T) is the standard

deviation of the capacity, and $s(\tau)$ is the standard deviation of the demand. The final equation substituting equation 2.4 into equation 2.2 gives:

$$e = KCPh^{1/2} I^{3/2} \qquad \text{Equation 2.6}$$

where K incorporates K_1 from equation 2.4 and M from equation 2.2, and P is from equation 2.5.

2.2.3.7 Runoff

Runoff is the flow of water across the land surface to the permanent stream network; it is the result of the rate of rainfall exceeding the rate of infiltration. There are two types of runoff, sheet flow and rill/gully flow.

Rill or gully flow is essentially the same as standard streamflow except that the flow is not permanent within the channels. Rills are smaller channels and represent the initial accumulation of water into concentrated flow; their position and route will usually vary from storm to storm. Gullies are larger and more permanent fixtures of the landscape, they represent larger scale permanent erosion where runoff channels have been cut into the hill slope. They do not, however, form part of the permanent stream network as they only have flow within them during storms.

Sheet flow is a much rarer form of runoff, and will only occur in specific circumstances. Sheet flow can theoretically occur during high intensity rainstorms when the infiltration rate into the soil has been reduced due to surface crusting and a very dry soil. Surface crusting occurs during a long hot, dry spell between rainfall when clay and silt particles settle on the surface of the soil forming a semi-impermeable layer. During high intensity rainstorms water is unable to immediately penetrate this layer, and thus runoff forms across a whole area as a thin sheet. There

is considerable dispute, however, as to whether sheet flow actually exists (see section 2.2.3.8.1).

2.2.3.8 Sediment Transport

Once particles have been detached from the soil matrix, assuming there is sufficient power in the flow then the particles will be transported downstream. The particles are transported in the flow by two different methods. The smaller, lighter particles (clays, silts and fine sands) are transported in suspension, i.e. the suspended load. The larger, heavier particles are transported along the bed by bouncing or rolling in a process known as saltation; this is known as the bed load.

There are various different approaches to the modelling of sediment transport, conceptual, empirical and physically based models have been proposed (see section 2.2.3.9) and at the most basic level, only distinguish between suspended loads and bed loads. However, at levels that are more complex, the depth of flow also makes a difference to the rules that govern transport, and thus distinctions occur between transport in shallow flow and in streamflow.

There are also different reasons for studying sediment loads and the transport thereof, and thus different theories arise.

The main drawback with sediment transport equations is that they are either completely theoretical or have been based on laboratory experiments, but this is largely because it is very difficult to run tests on natural streams.

Zhang and Summer (1998) summed up sediment transport very succinctly when they stated that developed transport formulae present a relationship between sediment discharge and hydrological as well as hydraulic factors, such as flow discharge, slope, river morphometry, sediment characteristics, etc. As these sediment

formulae were often gained from laboratory investigations under steady flow conditions, their basic applicability is limited to these flow conditions. However, in natural rivers most of the sediment displacement takes place during floods, which represent unsteady flow. Hence, one should be aware of the conceptual formula limitations and possible prediction errors.

With many inputs, quantification of sediment transport is not easy. As van Rijn (1984) states the transport of sediment particles by a flow of water can be in the form of bed-load and suspended load, depending upon the size of the bed material particles and the flow conditions. The suspended load may also contain some wash load, which is generally defined as that portion of the suspended load that is governed by the upstream supply rate and not by the composition and properties of the bed material.

2.2.3.8.1 Transport by sheet/overland flow

The phenomenon of erosion by overland flow in the form of sheet flow is arguably an event that does not need to taken into account within soil erosion modelling. This is largely because it is a very rare occurrence requiring very specific conditions to take place. Sheet flow is only feasible in the instance of a high intensity rainstorm on a relatively smooth surface of relatively low permeability. Sheet flow has only sufficient energy to transport eroded material downslope, not erode fresh material from the soil surface. As Nearing (1997a) states, the forces required to transport sediment down a slope are much less than those required to remove an in situ particle from the soil mass. Thus, even thin sheets of surface runoff are capable of transporting sediment short distances down a slope. These short distances are often

enough to carry sediment off the side slope of a rill into the flow at the bottom of the rill channel to be transported by channel flow.

2.2.3.8.2 Transport by streamflow

The transport of particles by streamflow is dictated by the velocity of flow and the volume of flow. The greater the flow rate, the more sediment can be transported, the farther it can be transported and the larger the size of particle that can be transported.

2.2.3.8.3 Transport by rill/gully flow

The transport of particles within rill and gully flow is essentially subject to the same principles as transport by streamflow, except that everything is on a smaller scale.

2.2.3.8.4 Deposition

The deposition of particles is an important process when calculating sediment yields but is not of consequence when dealing with soil loss. However, the issue of scale needs to be taken account of when deciding at what point deposition becomes a dominant factor. Whilst soil particles are transported by the flow of water, they are subjected to three forces when considering the system at a basic level. An upward force, lift, from the resistance of fluid to the downward force of gravity and a horizontal force induced by the flow of water through the channel. Depending upon the size of the particle there is a net difference between the upward and downward forces. The larger the particle the larger the net difference and the faster the particle

will fall through the fluid to the bottom. Hence, the faster the water flows the farther a particle in suspension in the fluid will fall until it becomes deposited on the bed of the stream.

This is where the issue of scale comes in. If studying erosion at the plot level then it can be assumed that deposition is not a factor because all particles that are in suspension will be carried off the plot due to the small distance over which the water will flow. When considering a full catchment, deposition will definitely be an aspect because some particles will be deposited on the streambed during the passage of flow to the catchment outlet. The point at which deposition starts to occur would have to be identified for studies in between the two.

However, the three forces would exist as they are only in an ideal fluid. In real streamflow, particles within the flow are also subjected to forces from turbulence that act on the particle in many different directions and can either speed up or slow down the descent of the particle through the fluid.

Fortunately, many empirical formulae have been derived to describe the transport of soil particles by water, which take into account deposition rates (see section 2.2.3.9).

2.2.3.8.5 Re-entrainment

Re-entrainment is the removal of soil particles, which have been deposited onto the streambed, back into suspension in the flow. The mechanics of this process differ slightly from the initial detachment of particles from the soil matrix. The forces holding a deposited particle are less than those connecting a particle that is already part of the soil matrix.

2.2.3.8.6 Transport capacity

As an alternative to the physically based sediment transport equations, some modellers have developed empirical sediment transport equations based on the concept that a particular flow regime has a defined transport capacity, i.e. the amount of sediment that a certain volume and velocity of flow can carry. If the sediment suspended in flow is less than the transport capacity, then the stream banks become vulnerable to erosion by the flow and previously deposited particles become re-entrained. However, once the transport capacity becomes exceeded then deposition will occur. The relevance of transport capacity is emphasised by Govers (1990) who states that the sediment transporting capacity of overland flow is a parameter of fundamental importance in the physically based description of soil erosion and deposition processes.

2.2.3.8.7 Stream power

Stream power is an alternative sediment transport concept based upon energy principles. Zhang and Summer (1998), state that sediment transport in natural rivers may be estimated on the basis of the stream power concept. The rate of energy dissipation derives from an energy balance which adjusts to the river bed's roughness, sediment discharge, channel geometry and cross section. The concept of stream power was first proposed by Bagnold (1966) and according to Williams et al (1985) is defined as:

$$SP = gqS_w \qquad \text{Equation 2.7}$$

where g is the density of water, q is the flow rate and S_w is the water surface slope.

2.2.3.9 Sediment Transport Formulae

Many sediment transport formulae have been derived covering all aspects of transport, bed loads, suspended loads, overland flow and streamflow. A selection of the more common equations follows.

Chadwick and Morfett (1993) list some transport equations such as the Shields (1936) bed load equation:

$$q_s = \frac{10 q S_0 \rho^2}{\rho_s} \frac{(\tau_0 - \tau_{CR})}{(\rho_s - \rho)^2 g D} \qquad \text{Equation 2.8}$$

the Ackers and White formula (White, 1972) which is a total load formula in three parts:

$$G_{gr} = \frac{q_s D_m}{qD}\left[\frac{u_*}{V}\right]^n = C\left[\frac{F_{gr}}{A} - 1\right]^m \qquad \text{Equation 2.9}$$

$$F_{gr} = \frac{u_*^n}{\sqrt{gD[(\rho_s/\rho)-1]}}\left(\frac{V}{\sqrt{32}\log(10 D_m/D)}\right)^{1-n} \qquad \text{Equation 2.10}$$

$$D_{gr} = D\left(\frac{g[(\rho_s/\rho)-1]}{\nu^2}\right)^{1/3} \qquad \text{Equation 2.11}$$

Other total load equations are listed by Hossain and Rahman (1998) and include:

the Engelund-Hansen equation (1967);

$$g_s = 0.05\gamma_s V^2 \sqrt{D_{50}/\{g(\gamma_s/\gamma - 1)\}}\left[\tau_0/(\gamma_s - \gamma)D_{50}\right]^{3/2} \qquad \text{Equation 2.12}$$

the Yang equation (1973);

$$\log C_t = 5.435 - 0.286\log(\omega D_{50}/\upsilon) - 0.457\log(u_*/\omega) + \{1.799 - 0.409\log(\omega D_{50}/\upsilon) - 0.314\log(u_*/\omega)\}\log(V S/\omega - V_{CR} S/\omega)$$

Equation 2.13

$$\frac{V_{CR}}{\omega} = \frac{2.5}{\log(u_* D/\nu) - 0.06} + 0.66, \quad 0 < \frac{u_* D}{\nu} < 70 \qquad \text{Equation 2.14}$$

$$\frac{V_{CR}}{\omega} = 2.05, \quad 70 < \frac{u_* D}{\nu}$$ Equation 2.15

and the Van Rijn formula (1984) for bed load and suspended load;

$$\frac{q_b}{ud} = 0.005\left(\frac{u-u_{cr}}{\left[(s-1)gD_{50}\right]^{0.5}}\right)^{2.4}\left(\frac{D_{50}}{d}\right)^{1.2}$$ Equation 2.16

$$\frac{q_s}{ud} = 0.012\left(\frac{u-u_{cr}}{\left[(s-1)gD_{50}\right]^{0.5}}\right)^{2.4}\left(\frac{D_{50}}{d}\right)(D_*)^{-0.6}$$ Equation 2.17

$$u_{cr} = 0.19(D_{50})^{0.1}\log\left(\frac{12R_b}{3D_{90}}\right) \quad \text{for } 0.1 \le D \le 0.5\text{mm}$$ Equation 2.18

$$u_{cr} = 8.5(D_{50})^{0.6}\log\left(\frac{12R_b}{3D_{90}}\right) \quad \text{for } 0.5 \le D \le 2.0\text{mm}$$ Equation 2.19

The Van Rijn formula is a simplified form for use when only mean velocity, flow depth and particle size are known.

2.2.3.10 Sediment Delivery Ratios

The delivery ratio is a useful concept that can be used to replace sediment transport formulae when insufficient data is available. The basic sediment delivery ratio is defined by Walling (1994) as:

Gross Erosion = Sediment Yield/SDR Equation 2.20

where SDR is the sediment delivery ratio. Walling goes further to define the magnitude of the SDR as a parameter influenced by a wide range of geomorphological and environmental factors, including: the nature, extent, and location of the sediment sources; relief and slope characteristics; the drainage pattern and channel conditions; vegetation cover; land use; and soil texture. Many empirical delivery ratios attempt to define the delivery as a function of catchment area, but more

recently developed models such as CALSITE (Bradbury et al., 1993, see section 3.6.4) have defined a delivery ratio that incorporates a simple sediment transport equation using parameters of runoff and slope.

2.2.3.11 Hydrological Processes

For more detail on the hydrological processes involved in stream flow and sediment transport there are many books available (e.g. ASCE, 1996 and Shaw, 1994). The following is a brief summary of some of the processes involved taken from Linsley et al. (1982).

There are three main routes of travel for rainfall to reach the permanent stream network once it hits the ground: overland flow, interflow and groundwater flow. Overland flow or runoff is water that travels over the ground surface to a stream channel. A channel refers to any depression in the ground surface that may carry turbulent flow during rain and for a short while after. Surface flow only occurs if the rate of rainfall exceeds the infiltration rate; this is therefore less likely on high permeability soils or if the soil is very dry. However, if the soil has been very dry for a long period then a cementation effect takes place that causes the infiltration rate to become much lower than normal. Hydraulic conductivity is also much lower in dry soils. This means that when it rains the rainfall rate can easily exceed the infiltration rate, causing large volumes of runoff and very high erosion rates.

Some water that infiltrates the ground surface may move laterally through the upper soil layers until reaching a stream channel. This water movement, known as interflow or subsurface flow, moves more slowly than surface runoff and reaches the stream later. Although slower than surface runoff, interflow may be much greater in

quantity and thus may be a principal factor in smaller rises in streamflow, especially during moderate storms.

The rest of the precipitation percolates downwards to the water table. Water eventually discharges into the permanent stream network as groundwater flow if the water table intersects stream channels of the watershed. However, the rate of groundwater flow is much slower than interflow. Therefore, the contribution of groundwater does not fluctuate rapidly because of its very low flow velocity.

The proportion of total runoff from each of the three components depends upon the physical conditions. Thin soil, covering rock favours substantial interflow and some surface flow, whereas, thick uniform permeable soil encourages downward percolation to join groundwater flow.

This means that watersheds with permeable surface soils and large effluent groundwater bodies give high, sustained stream flow with a small difference between mean and flood flows. Watersheds with low permeability surface soils and influent groundwater have large differences between mean and flood flows, and have low or even zero flows between floods.

The three components of flow can be interchangeable and sometimes for convenience, subsurface flow is incorporated with the surface flow. However, for the purposes of this study it would be inappropriate to incorporate surface and subsurface flow, as the subsurface flow has no influence upon surface erosion.

2.2.3.12 Infiltration

The infiltration rate is simply the rate at which rainfall is absorbed into the soil matrix. This is a very important base factor as it plays a crucial role in the erodibility of the soil and in determining the runoff rate from a soil. Runoff occurs once the rate

of rainfall exceeds the rate of infiltration. When rainfall first occurs, the soil absorbs the moisture to a point where the soil becomes saturated. Once saturated and the capacity of the soil is exceeded, then the excess water flows across the surface of the soil as runoff.

Generally, the higher the infiltration rate the lower the quantity of runoff. However, there are exceptions to this rule, in areas of infrequent but high intensity storms the soil surface will dry out and become crusted, increasing the impermeability of the soil at the surface and generating higher runoff rates than would normally be associated with the soil type. This is most common in sandy soils with relatively high clay contents.

2.3 Why model soil erosion?

2.3.1 Introduction

The context under which erosion is studied is very important. When studying erosion, it is necessary to appreciate the motives for the study such as; is the erosion damaging the natural environment or merely a part of the continuous cycle of loss and re-growth. There are different reasons for studying soil erosion arising from the many different issues that occur when soil erosion becomes a dominant factor in the development of the landscape. These can be largely categorised as either environmental and conservational issues or socio-economic issues. Further to this, there is then the question of what measure of soil erosion should be taken; soil loss or sediment yield.

As previously stated, soil erosion is the removal of surface particles by wind or water, in this study the removal by water is the main concern. However, as also previously stated, the process of soil erosion is only one type of land degradation;

many other processes also occur to degrade the land causing the overall effect of landscape denudation. Before going into detail about the measurement and prediction of the effects of soil erosion and the ways to control those harmful effects, it is helpful to look at all the overall processes and effects involved in landscape denudation to be able to place soil erosion in perspective.

Socio-economic issues include: whether the net soil loss from any one section of agricultural land has a significant effect on the production capabilities of that section of land; and, whether the quantification of erosion using methods from western science address the source of the problem at management levels higher than the peasant farmers who till the land.

From the point of view of western science in terms of the quantification of soil erosion, there are two main reasons to study erosion and these reasons link very well with the two types of soil erosion measure that are usually taken. The first reason is to study the on-site effects of the soil erosion; this includes loss of crop productivity, degradation of the land surface, loss of nutrients etc. These effects can be quantified by relating them to the results of soil loss calculations. Sediment yield however, is used to quantify the off-site effects of soil erosion. These effects include transport of pollutants (pesticides), siltation of reservoirs and lakes, etc.

When these topics are considered it will then place the erosion in context of natural landscape development not just the scientific definition from the point of view of land management and conservation. This is especially important in places like Africa and other developing countries where it is necessary to place the relevance of western science within local practices and knowledge, to find the best solution to the problem that is encountered.

2.3.2 Erosion in context/perspective

Kirkby (1980) discusses the perspective of soil erosion by rainfall and runoff within the context of all forms of degradation, the following section summarises the most salient points.

The broadest view of soil erosion is to compare it with other processes of landscape denudation, because soil erosion should only be recognised as the dominant process when it is the most rapid. This also allows the significance of soil erosion rates to be compared within a geological time-scale and asks what rates can be tolerated in the long term. Although the highest rate that can possibly be tolerated is one at which the rate of erosion does not exceed the rate of regeneration, its significance depends upon the depth of soil. For example, if the regeneration rate was 2mm/year less than the erosion rate, this would have a much greater consequence on a thin 10cm soil than on a deep 1m soil. A narrower view examines soil erosion in its immediate climatic and vegetational controls, and questions how well the processes involved, e.g. raindrop impact, flow generation and sediment resistance and transport, are understood at this level. Another way of looking at soil erosion is through its broad pattern in time and space. At present, the distributions of soil erosion through the year and around the world can only be partially explained, but the explanation helps to define the most urgent problems facing soil conservationists in various environments.

Soil erosion is a normal aspect of landscape development, but only in some parts of the world does it dominate other processes of denudation. In suitable environments, the other major processes, mass movement and solution, are the dominant processes. A brief survey of these three groups helps put soil erosion and

conservation problems in perspective on a geological time scale in a worldwide context.

In an uplifted mountain mass, commonly dissected by rivers into steep sided valleys, landslides, rock fall and other types of mass movement are highly effective in widening the valleys and lowering their slope gradients. Rapid mass movements are dominant at this stage, but are characterised by a threshold value below which slopes become stable. This value is broadly related to the bedrock and soil properties, but is also related to a lesser extent to rock structures, climate and groundwater conditions. Vegetation cover also plays a small part, so that land use changes can influence slope stability. During the mass movement stage, the slower processes of soil erosion and solution, although active, usually play a subsidiary role to mass movement such that they can be considered negligible by comparison. It should be pointed out that the speed of the process refers to the quantity of soil and other ground material lost over a given time period, i.e. the rate of degradation. Although soil erosion can occur very rapidly, the rate of degradation by soil erosion will also be much less than that of any mass movement processes.

Once slopes are at gradients that are stable with respect to rapid mass movements, the slower processes of soil erosion and solution become dominant. Where rainfall generally percolates into the soil, it flows slowly within the soil and rock pores and thus has no capacity to transport material along its flow. However, it is able to come to a near equilibrium state with the finest material in the soil making it highly effective at dissolving the soil and the bedrock. This not only lowers the surface of the soil but also progressively converts bedrock into new soil. The main feature of this process is that it is inherent in the nature of the process that solution can never have catastrophic effects, the higher the rate of solution the greater the rate of

lowering of the soil, but also the greater the rate of formation of new soil from the degradation of bedrock.

Soil erosion by water is therefore most active where solution is least active. For solution rates to be high the soil must be of fairly high permeability, for erosion by water to be significant the soil must be transported overland (not through the soil matrix) and thus permeability rates must be low. Therefore, where rainfall cannot infiltrate the soil, it flows over the surface and can carry away soil material by means of its hydraulic forces due to the relatively fast rate of flow. As relatively large depths of flow can flow over the surface, and exert correspondingly large forces, soil erosion can have catastrophic effects even on relatively flat gradients. This is most likely to occur in semi-arid areas, but fields cleared for cultivation are liable to such erosion in any climate. Severe soil erosion associated with gully incision can initiate mass movements from steepened slopes around gullies. Such mass movements play what may be an important role in the total sediment removed.

2.3.3 Socio-economic considerations

The socio-economic aspects of soil erosion are also very important. The long term affects of severely degraded land can put severe pressures on a country's agricultural production. In developing countries where a sound agricultural base is vital for economic stability and growth, then loss of agricultural land through mismanagement and soil erosion can have serious knock on effects. For a country to be economically stable then it has to be reasonably self sufficient in terms of its agricultural production.

As well as considering the causes and context of erosion with respect to the physical processes involved, it is also important to place erosion into perspective

taking into account the reasons for the mismanagement of the agricultural land. If this is done then a much broader explanation of soil erosion can be exposed than the narrow view provided by scientific and technical analysis of the erosion. Stocking (1995) states that the productivity and sustainability of the world's soils is, by most estimates, declining, even though aggregate production (in all continents except Africa) is being maintained or even increased. This statement demonstrates two important considerations; firstly, that soil as a resource is being put under more pressure than ever before; and, secondly, when considered with the fact that it has the largest population growth rates, it implies that in Africa, soils are so badly degraded that aggregate production is also in decline and potentially unable to support the population.

Stocking (1995) makes further comments on the socio-economic issues involved which are summarised as follows. Prediction models calculate how changes in land use or management may alter the erosion hazard, and most technical studies and consultant reports take only these obvious, tangible factors into account. The socio-economic, cultural and political contexts are, if considered at all, merely externalities that may marginally modify the core technical analysis. This view of the importance of site-specific technical analysis has unfortunate side-effects. From this viewpoint, it is very easy to blame the land user for the erosion and loss of productivity because many of the variables that the prediction models cite as the cause of erosion can be controlled by the land user. In the developing world, the land user is often a poverty-stricken farmer trying to create subsistence on steeply sloping land with poor soils and little vegetation cover.

The question that arises is why should the farmer utilise such bad practices when it is obvious that they are causing severe land degradation and jeopardising the

future cultivation of the land. The answer on a certain level can be very simple, it may be a choice between having enough food to survive but continuing to degrade the land, resulting in the land becoming barren and infertile later on, or conserving the land now but not having enough food to survive. Unsurprisingly, farmers choose the first option. It is not usually as stark and clear cut as that however, more a series of problems that conspire to contribute to a gradual decline in land quality. This is explained as the reproduction squeeze, whereby rural peasantry are caught between either maintaining current livelihoods or looking after conservation works. A small farmer must produce a primary product (e.g. maize, cassava) for sale to purchase commodities for production (e.g. tools, fertilisers) or for consumption (e.g. food, clothing). As the relative value of local production falls in comparison with the cost of purchases, a worldwide phenomenon, the small farmer must reduce the cost of production and/or increase primary product output. The result is an impoverished peasantry working harder on poorer, degraded, more distant soils. Labour time, essential for soil improvement or maintenance of conservation structures, is instead diverted into the immediate goal of primary production.

Stocking (1995) then goes on to discuss the global context. A further valid question is how this world's economic and political systems have developed to the state whereby it is the rational choice of land users to degrade their land. In such a milieu, market prices, the terms of trade, the structure of agrarian society, international economic relations, competing political interests and global politics become parts of the explanation. Explanation of soil erosion thus involves a wider political economy and a complexity of non-technical issues. Where natural systems of soil, water and vegetation are resilient, only major disturbances may cause degradation that has a substantial impact on production. Couple this with relatively

stable economies in societies that are not only willing and able to subsidise land users to ensure conservation, but also have a high degree of empowerment and local decision making, then land management is relatively easy. However, in a poor developing country with inequitable access to resources, corruption and many other pressing problems, it would be a brave land manager who might contemplate tackling international relations.

2.3.4 Soil loss vs. sediment yield

As stated there are many reasons to study both sediment yields and soil losses depending upon the requirements of the study. There are also many different advantages and disadvantages to both measures of soil erosion that should be clearly understood before selecting one for analysis.

According to Walling (1994), sediment yield measurements possess the advantage of providing a spatially integrated assessment of erosion rates in the upstream catchment area and thereby avoid many of the sampling problems associated with direct measurements. Thus, in principle, measurements of sediment yield at a single point at the basin outlet can provide information on average rates of erosion within the basin, whereas a large number of plot or similar measurements might be required in order to derive an equivalent average. Walling then recognises that there are, however, many disadvantages with this type of data when trying to provide meaningful results from the analysis of this data. These problems are summarised as follows.

Firstly, only a fraction of the sediment eroded from upland slopes within a catchment reaches the catchment outlet. Much of the eroded sediment is deposited and held in either temporary or permanent storage upstream of the catchment outlet.

The storage may occur on slopes, particularly where slope gradients decline and concave slopes occur, at the base of slopes, in swales, on floodplains and within the channels.

Secondly, problems arise when attempting to link downstream sediment yield to upstream erosion rates due to the temporal discontinuity involved in the process of sediment delivery. Eroded sediment may be deposited and remobilised several times before reaching the catchment outlet, giving rise to an unknown length of storage time, which has to be accounted for. Therefore, transported sediment at the catchment outlet may reflect the recent history of erosion within the catchment rather than the erosion resulting from a single storm.

The final problem involves relating sediment yield to soil erosion upstream when considering that the sediment transported to the catchment outlet is derived from a variety of sources other than erosion from upland slopes. These sources include channel and gully erosion, and mass movements such as bank collapses and landslips caused by intense rainstorms.

The advantages of soil loss measurements are that they can provide specific erosion rates at distinct points across the land surface. These assessments are useful for identifying areas of high potential erosion enabling conservation methods to be applied to the areas where they are needed most. As with sediment yield measurements there are disadvantages associated with this approach when quantifying soil erosion.

The first and most important disadvantage is that the individual parameters are generally empirically generated from experimental plot data. This means that for each different circumstance in which the model is used, parameters have to be re-calibrated for the conditions specific to that area. This then leads on to the problems associated

with the direct measurement of physical events to acquire the data needed for the calibration of these parameters. There are not as yet any totally reliable means of measuring suspended and bed sediment loads within streamflow. Suspended load measurement has become very sophisticated but requires expensive equipment; however, bed load measurement is still very primitive and prone to large, even unquantifiable errors.

Sediment yields also only provide an average loss of soil throughout a catchment, which has been transported out of that catchment; but cannot identify erosion hotspots that require additional conservation management. Therefore, whilst a model can predict that x amount of sediment is leaving a catchment and is silting up reservoirs, the only way to stop this is to identify from where the sediment is being eroded. The solution is therefore to create a model that provides both soil loss estimates over the catchment and sediment yield predictions to identify the harmful effects of the eroded sediment. The main drawback of this solution is the difference in time scale that is used in the two types of modelling. Soil loss models tend to operate on an annual basis, whereas sediment yield models operate on a daily or an even smaller time step. It is however, easier to adapt the soil loss model to the smaller time scale, than vice versa, as the soil loss information is required for each run of the simulation to provide sediment yield data. Soil loss is easily equated over a whole year, whereas the parameters required for calculating sediment yields are not.

2.4 Erosion in Ghana

2.4.1 Erosion and related studies in Ghana

Very few soil erosion studies have been undertaken in Ghana, although this applies to much of Africa. In Ghana most of the agricultural production is low

technology and restricted to shifting cultivation especially in the rural areas where secondary forest is predominant. Within much of the agricultural areas, the units are effectively self-sufficient smallholdings trading surplus in the large urban areas and towns. Small-scale cash crop production, such as cocoa beans, is also undertaken.

The climatic conditions in Ghana are semi-tropical with a bi-modal rainy season in the southern half of the country (April – July and September – November), in the north of the country considerable desertification has taken place, and only a single rainy season occurs (April – September), but with overall less rainfall.

The high intensity seasonal rainfall coincides with the early growing period for many of the crops grown, such as maize, cassava and yams, when the plants have a small leaf area and thus do not provide much protection to the soil. This means that the plots are potentially very susceptible to high rates of erosion when combined with farming areas on steep-sided valleys in the regions around the southern half of Lake Volta.

As previously mentioned in chapter one, the project that motivated this thesis set out to apply the agro-ecological zoning principle to Ghana; Boateng et al, 1998 state that the FAO/IIASA-AEZ suitability procedures that were developed for Africa and Kenya were adopted and modified to suit Ghanaian environmental and socio-economic conditions.

The report discusses at some length the socio-economic aspects of erosion, related to Ghana, which are detailed further in the next section (2.4.2). The project pays very little attention to the specific quantification of soil erosion, however, the AEZ method does allow for some of the main contributing factors that cause major soil losses to be taken into consideration. Through utilising land slope and soil type as two of the land use suitability classification parameters, the project does indirectly

attempt to protect the soil from the adverse affects of erosion. By accounting for slope and soil type and decreasing the suitability rating of the land resource for steeper slopes and poor quality, thin, friable soils, then the AEZ method recommends a decrease of land use on such resources, thus predicting and also preventing soil erosion. However, there is the drawback with this approach. If the climate, and thus rainfall, in a country like Ghana is considered then high intensity rainstorms could potentially prove more damaging to the soil depending upon the type of land use that was employed. One part of the AEZ crop growth model that does seem to be lacking is this consideration of the protection afforded to the soil by the specific land coverage.

Web searches for soil erosion in Ghana, produced many discussions upon soil erosion, its causes, consequences and some on the methods of prevention. However, there was little discussion on the quantification of that erosion.

2.4.2 Socio-economics and environmental planning in Ghana

As stated previously in section 2.3.3, in a developing country with an exponentially expanding population and high potential for economic growth, agriculture is a vital resource. Ghana is no exception to this rule. A good overview of Ghana is provided by Hens and Boon (1999), the relevant points from their paper are summarised and commented on as follows.

They start by simply stating that the environmental situation in Ghana is characterised by desertification, land degradation, deforestation, soil erosion, and inadequate water supply in the northern regions of the country. The population as a whole is growing at a rate of 3% per annum, with even greater urban growth rates,

due to rural out-migration. This statement portrays a fairly bleak picture of the problems in Ghana, but is not uncommon throughout much of Africa.

Next, they detail some of the facts and figures about the country and its geography. Ghana covers an area of 23 million hectares, spanning two major ecological zones. High forest is confined to the south western third of the country, while savannah woodlands cover the north and coastal areas. Within these zones rainfall ranges from 900 mm in the coastal savannah to 2100 mm in the forest belt. The highest precipitation occurs in the extreme southwest, reaching 3000 mm/yr. The rainfall pattern in the south is bimodal with a major peak in June/July and a minor one in September. The surface water regime is determined by 13 river basins. The largest is the Volta River, which has been dammed at Akosombo to form one of the largest man-made lakes in the world. The catchment area of the Volta covers about 70% of the country.

Following independence in 1957, Ghana embarked on a program of economic development to alleviate poverty and raise standard of living of its inhabitants. The progress of economic development in Ghana is, to a large extent determined by the mining and timber industries and a rapidly industrializing and export-oriented agricultural sector, mainly based upon cocoa and oil palm, but diversifying into a wide array of tropical fruits and vegetables. The nine main elements of key importance for Ghana's environmental quality are; land use, forestry and wildlife, human settlements, water quality, coasts and wetlands, industrial pollution, mining, hazardous waste, and chemicals and environmental displacements.

Land degradation is only one of the environmental stresses on agricultural land in Ghana. Deforestation has led to many environmental consequences such as local climatic changes, soil erosion, land degradation, instability in hydrological regimes,

and loss of biodiversity. The clearing of forests through the use of bushfires leads to low agricultural yields, which in turn puts more pressure on the land to be used for cultivation. This need for more agricultural land is important in a country where the agricultural sector accounts for more than 40% of the GNP and 75% of the population earns its living from agriculture. The traditional shifting cultivation method, crop rotation and uncontrolled cattle grazing, and the rapidly increasing use of agricultural chemicals, such as fertilizers and pesticides, also affect the quality of the soil. Annual loss of forest cover over the whole of the country is estimated at 22 000 ha.

In arid and semiarid areas, one of the extreme consequences of deforestation and the consequent misuse or overuse of the land is desertification. It is estimated that 35% of the total land area is subject to desertification. Many of Ghana's sources of water, especially those which do not drain human settlements, are still in pristine condition. Industrial and mining activities, improper use of agrochemicals and increasing urbanisation have led to increasing effluent discharges into existing water bodies. In addition, soil erosion by poor agricultural practices is causing increased sediment loads in rivers and suspended particles in water bodies. In summary, the impacts of land degradation include deforestation, changes in topography, changes in the drainage pattern, slope instability, accelerated erosion and soil degradation.

The fact that the Volta catchment covers such a large area of the country (16.1 million hectares) has significant implications when considering the usage of Lake Volta. Lake Volta was created in 1965 when construction of the Akosombo Dam across the River Volta was completed. The Lake is the main reservoir (irrigation) for Ghana and the hydroelectric plant within the dam provides a significant proportion (768 MW generating power) of Ghana's power. Increased sediment loads within the rivers that feed the Lake, will, in the long term, increase siltation rates within the Lake

decreasing its capacity to supply electricity and water putting pressure on the economy with the massive costs of running dredging operations.

Boateng et al (1998) state that the socio-economic needs of an increasing population is the main driving force in the allocation of land resources to various kinds of uses, with food production as the primary land use. They also state that policy makers and land users face two basic challenges: the need to reverse trends of land degradation in already cultivated areas by improving conditions and re-establishing their level of fertility; and to prevent the degradation of land resources to maintain productivity and minimize soil erosion.

Their final point is that land use is largely determined by environmental factors such as climate, topography, bio-diversity and soil characteristics, and by demographic, socio-economic and political factors, such as land tenure, markets and agricultural policies (not mentioned is also the conflict between spending priorities of any developing country's government with little enough money to distribute). Land is an indispensable resource for the most essential human activities: it provides the basis for agriculture, energy, and timber production, water catchment, recreation, and settlement. A continuing theme throughout history has been the conflict related to control over land and its use.

2.5 Summary

Soil erosion is a complex process with many different parts interacting with each other as well as independently being part of the whole. To assess properly the environmental damage caused by erosion, most researchers now concentrate on analysing sediment yields as well as soil loss. The process that defines yield incorporates three main parts, detachment of particles from the soil mass, transport of

those particles away from the place of detachment and subsequent deposition of those particles. Because the system is so complex it would be extremely difficult to model accurately, therefore the key factors involved in the process are conceptualised to create simple factors that encompass the principal and dominating parts of the process.

The key parameters that control the detachment are the factors of erodibility, erosivity, vegetational protection and topography. The factors that predominately dictate the transport and deposition phases are the runoff and flow rates of the transporting medium. These are generally modelled using sediment transport equations.

Chapter 3

Review of Erosion Modelling

3.1 Introduction

Having discussed the processes that influence soil erosion, this chapter now examines the various methods and models that have been employed to analyse erosion.

3.2 History of soil erosion modelling

There has been an awareness, and thus attempts to control, soil erosion for many centuries. The best example of this is the terracing system first adopted by Chinese farmers as long ago as the early centuries BC. However, it is only much more recently that scientists have tried to quantify the erosion.

The first recorded instance of a scientific study into the effects of erosion dates back to Wollny in the late nineteenth century (Kirkby, 1980). Subsequently, the first quantitative experiments were carried out in the US beginning with the forest service in 1915 and then by M.F. Miller in 1917 in a study of the effect of crops and rotations on runoff and erosion (Kirkby, 1980). Throughout the 1920s and 1930s, there was great concern over the dangers and effects of severe rates of erosion especially due to the dust bowl crisis throughout the mid-west.

The first empirical equation to appear was developed by Zingg (1940). This equation only related soil loss to slope length and slope steepness but was the start of the development of empirical equations using plot data. Through the late 1940s important developments were made. Ellison (1947) describes the individual processes involved in erosion and Musgrave (1947) developed an equation relating the amount of soil eroded to the rainfall characteristics. Through the 1950s and early 1960s the

mass of accumulated plot data collected in the USA was steadily growing, as was the refinement of the factors affecting soil erosion. By the mid 1960s, the parameters representing those factors had been finalised and this brought about the emergence of the Universal Soil Loss Equation (Wischmeier and Smith, 1965) or USLE for short. The original equation was designed for the western half of the USA, but a subsequent refinement (Wischmeier and Smith, 1978) was calibrated to be used anywhere within the USA. Theoretically, the equation could also be adapted for use anywhere in the world provided that a sufficiently extensive amount of calibration data could be accrued.

This was not the only work in progress. Despite an inclination towards empirical modelling throughout this period, research was still being undertaken on the processes involved in soil erosion. In 1969, Meyer and Wischmeier published a process-oriented model that considered the detachment and transport of soil particles by rainfall and runoff as individual processes.

The USLE was the dominant model for many years, but its major drawback was that it could only quantify sediment losses. However, the subsequent advances in erosion modelling and the inclusion of hydrological modelling, the birth of GIS and the growth of more advanced and powerful computer techniques have enabled scientists to produce more comprehensive sediment yield models since the early 1980s. Many of these models still reflect the early advances made by the USLE though, through the components within the models employed to calculate initial erosion at plot level before routing eroded sediment through the catchment. These models are discussed in more detail in section 3.6.

3.3 The Universal Soil Loss Equation

Before commencing an analysis of soil erosion, it is important to be able to identify the circumstances and conditions under which the land is susceptible to land degradation and in particular a significant net loss due to soil erosion. Thus, once this information has been established it is possible to select an appropriate study area in which a potential erosion risk exists so that the risk can be quantified.

To achieve this, a simple, reliable and efficient model is required that does not necessitate a large amount of input data or time to evaluate.

The USLE (Wischmeier and Smith, 1978) is a calibrated empirical model designed to predict long-term average annual soil loss estimates depending upon land type, topography, rainfall, land cover and land management practices. Its original purpose was to provide a simple but accurate model to predict the soil loss from cropland in the United States, especially in the mid-west after the dust bowl droughts in the mid 30s. The USLE takes the general form of:

$$A = R.K.LS.C.P \qquad \text{Equation 3.1}$$

where, A is the annual soil loss (t/ha), R is the rainfall erosivity factor, K is the soil erodibility factor, LS is a combined slope length/steepness factor, C is the land cover and crop management factor and P is the land management practice factor.

The USLE in its original form has drawbacks; its biggest criticism, states Nearing et al (1994), is that it has little relevance outside of its [original] scope of use. Zhang et al. (1996) say the greatest criticism of the USLE has been its effectiveness in application outside the range of conditions for which it was developed. In the original USLE equation, the parameters and their equations were all derived from empirical data generated from US records. This was the main reason for the use of the USLE being severely restricted outside of the US in areas where conditions differed from

those within the US. This is not strictly true as it can be used provided the parameters in the equations have been adapted to the conditions in which the equation will be used. Initially this meant extensive re-calibration of the factors for the study area, fortunately, much work has been done over recent years to establish equations for the various factors that are appropriate for selected specific environmental, geological and meteorological conditions. More recently, however, equations have been developed for some of the factors enabling their use in any conditions. In this respect its successor the RUSLE (Revised Universal Soil Loss Equation, Renard et al, 1991), proves to be a more useful tool than the USLE.

The other main drawback of the USLE largely relates to the distinctions between sediment yield, soil erosion and soil loss. The USLE was originally designed to calculate soil loss. Sediment yields, however, for which soil loss has to be calculated initially, can provide much more useful information to land conservation planners.

Another modification of the USLE, the MUSLE (Williams and Berndt, 1977), exists to tackle this second drawback, but it lacks the effectiveness of the RUSLE in improving the problem that it was designed to address. To this end, the R factor was replaced with a function of runoff volume and peak runoff, such that:

$$A = 1.586(Q \times q_p)^{0.56} DA^{0.12} \times K \times LS \times C \times P \qquad \text{Equation 3.2}$$

where Q is the runoff volume (mm), q_p is the peak flow rate (mm/h), DA is the drainage area (ha) and A, K, LS, C, P are as before. The MUSLE, whilst an interesting experiment, is restricted to homogeneous areas so is not much more effective than the USLE, and is not capable of replacing the more advanced sediment yield models such as AGNPS (Young et al, 1989).

The RUSLE was developed to address the lack of applicability of the equation to areas outside the US. Renard et al (1991) describe the RUSLE as having a lumped structure that does not explicitly consider runoff, processes of detachment, transport or deposition individually, but rather as a combination. The equation parameters are identical to the USLE, however, as Renard et al., (1994) state, whilst the basic USLE structure has been maintained, the algorithms used to calculate the individual factors have been changed significantly. The RUSLE is not without its criticisms though, according to Yitayew et al (1999) the algorithms used in computing RUSLE factors are somewhat complex, and because they are linked to each other, are difficult to calculate unless used with computers. However, with computers becoming ever more widely available, even in developing countries, and more powerful, this becomes less of a problem.

Despite its many criticisms, the USLE can provide a useful tool to land conservation and management planners for initial identification of areas of high potential risk to erosion. It still has support from many authors; Zhang et al (1996) state that the USLE is the most widely used empirical overland flow or sheet-rill erosion equation. Nevertheless, they do recognise the limitations as well in that: (a) gullying or mass movements are not considered; (b) deposition of sediment cannot occur within the area under consideration and (c) the slope length and steepness factors must be determined only on the area that is contributing runoff. Kertesz (1993) states that it is important to be fully aware of the problems of using the USLE for soil erosion assessment, but at the same time underlines that the USLE is the most widely used method of soil loss estimation. Molnar and Julien (1998) comment that the USLE is used by conservationists around the world in predicting the average annual soil loss due to sheet and rill erosion. These are just a few quotes, but they do

demonstrate the extent to which the basic structure of the USLE is still in use today, even if the algorithms used to calculate the factors no longer resemble the originals.

It has also been recognised by many modellers that the USLE, either in part or in full, can become an important part of a sediment yield model when used as an initial predictor of soil loss. This then provides the input to the routing section of such a model, which uses this information to calculate sediment yields (e.g. its use in AGNPS (Young et al, 1987) and ANSWERS (Beasley et al, 1982)). This is because the parameters in the equation represent all the physical factors that effect the removal of particles from the soil matrix. The importance of the USLE in this context is also supported by Perrone (1997) who found that the USLE factors were among the most sensitive parameters when utilising AGNPS simulations.

This chapter covers the details of deriving USLE factors for both an initial USLE analysis of Ghana to determine the location of the experimental catchment, and for the factors that were derived for the specific sediment yield modelling undertaken within that catchment. Methods for initial analysis and specific sediment yield modelling were in some cases similar but in others varied due to the nature of the data available and the required temporal scale, for example in the case of the rainfall factor.

3.4 USLE Factors

The six factors of the USLE, although calculated separately, are all inter-related within the original USLE. This becomes apparent when researching how the parameters were defined and from the way in which the equations for each parameter were developed, in most cases the remaining variables were held constant and the effects of an individual parameter tested. Subsequently there have been many

developments in the methods used to calculate the parameters; these are discussed in the following sections.

3.4.1 R Factor

The R factor represents the erosive power of the rain. Wischmeier and Smith (1978) define it as the rainfall and runoff factor, which equals the number of rainfall erosion index units. These erosion index units have been defined in many different ways by different researchers. Wischmeier and Smith (1978) found that when all other parameters are held constant, soil losses are directly proportional to the parameter EI and that the relationship was linear. The EI parameter is the energy intensity value of a particular storm, where E is the total storm kinetic energy and I is the maximum 30-min intensity. Wischmeier defined E as:

$$E = 916 + 331 \log_{10} I \qquad \text{Equation 3.3}$$

where I is the average intensity of the storm.

Oduro-Afriyie (1996) demonstrates a general agreement of this principle, stating that the most common expression of the erosivity of rainfall is an index based on the kinetic energy and momentum of runoff. Thus, the erosivity index of a rainstorm is a function of its intensity and duration, and of the mass, diameter, and velocity of the raindrops.

However, this is not the only definition that exists. Yitayew et al (1999) defined EI as:

$$EI = (E)(I_{30}) = \left(\sum_{r=1}^{m} e_r \Delta V_r \right) I_{30} \qquad \text{Equation 3.4}$$

where e_r is the rainfall energy per unit depth of rainfall per unit area, and ΔV_r is the depth of rainfall for the r^{th} increment of the storm hyetograph, which is divided into m parts of constant rainfall intensity.

Foster et al (1981) defined a rainfall erosivity factor such that:

$$R = 0.417[(P_{2-6})]^{2.17} \qquad \text{Equation 3.5}$$

such that R is rainfall erosivity factor (MJ-mm/ha-h-yr) (P_{2-6}) is 2 year frequency, 6 hour duration precipitation (mm).

The rainfall erosivity can often be as much a feature of the rainfall patterns in a particular climate or region as it is a function of energy and intensity, hence, many modellers working outside of the US have found it advantageous to calculate their own measure of rainfall erosivity. Bradbury et al (1993) developed their own equation to calculate R factors for the USLE section of their CALSITE model. They defined the R factor as:

$$R = \frac{P_a^2}{(100(0.073P_a + 0.73))} \qquad \text{Equation 3.6}$$

where P_a is the mean annual rainfall in mm. Whilst undertaking agro-ecological zoning in Kenya, Kassam et al (1991) defined the effects of rainfall as:

$$R = 117.6(1.00105^{MAR}) \text{ for MAR} < 2000\text{mm/yr} \qquad \text{Equation 3.7}$$

$$R = f(MAR) \text{ for MAR} > 2000\text{mm/yr} \qquad \text{Equation 3.8}$$

where MAR is the mean annual rainfall.

Oduro-Afriyie (1996) uses a climatic index, the Fournier index, to estimate rainfall erosivity indices for stations around Ghana, which were subsequently converted into a rainfall erosivity map. The Fournier index is defined as:

$$c = p^2/P \qquad \text{Equation 3.9}$$

where p is the rainfall amount in the wettest month and P is the annual rainfall amount.

The choice of this index by Oduro-Afriyie is based on the premise it was developed in West Africa under similar climatic conditions as Ghana with data that are readily available. In addition, it incorporates relief characteristics, which since it is a function of mean annual precipitation is itself dependent on relief (Bollinne et al, 1980). Thus, it is much better related to erosion.

3.4.2 K Factor

The K factor is a quantitative value, experimentally determined, and was defined by Wischmeier and Smith (1978) as, for a particular soil, the rate of soil loss per erosion index unit as measured on a "unit" plot. The unit plot is defined as a 72.6ft long, uniform lengthwise, slope of 9 percent, in continuous fallow, and tilled up and down the slope. Continuous fallow is defined as land that has been tilled and kept free from vegetation for more than 2 years. The plot is also re-tilled over time to prevent surface crusting. Thus, the resulting outcome, when all these conditions are met, is that L, S, C, and P factors all have a value of 1.0 and that K is defined as A/R or EI.

The dimensions of the unit plot are arbitrary values based on the predominant slope length and average gradient on which erosion measurements were taken in the US.

The K factor, like R, is slightly different from the other factors in that it is a measure of an inherent property rather than a measure of an effect of a circumstance. However, unlike R (if R is just taken as the rainfall and not runoff as well, then this does not apply) erodibility has to be evaluated independently of the other factors. It is

a measure of a physical property of the soil: a highly erodible soil may not show high erosion on a shallow slope when small rainstorms occur, yet a soil of low erodibility may show high rates of erosion on a very steep slope under high intensity rainfall.

The K factor is defined by Wischmeier and Smith (1978) as:

$$K = \left(2.1M^{1.14}\left(10^{-4}\right)\right)(12-a)+3.25(b-2)+2.5(c-3))/100 \qquad \text{Equation 3.10}$$

where M is the particle-size parameter which equals percent silt and very fine sand (0.1-0.002mm) times the quantity $(100-\%clay)$, a is the percent organic matter, b is the soil structure code used in soil classification and c is the profile permeability class. The equation does not necessarily have to be used; Wischmeier and Smith (1978) also provided nomographs to calculate the K factor. Wischmeier and Smith (1978) also state that to calculate K, it requires measurements to be made for a representative range of storm sizes.

The equation for the K factor was redesigned for the RUSLE, incorporating more data than the original USLE. Renard et al (1994) state that erodibility data from around the world have been reviewed and an equation has been developed that gives an estimate of K as a function of an average diameter of soil particles. The equation is defined as (from Renard et al. (1991) and Williams and Arnold (1997)):

$$K = \left(0.2+0.3e^{(-0.256SAN(1-SIL/100))}\right)\left(\frac{SIL}{CLA+SIL}\right)^{0.3}\left(1-\frac{0.25C}{C+e^{(3.72-2.95C)}}\right)\left(1-\frac{0.7SN1}{SN1+e^{(-5.51+22.9SN1)}}\right)$$

Equation 3.11

where SAN, SIL, CLA and C are the %sand, %silt %clay and %organic matter content of the soil and $SN1 = SAN/100$.

It is worth noting that the term representing the organic matter content always equals 0.75 for soils of higher than 6% organic matter content.

The K factor is not without issues. The main point of argument is whether the value of K varies with time and if so on what scale of time does it vary. On a geological time-scale then K will almost certainly vary, as the soil develops and new layers and horizons form. However, Smyth and Young (1998) state that erodibility is a measure of the average susceptibility to soil loss from a given soil, which, as would be expected, varies throughout the year. The most likely reason for this variability in the value of K, is the change in weather throughout the seasons, which would be especially noticeable in temperate climates. Several meteorological factors may affect this, for example rainfall, temperature and humidity. This means that in tropical climates around the equator, the only variable to be significantly affected would be the rainfall and as the majority of erosion occurs during the rainy seasons, K can be assumed constant throughout this period.

The RUSLE method is only available if the appropriate soil data can be obtained. If particle size distribution data is not available then data from other research has to be relied upon to fill in the gaps, however, in terms of the initial estimations of soil loss, this method is adequate to provide reasonably accurate assessments.

Table 3.1 gives examples of K factor values for various soil types taken from other projects that utilised the USLE.

Perrone (1997)		Molnar and Julien (1998)	
Soil Type	K Value	Soil Type	K Value
Sand	0.1		
Sandy Loam	0.24		
Fine to Very Fine Sandy Loam	0.35	Very Fine Sandy Loam	0.47
Loamy Very Fine Sand to Sandy Loam	0.31		
Loam	0.28		
Loam to Sandy Loam	0.26		
Silty Loam to Silty Clay Loam	0.37	Silt Loam	0.48
Silty Clay Loam	0.32		
Silty Clay Loam	0.33		
Clay to Clay Loam	0.27		
Clay Loam	0.25		
Clay	0.29		

Table 3.1 Examples K Factors

3.4.3 LS Factor

The LS factor is the combined slope length (L) and slope steepness (S) factor that Wischmeier and Smith (1978) amalgamated into a single topographic factor because of convenience. The LS factor is the most controversial and widely disputed of all the USLE factors, due to the issue of slope length.

The slope steepness component does not usually cause much concern in terms of calculating the S factor, but various issues arise when calculating the angle of the slope in order to calculate S. These arise from the problems encountered when defining the two points to create the line (the arccosine) from which the slope angle is derived.

According to Hickey et al (1994), generating LS values poses the largest problem in using the USLE. Renard et al (1994) state that more questions and concerns are expressed over the L-factor than any of the other USLE factors. These two statements demonstrate the contentions that arise from the use of slope length. One reason for this is that the choice of slope length involves judgement; different

users choose different slope lengths for similar situations. This then has an effect on the slope angle, as this will be defined from the same points for which the slope length is defined.

The slope length is defined as the distance from the origin of overland flow to the point where, either the slope gradient decreases sufficiently so that deposition begins, or the runoff water enters a well-defined channel that may be part of a drainage network or a constructed channel (Smith and Wischmeier, 1957). Wischmeier and Smith (1978) then further specified that a change in land cover or a substantial change in gradient along a slope does not constitute the start of a new slope length for the purposes of soil loss estimation.

The slope steepness originates from the discovery by Wischmeier and Smith (1978) that despite no direct relationship between runoff and slope steepness unless other factors were considered, there was a relationship between soil loss and slope steepness. The function for S is expressed as a function of the sine of the angle, rather than the tangent, because a component of the raindrop-impact forces act along the surface and runoff shear stress are functions of the sine.

The LS equation was defined by Wischmeier and Smith (1978) as:

$$LS = (\lambda/72.6)^m (65.41\sin^2\theta + 4.56\sin\theta + 0.065) \qquad \text{Equation 3.12}$$

where λ is the slope length in feet, θ is angle of slope, m is 0.5 if the slope is greater than or equal to 5%, 0.4 on slopes 3.5 to 4.5 %, 0.3 on slopes 1 to 3 %, 0.2 on uniform gradients less than 1 %. The first term of the equation $(\lambda/72.6)^m$ defines the L factor for slope length and the second term $(65.41\sin^2\theta + 4.56\sin\theta + 0.065)$ defines the S factor, the slope steepness. This is not the only form of the equation however; many variations can be encountered merely due to rearrangements of the equation to account for variations in the units used for the equation parameters. If the gradient is

specified in percent instead of degrees, then the S term becomes $(0.065 + 0.045s + 0.0065s^2)$. If the slope length is specified in metres instead of feet then the L term becomes $(\lambda/22.13)^m$. It is worthwhile noting that the L term contains a parameter of slope gradient indicating that to an extent slope steepness plays a part in affecting runoff and therefore erosion.

Other forms of the equation include the variation found in the EPIC (Williams et al 1984) such that:

$$LS = \left(\frac{\lambda}{22}0.1\right)\xi(65.41S^2 + 4.56S + 0.065) \qquad \text{Equation 3.13}$$

where S is the land surface slope (m/m), λ is the slope length (m) and ξ is a parameter dependent upon slope such that $\xi = 0.3S/\left[S + e^{(-1.47+61.09S)}\right] + 0.2$. Kassam et al (1991) defined a two-part LS factor such that:

$$LS = (l)^{0.5}(0.0138 + 0.00965s + 0.00138s^2) \text{ for s}\leq 20\% \qquad \text{Equation 3.14}$$

$$LS = (l/22.1)^{0.6}(s/9)^{1.4} \text{ for s}>20\% \qquad \text{Equation 3.15}$$

where l is the slope length (m) and s the slope steepness (%). McCool et al (1987) also defined the LS equation for the RUSLE as a two-part equation such that:

$$LS = (l/22.1)^m(10.8\sin\theta + 0.03) \text{ for s}<9\% \qquad \text{Equation 3.16}$$

$$LS = (l/22.1)^m(16.8\sin\theta - 0.50) \text{ for s}\geq 9\% \qquad \text{Equation 3.17}$$

where θ is the slope angle (a 9% slope corresponds to a 5.14° slope angle), l is the slope length, and m represents the same parameter as that used in the USLE. It is worth noting that RUSLE is normalised to a 9% slope, the slope on which USLE readings are based (the standard plot) whereas Kassam et al. use 20% as the change point in equations.

The effects of slope length and steepness have been described in many forms from the beginning of soil erosion modelling, including Zingg (1940):

$$A = CS^m L^{n-1} \qquad \text{Equation 3.18}$$

and Smith and Whitt (1948):

$$A = a + bS^n \qquad \text{Equation 3.19}$$

where A is annual erosion, S is the land slope, L is the slope length, C is a vegetation cover factor and a, b, m and n are independent coefficients.

The slope length has always remained a power function. However, more recently, Nearing (1997b) notes that relationships have described the effect of slope steepness as a linear function of the sine of the slope angle. Nearing (1997b) analysed three different slope functions: those used in the RUSLE for slopes less than 9% and for slopes from 9% to 22% as proposed by McCool et al (1987) (see equations 3.15 and 3.16); and an equation developed by Liu et al (1994) for slopes up to 55%. The objectives of the study were to establish a single continuous function to describe the influence of slope steepness on soil loss that fitted the various parts of the three equations given. Nearing (1997b) established the equation for the slope steepness factor, S, such that:

$$S = -1.5 + 17/\left[1 + \left(2.3 - 6.1\sin\theta\right)\right] \qquad \text{Equation 3.20}$$

where θ is the slope angle in degrees.

Bradbury et al (1993) also defined the topographic effects as a function of slope only such that:

$$S = 0.2s^{1.33} + 0.10 \qquad \text{Equation 3.21}$$

where s is the slope in percent.

3.4.4 C Factor

The C factor, also known as the land use factor, represents the effects of vegetational cover and the cropping management of the land.

The C factor is defined by Wischmeier and Smith (1978) as the ratio of soil loss from land cropped under the specified conditions to the corresponding loss from clean-tilled, continuous fallow. The loss from such a plot would be equivalent to the product of the R, K, and LS factors.

Under clean-tilled, continuous fallow, the equivalent value of the C factor is equal to one, and applying the USLE to these conditions will give the maximum possible amount of soil loss from any particular plot. Any vegetation or different tilling conditions will give a reduction in the C value and thus less soil loss. For this reason, the C factor is probably the most important factor within the USLE as it is the one factor that can be varied most easily by either changing the vegetation or the cropping conditions. Folly et al. (1996) confirm this, stating that the C factor is the most important parameter since it measures the combined effect of all interrelated cover and management variables and it is the factor most easily changed by man.

Despite being the most important factor influencing soil erosion, it is also the most neglected. This is for two reasons: (a) it is hard to quantify, as there are a number of different sub-processes involved that are all inherently inter-related and not easy to measure in practice; and (b) it is often not recognised as being the hardest to quantify – this is probably the greater of the two problems. All too often researchers do not calculate C factors properly and considering the difficulties of measurements this is not surprising, but very few researchers seem to recognise this fact, the C factor is usually borrowed from somewhere else and the justification conveniently ignored.

One of the most complex issues to be resolved when calculating the C factor is seasonality and the variability of conditions throughout the period of assessment of soil erosion. The USLE calculates annual soil loss, thus the C factor has to represent the changing conditions of the vegetation throughout this period. This can also necessitate calculations on prior years' land use so that the full effect of crop rotations is known. This largely results in a weighted average for the area over the given period. However, this also means that when utilising the USLE as a measure of initial source erosion, then evaluation of the C factor becomes much simpler as it is taken as an instantaneous measure of the effectiveness of the land use at protecting the soil. This also means that the land management considerations in the cover management factor become negligible, as their effects are more significant over a longer period. Therefore, the parameters of the C factor reduce to those that describe the protective cover from the plants above ground. There is one obvious drawback with this; the C factor needs to be constantly re-evaluated each time the analysis is run. Nevertheless, with remote sensing and GIS technologies as they currently stand, this task, once initial interpretation and ground truthing of the remote sensed images has been completed, becomes a relatively easy task. Table 3.2 shows example C factors from other USLE projects.

Within the RUSLE, the calculation of the C factor has been formalised into a specific equation using sub factors to represent the different influences. It is defined as:

$$C = PLU \times CC \times SC \times SR \qquad \text{Equation 3.22}$$

The four sub factors are defined as follows: PLU is prior land use, CC is crop canopy, SC is surface or ground cover and SR is the surface roughness. Some definitions of

the C factor equation can be found (e.g. Weltz et al, 1998) where a fifth sub-factor, SM, is included to represent soil moisture.

Perrone (1997)		Roslan and Tew (1997)		Cox and Madramootoo (1998)		Folly et al. (1996)	
Land Use	C Value	Land Use	C Value	Land Use	C Value	Land Use	C Value
Corn	0.38			Rainforest	0.001	Quercus Ilex (evergreen oak)	0.003
Grain	0.15	Cropland	0.3-0.4	Mangrove	0.001	Quercus Pyrenaica (type of oak)	0.003
Hay	0.1	Grassland/Hay	0.003	Plantation	0.001	Pinus Halepensis (Aleppo Pine)	0.003
Pasture	0.03	Rangeland (grass and weeds)	0.007-0.45	Scrub	0.01	Pasture	0.05
Soybeans	0.27	Construction Areas	1	Grass and Open Woodland	0.01	Upland Pasture	0.075
Vegetables	0.2	Impervious Areas	0.005	Mixed Farming	0.08	Shrubs	0.088
Forest	0.02	Forest	0.003	Intensive Farming	0.12	Degraded Shrubs	0.113
Residential	0.01	Residential	0.003	Densely Vegetated Farming	0.003	Winter Crops	0.375
				Flatland Intensive Farming	0.12	Summer Crops/Sunflower	0.375-0.755
				Eroded Agricultural Land	0.5	Fallow/Olive	1-0.7
				Agriculture (bananas, vegetables, root crops, tree crops)	0.12		
				Agriculture/Agroforestry (crops as before)	0.06-0.08		
				Forestry	0.001		

Table 3.2 Examples of C Factors

3.4.5 P Factor

The support practices factor covers the reductive effects of farming practices employed to lessen soil erosion. Wischmeier and Smith (1978) define the factor as the ratio of soil loss with a specific support practice to the corresponding loss with up-

and-down-slope cultivation. Support practices are designed to reduce erosion by slowing the rate of runoff water, thereby reducing its transport capacity and erosive power. The most common support practices include contour ploughing, strip cropping on the contour and terracing. It is important to note that a stabilised drainage network for removal of excess rainfall is a necessary requirement for the success of each of these practices. Currently in Ghana, from observations made during fieldwork, support practices are not used by farmers. Thus, more detail about the support practices is not necessary here.

3.5 Types of soil erosion models

3.5.1 Introduction

Soil erosion models can be distinguished in many different ways. They can be classified using general model classifications and they can be classified according to the resultant output from the model. Both of these classifications are described in this section.

3.5.2 Model classification

Several different classifications exist that are applicable to soil erosion and sediment yield models. Classifications of model depend upon the distinctions made about the models structure, realism, calibration or spatial orientation.

According to Bradbury *et al.* (1993), the initial distinction in modelling is between deterministic and stochastic models. Whereas deterministic models presume that a certain set of events lead to a uniquely definable outcome, stochastic models presuppose the outcome to be uncertain and are structured to accommodate this uncertainty.

Deterministic models are then sub-divided into three types: empirical, conceptual and physically based. Empirical models are based solely on the statistical relationship between different environmental factors, established from field experiments, and have no regard for how and why such relationships occur. A physically based model is based upon physical laws and attempts to model individual physical processes. The distinction between the two is not clear-cut. Between the two extremes are models which are based upon concepts about physical laws but rely on empirical data. These are termed conceptual models. Physically based models are often developed with the aid of empirical data, either by making use of laws that are derived empirically, or by using empirical data to test and modify the model (Bradbury et al., 1993).

The USLE is the empirical model that has been used most widely for predicting soil erosion. The greatest criticism of the USLE has been its ineffectiveness in applications outside the range of conditions for which it was developed. Adaptation of the USLE to a new environment requires a major investment of resources and time to develop the database required to drive the model.

Physically-based models are intended to represent the essential mechanisms controlling erosion. The power of physically-based models is that they represent a synthesis of the individual components which effect erosion, including the complex interactions between various factors and their spatial and temporal variabilities. The result is synergistic, the model as a whole represents more than the sum of the individual pieces. The research scientist can use the physically-based erosion models to help identify parts of the system that are most important to the overall erosion process, and therefore should be given attention in research and development of

erosion prediction and control technology. The focus of conceptual models has been to predict sediment yields, primarily using the concept of the unit hydrograph.

Very few soil erosion or sediment yield models are stochastic in nature, although such a model would be appropriate given that most of the factors governing soil erosion are uncertain. Although this seems a very reasonable approach, because stochastic models are based on uncertainties, it would only be logical to include all possible factors in a stochastic model to account for all possibilities. This would result in a very complex model. Therefore, most soil erosion models fall under the category of deterministic models.

On a spatial level there are two different classifications depending upon the degree of spatial variability of the parameters that are being modelled. A lumped model is one in which there is a low spatial variability of the parameters, i.e. they have been lumped together. For example, the assumption of an even distribution of rainfall across a catchment during an event would add a degree of lumping to a hydrological model. The opposite of the lumped model is the distributed model in which there is a high spatial variability of parameters within the model, an example of which is the calculation of individual slope and aspect ratios between cells in a raster model. This particular distinction between models is, however, a very subjective measure of model classification. In the slope and aspect example given, the degree of distribution would rely upon the cell size relative to the area being studied. There are many cases where the descriptions are far more applicable to the parameters within the model rather than the model as a whole, as a model may contain both lumped and distributed parameters. There is also the difficulty of defining the point at which a lumped model or parameter becomes a distributed parameter. The extremes of the

distinction are easy enough to identify, but it is very difficult to establish the degree of variability required for a lumped model to become a distributed one.

The spatial variability of the model can be dictated by both the user and the developer, there are some models in which the degree of spatial variance can be increased or reduced by the user of the model. In the examples using rainfall and slope, it is assumed that the degree of variance is being decided by the user. However, there are models in which restrictions of variance is imposed by the developer, i.e. those parameters used internally within calculations about which a user has no input.

Each type of model has specific implications on the accuracy of the predictions made by the model. The various issues are discussed in further detail in chapter 9.

The spatial variability has the most complex implications. It would be logical to assume that the more spatially varied the parameters in a model, the more detailed is the analysis that can be carried out, thus making the model more accurate. This is not, however, always the case. When applying routing models, the issue of scale is very important. The scale of the model can logically be too large, but can also be too small. If the scale, and thus cell size, is too large then important features such as small valleys can be missed out and valley bottoms are not properly mapped resulting in the incorrect representation of the stream paths. If the scale is too small, this could produce problems such as the generation of excessive slopes when producing a slope map from a DEM which would result in over estimation of erosion, flow rates and thus transport rates.

3.6 Review of selected soil erosion models

After the USLE, the next major development in erosion modelling came with the emergence of the first modellers to incline towards a more physically based nature to their models, such as ANSWERS (Beasley et al, 1982), AGNPS (Young et al, 1987) and WEPP (Laflen et al., 1991).

3.6.1 Empirical Soil Loss Models

Many different soil loss models have been developed over the years of which the USLE is the most commonly used. The USLE has already been discussed in detail. Other models that have been created will be looked at here. The models have many similarities mainly due to the comprehensive understanding that scientists have of individual factors that affect the rate of erosion at plot level. Thus, although the models have many identical parameters the main differences are how the parameters are calibrated, with some of the models having additional parameters to cover aspects of the erosion process that are more advanced.

RUSLE (Revised USLE) (Renard et al., 1993) and MUSLE (Modified USLE) (Williams, 1976) are both adaptations of the USLE although both have very different changes from each other.

The RUSLE maintains the basic structure and parameters of the USLE, however, the important difference as stated by Renard et al. (1994) is that the algorithms used to calculate the individual factors have been changed significantly. The K and R factors have remained largely the same; the major change is the inclusion of a much larger data set improving the accuracy of those parameters. In recognition of the lack of applicability of the K factor outside of the US, an equation to calculate K as a function of average particle diameter and grading has been

developed using data from around the world (Renard et al., 1994). The C factor is calculated using SLRs (soil loss ratios) as in the USLE, however, the SLRs for RUSLE are calculated using a sub-factor method instead of the immensely long and complicated procedure used originally. This enables the C factor to be derived directly using the following equation:

$$C = PLU \times CC \times SC \times SR \qquad \text{Equation 3.22}$$

where PLU is the prior land use, CC is the crop canopy, SC the surface or ground cover and SR the surface roughness.

The MUSLE was proposed to estimate sediment yield from single rainfall-runoff events. The MUSLE retains most of the basic parameters from the USLE except for the R factor, which is replaced by a function of runoff volume and peak discharge. The equation takes the following form:

$$Y = 11800\left(Q \times q_p\right)^{0.56} K.LS.C.P \qquad \text{Equation 3.23}$$

where K, LS, C and P are standard USLE factors, Q is the runoff volume and q_p is the peak runoff rate. The equation, whilst an interesting experiment in adapting the USLE to be able to calculate sediment yields for single events, has one major limitation. This is that its use is restricted to homogeneous catchments, which considerably reduces its applicability in real situations.

SLEMSA (Soil Loss Estimator for Southern Africa), was developed by Elwell and Stocking (1982) and is very similar in principle to the USLE. The model considers factors of crop, climate, soil and topography.

The model exhibits the simplicity of soil loss modelling also shown by the USLE, but as Stocking (1995) notes, predictions [using such models] are only as good as the database used to give physical values to the control variables.

3.6.2 AGNPS

AGNPS (Agricultural Non-Point Source pollution model) (Young et al., 1987) is a distributed, physically based sediment yield model developed to simulate individual storm events. The model was developed to simulate surface runoff, erosion, and sediment and nutrient transport for agricultural catchments. The nutrient transport options can be turned off, however, if sediment transport analysis only is required.

Young et al. (1989) state that the model was developed to analyse and provide estimates of runoff water quality from agricultural watersheds ranging in size from a few hectares to upwards of 20,000 ha (50,000 a). AGNPS operates on a grid-based system dividing the catchment into square cells that have associated properties, and like many of the sediment yield models is usually integrated with a GIS to make input and output of large amounts of data more viable.

The model is run in three stages or loops. The first loop calculates for each cell, upland erosion, overland runoff volume, time of concentration of overland flow, levels of soluble pollutants and point source pollutants. The second stage calculates sediment and runoff leaving impoundments, sediment yields for primary cells and breaks down sediment yields into five particle size classes. The third loop then routes sediment and nutrients through the watershed. A wide variety of outputs can be gained from the model including the runoff volume (per cell), peak runoff rate, total sediment yield (with particle size class sub-totals), upland erosion per cell, deposition rates and also all the nutrient data. The key equations in the model are the peak runoff rate, the runoff volume, upland erosion and the routing equation. The peak runoff rate is taken from the CREAMS (Smith and Williams, 1980) model and is as follows:

$$Q_p = 3.79A^{0.7}CS^{0.16}\left(RO/25.4\right)^{\left(0.903A^{0.017}\right)}LW^{-0.19} \qquad \text{Equation 3.25}$$

where Q_p is the peak flow rate in m^3s^{-1}, A is the drainage area in km^2, CS is the channel slope in m/km, RO is the runoff volume in mm, and LW is the watershed length width ratio, calculated by L^2/A where L is the watershed length. Runoff volume is based on the SCS (Soil Conservation Service) curve number method (SCS, 1986) and is given by:

$$Q = \frac{(P - 0.2S)^2}{P + 0.8S} \qquad \text{Equation 3.26}$$

where Q is the runoff volume, P is the rainfall, and S is a retention parameter dependent upon curve number, all dimensions in meters. The upland erosion equation is a variation on the standard USLE equation:

$$SL = (EI)KLSCP(SSF) \qquad \text{Equation 3.27}$$

where SL is soil loss, EI is the product of the total storm kinetic energy and maximum 30-minute intensity (replacing the USLE R factor), K, LS, C and P are all standard USLE factors, and SSF is a slope shape factor for each cell. The routing equation is derived from a basic steady-state continuity equation and for each of the five particle size classes is as follows:

$$Q_s(x) = \left[\frac{2q(x)}{2q(x) + \Delta x V_{ss}}\right]\left[Q_s(o) + Q_{sl}\frac{x}{L} - \frac{w\Delta x}{2}\left[\frac{V_{ss}}{q(o)}[q_s(o) - g'_s(o)] - \frac{V_{ss}}{q(x)}g'_s(x)\right]\right]$$

Equation 3.28

where $Q_s(x)$ is the sediment discharge per cell, q(x) is the [flow] discharge per unit width, Δx is , V_{ss} is the particle fall velocity, $Q_s(o)$ is the sediment discharge into the cell, Q_{sl} is the lateral sediment inflow rate (i.e. upland erosion from that cell), x is , L length of the flow direction across the cell, w is the average channel width, q(o) is the [flow] discharge per unit width into the cell, $q_s(o)$ is the sediment inflow per unit

width into the cell, $g'_s(o)$ and $g'_s(x)$ are the effective transport capacities for flow into and out of the cell respectively.

Despite having been developed within the US, AGNPS has been successfully tested, adapted and run in other environments. Kusumandari and Mitchell (1997) used AGNPS in West Java, Indonesia, to model soil erosion and sediment yield in forest and agroforestry areas. They compared the calculated erosion rates for the Citarik catchment from the AGNPS and USLE models with field observations to establish the merits of agroforestry as an effective method of reducing erosion rates from agricultural land.

Perrone and Madramootoo (1997 &1999), evaluated the AGNPS model for sediment yield prediction in Quebec, Canada, a region where AGNPS had not been previously tested.

Contradictorily, Kusumandari and Mitchell (1997), state that one of the main limitations of AGNPS is its lack of applicability to large watersheds, the maximum recommended size being 800 ha although it is unclear from where this conclusion has been drawn. Young et al. (1989) do address this issue, stating that for watersheds exceeding 800 ha (2,000 a), cell sizes of 16 ha are recommended, for smaller watersheds smaller cell sizes are recommended. However, once cell sizes approach 16 ha, accuracy decreases as a result of treating larger areas as homogeneous, and the question of spatial scale needs to be taken into account, this is discussed in more detail in chapter 6. Another limitation mentioned by Kusumandari and Mitchell (1997) is the lack of land use types recognised by the AGNPS model, this can be rectified, however, by modifying certain parameters within the model. The other main limitations of the model are that the input values are sometimes limited to a small range of categories and that the number of drainage paths across a cell is

limited, based loosely on the D8 algorithm but containing only three possible outcomes. This results in drainage cells that are incorrectly modelled (see section 3.5.4 for more on flow routing algorithms).

3.6.3 ANSWERS

ANSWERS (Areal Non-point Source Watershed Environment Response Simulation) like AGNPS is another event based runoff erosion simulator although can be considered slightly more conceptual than AGNPS. In addition, like AGNPS and many of the other models reviewed here ANSWERS was developed by scientists working for the USDA ARS (United States Department of Agriculture, Agricultural Research Service). Beasley et al. (1982) describe ANSWERS as a distributed parameter model for simulating runoff and soil erosion.

The model has seven component relationships that dictate the major hydrological processes in generating runoff, and the detachment and transport of sediment (from de Roo et al., 1989). The first relationship is a simple continuity equation of the form:

$$I - Q = \frac{dS}{dt} \qquad \text{Equation 3.29}$$

where I is the inflow of water to a cell including rainfall and flow from other cells, Q is the outflow rate, S is the volume of water stored in a cell, and t is time. The next equation describes surface storage potential and is represented by:

$$DEP = HU \times RC \times \left[\frac{H}{HU}\right]^{1/RC} \qquad \text{Equation 3.30}$$

where DEP is the volume of stored water in mm, H is the height above datum in mm, HU is the height of maximum micro relief in mm, and RC is a surface characteristic

parameter, this equation is based on work by Huggins and Monke (1966). The third equation represents infiltration from Holtan (1961) such that:

$$FMAX = FC + A \times \left[\frac{PIV}{TP} \right]^{P} \qquad \text{Equation 3.31}$$

where FMAX is the infiltration capacity with surface inundated, FC is the final infiltration capacity, A is the maximum infiltration capacity in excess of FC, TP is the total volume of pore space within the considered infiltration depth, PIV is the volume of water stored prior to saturation, and P is a dimensionless coefficient relating decreasing infiltration rate with increasing soil moisture. The drainage is given by:

$$DR = FC \times \left[1 - \frac{PIV}{GWC} \right]^{3} \qquad \text{Equation 3.32}$$

where DR is the drainage rate, and GWC is the gravitational water capacity (total porosity minus field capacity). Detachment of soil particles by raindrop impact is based on work by Meyer and Wischmeier (1969) such that:

$$DETR = 0.108 \times C \times K \times A_i \times R^2 \qquad \text{Equation 3.33}$$

where DETR is the rainfall detachment rate in kg min^{-1}, C is a cropping and management factor (C*P from USLE), K is the K factor from USLE, A_i is the area increment in m^2, and R is the rainfall intensity rate in mm min^{-1}. Detachment of soil particles by overland flow is also from Meyer and Wischmeier (1969) but modified by Foster (1976) and is of the form:

$$DETF = 0.90 \times C \times K \times A_i \times SL \times Q \qquad \text{Equation 3.34}$$

where DETF is the overland flow detachment rate in kg min^{-1}, SL is the slope steepness in percent, Q is the flow rate per unit width in m^2 min^{-1}, C, K and A_i are as before. The final relationship represents the transport capacity based on Yalin (1963), and Meyer and Wischmeier (1969), and is given by:

$$TF = 161 \times SL \times Q^{0.5} \text{ if } Q \leq 0.046 \text{ m}^2 \text{ min}^{-1} \qquad \text{Equation 3.35}$$

$$TF = 16320 \times SL \times Q^{2} \text{ if } Q > 0.046 \text{ m}^2 \text{ min}^{-1} \qquad \text{Equation 3.36}$$

where TF is the potential transport rate of sediment in kg min^{-1} m^{-1}, and Q and SL are as before.

The component relationships do not cover all the equations utilised within the model, many of the parameters are derived attributes such as the flow rate per unit width, which is derived from Manning's *n*. However, the seven component relationships described above form the main theoretical structure of the model and demonstrate the processes that are simulated, hence it is unnecessary to list all the other equations involved.

There are interesting points to note from the equations used within the model. Firstly, as briefly mentioned earlier, the degree of conceptuality is much higher in ANSWERS than in AGNPS, especially when considering the routing structure. Whereas AGNPS uses a quite complex differential equation to route sediment and flow from cell to cell through the catchment, ANSWERS uses a very simple continuity equation combined with a water/sediment balance equation. This involves runoff from the continuity equation, the detachment equations and the transport capacity equation. The attempt to model the exact physical processes by mathematical equations is much less in ANSWERS.

It is also worth noting the parameters involved within the detachment equations. The equations are based upon the factors that influence the removal of soil particles by water and to some extent reflect the structure of the USLE, but have split the two types of detachment into separate equations, whereas the USLE uses only one. The parameters used also reflect some of the criticisms made of the USLE. For the

detachment of particles by raindrop impact only the C, P, K and R factors are used, the R parameter although not defined as a USLE factor, the two are analogous.

There is also no consideration of slope steepness or length. Within the equation for detachment by overland flow the C, K and S factors are used. The slope length is ignored and the R factor is replaced with the flow rate. These approaches seem appropriate for the application, as slope length is a contentious issue, and as the two types of detachment are different processes, then two equations would be sensible. However, the exclusion of slope steepness from detachment by rainfall may not be entirely correct, because forces from the raindrops would have a greater influence the steeper the slope and the inclusion of area increments is not fully understood.

3.6.4 CALSITE

The CALSITE (Calibrated Simulation of Transport Erosion) model (Bradbury et al, 1993) is a conceptual sediment yield model that was originally developed and tested on the Magat catchment in North Central Luzon in the Philippines.

CALSITE is a two-stage model, the first stage calculates source erosion and then after calibration of erosion rates, the second stage calculates transported erosion. Thus, the model is essentially divided into two main sections; a section for calculating soil loss and a section for routing eroded sediment through the watershed.

Soil loss is calculated using the USLE although methods for calculating the various factors differ from the original methods detailed by Wischmeier and Smith (1978). The equations for the LS and R factors are discussed in more detail in chapter 3. The C and K factors, like many other studies of its kind are based upon previous individual research on the specific topics.

The routing structure of the model is unusual compared with most modern soil erosion models. Unlike ANSWERS or AGNPS, CALSITE does not use a hydrological model based on a continuity equation, but instead uses a delivery ratio. Whereas most sediment yield models use a progressive algorithm that by continuously looping moves sediment from cell to cell to the catchment outlet, CALSITE uses a different approach. CALSITE analyses the route to the catchment outlet from each cell and based upon criteria of slope, aspect and drainage area, calculates a delivery ratio that determines how much of the sediment eroded from each cell will be transported to the outlet.

To calculate the transported erosion the first step is to calculate a delivery index image. The delivery index is derived from an understanding of the relationship between sediment transport capacity (T), liquid discharge (Q) and channel slope (S), such that:

$$T = kQ^a S^b \qquad \text{Equation 3.37}$$

where k, a and b are constants. Alternatively, the relationship can be rearranged in terms of the concentration of the transported sediment (X) such that:

$$X = T/Q = k_1 Q^{a-1} S^b \qquad \text{Equation 3.38}$$

The sediment concentration is used as opposed to the transport capacity, as it is independent of the position along the flow path. Values for a and b are derived from work by Govers (1990), whose experimental studies looked at the sediment transport capabilities of varying sediment sizes in a sloping laboratory channel. The delivery index (DI) image is then created for each pixel within the catchment, such that the delivery index per pixel (DI_p):

$$DI_p = \min X_f \qquad \text{Equation 3.39}$$

where min X_f is the minimum sediment concentration transporting capacity along a flow path from each source pixel to a defined stream channel. It is assumed within the model that all sediment, once having entered the permanent stream network, is transported to the catchment outlet. This, although not entirely accurate is a reasonable assumption to make when information is not known about the exact nature of sediment transport within a stream network. Although some sediment is held in temporary storage, (see section 2.3.4) it is logical to assume that after a certain period there is a reasonable balance of exchange of sediment between the transported and stored sediment within the stream network. The actual situation is more complex with high intensity storms 'flushing' sediment from stores giving elevated readings of sediment discharge for those storms, and giving lower readings for subsequent smaller storms as stores are recharged.

Within the delivery index equation, the Q parameter is not easy to calculate directly. Overland flow paths are also calculated, such that another image is created, for which a score (F) is kept of the number of upstream flow paths which cross a particular pixel, the higher the value of F, the more likely it is that a pixel will contain a definite stream channel. However, the F value can also be used to define a 'catchment' size, i.e. the number of upstream cells contributing runoff, and thus giving a likely scale of the annual discharge, V_a, across the pixel, when combined with the annual rainfall, P. V_a is related to the annual rainfall and 'catchment' size, thus:

$$V_a = FP^c \qquad \text{Equation 3.40}$$

The parameter c is a constant based upon the relationship between annual rainfall and runoff. Combining equations 3.38, 3.39 and 3.40, then gives the delivery index for each pixel as:

$$DI_p = \left[F^{a-1} P_a^{(a-1)c} S^b\right]$$ Equation 3.41

Delivery index values are scaled to fit a range from 0 to 100. The delivery ratio (DR_p) is given by:

$$DR_p = \frac{1-\cos\left(\pi \times \left(DI_p - t\right)/\left(s-t\right)\right)}{2}$$ Equation 3.42

where t is a lower threshold below which $DR_p = 0$, and s is an upper saturation value above which $DR_p = 1$ (CALSITE provides all solutions for combinations of t from 0 to 50 and s from 1 to 100). The final delivery ratio is then defined as a function of the delivery index, dependent upon calibration:

$$DR_p = f\left(DI_p\right)$$ Equation 3.43

Transported erosion is then given by:

$$TE = SE \times f\left(DI_p\right) \times k$$ Equation 3.44

where k is a calibration constant incorporating all constants from the previous equations and SE is the annual source erosion derived from the USLE.

CALSITE also recognises the difficulty in the concept of slope length and when calculating the LS factor from USLE, Bradbury et al. (1993) state that although average land slope(s) may be determined with reasonable accuracy from elevation data, slope length cannot easily be determined. Thus within the CALSITE model they assume slope length to be constant. Although not mentioned in the report a secondary reason for not using slope lengths in the USLE LS factor is that the slope lengths were originally included in the USLE to deal with runoff, and as the CALSITE model has a separate section effectively dealing with runoff, then slope lengths are not needed to calculate source erosion.

CALSITE's main limitation is due to its relatively high degree of empiricism. Despite being a conceptual model, because very few parameters are used and the

conceptual nature of the routing process, a long data set is required to calibrate these parameters, which have to be calibrated for each individual catchment to which the model is applied. High quality data sets such as these are not often available in developing countries, especially on smaller catchments, which are more suited to the development and testing of sediment yield models before they are applied to larger catchments.

3.6.5 WEPP, EPIC, SWAT, CREAMS and other models

Many other models have been developed for sediment yield predictions with varying levels of complexity; a brief summary of some selected models follows.

CREAMS (Chemicals Runoff and Erosion form Agricultural Management Systems) (Knisel, 1980), EPIC (Erosion Productivity Impact Calculator) (Williams et al., 1984), SWRRB (Simulator for Water Resources in Rural Basins) (Williams et al., 1985; Arnold et al., 1990) and SWAT (Soil and Water Assessment Tool) (Arnold et al., 1993) are all part of a comprehensive family of models that share many common components. The models are intended for use on ungauged catchments and cover all aspects of the erosion process. They contain full hydrological models including weather generators and full flow routing (including overland flow and all types of groundwater flow), erosion and transport sections, and crop growth models. All of the components are interlinked so that the models run on a daily time step for, if desired, a sequence of several years. There is one major disadvantage with these models, which is due to the comprehensive modelling structure and the design for use on ungauged catchments. The models are therefore very data intensive and require many input parameters.

The WEPP (Laflen et al., 1991) models were initiated in 1985 and there have been many other contributing authors including Nearing and Lane (1989), Foster and Lane (1987), Foster et al. (1989), and Flanagan and Laflen (1997). The WEPP models are slightly different to the models described before because they have gone a stage further by replacing the USLE with an alternative source erosion component.

WEPP is a daily simulation model and has three versions (Flanagan and Laflen, 1997). A Hillslope Profile version, which is a direct replacement for the USLE, for computing sheet and rill erosion and deposition for overland flow profiles. A Watershed version that computes sheet and rill erosion by overland flow, detachment and deposition in concentrated flow channels and deposition in impoundments. The Grid version of WEPP covers a watershed with grid elements, computes the same information as the Watershed version for each cell and then routes the water and sediment from cell to cell to the outlet point of the watershed. The first two versions are presumably limited to homogeneous areas because they do not have a grid structure, whereas the final version must be able to handle non-homogeneous areas. The additional components within WEPP are a winter processes component, a soil component that adjusts the hydrologic and erosion parameters of the soil depending on tillage and consolidation, a plant growth and residue decomposition component and an irrigation component.

As mentioned above a key feature of the WEPP models is the replacement of the USLE for predicting rates of erosion. The basic replacement equation is a steady state sediment continuity (from Lane et al., 1997b) equation such that:

$$dG/dx = D_i + D_r \qquad \text{Equation 3.45}$$

where G is the sediment load in the flow down a hillslope ($kgs^{-1}m^{-1}$), x is the distance downslope (m), D_i is the interrill sediment delivery rate ($kgs^{-1}m^{-2}$) and D_r is the rill detachment or deposition rate ($kgs^{-1}m^{-2}$). The interrill component is given by:

$$D_i = K_i I_e^2 G_e C_e S_f \qquad \text{Equation 3.46}$$

where K_i is the interrill erodibility ($kgs^{-1}m^4$), I_e is the effective rainfall intensity (ms^{-1}) occurring during the period of rainfall excess, G_e is a ground cover effect adjustment factor, C_e is a canopy cover adjustment factor, and S_f is a slope adjustment factor. I_e is computed through a procedure that examines the time period over which rainfall excess occurs. S_f is a function of interrill slope such that:

$$S_f = 1.05 - 0.85\exp(-4\sin B) \qquad \text{Equation 3.47}$$

where B is the interrill slope angle. The rill detachment rate is predicted to occur when the flow shear stress exerted on the soil exceeds a critical threshold value and sediment transport capacity is greater than the sediment load:

$$D_r = K_r(\tau - \tau_0)(1 - G/T_c) \qquad \text{Equation 3.48}$$

where, K_r is the adjusted rill erodibility parameter ($kgs^{-1}m^{-1}$), τ is the flow shear stress (Pa), τ_0 is the critical flow shear stress (Pa) and T_c is the flow sediment transport capacity ($kgs^{-1}m^{-1}$). Sediment transport capacity is predicted using:

$$T_c = k_t \tau^{1.5} \qquad \text{Equation 3.49}$$

where k_t is a transport coefficient ($m^{0.5}s^2kg^{-0.5}$). The coefficient k_t is calibrated and obtained using the Yalin equation (see section 2.2.3.9). Finally, when sediment load exceeds the sediment transport capacity the equation used to predict deposition is:

$$S_r = BV_{eff}(T_c - G)q^{-1} \qquad \text{Equation 3.50}$$

where S_r is the rill deposition rate ($kgs^{-1}m^{-2}$), B is a rainfall-induced turbulence factor (taken as 0.5), V_{eff} is an effective particle fall velocity (ms^{-1}), and q is the flow discharge per unit width (m^2s^{-1}).

All the models discussed in this section have one important common goal. The reason they are related and share common components is that they have been designed with the intention of producing a complete and comprehensive agricultural and environmental simulation model. Only some of the components (those most relevant to this thesis) have been discussed so far, however, the models contain many more. As the models are continuous, daily simulation models then components have been included that model the growth of vegetation, and the decomposition of vegetation on the ground surface. The hydrological sections not only model the flow of water once it has fallen as rainfall, but also include a weather generator that predicts the daily amount of rainfall, temperature, solar radiation etc. Soil moisture is altered continuously as dew falls overnight and sunshine dries the soil out, both directly and indirectly through evapotranspiration.

However, there is one other common feature between all these models, due to the tremendous quantity of variables; calibration requires very long and comprehensive data sets, which are largely unavailable outside developed countries.

3.7 Summary

There are many different approaches to modelling soil erosion, from the simpler conceptual models to the more advanced physically based models. As the more complex models require more input parameters, the selection of model is often based upon the data that can be accrued for calibration.

The breaking down of the erosion process into two phases, detachment, and transport and deposition, is a common theme in many of the models that have been reviewed. The other common feature is the use of the USLE, in part or full, or similar functions, to predict the quantity of erosion that is detached from the area of interest and then the use of routing components to assess the quantity of eroded material that is transported away by the river systems.

Chapter 4

The GIS Environment

4.1 Introduction to GIS

GIS are geographical information systems; they are usually computer software applications that reference items of data to a physical location in space. This enables the spatial relationships between the data items to be analysed.

Burrough and McDonnell (1988) define GIS as [a set of] powerful tools for collecting, storing, retrieving at will, transforming and displaying spatial data from the real world for a particular set of purposes. They also include a definition from the DoE (1987) [that GIS is] a system for capturing, storing, checking, manipulating, analysing and displaying data which are spatially referenced to the earth.

There are two main formats of representing spatial data in a GIS, raster and vector. Vector data takes three forms: point, line and area. Figure 4.1 demonstrates these types; figure 4.1a shows the points which are specified by x and y coordinates. In some very modern applications, three-dimensional representations can be modelled in which the point would also have a z coordinate. By joining two points together, a line is formed (figure 4.1b) and by joining three or more lines, a polygon is created (figure 4.1c). Each form of vector data can have attributes related to it that are stored in the database attached to the GIS.

The raster format is generated by taking an area and dividing it into small uniform squares or cells. Each of the squares has an attribute value attached to it, which is stored in the database. The main principle of the raster format is to achieve the right cell size so that the attribute is a homogeneous representation of the spatial area covered by the cell. In practice, this is not always possible.

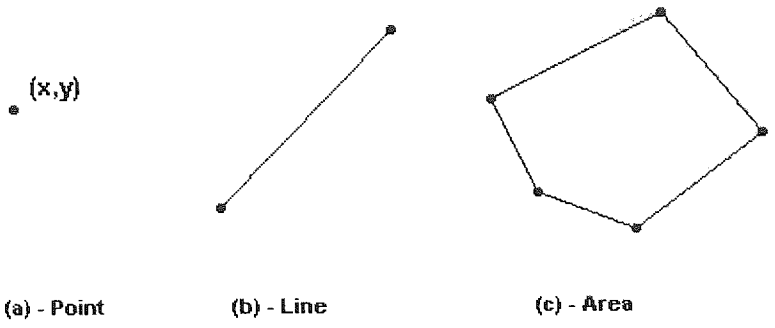

Figure 4.1 The Three main Constructs of a GIS

The attributes are probably the most important aspect of either of the two formats. The raster and vector representation models provide the spatial distribution, but the attributes contain the data that is being spatially represented.

The two main forms of digital map used in GIS as described by Burrough and McDonnell (1988), are topographical maps and thematic maps. Topographical maps are general purpose maps that represent the natural and man-made surfaces and features of the Earth. Thematic maps contain information about a specific subject or theme. Of the various types of topographical map, on of the most important is the digital elevation model (DEM). DEMs are a represent the terrain of the Earth's surface as the height above sea level at various points on the map. The location and frequency of the defined points is determined by the type of format (i.e. raster or vector) of the DEM, and the resolution of the DEM. DEMs, their derivation and the issues with their use is covered in more detail in chapter 5.

4.2 Benefits of GIS

GIS started to be developed as a result of the inadequacy of the paper map to fulfil the requirements for spatial representations. As Burrough and McDonnell

(1988) state, the growing demand for more spatial data and for better means to analyse them can only be met by using computers. Before computer mapping tools were available, all kinds of mapping had one major limitation, namely that the spatial database was a drawing on a piece of paper. The biggest advantage of GIS is that the information held within the spatial database can be compared, analysed, drawn and redrawn with relative ease compared with the traditional paper map.

Digital representations of the earths surface and the ability to reference a database of information to a spatial location means that GIS can provide a powerful platform for various forms of modelling. Burrough and McDonnell (1988) list examples of the users of GIS including: earth scientists, urban planners, civil engineers, emergency services, epidemiologists, commercial industries (for market analysis), utilities (water, gas, electricity) and archaeologists. Similarly, those involved in soil erosion modelling have been able to gain from the many benefits of using GIS.

4.3 GIS Software

There are many GIS software packages available on the market, each with their own advantages and drawbacks.

Many of the commercial packages available tend to be vector-based systems, such as ESRI's Arc suite (ESRI, 2004) and the MapInfo (MapInfo Corporation, 2006) packages. Licences for these systems are expensive and the additional modelling functionalities within them bring on additional costs as well. In terms of cost, efficiency and capabilities of the software, it is better to look at experimental research packages.

4.3.1 GRASS-GIS

The GRASS (Geographic Resources Analysis Support System) GIS (GRASS Development Team, 2003), has many unique advantages over the other commercial and research software packages. In the author's experience of GIS it is the most wide ranging and comprehensive GIS software package.

GRASS can model and represent many different aspects of the processes involved in GIS, not only does it cover the basic raster and vector formats, but also includes a sites format which has specially developed routines for point data, as well as routines for ortho-rectifying aerial photographs. Within each of the types of format, it not only covers the basic manipulations and functions of those types of format, but also includes a range of pre-defined environmental models.

If GRASS has any one drawback then it would be its graphical capabilities, especially in terms of its output specifications, however this is also due to the systems on which the package is installed. It is worth noting that since the completion of the modelling work in this PhD, the package has many improvements in respect to those criticisms. The main advantage in terms of the research being undertaken, however, is the programmability of GRASS.

4.4 Programming in GRASS

As stated above, the main advantage with the GRASS-GIS is its programmability. The package is created using source coded C programs, in the same way in which the UNIX/Linux platform is designed. Programming within the GRASS-GIS package is also undertaken using the C programming language. Unlike most Microsoft Windows based packages that run on a PC, where software is machine coded, because the GRASS package is source coded the original programming can be

seen and adapted in which ever way a developer would want. This means that modules could be created in GRASS to run the soil erosion model that was to be developed for evaluating the erosion rates in Ghana.

Despite the many advantages of GRASS, its allowance of customisation through source code programming and its simple but powerful mathematical functionality, it does have disadvantages. Because it is built for the UNIX and Linux platforms, machine dependencies exist that can cause bugs and errors in relatively simple code.

4.5 Application of GRASS for Soil Erosion Modelling and USLE Estimation

The multi-layer analysis and programming capabilities of GRASS enable soil erosion modelling and USLE application to be performed with relative ease. Multi-layer analyses enable several different layers, representing the same geographical region but containing different attribute values, to be effectively superimposed over each other. Once this has been achieved, mathematical manipulations can then be performed between the layers. Layers can also be manipulated using look-up tables. A look-up table can also be used to equate the attribute value to a parameter or factor by ranges or equations.

4.6 Summary

The modelling tools available within an advanced GIS such as the GRASS package enable many of the different types of environmental and geographical models to be carried out effectively and efficiently. Soil erosion modelling is no exception to this with multi-layer analyses enabling source erosion and transport functions to be simulated on a representation of a study catchment.

Chapter 5

Scale, Resolution and Topographic Attributes

5.1 Introduction

Scale is a very important consideration in any modelling, and in erosion and hydrological modelling has many affects on many different areas. It not only influences the result and accuracy of parameter calculations and thus the end result, but also influences which parameters are dominant within a model.

In particular scale has an effect on the DEM and its derived topographic attributes. This is because the attributes derived from the DEM will change depending upon its scale. The scale at which a DEM is created is usually referred to as the resolution.

Attributes derived from other maps within the GIS are affectedly differently depending upon the scale that is used. The scale of the available DEM dictates the scale at which the other maps are set. The scale will not necessarily effect the derived parameters, but will instead result in a change of the spatial variability. To avoid confusion this will be referred to as the modelling scale.

Therefore, in terms of modelling there are two distinct areas that are influenced by scale: those dominant processes that act at a given modelling scale and the values of the various topographic attributes which change depending upon the resolution.

5.2 Modelling scale

Many authors have defined different scales for different applications. Lane et al. (1997a) identified three distinct modelling scales for erosion modelling. For each of these scales there are distinct differences in the processes that dominate and control

sediment yield at such scale and the applicability of results that can be achieved from modelling at each scale.

The smallest is the plot, or hillslope, scale covering areas from approximately 10^{-6} to 10^{-2} km^2. Lane et al (1997a) states that within this scale, it is rainfall erosivity (amount and intensity), vegetative canopy cover, surface ground cover and topography that largely determine the sediment yield, with the spatial variability of each factor playing a large part in determining the extent of the impact. This is because at this scale soil detachment and runoff are the controlling processes, which in turn are dictated by the amount of sediment available for transport and the amount of runoff to transport the sediment. Soil erodibility and land-use are also important at this scale, the latter inherently influencing the canopy and ground cover, though not as dominant as the others.

The sub-watershed or sub-catchment scale, at 10^{-2} to 10^{1} km^2 is the middle scale. At this scale although rainfall erosivity and runoff generation remain dominant processes, gully and channel processes and vegetation type take over from canopy and surface cover, and topography in controlling sediment yield. The channel and gully processes become the most important at this stage. As runoff accumulates into distinct channels, detachment, transport, and deposition phases within the channel flow become the major influence on sediment yield. It should be noted however, that the other processes and properties such as soil erodibility, vegetative cover, topography and land-use still have a significant effect on sediment yield.

The largest of the three defined scales for areas of 10^{1} km^2 upwards is the catchment or watershed scale. At the largest scale, rainfall erosivity, stream and channel processes, runoff rates and sediment transport capacities become the dominant processes. The processes involved at the hillslope and sub-catchment scale

still have a major influence on sediment yields but become aggregate parts of the whole in terms of their importance.

Lane et al (1997a) also introduce the simple conceptualised ideas of Schumm's (1977) theory of the fluvial system. The system conceptualises the catchment in to three major zones and process stages, sediment source, transport and sink. In Schumm's system, zone 1 represents the drainage basin, a source of sediment and runoff, zone 2 as the network of stream and river channels and sediment transfer, and zone 3, the sink, is the alluvial channels, fans and deltas. Zone 1, the sediment source, is comparable to Lane's hillslope scale, zone 2 and zone 1 together include the sub-catchment scale and zones 1, 2 and 3 together encompass the whole catchment. However, Lane et al (1997a) go further to suggest that Schumm's theories cannot only apply to the full catchment scale but is also repeated across both larger and smaller scales. They state that the three-zone behaviour is exhibited when examined carefully on a small plot, but can also be applied to large-scale (10^3 km^2) multi catchment systems. The individual zones within each scale can be defined using stream orders, zone 1 consists mainly of first order streams, and the addition of higher order streams progresses the system into zones 2 and 3.

Lane et al. (1997a) and Schumm's (1977) conceptualisation of the catchment scale and the processes involved, also provide a very useful template for the creation of sediment yield prediction models. Schumm's three-zone model provides the general structure for a sediment yield model. It can be seen from studying most of the current sediment yield models, ANSWERS (Beasley et al., 1982), EPIC (Williams et al., 1984), WEPP (Foster & Lane, 1987), AGNPS (Young et al., 1989), SWAT (Arnold et al., 1993) and CALSITE (Bradbury et al., 1993) that they all stick to the general format of a three stage model, although the latter two stages of transport and

deposition are often merged as the processes are inherently related. The work by Lane et al. (1997a) provides useful guidelines as to what the critical processes are for the scale at which modelling is undertaken. Of the models listed above ANSWERS, AGNPS, SWAT, CALSITE and EPIC all concentrate upon the hillslope and catchment scales, source erosion is based upon the USLE at hillslope scale with various different routing equations and sediment delivery ratios at the catchment scale. WEPP however is slightly different and provides three separate models for each of the scales, although this is hardly surprising as Lane was one of the main contributors to the WEPP project.

Hutchinson and Gallant (2000) also define a series of scales but in addition define the modelling applications and DEM resolutions applicable at those scales (see table 5.1). Soil erosion modelling in the form of sediment yield modelling is usually performed at either fine or coarse toposcales, whereas soil loss estimation can be carried out at all four scales.

Scale	DEM Resolution	Common topographic Data Sources	Hydrological and Ecological Applications
Fine toposcale	5 – 50m	Contour and stream-line data from aerial photography and existing topographic maps at scales from 1:5,000 to 1:50,000 Surface-specific point and stream-line data obtained by ground survey using GPS Remotely sensed elevation data using airborne and spaceborne radar and laser	Spatially distributed hydrological modelling Spatial analysis of soil properties Topographic aspect corrections to remotely sensed data Topographic aspect effects on solar radiation, evaporation, and vegetation patterns
Coarse toposcale	50 – 200m	Contour and stream-line data from aerial photography and existing topographic maps at scales from 1:50,000 to 1:20,000 Surface-specific point and stream-line data digitised from existing topographic maps at 1:100,000 scale	Broader scale distributed parameter hydrological modelling Subcatchment analysis for lumped parameter hydrological modelling and assessment of biodiversity
Mesoscale	200m – 5km	Surface-specific point and stream-line data digitised from existing topographic maps at scales from 1:100,000 to 1:250,000	Elevation-dependent representations of surface temperature and precipitation Topographic aspect effects on precipitation Surface roughness effects on wind Determination of continental drainage divisions
Macroscale	5 – 500km	Surface-specific point and stream-line data digitised from existing topographic maps at scales from 1:250,000 to 1:1,000,000 National archives of ground surveyed topographic data including trigonometric points and benchmarks	Major orographic barriers for general circulation models

Table 5.1 Spatial Scales of Applications of Digital Elevation Models (DEMs) and Common Sources of Topographic Data for Generation of DEMs (Hutchinson & Gallant, 2000)

5.3 Topographic attributes

As well as scale, resolution is a very important aspect of soil erosion modelling. The resolution, or spatial scale, primarily affects the topographic attributes derived from the DEM, and thus the resolution of the DEM usually dictates the resolution used within the GIS for all the modelling work, with the resolution and data of the other input maps adjusted to suit. The resolution not only affects the

attributes from the DEM however, the spatial variability of land-use classifications and rainfall distributions also have to be taken into account.

Firstly, it is useful to define the topographic attributes being utilised within the model. All the attributes used are primary attributes, i.e. they are derived directly from the DEM. The attributes used are aspect, catchment area and slope.

5.3.1 Slope

Slope can be defined in several different ways depending upon the requirements. The most common method for deriving slope is the finite differences method, which determines the maximum downhill gradient across the centre grid cell of a 3×3 window. The finite difference method calculates slope using the elevation values of the four cardinal directions, and thus from figure 5.1,

$$Slope_{FD} = \sqrt{\left(\left(\frac{z_1 - z_5}{2h}\right)^2 + \left(\frac{z_3 - z_7}{2h}\right)^2\right)} \qquad \text{Equation 5.1}$$

This is a second order finite difference method and the most popular of the finite difference methods. The first order derivative calculates the maximum downslope difference from the 3x3 window in four directions horizontally, vertically and the two diagonals. This is known as the maximum downhill slope or downward gradient. This first order derivative is given by, (with reference to fig 5.1),

$$S_{D8} = \max \frac{z_m - z_n}{2h\phi(i)} \qquad \text{Equation 5.2}$$

where m = 1,2,3,4 and n = 5,6,7,8, and $\phi(i) = 1$ for m = 1,3, n = 5,7 and $\phi(i) = \sqrt{2}$ for m = 2,4 n = 6,8.

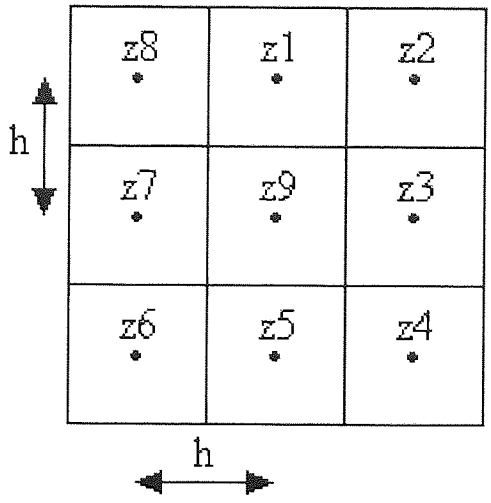

Figure 5.1 Schematic Diagram of a 3x3 Cell Neighbourhood for Calculating Slope and Aspect

However, according to Burrough and McDonnell (1998) this method has the disadvantage that local errors in terrain elevation contribute heavily to errors in slope. A third order derivative also exists that utilises all eight surrounding grid cells; although Gallant and Wilson (2000) state that there is little difference between the results of the first and third order derivatives.

A second method for calculating slope is the D8 method. This method is like the first order finite difference derivative except that instead of calculating maximum downward slope from one nearest neighbour across the centre square to the corresponding nearest neighbour, it calculates the steepest downhill slope from the centre grid square to one of the eight nearest neighbours, again using figure 5.1,

$$S_{D8} = \max_{i=1,8} \frac{z_9 - z_i}{h\phi(i)} \qquad \text{Equation 5.3}$$

where $\phi(i) = 1$ for $i = 1,3,5,7$, and $\phi(i) = \sqrt{2}$ for $i = 2,4,6,8$. This accounts for the longer distance between cell centres to the non-cardinal (diagonal) neighbours.

Wilson and Gallant (2000) also note that the D8 slope estimate is useful when the slope of channels is required, because the finite difference estimate of channel slope may be affected by steep slopes adjacent to the channel.

There is often confusion over the definition of the terms for the D8 method and the first order finite difference derivative, Hickey et al (1994) refer to the D8 as the maximum downhill slope and the first order derivative as the maximum slope from a 3x3 neighbourhood. For the purposes of this thesis, the terms used shall be maximum downhill slope for the D8 method and maximum downward gradient for the first order finite difference derivative, the second order finite difference method will be known as just the finite difference method.

5.3.2 Aspect

Aspect is defined as the direction, usually measured in degrees clockwise from due north, of the path of steepest descent across a grid cell. Aspect is calculated as the arctangent of the north south gradient divided by the east west gradient, such that from figure 5.1,

$$Aspect = \arctan\left(-\left(\frac{z_1 - z_5}{2h}\right) \Big/ -\left(\frac{z_3 - z_7}{2h}\right)\right) \qquad \text{Equation 5.4}$$

where, z_i is the elevation value at each of the grid cells and h is the cell width, all as shown on figure 5.1. An alternative to aspect is the primary flow direction, which is equivalent to the maximum D8 slope. The primary flow direction is given by,

$$FLOWD = j, \text{ where, } j = \arg\max_{i=1,8} \frac{z_9 - z_1}{h\phi(i)} \qquad \text{Equation 5.5}$$

which gives the aspect direction based upon the D8 direction numbering system.

The choice of whether aspect or the primary flow direction is used is largely down to which slope calculation is utilised. Gallant and Wilson (2000) state that

using the D8 slope option guarantees that the slope calculated at a cell corresponds to the slope in the primary flow direction. Thus, when using the finite difference method aspect should be used as these two measures are also corresponding.

5.3.3 Primary cells

Primary cells are defined as those grid cells that do not receive flow from any of the surrounding grid cells, i.e. the elevation of the cell is higher than that of its neighbours.

5.3.4 Drainage area

The other important topographic attribute that needs to be derived from a DEM for sediment yield modelling is the drainage area, also known as the upslope contributing area or specific catchment area. The drainage area is defined as the area above a certain point in the catchment, which contributes flow to that area. The drainage area, although a primary topographic attribute, can only be calculated once certain other attributes have been calculated, i.e. flow routing directions and depressions and flat areas.

5.3.4.1 Flow routing algorithms

There are various methods available for routing flow through a catchment using a DEM. They all are based upon indicating the direction of flow from a single grid-cell to one or more of the eight surrounding cells, providing they are downslope of the central square. According to Gallant and Wilson (2000) there are at least six algorithms that have been proposed for routing flow and computing contributing areas from square grid DEMs. Five of these algorithms – the D8 (deterministic eight-node)

algorithm of O'Callaghan and Mark (1984), the Rho8 (random eight-node) algorithm of Fairfield and Leymarie (1991), the FD8 and FRho8 algorithms, and the DEMON algorithm of Costa-Cabral and Burges (1994) – have been implemented in TAPES-G (Moore, 1992, Wilson and Gallant, 1998). The sixth method uses a vector-grid approach and has been implemented as the *r.flow* routine in the GRASS-GIS (Mitasova and Hofierka, 1993, Mitasova et al., 1995, 1996).

It should be noted that the DEMON and FD8 algorithms discussed here are not exact replications of the original models but algorithms implemented from information given in papers on the algorithms. The general philosophies behind the algorithms have been adhered to, but the exact nature of the routing proportions and weightings are of the author's own invention and may differ from the originals.

The simplest algorithm, and most popular amongst the older sediment yield models, is the D8 (deterministic eight-node) routing algorithm. However, in terms of accurately modelling the actual flow network, this is the least satisfactory. The D8 algorithm routes flow from a single cell to only one of eight surrounding cells depending upon the aspect direction. In terms of programming the algorithm, the cells are numbered from 1 to 8, starting at due north (this is illustrated in fig 5.2a). For example if the aspect is 45°, then flow would be directed northeast to the top right (number 2) cell. This method contains obvious inaccuracies; the flow travelling to only one cell will only be reasonable in the instances whereby the aspect direction is a multiple of 45, but in the D8 algorithm all aspect directions between 22.5° and 67.5° will be routed to the number 2 cell (45°) (see figure 5.2b).

Routing to only one downslope cell is not necessarily always logical. Unless a distinct stream channel exists along the pathway indicated from the D8 algorithm, it is reasonable to assume that flow will disperse to all downslope cells not just the one of

steepest descent (as calculated from finite differences), and even in the case of a distinct stream channel, some flow may disperse to other downslope cells. As Gallant and Wilson (2000) comment, this popular algorithm is often criticised because it tends to predict flow in parallel lines along preferred directions that will agree with aspect only when aspect is a multiple of 45° and it cannot model flow dispersion.

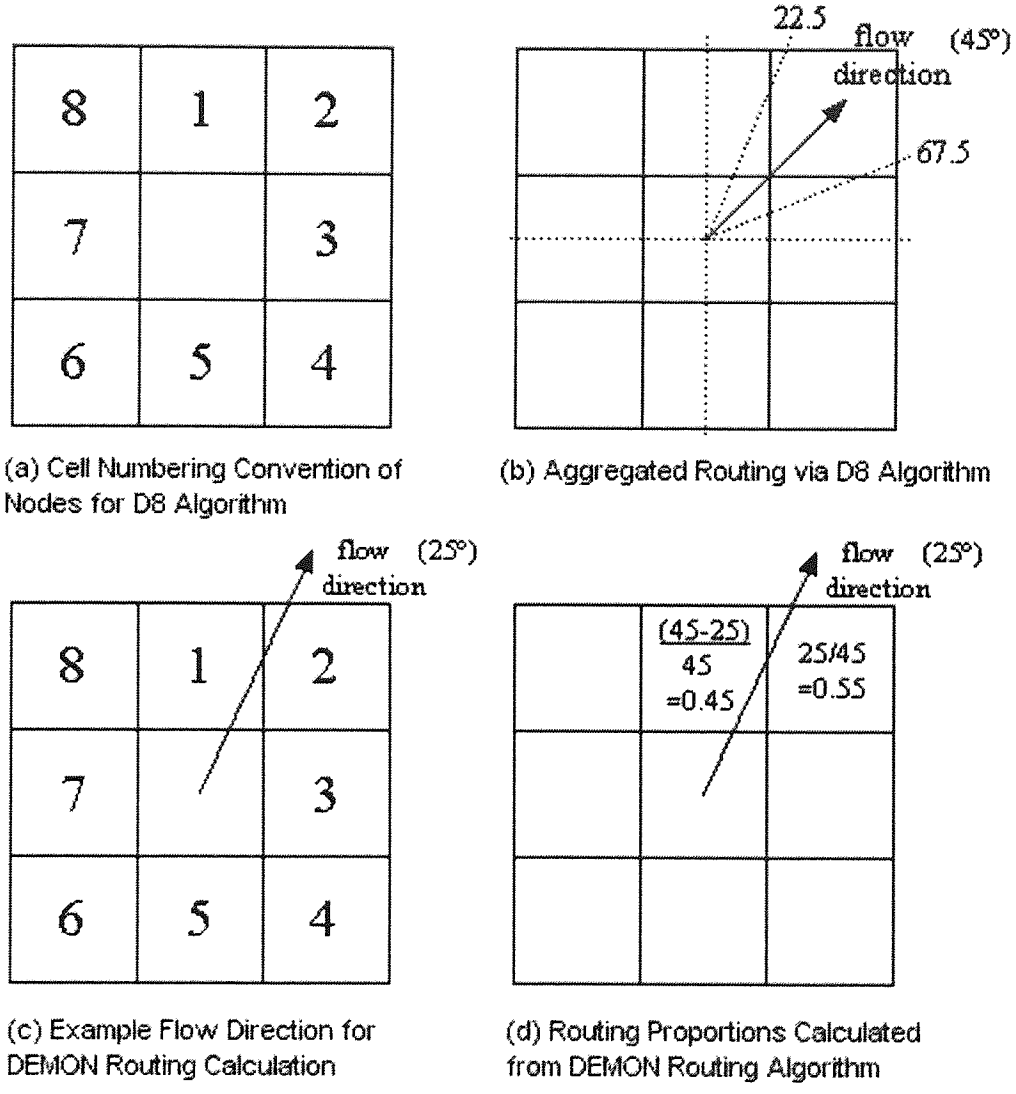

(a) Cell Numbering Convention of Nodes for D8 Algorithm

(b) Aggregated Routing via D8 Algorithm

(c) Example Flow Direction for DEMON Routing Calculation

(d) Routing Proportions Calculated from DEMON Routing Algorithm

Figure 5.2 Flow Routing Algorithms Operational Diagram

The next progression of routing algorithms is again based upon D8 aspect routing but allows flow to pass to the two cells either side of the aspect direction

unless the aspect is a multiple of 45°, in which case the flow is passed to just one cell. This is essentially the basis for the DEMON routing algorithm. According to Gallant and Wilson (2000), DEMON avoids these problems [those experienced with the D8 algorithm] by representing flow in two directions as directed by aspect. This approach permits the representation of varying flow width over nonplanar topography (similar to contour-based models). DEMON is an aspect driven algorithm such that, flow is routed to each of the two cells proportionally depending upon the aspect, the closer the aspect to a multiple of 45°, the more flow will be passed to the cell along that D8 flow line. For example, if the aspect direction is 25°, then 55% of the flow will pass to cell 2 and 45% of the flow will pass to cell 1 (see figs 5.2c and 5.2d).

The third and most advanced progression of routing is to allow flow to pass to multiple nearest neighbours. This is the most realistic method of flow routing as it allows flow to be routed to all cells that are downhill of the source cell as determined by the DEM. The FD8 routing algorithm is one such algorithm that allows flow to be distributed to multiple nearest neighbours in upland areas above defined channels and uses the D8 algorithm below points of channel initiation (Wilson and Gallant, 2000). They go further, explaining that flow in upland areas is assigned to multiple downstream nearest neighbours with these algorithms in TAPES-G using slope weighted methods similar to those of Freeman (1991) and Quinn et al. (1991).

As with the DEMON model the exact weighting proportions are not known and the algorithm has been implemented based on information given in papers. As such, the slope weighting method is the author's choice. The simplest method of slope weighting and the one selected for use in the model is to distribute flows so they are directly proportional to the sum of the downhill slopes. For example, figure 5.3a shows the elevations for a cell and its neighbours. Cells 3, 4 and 5 (using the D8

numbering system, see figure 5.2a), are the three downstream cells. Assuming the cell width is 50m the slope for cells 3 and 5 is the elevation difference divided by the cell width and for cell 4, it is the elevation difference divided by the cell width multiplied by the square root of two. The length to a diagonal cell is longer than the length to an adjacent cell. The slope for each cell is then shown in figure 5.3b. The proportional flow to each cell is then shown in figure 5.3c, the proportions calculated from the slope for each individual cell divided by the sum of the downstream slopes.

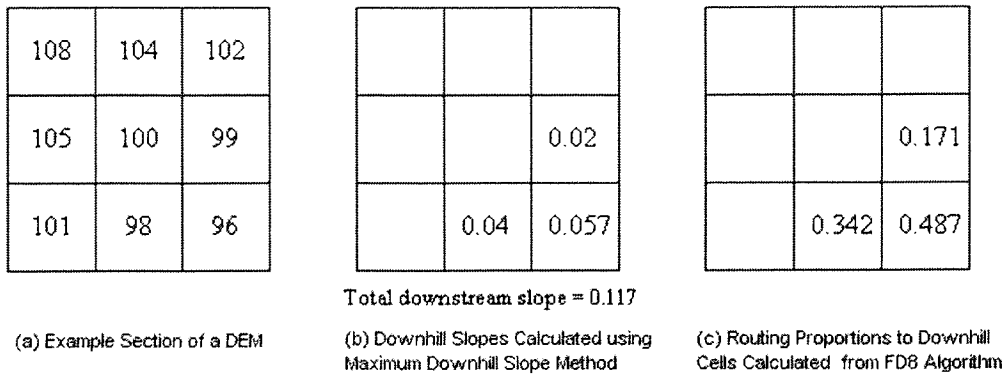

Figure 5.3 Example Calculations for the FD8 Routing Algorithm

5.3.4.2 Depressions and flat areas

Before calculating drainage area, it is also necessary to remove depressions and flat areas from the DEM. Depressions and flat areas are anomalies in the DEM that generally arise due to the resolution used, because elevations are taken only at the centres of the grid cells (e.g. 50m centres) in raster format the exact nature of the land surface can be misrepresented when features that appearing between grid centres are not included. They become a problem when applying the routing algorithms because they prevent the routing algorithm taking flow through those grid cells, thus resulting in inaccurate drainage area estimations. Any grid cell that does not have a nearest

neighbour with an elevation value lower than its own will be either a flat area or depression. For example, figure 5.4a shows a cross section of a land surface demonstrating how flat areas can arise between two cells of a DEM. Points A, B, C and D represent the centres of four consecutive grid cells at which the elevation is recorded; despite the dip in the landscape between points B and C, the elevations at points B and C are both the same, thus a flat area results in the DEM. Figure 5.4b shows an aerial view of a 3x3 section of a DEM with the contours overlaid. The centre cell of the section represents a depression; despite the contours showing that water would exit that grid cell in the bottom right hand corner, the way in which the contours lie with respect to the centres of the grid cells means that the centre square appears to be enclosed by higher ground on all sides. There are some cases where it is not appropriate to fill depressions; Gallant and Wilson (2000) mention sinkholes in karst landscapes as one example.

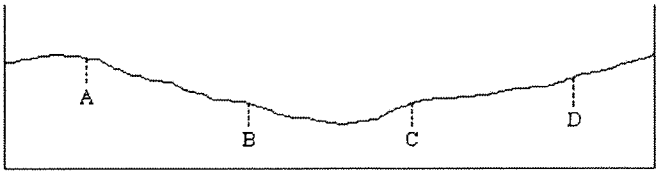

(a) Example of how Flat Areas occur within a Raster DEM. A, B, C & D are cell centres, height at B is the same as the height at C, thus flow will not pass from B to C in Raster representation

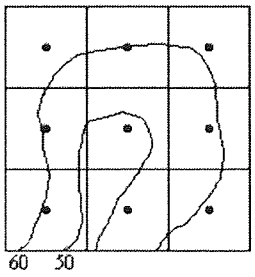

(b) Demonstration of how Landscape Contours may Produce a Depression in a Raster DEM

Figure 5.4 Example of how a Depression forms in a Raster DEM

However, in the case of a landscape with natural ponds and depressions, these still need to be filled to represent effective contributing areas to a downstream cell, as

these would naturally fill with water and excess would add to the contributing flow downstream.

As these depressions and flat areas can distort the results of the drainage area calculations they must be removed before routing algorithms are applied to the DEM. The errors in the DEM are rectified by artificially raising or lowering the elevation of the grid cells within the problem area so that the theoretical flow of water across the landscape is uninterrupted. This can be undertaken, largely dependent upon the practicalities and requirements, by two different methods. The first method is to apply one of the various algorithms (e.g. Jenson & Domingue, 1988) that have been designed to remove the flat areas and depressions. The second method is to use algorithms to identify potential flat areas and depressions and then to correct these manually rather than under the control of an algorithm. The second method allows more user control in correcting these errors and thus allows local knowledge of the area covered by the DEM, and comparisons with 1:50000 maps, to be utilised. There is not necessarily a single solution for correcting these errors with this method; hence alternative solutions can be used. However, the second method is far more time consuming and is therefore not always practical on larger areas of a DEM.

5.3.4.3 Derivation of Drainage area

Drainage areas are derived from the flow routing algorithms by cumulatively summing the number of cells through which flow has been directed. There are at least two methods of calculating the drainage area. The first method is to route flow from primary cells only cumulatively adding the cell area to the total drainage area as it passes over each cell, this total drainage area is added to the value within the cell for each cell crossed. The alternative method to this, which does not require the use of

primary cells, is to route the flow from every cell within the catchment. In this instance, cumulative totals are not used as flow is routed from the start cell to the catchment outlet; for each cell that is crossed between the start cell and the outlet only the cell area is added to the drainage area total. However, as flow is routed from each cell, the same results are achieved as when routing from primary cells.

5.3.5 Accuracy of methods of calculation of topographic attributes

To select the most appropriate method for calculating each of the topographic attributes, advice was taken from various literature sources, as well as direct comparisons of the various methods on the corrected DEM of the experimental catchment in Ghana (see section 7.3).

5.3.5.1 Slope

The method used to calculate slope has been found by some researchers to make a marked difference upon the results of soil erosion estimation. Both Burrough and McDonnell (1998) and Hickey et al (1994) agree that the maximum downward gradient provides more inaccurate estimates of slope than the finite difference method. Gallant and Wilson (2000) note that the D8 method gives slightly smaller average slopes than the finite difference method, because the direction in which the elevation difference is calculated is not always that of the steepest descent. They also go on to say that the finite difference method is preferred because of its greater accuracy. Hickey et al (1994) also discuss the relative accuracies of the slope methods. They made an example comparison between the finite difference and downhill slope methods. Figure 5.5 is taken from Hickey et al (1994) and shows a section of a DEM and slope angles calculated from the two methods. Figure 5.5a

shows the original section of DEM and 5.5b and 5.5c show the results of the two methods. Averages and standard deviations have been calculated for each method and are displayed in table 5.2. From this it can be seen that the maximum downhill slope method gives a higher average slope than the finite difference method. However, this is not necessarily the case as the sample size is very small, if a 7x7 grid or a 3x3 grid had been used instead of a 5x5 grid, steeper or shallower changes in elevation around the edges could easily make such a difference that the effect is reversed. This is demonstrated in figures 5.5d to 5.5f (a 3x3 grid), which also includes estimations for the maximum downward gradient. In this instance, the maximum downhill slope gives a very similar average slope to that of the finite difference method. These results may be different again when considering a whole catchment and have the potential to vary considerably between different catchments.

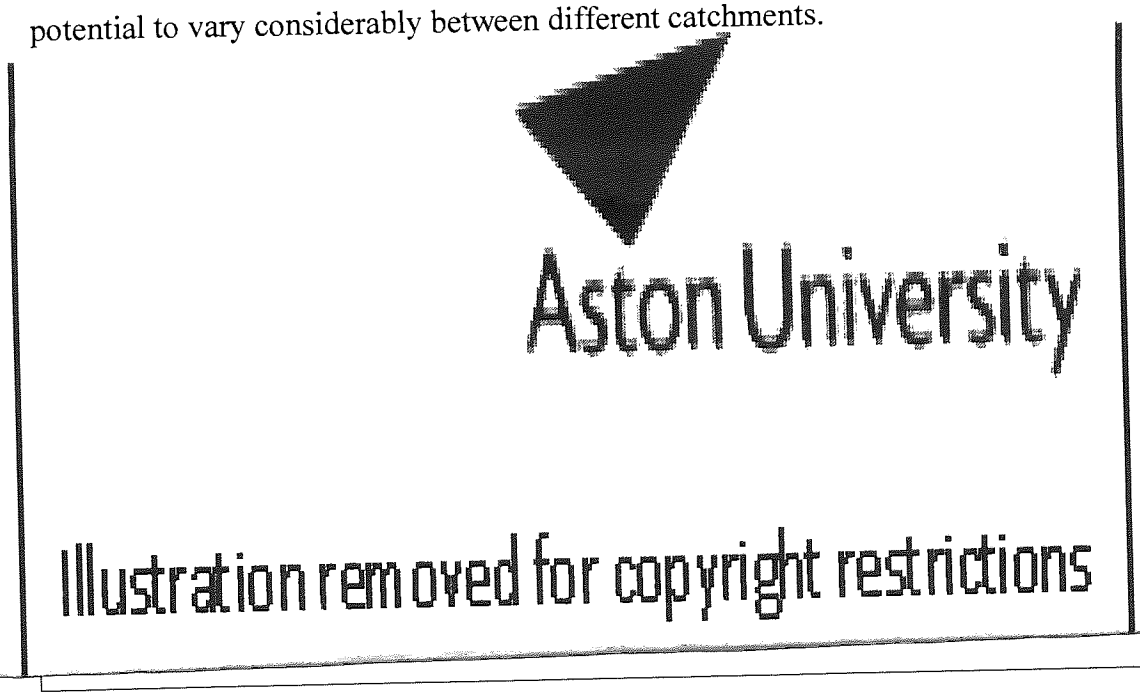

Figure 5.5 Slope Calculation Example (from Hickey et al., 1994)

Slope Prediction Method (diagram no.)	6.5b	6.5c	6.5d	6.5e	6.5f
Average (mean)	46.4	52.7	56.3	56.5	60.6
Standard Deviation	13.3	15.3	7.7	11.9	9.5

Table 5.2 Averages and Standard Deviations for Slope Calculations in Figure 5.5

Srinivasan et al. (1994) also studied the effect of various slope prediction methods upon values of slope and USLE LS factor values. They found that the average slope varied from 2.1% for the maximum downhill slope method to 4.3% for the maximum downward gradient. They concluded that the lower slope values from the maximum downhill slope method gave the best estimates of mean erosion from ten rainfall events.

However, this leads to some contradictions. Although the majority of researchers agree that the maximum downhill slope method under-predicts slope compared to the finite difference method, and that the finite difference method is also more accurate than the maximum downward gradient, not each of these methods is always applicable for sediment yield modelling. This depends upon the way in which routing throughout the catchment is undertaken. When using D8 routing any of the three slope methods discussed may be applied, although when using the maximum downward gradient, care must be taken to check that the direction corresponds with that of the aspect. Likewise, this also applies when using the DEMON routing algorithm. However, when using the FD8 routing algorithm, the only slope calculation method that can be realistically used is the maximum downhill slope method, although instead of using just the maximum slope, all downhill slopes are used as flow is directed to multiple nearest neighbours.

All three methods were applied to the DEM of the experimental catchment in Ghana (see section 7.4). Figures 5.6 to 5.8 show the results for the slopes as calculated for each of the three methods. Table 5.3 shows the mean and standard deviations for each of the methods.

Slope Method	Average (mean)	Standard Deviation
Finite Difference	11.94	8.10
Maximum Downward Gradient	11.82	7.58
Maximum Downhill Slope	6.24	4.73

Table 5.3 Comparison of Statistical Measures for Slope Calculation Methods

From these results, it can be seen that the finite difference and maximum downward gradient methods give very similar results, but the average maximum downhill slope method is approximately half of the other two methods. These results concur with the work by Srinivasan et al. (1994), in that the maximum downhill slope method gives an average slope of approximately half that of the maximum downward gradient across a whole catchment.

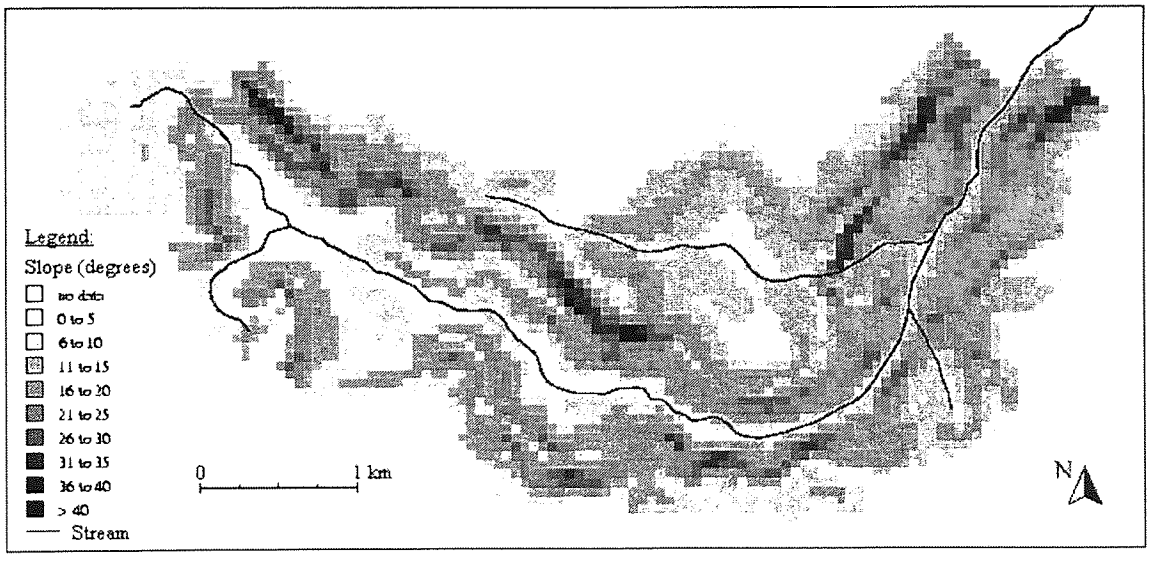

Figure 5.6 Finite Difference Slopes Calculated for Experimental Catchment

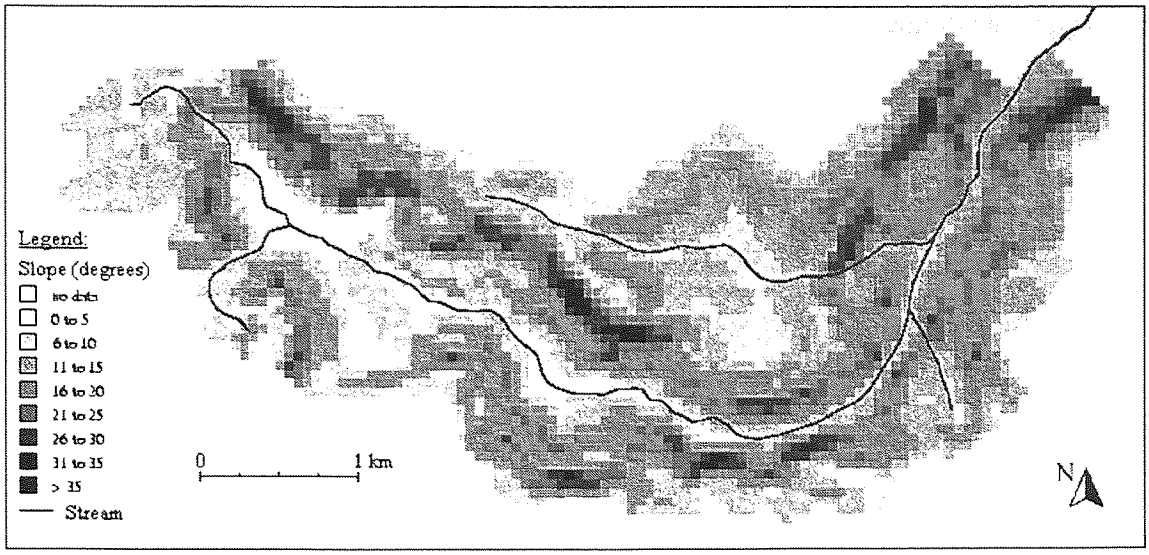

Figure 5.7 Maximum Downward Gradient Slopes Calculated for Experimental Catchment

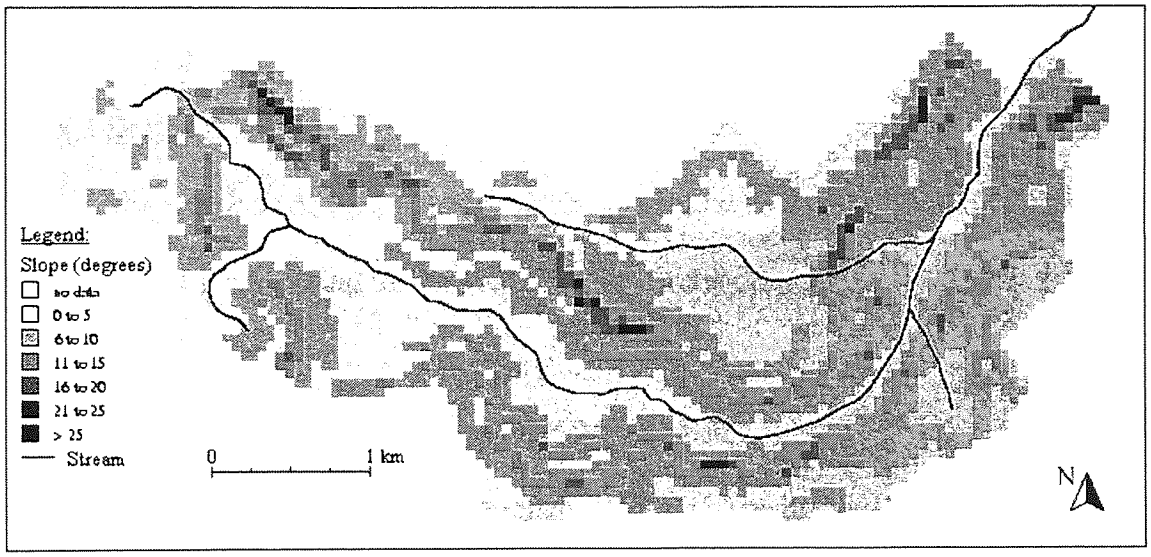

Figure 5.8 Maximum Downhill Slopes Calculated for Experimental Catchment

Although there is a general trend that shows the finite differences method gives slightly higher average slope values than the maximum downward gradient method, which in turn gives much higher values than the maximum downhill slope method, the exact degree of difference between the various methods cannot be determined as this varies from study to study. The degree of difference appears to vary depending upon the topography of the area under observation. A region with

generally steeper slopes tends to produce a greater difference between the average values of different methods than a region where slopes tend to be flatter. The variance of the elevation values also would make a difference to the overall average values calculated from each of the methods.

5.3.5.2 Aspect

Due to the method of aspect calculation being dependent upon the method used to calculate slope (i.e. true aspect when using finite differences and the surrogate aspect, primary flow direction, for maximum downhill D8 slope) a comparison of accuracies of the two methods becomes meaningless.

5.3.5.3 Drainage area

The accuracy of the calculated drainage area relies upon two factors. Firstly, the method of flow routing that is used to calculate the drainage area and secondly the resolution of the DEM.

In terms of the resolution of the DEM, the accuracy of drainage area calculations is directly proportional to the resolution. The higher the resolution the more accurate the calculations are because of more accurate modelling of the terrain surface. The effects of DEM resolution are discussed in more detail in the next section (5.4).

When considering the affect of the routing method used upon the accuracy of the drainage area, the general rule is that the more accurate the routing algorithm at representing the actual flow paths of the water across the land surface then the more accurate the drainage area calculations will be. The D8 routing algorithm is the least accurate of the flow path methods and therefore unsurprisingly gives the least

accurate results. According to Gallant and Wilson (2000), there are several occurrences within a calculated flow path network that are unrealistic and that the D8 algorithm is unable to cope with.

The first problem is that the D8 algorithm is better at mapping flow convergence within a valley than divergence along a ridge. This is a result of the fact that flow into a cell can come from multiple directions, but flow out of a cell is restricted to just one direction. A second problem of this algorithm is a tendency to produce parallel flow lines in preferential directions that are not in agreement with the aspect direction. This is again a result of the flow out of a cell being restricted to just one direction as dictated by the aspect corrected to the nearest multiple of 45°. Another artefact of the D8 algorithm is to produce lines of least contributing area that are not aligned with the catchment boundary as derived from contour lines on a map. However, it is usually not more than one or two cells out of alignment. The final artefact of the algorithm is an occasional lack of convergence of flow lines within ill-defined valleys and wide flat valley bottoms. This can result in disproportionate contributing areas, with cells at edges of valleys having values that are too high and those in the middle of the valley, where the stream actually exists, having values that are too low.

The FD8 rectifies most of the problems created by using the D8 algorithm but instead produces its own. The algorithm provides much more realistic distributions of contributing area in upslope areas, while also eliminating parallel flow paths that occur with the D8 algorithm (Gallant and Wilson, 2000). However, due to the distribution of flow from a cell to multiple nearest neighbours, the FD8 algorithm tends to produce considerable dispersion of flow in wider valley bottoms. This effect

is less noticeable in v-shaped valleys as the cells at the valley bottom tend to have only one downslope nearest neighbour.

The DEMON stream tube method, according to Gallant and Wilson (2000), gives similar or better results when compared with the FD8 routing algorithm It gives smooth variation of contributing area in upslope regions, like the FD8 algorithm, whilst producing well-defined stream channels in valley bottoms, similar to the D8 algorithm. It also produces few artefacts, the most noticeable being a slight preference to the cardinal directions, either north-south or east-west.

The results for the D8 and FD8 routing algorithms calculated for the experimental catchment (see section 7.3) can be seen in figures 5.9 and 5.10.

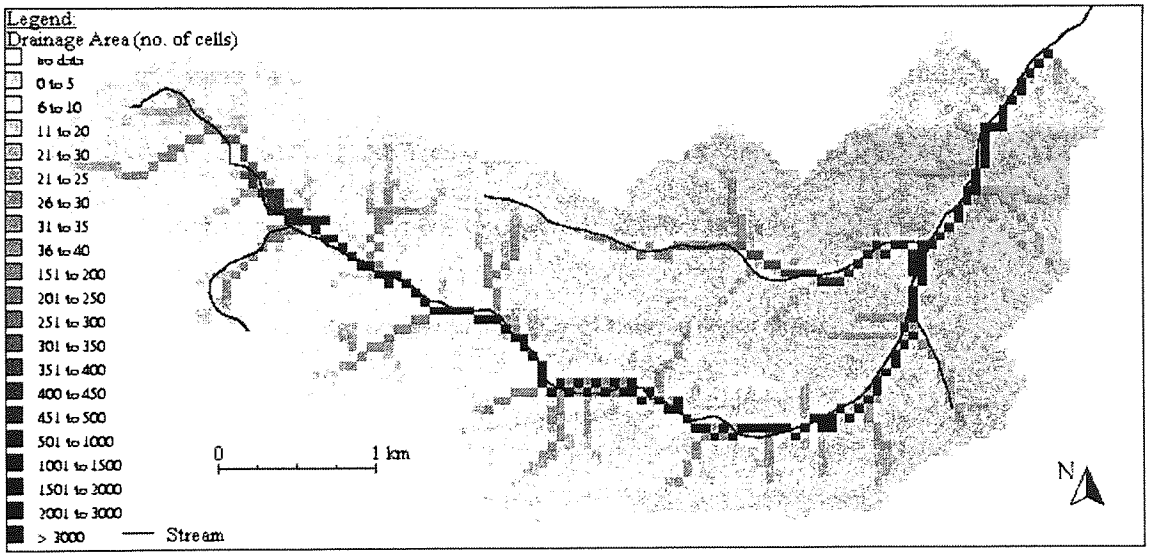

Figure 5.9 Drainage area Calculated using the D8 Algorithm

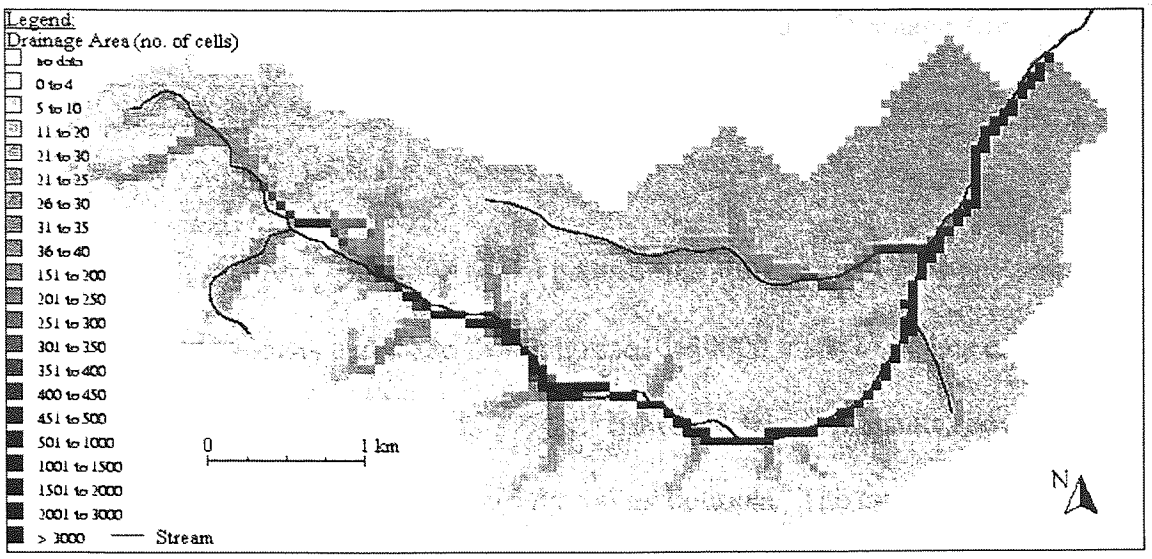

Figure 5.10 Drainage Area Calculated using the FD8 Algorithm

It can be seen by comparing the figures 5.9 and 5.10 that the D8 algorithm concentrates flow into defined stream paths with the areas in between having a lower drainage area than in the FD8 algorithm as expected. This is also demonstrated by the cumulative frequencies of the size of drainage area in each cell (figure 5.11). The average drainage areas per cell for each method are given in Table 5.4

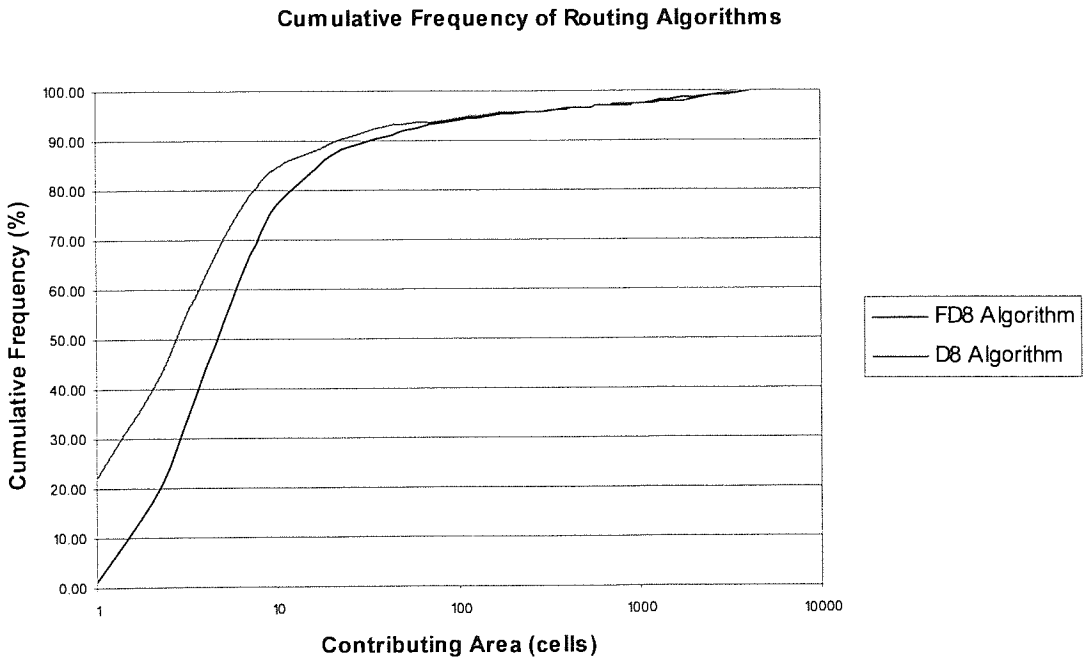

Figure 5.11 Cumulative Frequencies of Drainage Area Calculations

Drainage Area Method	Average Drainage Area
D8	76.94
FD8	71.70

Table 5.4 Average Drainage Area per Cell

Both algorithms model the actual paths of the stream reasonably accurately (marked on both figures and taken from digitised 1:50000 maps of Ghana created for the GERMP project, (Boateng et al., 1998)). However, the FD8 results show the characteristic dispersion of flow within the valley bottoms. The cumulative frequency graph also shows that the D8 algorithm produces more cells that have a drainage area of just one cell.

5.4 Resolution

It is not just the method of calculation that affects the accuracy of topographic attributes. The resolution of the DEM is also very important, especially when utilising slope in erosion parameter estimation.

The resolution of the DEM is the distance between the centres of grid cells in the representation of the DEM. It has already been seen in section 5.3.4.2, that due to the raster representation of a DEM, flat areas and depressions can occur. This will happen even at relatively high resolutions, though at higher resolutions the depressions become shallower as the detail level of features in the landscape are more accurately modelled.

Resolutions used by researchers vary considerably, with higher resolutions of around 30m (e.g. Hickey et al, 1994 and Roslan and Tew, 1997) to very low resolutions of 1km (Smyth and Young, 1998). The resolution that is used depends upon many different factors, which are often contradictory in their requirements. Some parameters are more accurate in high resolution DEM's, others work better

under lower resolutions, thus a balance has to be found that compromises each of the parameters as little as possible.

5.4.1 Resolution as Determined by the DEM

The resolution of any DEM is firstly dictated by the source from which the DEM was derived. This is in recognition of the errors that may exist within the original source and will decide the smallest possible grid size that can be obtained from the source data.

5.4.2 Effects of Resolution on Topographic Attributes

Although the resolution will affect all the topographic attributes, slope is probably the most important and has the greatest influence, especially when taking into account modelling soil loss and calculating source erosion.

With respect to slope, then the higher the resolution the higher the estimate of slope, this applies whichever method of calculating slope is used. Molnar and Julien (1998) found that at coarser grid resolutions, slopes decrease significantly. Thus, for larger grid resolutions the S value in the USLE also decrease and hence estimated erosion will also decrease. Molnar and Julien (1998) also found that in terms of estimated erosion a change in grid size from 30m to 690m resulted in a decrease of maximum estimated erosion from 200 tons $acre^{-1}$ to 30 tons $acre^{-1}$. Although this is a relatively small decrease (grid size increases by 23 times compared to an approximately 6.5 fold decrease in estimated erosion) the rate of decrease in predicted erosion is more significant with smaller changes in grid size, i.e. up to 120m. More importantly, Molnar and Julien also state that USLE is theoretically only applicable at grid sizes less than 1ha. However, they do not give a minimum value under which

USLE is no longer applicable. This has two main implications. Firstly, assuming the maximum theoretical applicable resolution for use of USLE is based upon underestimations of slope leading to underestimations of erosion, then there is possibly a point at which the grid resolution becomes so small that overestimations of slope and thus erosion occur. Secondly, due to the inapplicability of the USLE at resolutions greater than 1ha, then this means that the sediment yield models using USLE to calculate source erosion must also be subject to a maximum grid size of 1ha.

With respect to the first problem, however, very little research has been done with grid sizes smaller than 30m. Cox and Madramootoo (1998) began with a DEM with a grid size of 8.857m, but for the purposes of obtaining USLE estimates at the watershed scale, reduced the resolution to 97.43m by aggregating grid cells.

de Roo et al. (1989) also found significant differences in predicted erosion rates and runoff from the ANSWERS model at different resolutions. They found that in the distributed case (4275 grid units) total runoff was 46% higher, soil loss 36% higher and peak runoff 42% higher than in the lumped case when only 20 grid units were available.

Hickey et al. (1994) provide some discussion on the use of very high resolution DEM's. They actually define a 30m grid size as a typically low resolution and discuss how at these resolutions microfeatures that slow runoff, and therefore erosion, are lost. These discussions are in reference to slope length but are still relevant to the issue of the effects of resolution. Although slope length is neglected in many sediment yield models, runoff is dealt with in other sections in the model, and thus these features that slow runoff would have to be accounted for in the drainage area and routing sections of such a model. Hickey et al. (1994) also observe that at the lower resolutions, LS [from USLE] estimates will be greater than actual values,

which in the absence of the use of slope length within a model, will instead apply to the routing structure of the model.

This results in a currently irresolvable contradiction. In one case, the lower resolutions decrease slope steepness values and thus reduce erosion estimates, whilst at the same time higher resolutions increase runoff quantities, which in turn will raise erosion estimates. However, it is not illogical to assume there will be a grid resolution somewhere in the mid-range that will neutralise the two effects, thus generating realistic estimates of erosion. Based upon the work of most other researchers it appears that a resolution in the range 30-100m provides the necessary balance to reduce the negative effects of the incompletely modelled terrain in a DEM.

5.5 Terrain Modelling, DEM's and GIS

The various principles, equations and methods discussed throughout this chapter can all be very effectively modelled using GIS. There are two basic representations of a DEM using GIS, the TIN (triangular irregular network), a vector based methodology, or the altitude matrix, a grid or raster based representation (see Burrough & McDonnell (1998) for a full discussion). Using a raster based GIS provides the grid basis for all the modelling techniques discussed in the chapter.

5.6 Summary

Modelling scale and resolution both play an important part when considering options and parameters. At different scales, different parameters become dominant factors thus making the parameters in a model that represent those factors more sensitive. Resolution is also important. If it is too large, then key processes at smaller scales may not be included; however, if the resolution is too small, this can lead to

over representation of certain factors, giving results that are much greater than what is happening in reality.

It will also be important to establish the correct methods for representing flow paths within the terrain. The D8 method is probably too simplistic especially when considering the more recent adaptations like the FD8 algorithm, which gives a much more realistic representation of the overland flow. In addition the selection of methods for calculation of slope and aspect needs to be consistent with other parameter estimations elsewhere within a model.

All these methods can be effectively implemented using raster modelling in GIS.

Chapter 6

Application of the USLE for Field Site Identification

6.1 Introduction

The USLE has already been shown to be a useful predictor of soil loss potentials so the next stage of the research was to conduct an analysis of southern Ghana to identify potential field sites. Once potential field sites had been established one or more of these could be selected in which to set up the experimental equipment to collect data for calibration of the sediment yield model. Firstly, however, the USLE parameters had to be assigned to the model.

6.2 Selection of parameter equations and factor values to apply USLE in Ghana

It was shown in chapter 3 that there are many different possible equations for working out the various factors to use with the USLE. This next section discusses the choices made when selecting which equations were to be used to calculate the factor values for Ghana.

The main aim of applying the USLE is to quantify soil loss and thus reduce it if necessary. This achieved by identifying the factors of largest influence and then affecting changes to reduce the impact of these factors. However, before applying the USLE and interpreting the results from any experiments, it is important to recognise the limitations, not only of the equation, but also of the processes it is trying to represent This is especially in terms of how remedial measures can be imposed once an area is identified that may be susceptible to erosion.

The erosivity and quantity of rainfall are outside of the control of humans and so is the erodibility of the soil. This means that the R and K factors are controlled by the natural environment. However, the vegetative cover and management of the area under study, and to some degree the slope length and steepness can be positively affected to reduce erosion. Although the topography of the land cannot be altered drastically, physically changing slope length and angle would be both extremely expensive and time consuming, there are other methods to reduce these affects. Length and steepness of slope can be indirectly reduced by introducing support practice methods such as terracing or contour ploughing, introducing drainage channels and runoff breaks can also help to control rates of erosion. Whilst working within a GIS, utilising a DEM, slope lengths and steepnesses would appear the same when using a sensible scale despite these remedial measures. This is why the P factor is included in the equation, to allow for such practices that reduce erosion. However, it is often assigned a value of one by researchers working in developing countries where there are no such remedial measures.

The LS and C factors are therefore the most important factors within the USLE as they represent the physical properties that are the most changeable. As Renard et al (1994) state, the C factor is perhaps the most important USLE/RUSLE factor because it represents conditions that can most easily be managed to reduce erosion. This can be achieved by increasing the protective cover through either changing the type of vegetation or by growing additional plants between row crops that are traditionally widely spaced. However, as discussed previously it is also one of the hardest to quantify (section 3.4.4). This also applies to the LS factor, it is only appropriate to start remedial measures if the sums are correct first.

6.2.1 R Factor

The R factor was originally designed as an empirical measure to represent the averaged affect of annual rainfall. Therefore, if the R factor is used to initiate soil erosion for a single storm model as opposed to a cumulative annual effect, it is possible to over generalise the erosive power of the rainfall. Also, because the factor is often empirically derived, some equations, such as the Fournier index, also require long datasets before meaningful results can be obtained.

Although many R factor equations are developed for annual rainfall, they can be applied to single storms in certain cases. In single storm modelling, erosion is specified as the detachment of soil particles by rainfall. As this relationship between rainfall amount and erosion has been established to be linear (Nearing, 1997a) then provided an annual equation satisfies that linear relationship it can be substituted within a model that is providing single storm simulations.

Figure 6.1 shows a comparison between the CALSITE rainfall index (Bradbury et al, 1993) (eq. 3.6; a linear relationship) and the rainfall erosivity index used by Kassam et al (1992) in the AEZ Kenya program (eqs. 3.7 and 3.8, a non-linear relationship). The CALSITE model was also developed, and thus the rainfall index derived, for a bimodal sub-tropical rainfall pattern similar to that in Ghana as described in Hens and Boon (1999) . It also has the advantage that it is based on rainfall amount alone; other indices were rejected due to the unavailability of the required site-specific data. Because the CALSITE rainfall index is a linear relationship, then the R factor can be consistent between the annual estimations to be used to identify potential study areas and the R factor which was used in the subsequent single storm model.

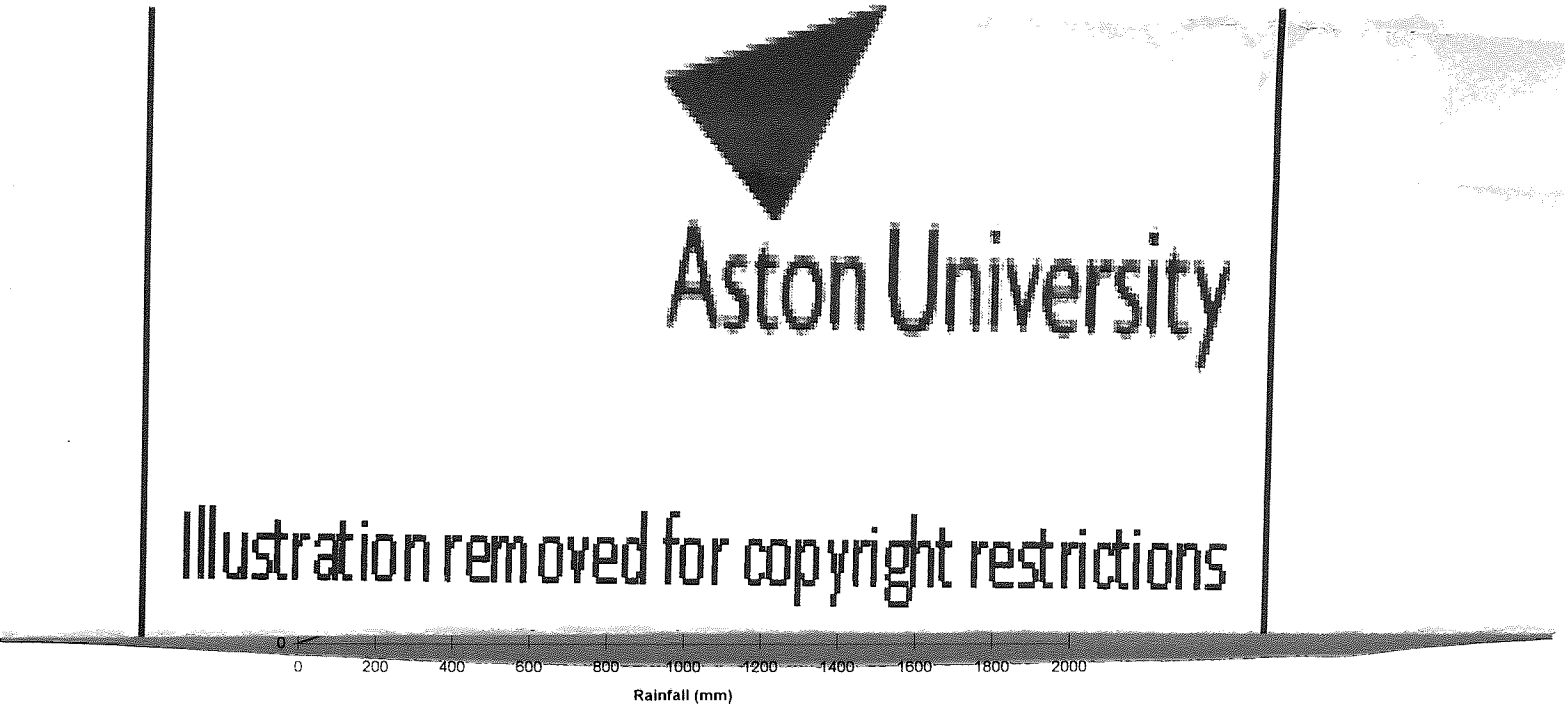

Figure 6.1 Comparison of R Factor Equations

Oduro-Afriyie's (1996) index for Ghana (eq. 3.9) was rejected because it is calculated on an annual basis as a long-term average and is independent of the quantity of rainfall that may fall at a specific time. The requirements for the rainfall erosivity factor for the model to be used in the current research was that it could be adapted to be used on a single storm basis (as well as annual readings for initial USLE estimates) and thus must be based upon rainfall amount.

Therefore, for the following reasons: available data, consistency of linear relationship and lack of applicability of the current Ghanaian rainfall index, the rainfall index developed for the CASLITE model was selected to be used to calculate R factors.

6.2.2 K Factor

The selection of method for calculating the K factor value is the easiest to decide, mainly due to lack of possibilities from which to choose. Use of the nomographs developed by Wischmeier and Smith (1978) are not an option due to their inapplicability outside of the US. Plot data in Ghana is not widely available, thus working out K from the procedure within the USLE, holding other parameters constant is also not feasible. Use of the equation by Renard et al (1991) (eq. 3.11) from the RUSLE was initially ruled out because before the Ghana field study (chapters 7 and 8) no plot data was available to verify the results of the equation.

Therefore, for the initial USLE analysis of Ghana, as sufficient data on the particle size distributions of the soils are not available, K factor values were interpreted from work by Kassam et al (1992) using FAO (1990) documentation to cross reference classification terminology of soil types (Bambury, 1999). Table 6.1 shows the K factors associated with the FAO classification of soil type.

After the field trip to Ghana, some plot data was obtained from Kumasi, which could be used for verification purposes. This meant that the equation developed for the RUSLE (eq. 3.11), which has a wider range of use than the original USLE equation, could now be utilised. The plot data from Kumasi can be used to verify that the equation is valid when applied to Ghanaian soils. The equation is ideal for circumstances where information is not available on aggregate stability and infiltration capacities, and thus erodibility values have to be based upon soil texture information alone, which was available for the soils within the study catchment. Providing plot data could be verified, use of the equation would then allow accurate estimations of K factors for soils within the experimental catchment.

	Sand	Loamy Sand	Sandy Loam	Loam	Clay Loam	Sandy Clay Loam	Sandy Clay	Clay	Silty Clay	Silty Clay Loam	Silty Loam
Acrisol			0.28	0.28	0.18	0.11	0.04	0.04	0.11	0.18	
Alisol			0.28		0.28	0.18	0.11	0.18			
Arenosol	0.18	0.18	0.28		0.18		0.18				
Cambisol			0.28	0.42	0.28	0.18	0.11	0.18	0.28	0.42	
Ferralsol			0.28		0.18	0.18	0.11	0.11	0.11		
Fluvisol		0.28	0.28	0.42	0.28	0.28	0.11	0.18	0.28	0.28	0.6
Gleysol		0.28		0.28		0.18	0.11	0.18	0.28		
Leptosol	0.42	0.42	0.42	0.42	0.28	0.28	0.18	0.28	0.42	0.42	0.6
Lixisol	0.18	0.18	0.18	0.18	0.18	0.18	0.11	0.18	0.28	0.42	
Luvisol			0.18	0.18	0.18	0.18	0.11	0.18	0.28		
Nitisol			0.18					0.28	0.42		
Planosol	0.42	0.42	0.42	0.42	0.28	0.28	0.18	0.18		0.42	
Plinthosl	0.42	0.42	0.42	0.42	0.28	0.28	0.18	0.28	0.42	0.42	0.6
Regosol	0.18		0.28	0.42	0.28	0.18	0.11	0.18			0.8
Solonchak			0.42	0.6	0.42	0.28	0.18	0.28	0.42		0.8
Solonetz	0.28		0.42		0.28	0.28	0.18	0.28			0.6
Vertisol				0.42	0.42	0.42		0.42		0.42	

Table 6.1 FAO (1990) Soil Classifications and Associated K Factors

6.2.3 LS Factor

As has been previously discussed in section 3.4.3, there is much debate about the use of the LS factor and whether the inclusion of slope lengths is appropriate. Figure 6.2 shows the varying slope length curves for differing values of m within equation 3.12 (the metric version has been used for the graph) and figure 6.3 shows the effects of slope length upon inclusion into the LS factor taking slope length to be 200m.

It can be seen from these figures 6.2 and 6.3 that the inclusion of slope length, apart from being contentious, will also have a considerable impact on the resultant estimations of soil erosion. From figure 6.2 it can be seen that the higher the degree of slope and the longer the slope length, the larger the LS factor will be. Figure 6.3 demonstrates how this compares with just the slope steepness factor alone.

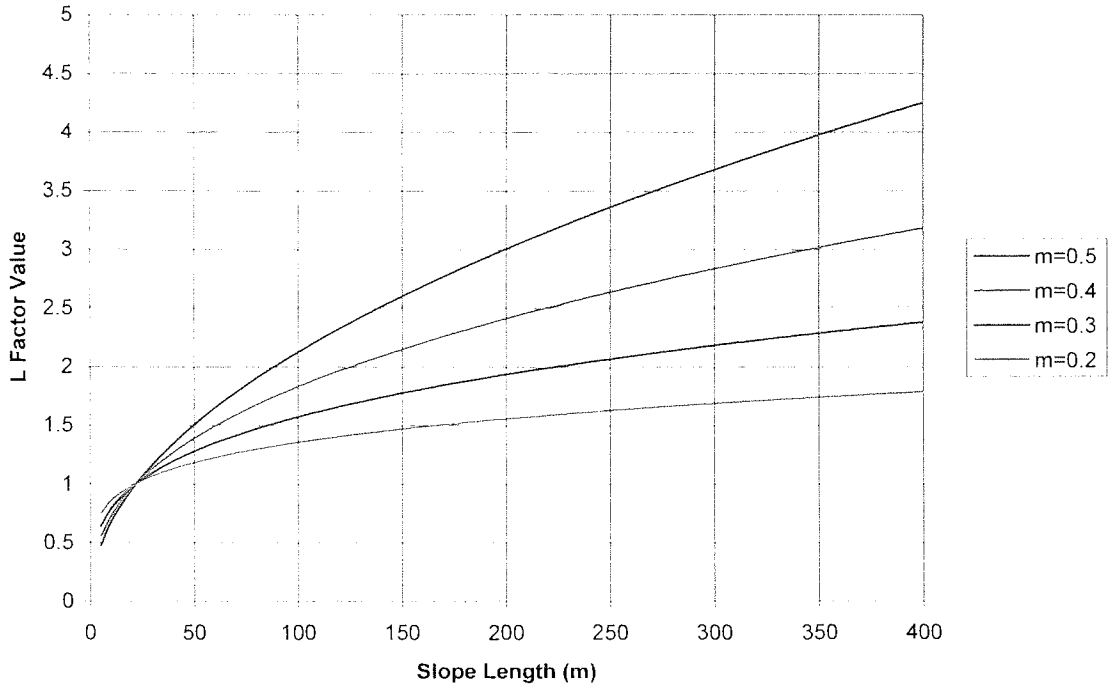

Figure 6.2 Effect of Changing Slope Length on L Factor in Equation 3.12

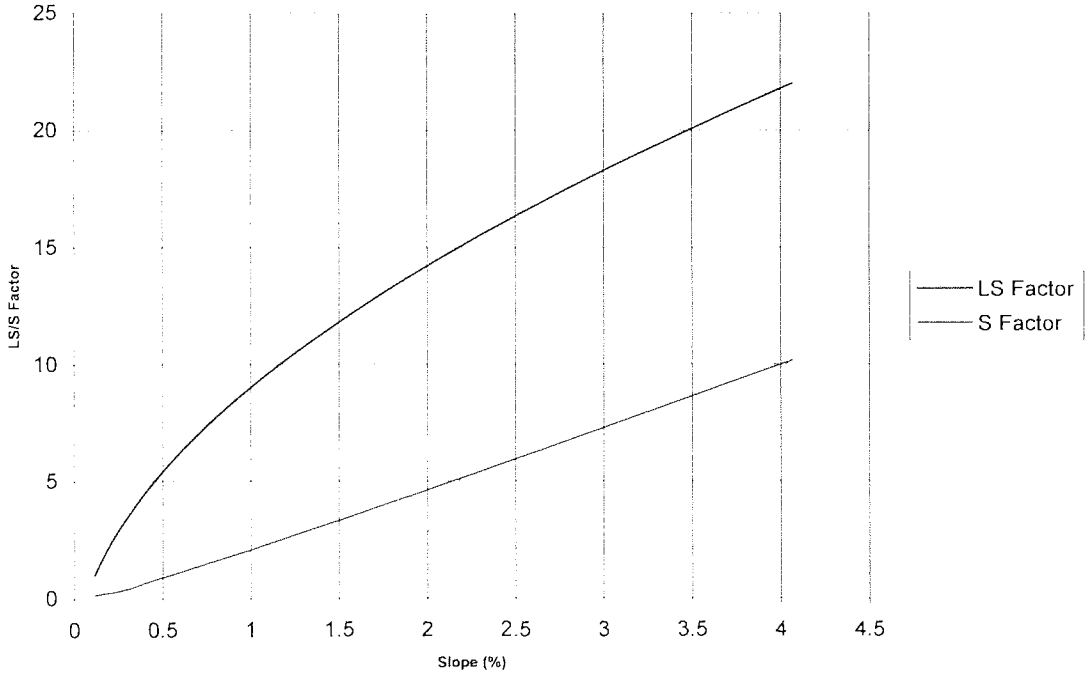

Figure 6.3 Comparisons between LS Factor and S Factor for Equation 3.12

With regards to the inclusion of the slope length, there is no definitive answer. However, the most logical reasoning depends upon the type of modelling that is

undertaken, i.e. soil loss modelling or sediment yield modelling. In the case of soil loss modelling, most notably the USLE, runoff is included within the equation of erosion and thus, as Wischmeier and Smith (1978) have convincingly argued, there is a need to take into account the effects of slope length as an inherent measure of the runoff and its transport capabilities. However, when modelling sediment yield, runoff and transport are dealt with separately, generally either by hydrologic and sediment transport equations or by delivery ratios. In this instance when dealing with the initial erosion of soil particles from the matrix, slope length does not need to be taken into account, and when using equations like the USLE for this purpose, therefore, slope length factors should be neglected. Because the model to be developed was a sediment yield model, it was decided that for this research the LS factor would only take into account slope steepness.

Subsequently, various S factor graphs were produced (see figures 6.4 and 6.5), in all cases separating the S term away from the L term so that comparisons of each equation could be made.

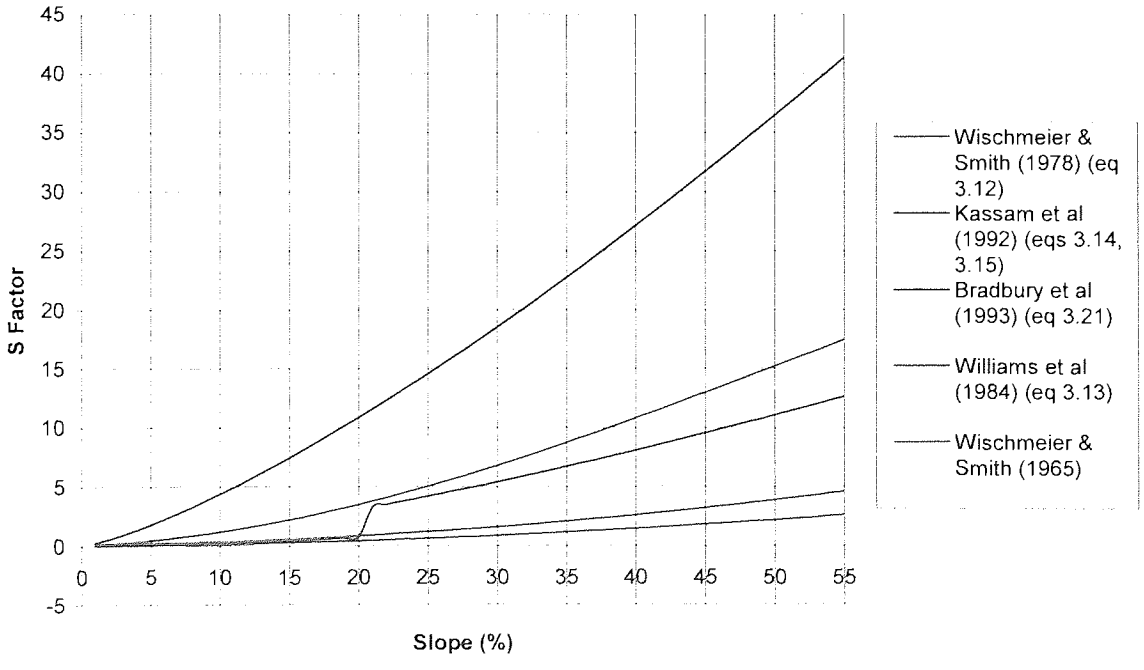

Figure 6.4 Comparisons of S Factor Equations

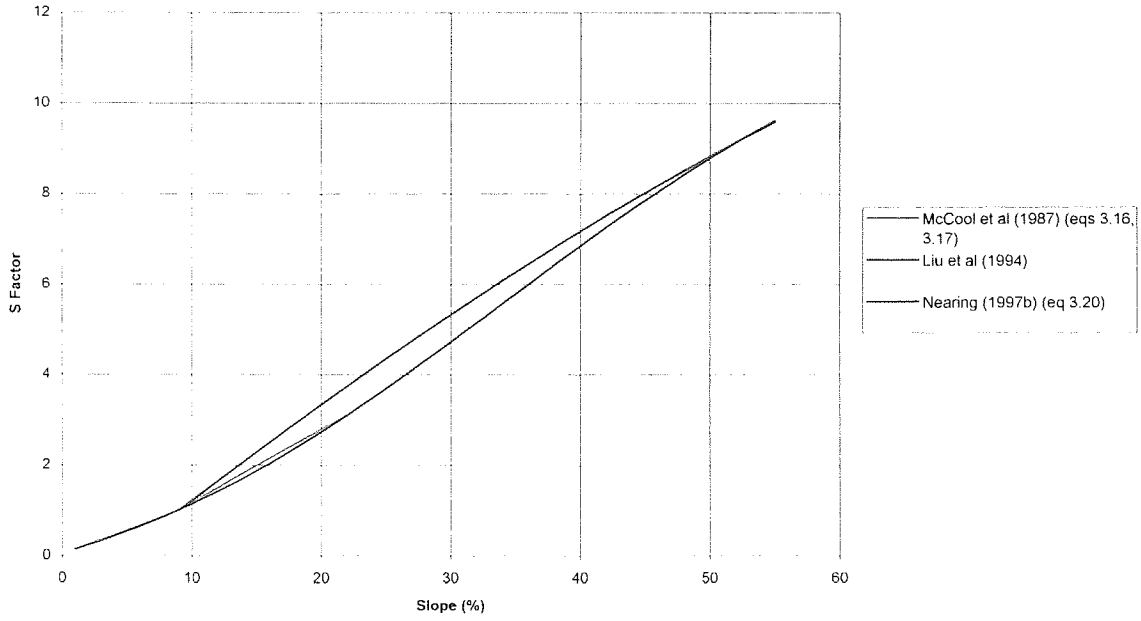

Figure 6.5 Further Comparisons of S Factor Equations

The first equation to be disregarded was the equation developed by Bradbury et al (1993) for the CALSITE model. Despite having been developed specifically as an equation to account for slope only, it predicts much higher values of S than all the other equations. This may be overcompensation because the CALSITE model relies on an S factor alone. However, if this were the case it would still not be applicable as the effects of slope steepness alone are required.

The two Wischmeier and Smith equations (1965 and 1978) were both rejected because of the inapplicability of the USLE in conditions for which it was not designed (see section 3.3). The equation developed by Kassam et al (1992) for the AEZ Kenya report was rejected because of the large kink in the curve where the two different equations overlap. The formula by McCool et al. (1987) was rejected like the Kassam equations because it was a two-part equation; thus creating a discontinuity at the point where the equations met, which whilst not as drastic as that experienced with the Kassam equations is nevertheless noticeable. Liu et al (1994) were disregarded because although the equation was capable of dealing with slopes up to 55%, it has to

be normalised for slopes below 9% otherwise the equation becomes negative below approximately 5%.

This leaves the equation developed by Nearing (1997b) and the one used in the EPIC model. The equation for the EPIC model was based upon the USLE and although it contains a correction factor, it is still too closely related to the original USLE and is likely to carry some of the original problems. Therefore, the selected equation is that developed by Nearing (1997b). This equation (eq 3.20) was developed from a wide variety of sources and is the only one capable of covering a broad range of slopes. It addition, when plotted its graph falls approximately in the middle of all the others (see figure 6.6).

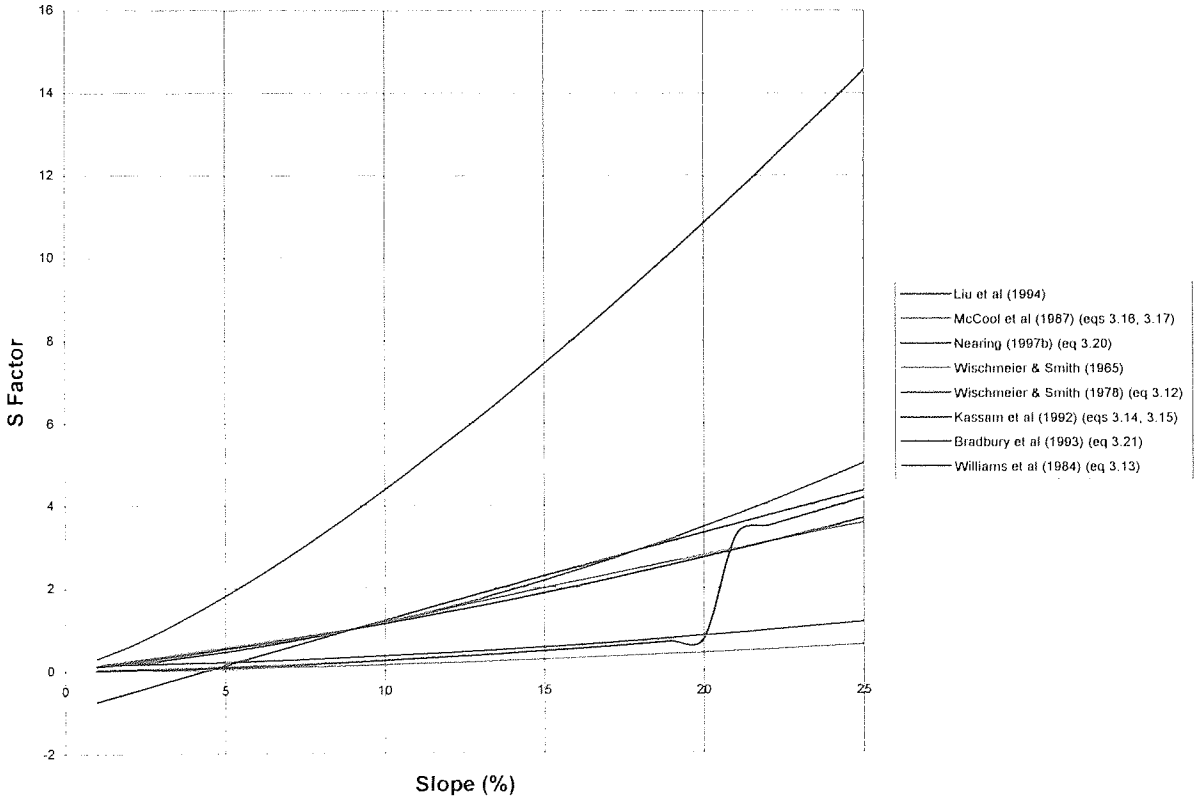

Figure 6.6 Comparisons of all S Factors Considered

In the original USLE work in Ghana (Bambury, 1999), the CALSITE equation was used to calculate the LS factors.

6.2.4 C factor

As previously stated (section 3.4.4), the C factor is one of the hardest factors to define due to the difficulties and expense involved in obtaining the required data. This point is reiterated by Cox and Madramootoo (1998) who intended to use the RUSLE version of the C factor equation (eq. 3.22), but found that it was not possible to determine the magnitude of the various sub-factors from the data available. Their data defined only broad land-use categories that did not provide sufficient information to be able to derive each of the individual sub-factors. To define the sub-factors considerable ground-truthing data is required, which is expensive to gather and over large areas generally impractical. Folly et al. (1996) found that although the sub-factor approach to calculation of C factors is the ideal method, it is not always the most practicable.

Utilising earlier work on the USLE in Ghana (Bambury, 2000) and cross-referencing with C factors in table 6.2, the following C factors were used for the initial USLE analysis of Ghana.

Land Use Category	C Factor
No Data	0
Medium Density Forest	0.004
Fairly Dense Mixed Forest	0.002
Fairly Open Mixed Forest	0.006
Open Scrub	0.014
Agricultural Land	0.38
Bare Land	1

Table 6.2 C Factor Values for Land Use Types (from Bambury, 1999)

6.2.5 P factor

Due to the lack of support practices being utilised by Ghanaian farmers, for the purposes of the analysis, P factor values are taken as 1.0, effectively removing the variable from the equation.

6.3 Application of USLE in Ghana

6.3.1 Creation of factor maps

Maps for the various factors were created for use within the GRASS GIS (GRASS Development Team, 2003) software environment. The four factors and their values described in the previous sections and the brief methodologies in the subsequent sections were revised from initial work done as a final year research project (Bambury, 1999). The main methods used to produce the factor maps were look-up tables and multi-layer analyses as discussed in section 4.4. Look-up tables were used to convert basic data (land-cover, soil type, rainfall surface and topography) into the individual factor maps and then a multi-layer analysis was used to combine these maps into a final USLE estimate.

6.3.1.1 R Factor

The R factor map was created by firstly developing a rainfall surface from the point data of average annual rainfall amounts using a kriging algorithm and then subsequently converting this surface into a GRASS compliant raster format. This rainfall surface was then converted to an R factor map using a look up table (LUT) and the *r.reclass* GRASS command. Rainfall data was provided by the Ghana Meteorological Office.

The R factor map for source erosion calculation for the sediment yield model was created in the same manner, except for the initial rainfall surface where a constant value from the daily rain gauge reading for the catchment was taken.

6.3.1.2 K Factor

The K factor map was derived from soils maps of Ghana that were created for the GERMP project (Boateng et al, 1998). The soils maps were imported into GRASS in raster format and then by using LUTs, soil types were assigned a K factor value by using the *r.reclass* GRASS command.

6.3.1.3 LS Factor

LS factors were created from a DEM of Ghana (again generated for the GERMP project (Boateng et al, 1998)) at 250ft (76.2m) scale using GRASS GIS program modules. For the initial USLE estimations the *r.slope.aspect* module (which utilises the 3x3 neighbourhood method) was used to calculate slopes; these were then converted to LS values using an LUT. For the sediment yield model a self-coded module called *r.max_slope* (which utilises the maximum downhill slope method) was used to obtain slopes, which were again converted to LS values using an LUT.

6.3.1.4 C Factor

The C factor map was derived from land use maps taken from Landsat 5 images that were interpreted and classified for the GERMP project (Boateng et al, 1998). The C factor map was created in GRASS using an LUT and the *r.reclass* command.

6.3.1.5 Production of USLE Maps

Production of the final USLE estimation maps was performed using a multi-layer analysis technique. GRASS provides a module for performing mathematical functions on a combination of layers called *r.mapcalc*. This was used to produce the final USLE estimation map by multiplying corresponding gird cells from each of the four factor maps as defined in the USLE (eq. 3.1).

6.3.2 Results

Figure 6.7 shows the results of the full USLE analysis for the southern region of Ghana (below 7°N). The second figure, 6.8, shows the same area but with the results classified into broader categories, so the high risk areas can be more easily identified. Finally, to simplify the site selection process, a higher threshold value of 100 t/ha/yr was employed. The resulting high risk areas are shown in figure 6.9.

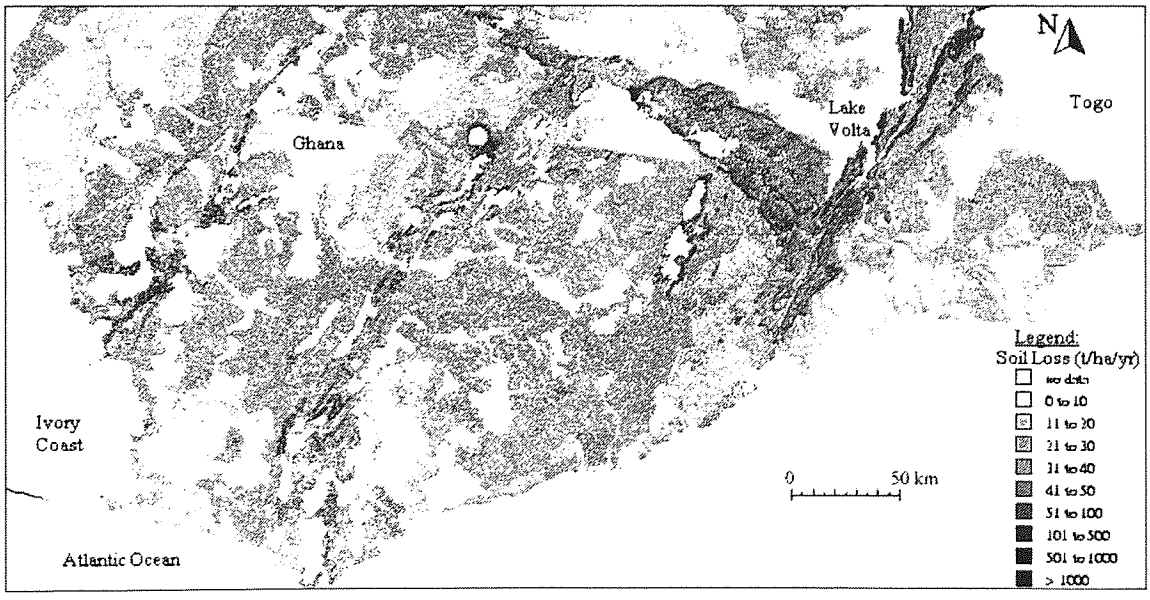

Figure 6.7 Soil Loss (USLE) Calculations for Southern Ghana (Below 7°N)

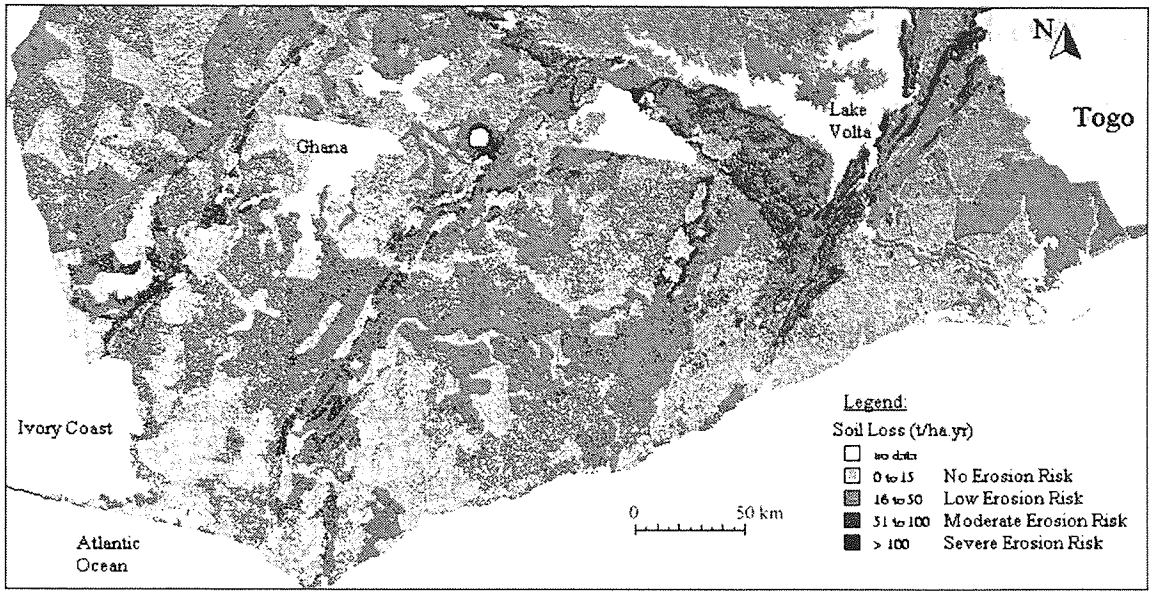

Figure 6.8 Soil Loss (USLE) Calculations Re-Classified into Erosion Risk Categories

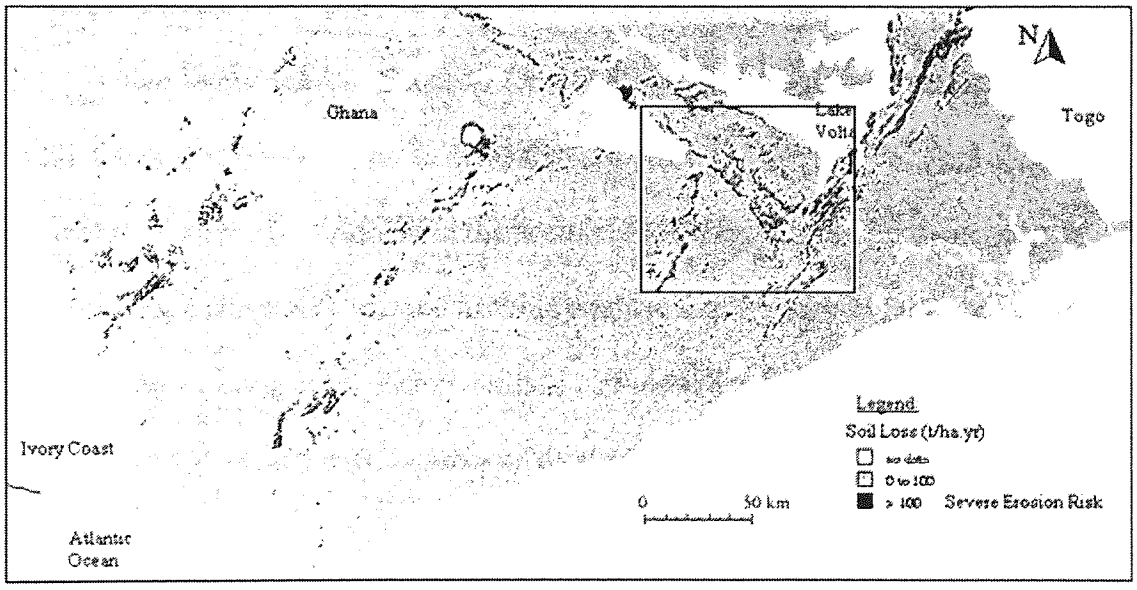

Figure 6.9 Soil Loss (USLE) Calculations Showing High Risk Areas Over 100t/ha/yr (the inner square shows the extent of the enlarged section of figure 6.10)

6.3.3 Interpretation

It can be seen from figure 6.9 that the area to the south of Lake Volta has large areas of high potential erosion risk. The areas of high potential erosion are those in which there is a combination of both high slopes and high C factor values due to agricultural activity.

It should be noted that the LS factors in the initial analysis (section 6.3.2) have been calculated using the finite differences method. There are other methods available for calculating slope that would give differing values of source erosion and these are discussed in section 6.3.1. Each slope method has differing accuracies but their use depends upon the situation and requirements. However, for the purpose of a preliminary, non-definitive, analysis with the USLE, the comparative potential for erosion, i.e. identifying regions of higher possible soil loss, is the required result so the issue of slope is not as important.

Other factor values calculated for this initial analysis of potential soil erosion within Ghana are not the same as those that are utilised when the USLE is used as a calculator of source erosion within the sediment yield model. In the experimental catchment (see chapter 7), ground truthing enabled a more accurate map of land-use to be created, altering the C factors utilised and more detailed analysis of the soil types allowed K factors to be confirmed or altered slightly.

6.4 Selection of Potential Catchments to Study in Ghana

Once the areas of high erosion risk had been established, a small individual catchment had to be selected for the field study. The size of catchment had also to be suitable for modelling as described in sections 5.2 and 5.4. However, it was unwise to decide on a final catchment based upon computer simulations carried out in the UK,

as the factors and conditions of the catchment would only become known once actually out in the field in Ghana. Therefore, a selection of catchments was chosen using the computer simulation for review in the field in Ghana. The final decisions are described in chapter 7.

The first stage of this initial selection process involved the use of the GRASS-GIS software package to delineate catchments based upon the DEM using a function called *r.watershed.* Based upon user defined inputs, such as minimum number of units required to constitute a catchment, the package calculates watershed boundaries and therefore, catchment areas. The data for areas of high erosion risk can then be overlaid to produce a combined map of catchment areas and erosion risk. From this map, a selection of catchments can be selected for suitability analysis in the field within the desired region to the south of Lake Volta.

USLE analysis for the southern half of the country (figure 6.9) shows the areas of high erosion risk to the south of Lake Volta. Figure 6.10 is an enlarged section with individual catchments delineated, onto which has been overlaid the USLE analysis. From this map, those catchments at greatest risk and their locations were identified, which enabled the final selection of the study site as discussed in section 7.2.

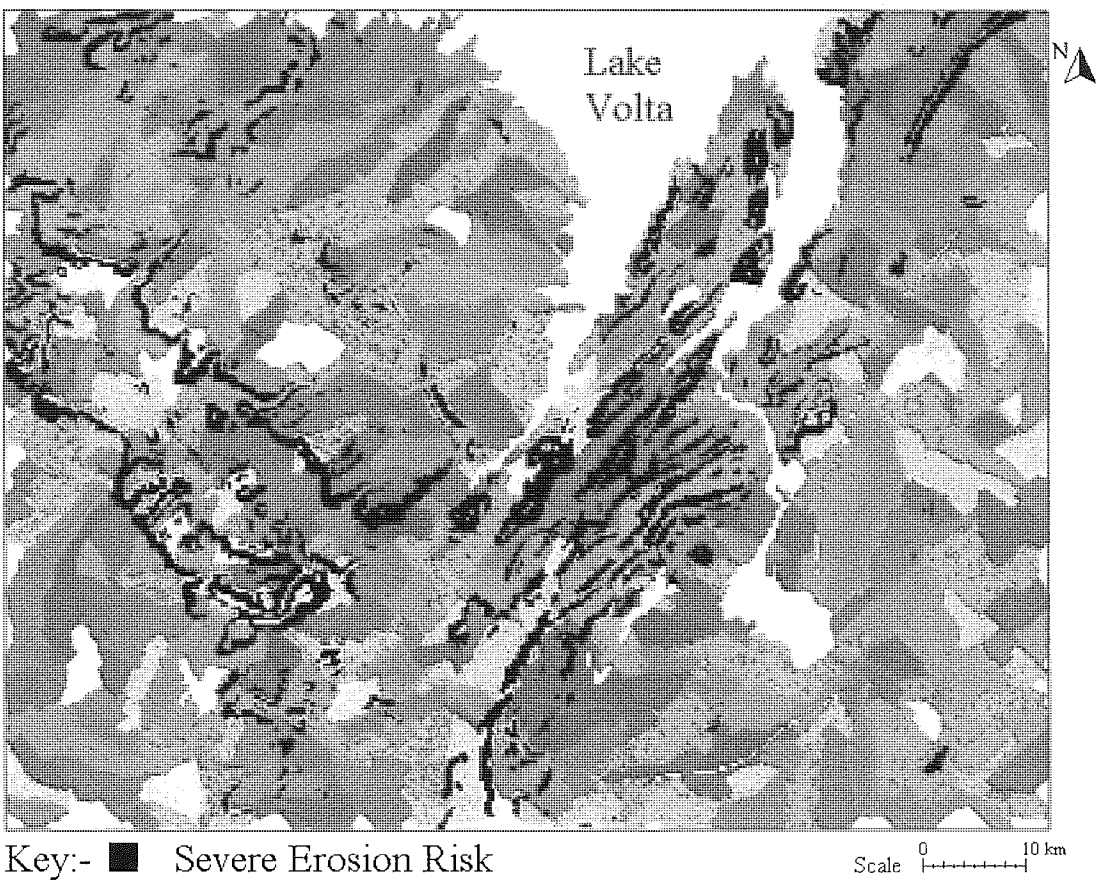

Figure 6.10 Detail Section with Location of Severe Erosion Risk Overlaid on Potential Study Catchments

6.5 Summary

There are various options to choose from when making use of the USLE, many researchers have investigated and used it, presenting future users a wide variety of equations and formulae from which to derive parameter values for their own use. The key to successfully employing the USLE is understanding it's limitations and then selecting the methods that most ideally suit the type of modelling to be undertaken and the conditions to be represented. Several such crucial decisions were discussed in this chapter the outcomes of would be taken forward for use in later stages of the research.

Chapter 7

Experimental Field Exercises within Ghana

7.1 Introduction

A month long field trip to Ghana was undertaken from August to September 2000 to acquire data for purposes of calibration and verification of the model, as well as to become familiar with the systems being modelled. The field trip to Ghana provided an important insight into the mechanisms of the soil erosion problem at the very basic level in the field.

7.2 Selection of Final Catchment

To enable the research objectives to be achieved a small catchment was required, that met the criteria of both accessibility and suitability for analysis. The main criteria for accessibility were: could relevant points in the catchment, i.e. the catchment outlet and various measuring sites, be accessed easily and efficiently, i.e. was the catchment easily traversable; and, was the catchment within travelling distance of a suitable base on a daily basis. The main criteria of suitability for analysis were as follows. Firstly, whether the catchment contained areas of land that were relevant to the study, i.e. areas of farmland and steeply sloped areas of poor soil types. Secondly, was the catchment the right size, approximately 10-30km^2 (see section 5.2 and 5.4), and finally did it contain a stream of sufficient flow regime. Of those identified from the desk study (section 6.4) this would generally be the case because they were some of the main criteria used in the initial USLE identification. However, the area still had to be checked usually in case a catchment that had been identified could have resulted from an anomaly or miscalculation.

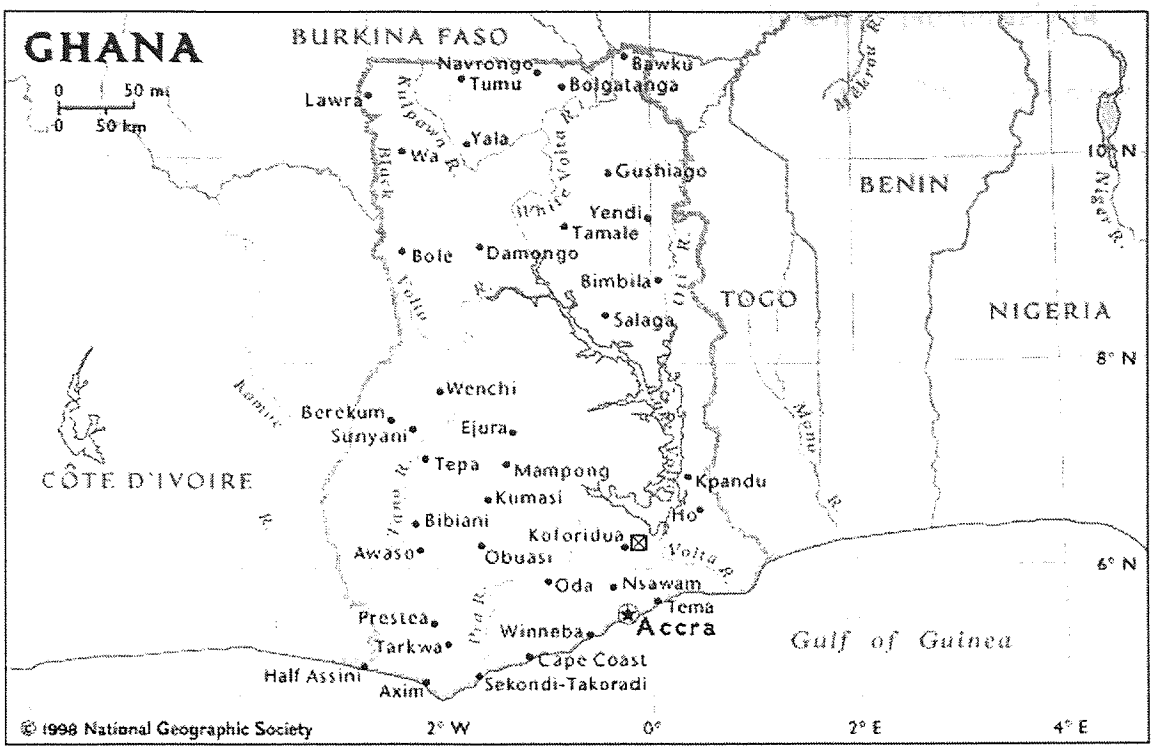

Key:-

⊠ - **Location of Study Catchement**

Figure 7.1 Map of Ghana with the location of the Study Catchment

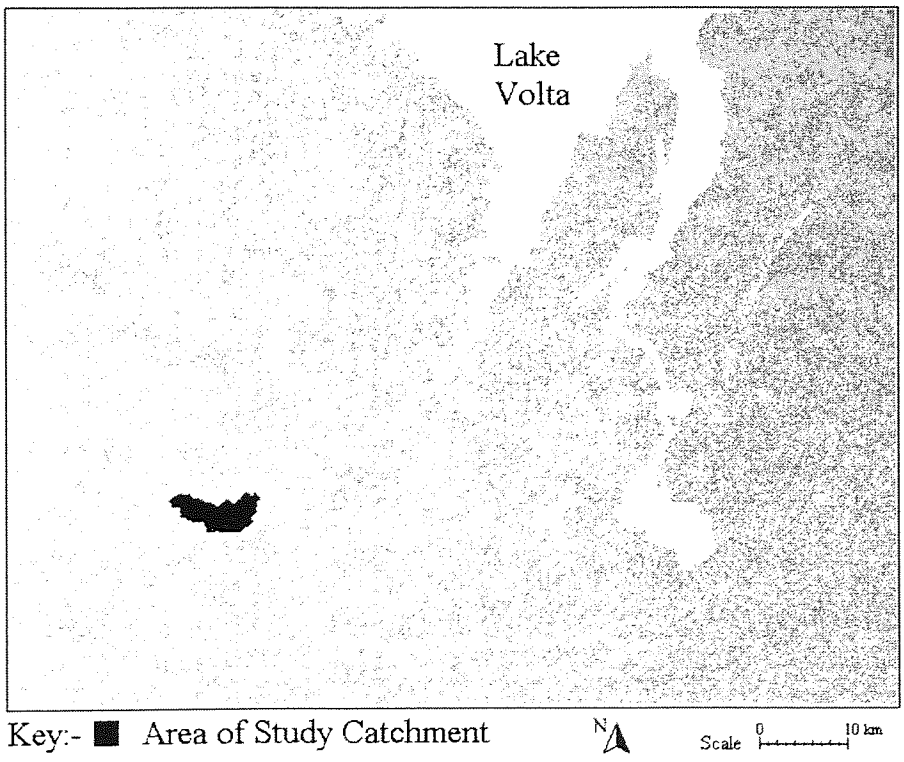

Figure 7.2 Experimental Catchment Highlighted from the Delineated Catchments (figure 6.10)

The site that was finally selected was a small catchment (approximately 14 km^2), see figures 7.1 and 7.2, containing a tributary of the Pompom River, which met most of the criteria reasonably well. The catchment was approximately an hour and a half drive from the base in Accra and could be accessed by main roads to the village of Huhunya, and then by a dirt track to the small village of Akpamu, 5 minutes walk from the catchment outlet. The catchment contained farming on steep slopes and poor soils, a path network enabling relatively easy transit around the catchment and a stream with sufficient flow regime (i.e. non-seasonal). Figure 7.3 shows an enlarged section of a 1:50000 map (Survey of Ghana, First Edition) on which the catchment is highlighted. Figure 7.4 is a further enlarged section of the 1:50000 map (Survey of Ghana, First Edition) which shows the catchment, on which are identified the locations of the photographs of key sites described in the following section.

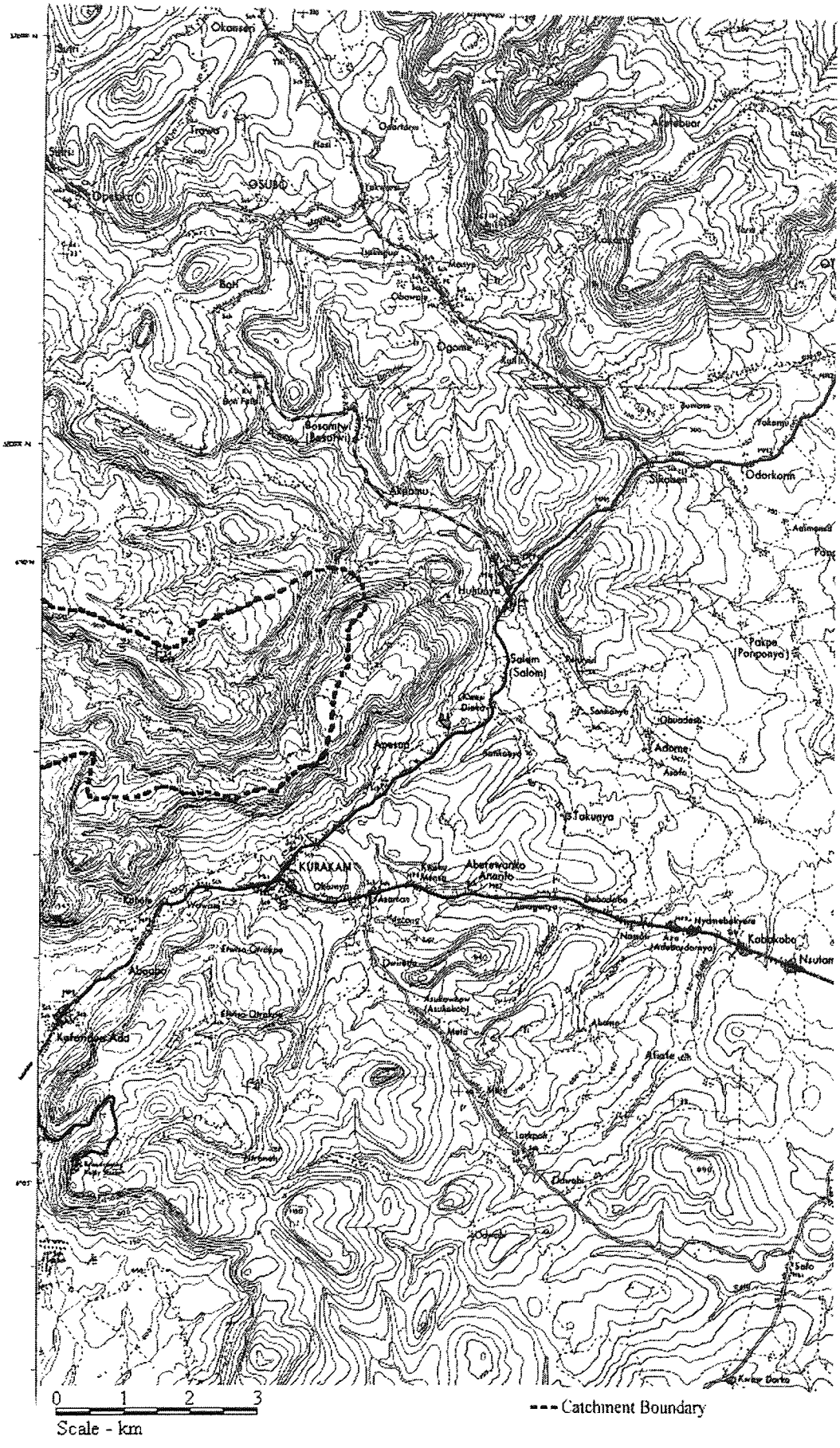

Figure 7.3 A copy of a 1:50000 Map of Area Around Catchment

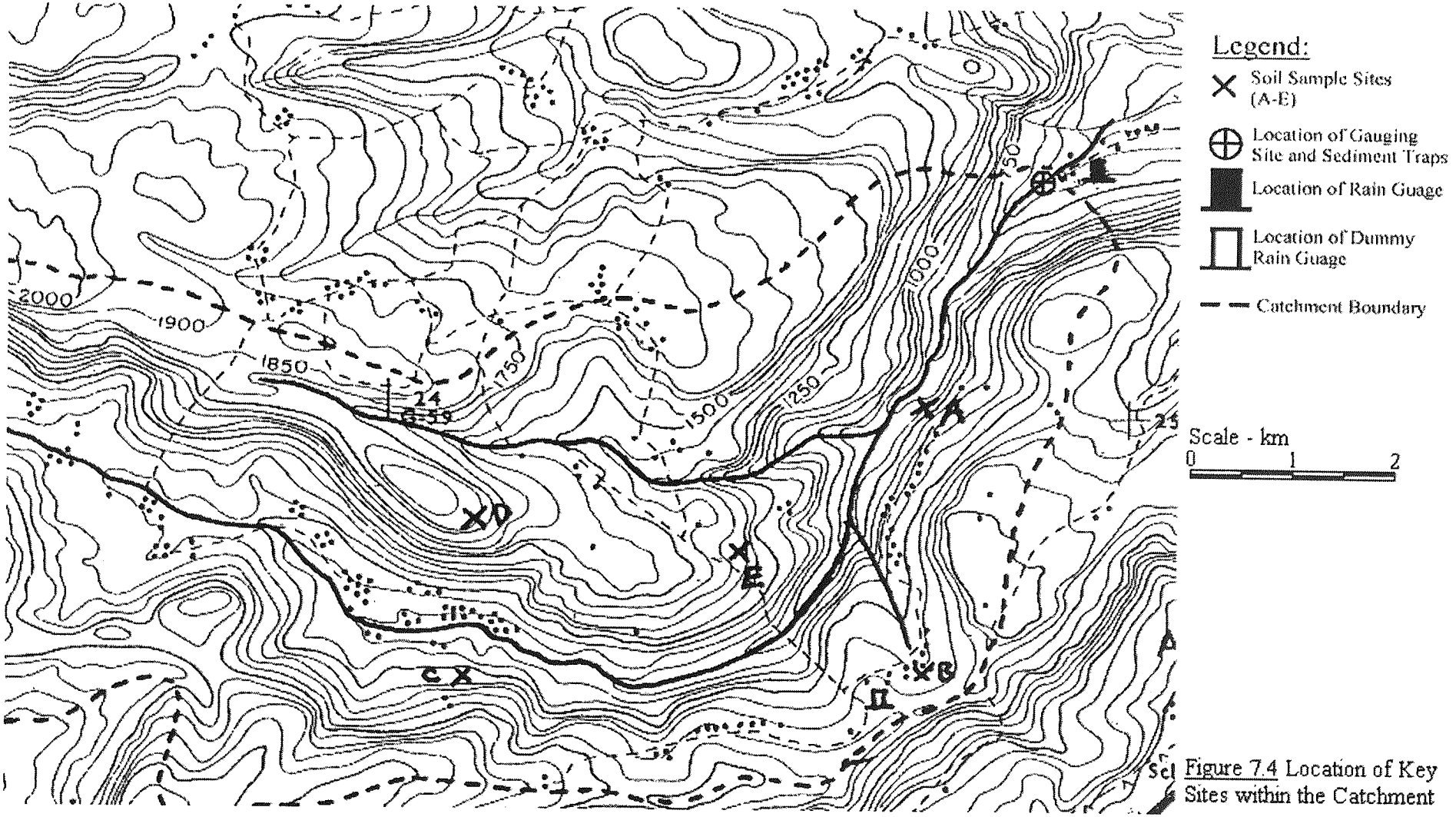

Figure 7.4 Location of Key Sites within the Catchment

7.3 Description of Catchment

During a tour around the selected catchment using local villagers as guides and labourers, the following key features were identified including many examples of extensive erosion and poor farming practices, which can be seen in the following photographs and sketches.

The catchment mainly consists of secondary rainforest, which on the southern side of the tributary is the dominant land cover. Plate 7.1 gives an idea of how dense the jungle actually is. On the northern side of the valley, the western half is again dominated by secondary rainforest whereas the eastern half is more scrubland, which can be seen in plate 7.2. On both sides of the valley however are dotted with settlements and large plots of land (0.5-2 ha) that have been cleared of forest to make way for row crops such as cassava, maize and yams.

Plate 7.1 Example of Natural Forest Vegetation within the Catchment

The catchment is also criss-crossed with a network of paths that the villagers use to navigate the valley, these paths however also play an important part in the erosion process acting as temporary rills and gullies to help take excess rainfall as overland flow down to the main streams.

Plate 7.2 Open Scrub on the North Eastern Section of the Catchment

The villages were mostly situated on the lower slopes of the valley above the level of the flood plain. Some of the villages are very old and give the best and most alarming examples of the extent of the erosion. Figure 7.5 shows a sketch of some buildings in the oldest and main village in the valley (approx. 100 years old according to local knowledge). As figure 7.5 shows, the building has a strange appearance at first glance seeming odd that the entrance door be constructed on the upper storey of a two-storey building. Closer examination of the surrounding area shows channels in the bare soil between the two buildings and the lower storey of each building has a rough eroded appearance whereas the upper storey has a smoother more constructed

feel to it. These observations then lead to the conclusion that the building was originally a single-storey building, what is now the upper storey, and that the lower storey has been created by erosion of the surrounding bare soil within the grounds of the settlement. Further evidence for this theory can be found by observing that some of the other obviously younger buildings are one and a half storeys high and that the trees surrounding the clearing of the settlement have large areas of exposed roots. Figure 7.6 demonstrates the erosion where a deep gully has been scoured out between two huts in the village.

The catchment outlet was situated in an area of dense jungle (figure 7.1) that covers most of the valley bottom in the lower half of the catchment. The site of the experiments was located about 50m from the outlet at a convenient position where there was a relatively straight stretch of water and a slight clearing of the jungle, which coincided with a small cassava field situated in an area of flood plain. The site is marked as location A in figure 7.4. Plates 7.13 to 7.18 (section 7.5) show the site of the experiment and the equipment that was used. Plates 7.3 and 7.4, taken at the experimental site, are interesting as ripple and dune patterns can be seen on the riverbed. This implies that the riverbed is constantly moving, a fact verified by the bed-load measurements, but it also demonstrates that a large proportion of the eroded material was transported as bed-load, presumably by the action of saltation.

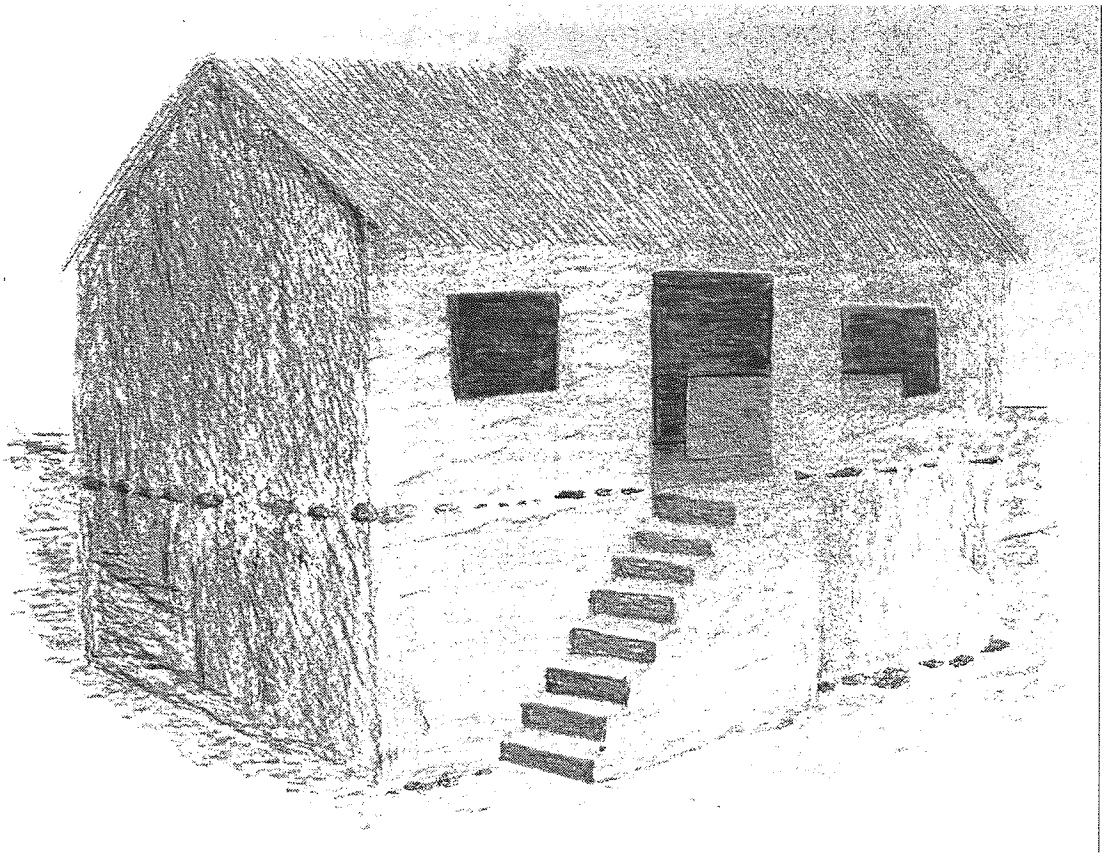

Figure 7.5 Sketch of an Old Building within the Village

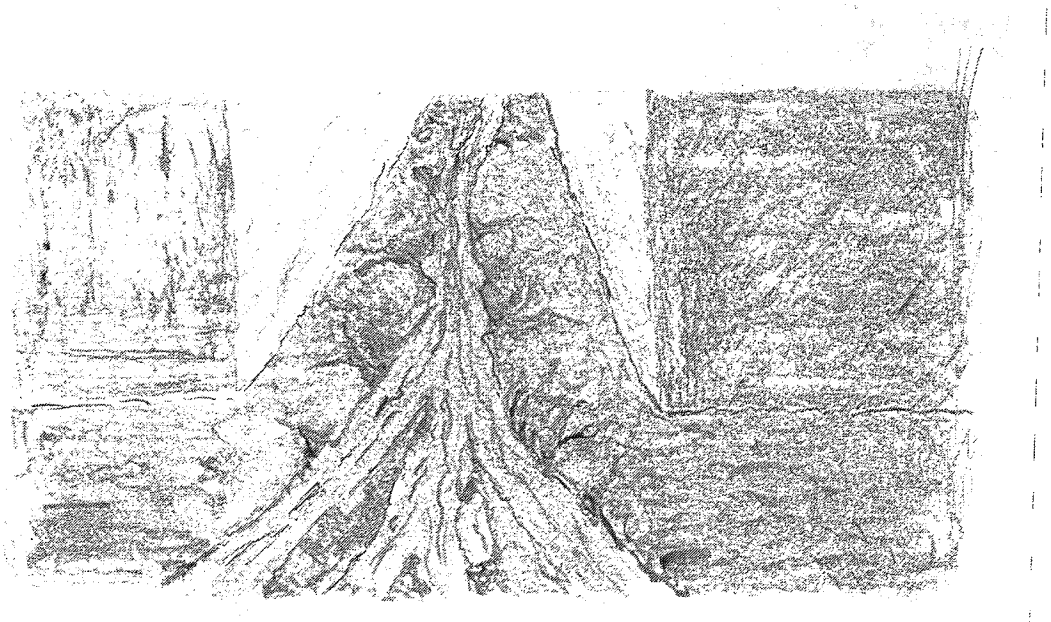

Figure 7.6 Sketch of Erosion between Buildings in the Village

Plate 7.3 Dune Formations on the Sandy River Bed

Plate 7.4 Further Examples of Dune Formations on the River Bed

The main village is then situated about 250 metres south-west along the valley from location A (figure 7.4). Beyond the village, the first of the larger plots can be seen at the path side. This has the consequence that as well as the paths acting as temporary rills the fields drain directly onto the paths exacerbating the situation and increasing the potential for the transport of eroded soil.

Proceeding around the southern side of the valley towards location B the first point to note is demonstrated in plate 7.5. The photo shows an area that has recently been cleared to make way for crops. The steepness of the slope can be clearly seen by comparing the lie of the land with the trees and the people walking along on a pathway at the far right of the photo. A rill or gully can also be seen running down the middle of the field just below the arrow showing direction of flow.

Plate 7.5 Steeply Sloping Land Recently Cleared Vegetation for Cultivation

The next photo shows the location of site B, plate 7.6. The location is in the middle of a maize plot. Again, the steep slopes of the valley can be seen, by comparison with the vertical stems of the maize.

Plate 7.6 Location of Site B in a Steep Sloped Maize Plot

Traversing between sites B and C the extent to which the gullies can develop can be seen in plate 7.7. The gully is approximately 300mm deep and 600mm wide and shows how extensive erosion can be when sloped plots are used. The plot shown is especially vulnerable because the photo was taken in early September at the start of the rainy season and the plot shown was bare.

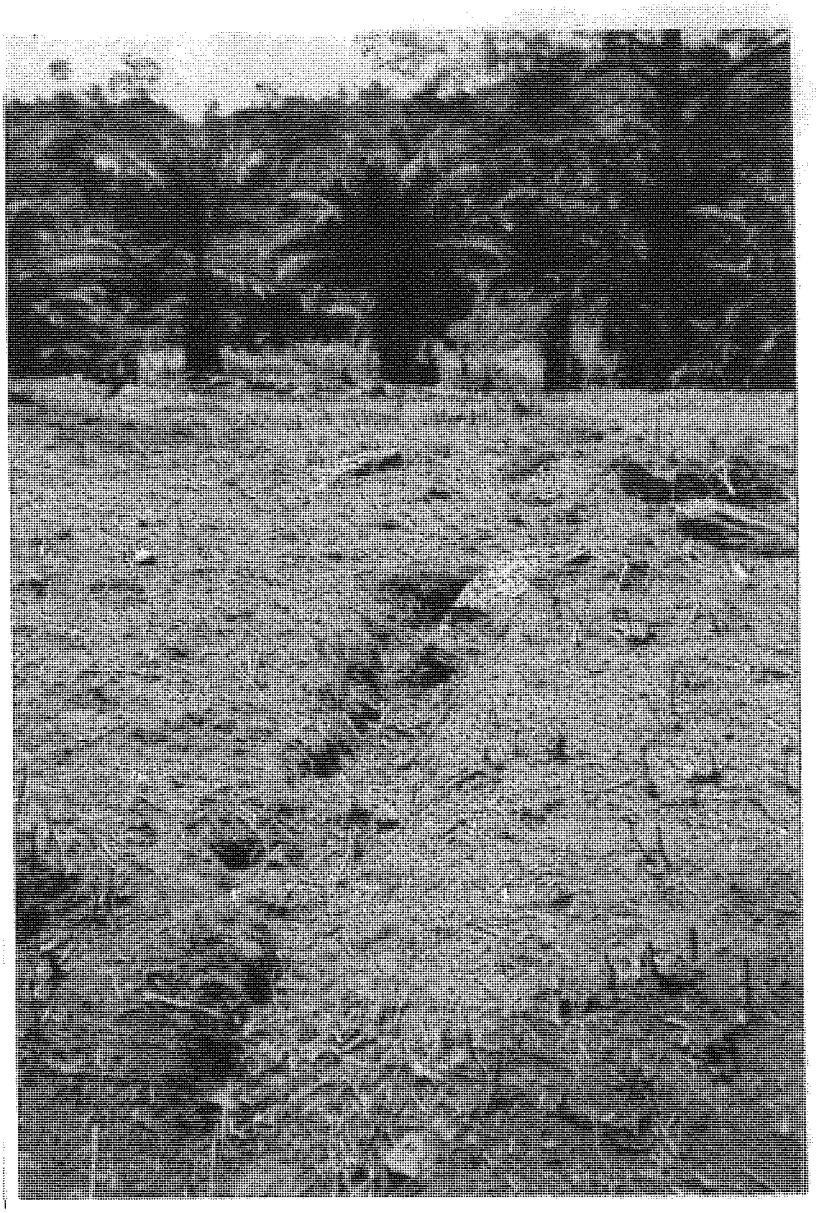

Plate 7.7 Example of Severe Gully Erosion in the Middle of an Agricultural Plot

Just further up the path from the exposed gully in plate 7.7 can be seen a good example of how the network of paths acts as a gully system for the draining water of the valley. Plate 7.8 shows the low point of a pathway, the path rising from the middle to the left and right of the photo. Here the runoff water has cut a channel out of the path from the low point to further its progress downslope.

Plate 7.8 Pathway Acting as a Drainage Gully, the Gully branches downhill upwards in the centre of the photograph

A further example of the paths/gullies through the valley can be seen near location C, seen here in plate 7.9. The pathway is again acting as a temporary channel, which is shown by the lighter material that has been deposited in the pathway by the runoff. The material in the bottom of the pathway is a light orange coloured fine sand, very similar to the material caught in the bed load traps in the stream. Another example of this can be seen at location D, plate 7.10. Here again the lighter sandy material can be seen in the bottom of the pathway. It can also be noted from this photo the steepness of the slope on which the cassava is being grown and the spacing of the cassava plants leaving the soil vulnerable to intense rainstorms. Again, it can be seen how close the pathway is to the edge of the plot with very little vegetation in between allowing soil to be washed directly into the 'gully'.

Plate 7.9 A Pathway acting as a Rill or Gully

Plate 7.10 A Steep Sloped Cassava Plot

It is also demonstrated in plate 7.10 how plots are not protected by any sort of runoff boundaries, thus increasing the erosion risk. The next photo, plate 7.11, shows

the location of site E within the middle of a cassava plot. This also demonstrates the large amount of space and exposed earth between each plant. The final photo, plate 7.12, shows the location of the rain gauge, which is also shown on the 1:50000 map as just outside the head of the valley.

Plate 7.11 Location of Site E

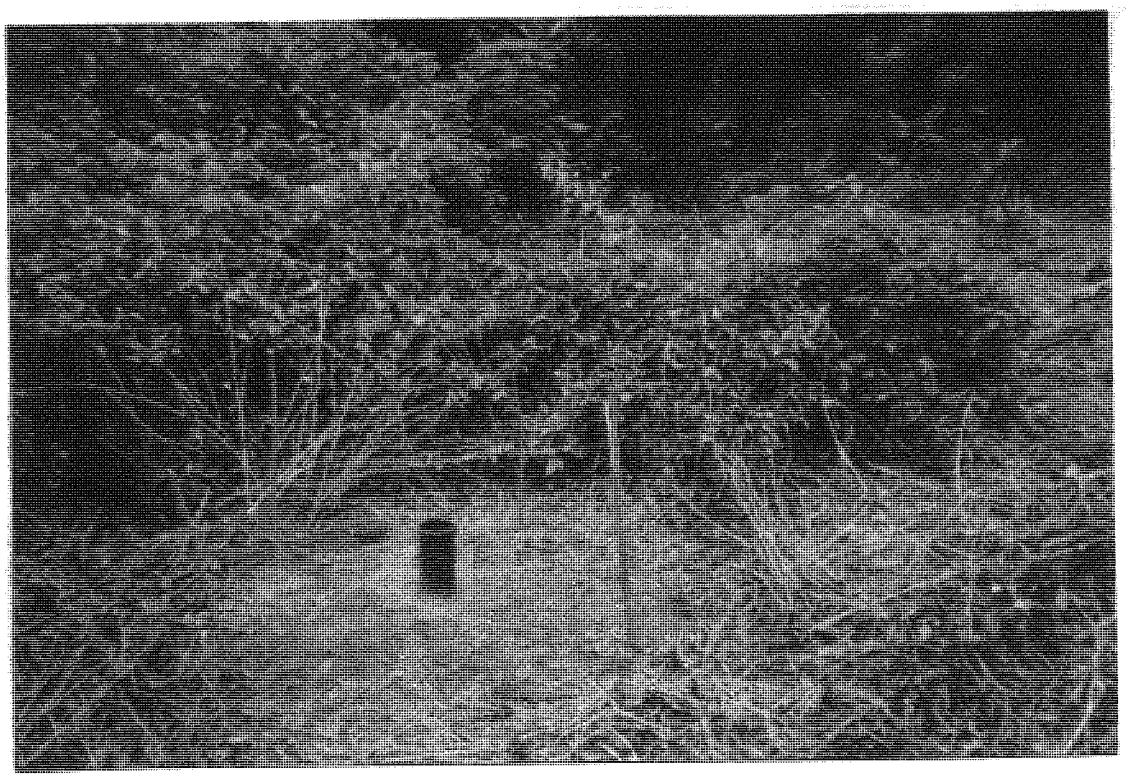

Plate 7.12 Location of Rain Gauge

A brief unpublished written report (section 7.4) of the area was also supplied by Mr Timothy Ayamga, a soil scientist working with the SRI (Soil Research Institute) based in Accra, who was assisting with the fieldwork and provided substantial local knowledge enabling many areas to be resolved quickly.

7.4 SRI Report (Ayamga, 2000, unpublished)

7.4.1 Geology and Soils of the Study Area

7.4.1.1 Geology

The geology of the study area falls under the Togo Formation. The Togo rocks are chiefly sandstones, quartzites, quartz and Sericite schists (McCallien and Burke, 1957).

7.4.1.2 Geomorphology, Relief and Drainage

A close examination of the study area revealed that very old rocks in the past have been lifted up and worn down several times and as a result, the relief and soils are inherited from previous cycles of erosion.

The relief of the study area can be described as high land to steeply dissected, with slopes of greater than 30%.

The study area is drained by two tributaries of the Pompom River. One [the main stream that runs the length of the catchment west to east, see figure 7.4] is seasonal while the other flows through out the year.

7.4.1.3 Vegetation

The vegetation of the study area may be described broadly, as degraded semi-deciduous forest zone.

Scattered patches of secondary or broken forest are present but most of the larger trees among which are Triplochinton Scleroxylon (Wawa), Antiaris Africana (Kyenkyen) and Ceiba Pentandra (Oyina) are now few, occurring as scattered emergence. The rest of the land is under food crops or young forest re-growth.

7.4.1.4 Agriculture and Land Use

Clearings are made through out the main and minor dry season on all sites ranging from summits to very steep sided upper and lower slopes.

Food crops grown in the area include cassava, maize, plantain, cocoyams, yams and vegetables. Cash crops grown include cocoa, oil palm and citrus.

7.4.1.5 Soils

Soil types encountered in the study fall under Fete-Bediesi soil association. The soils of this association are derived from sandstones of the Togo rocks, and are mostly piedmont drifts. The sandstone gives rise on weathering to very deep, sandy loams and sandy clay loams, which are normally free from concretions, gravels and stones.

7.4.1.6 Descriptions of the Soils

7.4.1.6.1 Sutawa Series (Gleyic Arenosols, FAO 1990)

These soils comprise deep, moderately well drained loamy sands occurring on middle to lower slopes sites.

The profile is made up of 0-20cm of dark brown (10YR3/3), loamy sands overlying from 20-55cm of brown (10YR 5/3)) loamy sand. The above layer grades into 55-125cm of strong brown (7.5YR 5/6) and yellowish brown (7.5YR 5/8) sandy loam to sandy clay loam.

7.4.1.6.2 Bejua Series

Bejua soils are very deep (>200 cm), poor to very poorly drained, transported alluvia, which are found on lower slopes and valley bottom sites.

The soil is made up of 0-10cm of dark greyish brown (10YR 4/2), loamy fine sand overlying, from 10-56cm, greyish brown (10YR 5/2) to pale brown (10YR 5/1) mottled yellowish brown (10YR 5/8), sandy loam. This layer grades into 56-125cm of pale brown (10YR 5/1) and whitish grey (10YR 7/2) sand with yellow mottles.

7.4.1.6.3 Fete Series (Lithic Leptosols, FAO 1990)

The series comprise excessively drained brashy soils developed on steep upper slopes over quartzite and sandstone of the Togo range.

The profile consists of a very shallow, sandy, humus topsoil (0-8cm) containing pieces of rock, merging into pale grey-brown to pale yellowish brown (8-12cm), loamy sand containing abundant pieces of rock. They occur among rock out crops.

The Fete series is similar in morphological formation to type 2B, (Nsuta village).

7.4.1.6.4 Bediesi Series (Haplic Nitisols, FAO 1990)

Bediesi soils are deep to very deep (>100cm), well-drained, non-gravely sandy loam to sandy clay loam, occurring at summits, and upper and middle slope sites.

The profile consists of about 0-20cm of Dark brown (7.5YR ¾), sandy loam, grading into 20-50cm of strong brown (7.5YR 5/8) sandy loam. The layer overlies reddish brown (2.5 YR 3/1), sandy loam grading into 80-125cm of red (2.5YR 5/8) sandy clay loam.

7.5 Experimental Sites

There were several experimental sites around the catchment for each of the different types of measurements that needed to be taken. The main experimental site at the catchment outlet was for the sediment traps and stream gauging. A site further upslope in a clear area was needed for the rain gauge. Finally, several sites around the catchment were required for daily soil moisture readings. Figure 7.7 shows the

locations of the various experimental sites around the catchment outlet (see gauging site and sediment traps, figure 7.4).

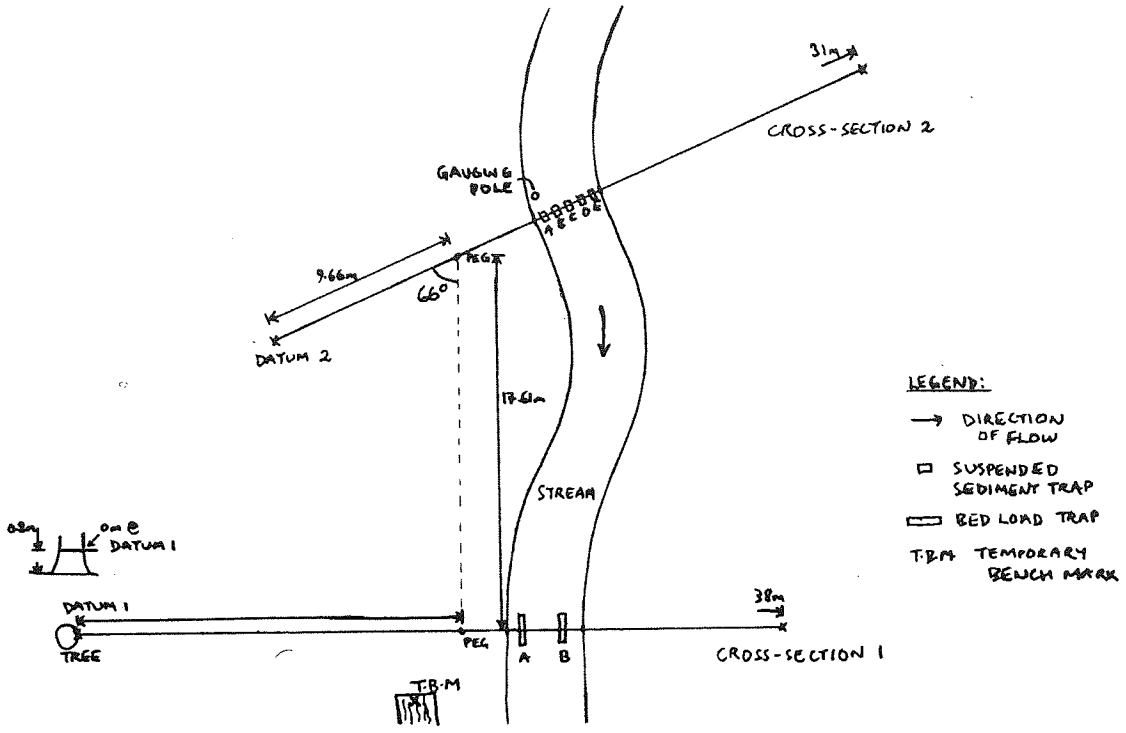

Figure 7.7 Sketch of the Experimental Sites at the Catchment Outlet

7.5.1 Selection of Measuring Sites and Equipment used

The sites were selected according to different criteria depending upon what measurements were to be taken at that site. Full experimental procedures for each of the types of site can be seen in Appendix B.

7.5.1.1 Rainfall Gauge

The rain gauge that was used was a Meteorological Office rain-gauge Mk II type daily rain-gauge as described in HMSO (1961). The rain gauge was set up and measurements recorded in accordance with guidelines set out in the Handbook of Meteorological Instruments, Part 1 (HMSO, 1961). Figure 7.8 shows the type of rain gauge used and how it should be installed. In summary, the guidelines state that the

gauge should be in a clear area with no over hanging or nearby ground vegetation, as this may falsify the results, and set up at the correct height above the ground (fig 7.8). The gauge must also be set up in a site so that rainfall collected is representative of whole of catchment, but due to time limitations, in a position that could be easily accessed. This is obviously not easy in a steeply sided catchment covered mostly in dense jungle. A site was eventually found situated on a clearer, flatter area near the catchment outlet (see figure 7.4 and plate 7.12). Rain gauge measurements were taken using a 10mm tapered model rain measure.

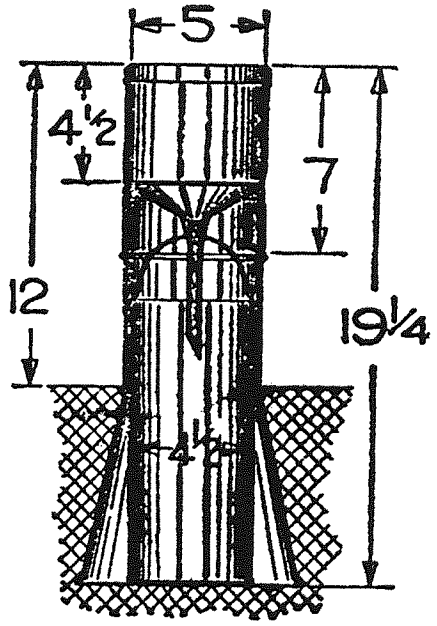

Figure 7.8 Meteorological Rain Guage Mk II
(from HMSO, 1961)

7.5.1.2 Sediment Traps

To capture the yield of the entire catchment, the equipment for sediment monitoring was set up as near to the catchment outlet as possible. Guidelines for the positioning and use of sediment traps was taken from Linsley et al (1982).

Sediment traps should be set up on a non-meandering section of channel with no major obstructions, pools etc. a significant distance upstream or downstream of the traps. The catchment outlet was located with assistance from local knowledge and a suitable section of the stream chosen. Due to the stream's size and the surrounding well-established large trees, a long straight section of stream was not easy to find as the stream took a meandering course. As a result, two separate sites were selected, one for the bed load traps and a second approximately eighteen metres upstream for the suspended load traps. Photographs taken at the sites can be seen in plates 7.13 to 7.18, fig 7.7 shows the area of both sites, figs 7.9 and 7.10 are cross sections showing the topography of the sections, and figs 7.11 and 7.12 are detail sections of the suspended sediment traps site showing the positions of traps and the gauging points for stream gauging.

Plate 7.13 Photo of the Inner Section of the Bed Load Traps

Plate 7.14 The Outer Section of the Bed Load Trap with the Grille Top

Plate 7.15 A Bed Load Trap Placed in the Stream Bed

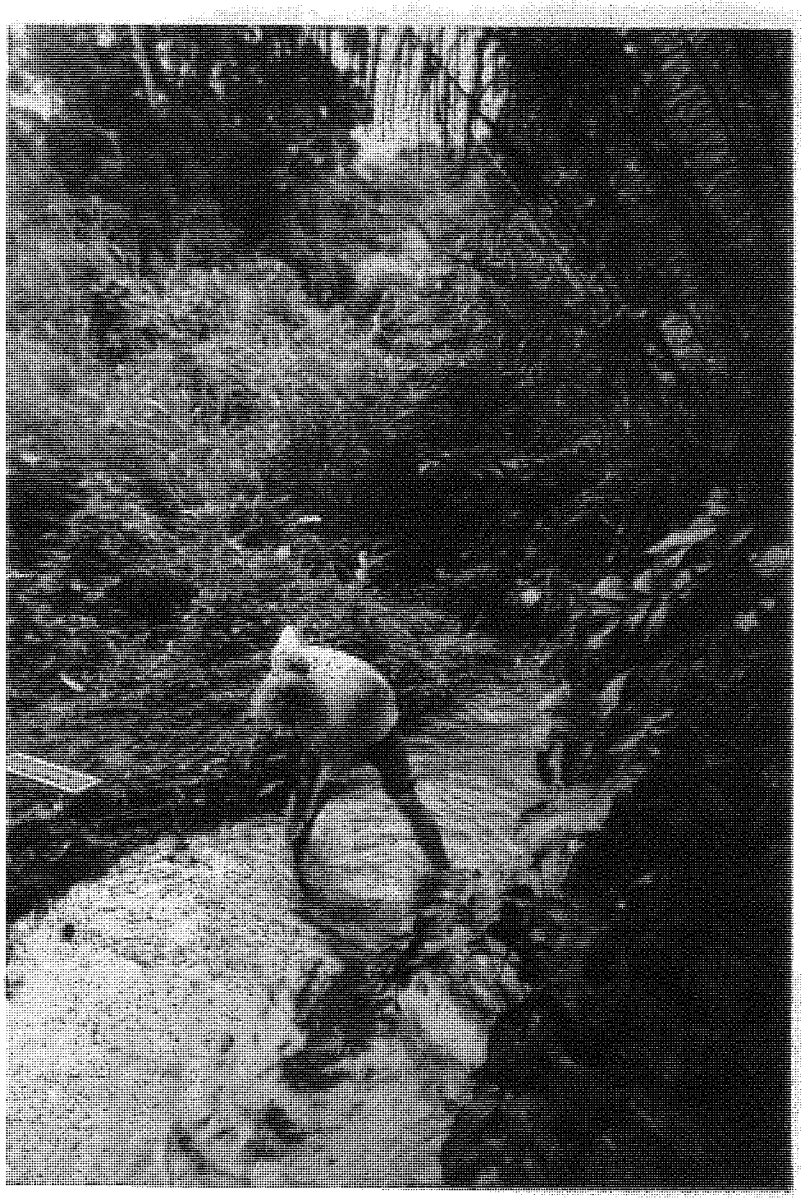

Plate 7.16 The Stream Bed Under Preparation for a Bed Load Trap

Figures 7.13 and 7.14 show details of the bed load and suspended load traps.

The collection of suspended sediment samples created some difficulties. With sufficient funding and equipment, suspended sediment samples can be taken using electronic samplers and data loggers allowing 24hr monitoring of suspended sediment loads. Such equipment was not available in Ghana, however, so instantaneous samplers were used. Instantaneous samplers only give the sediment concentration at a set point in time.

Plate 7.17 Suspended Load Traps Positioned in the Stream

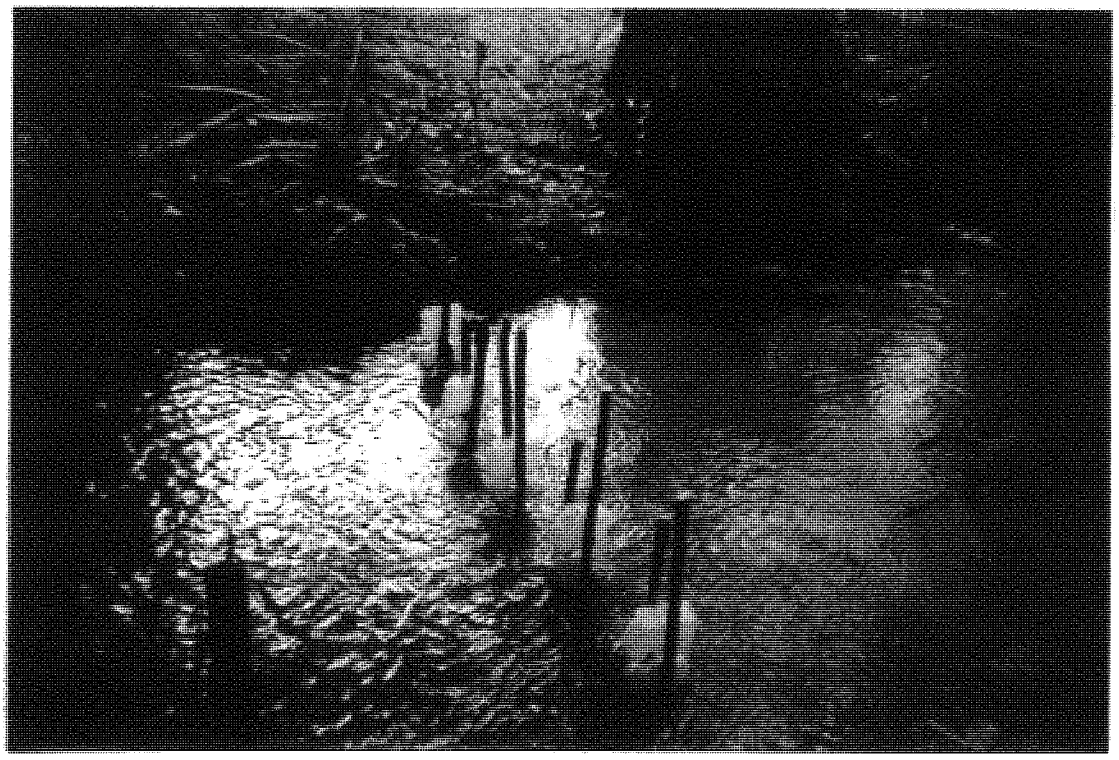

Plate 7.18 Suspended Load Traps Viewed from the Bank

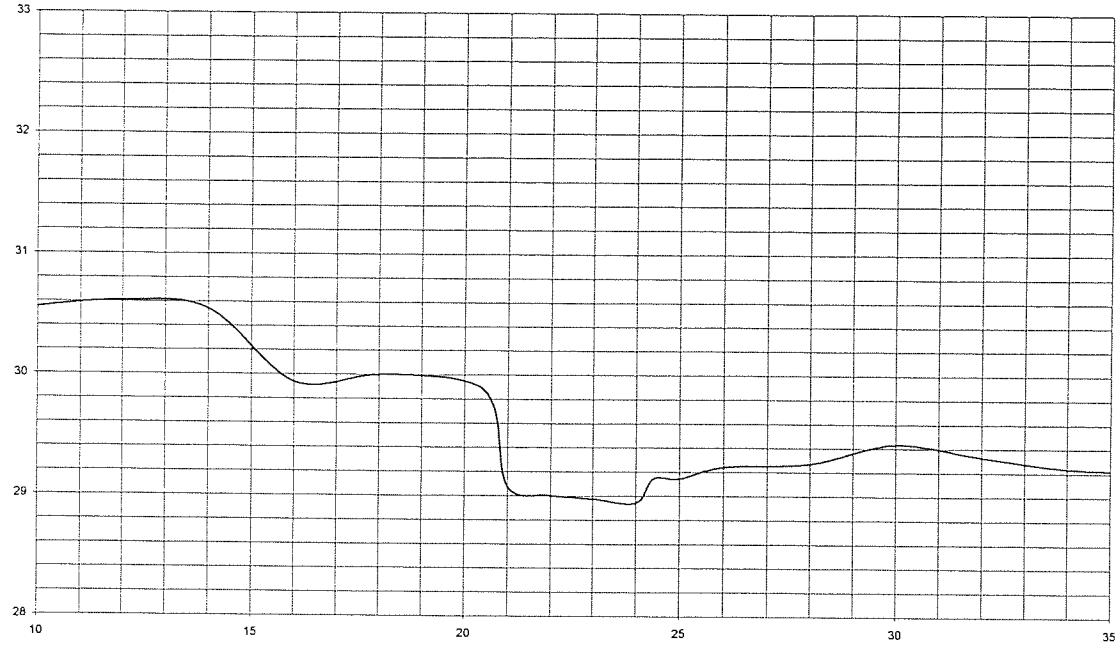

Figure 7.9 The Topography at Cross-Section One

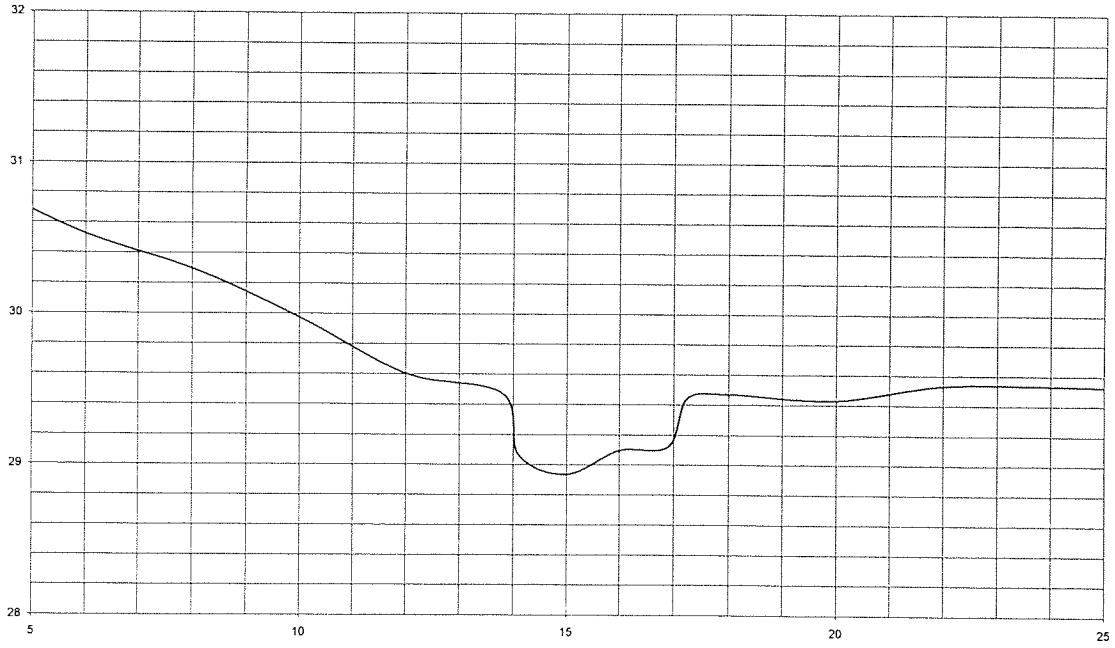

Figure 7.10 The Topography at Cross-Section Two

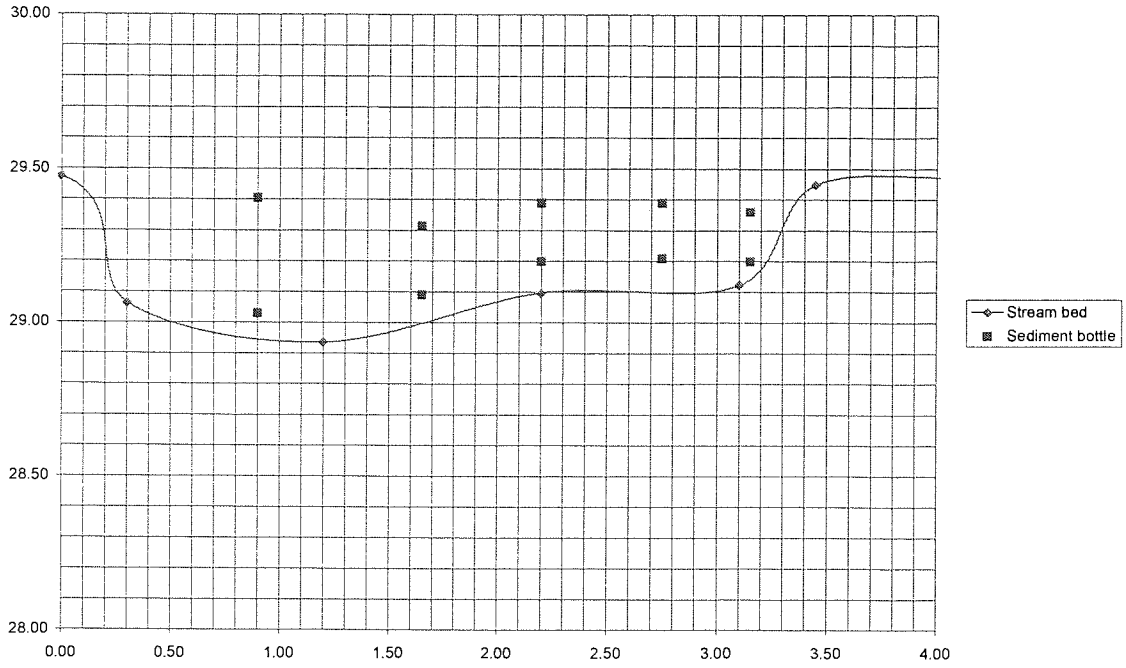

Figure 7.11 The Positions within the Stream Flow of the Suspended Sediment Traps

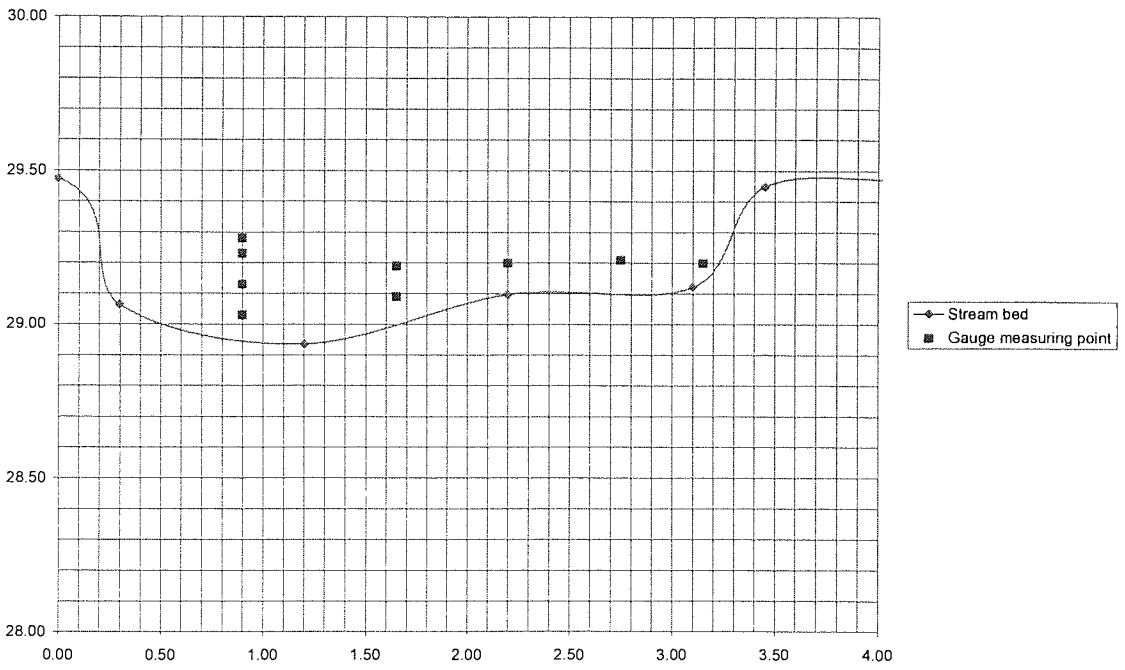

Figure 7.12 The Positions within the Stream Flow of the Gauging Points

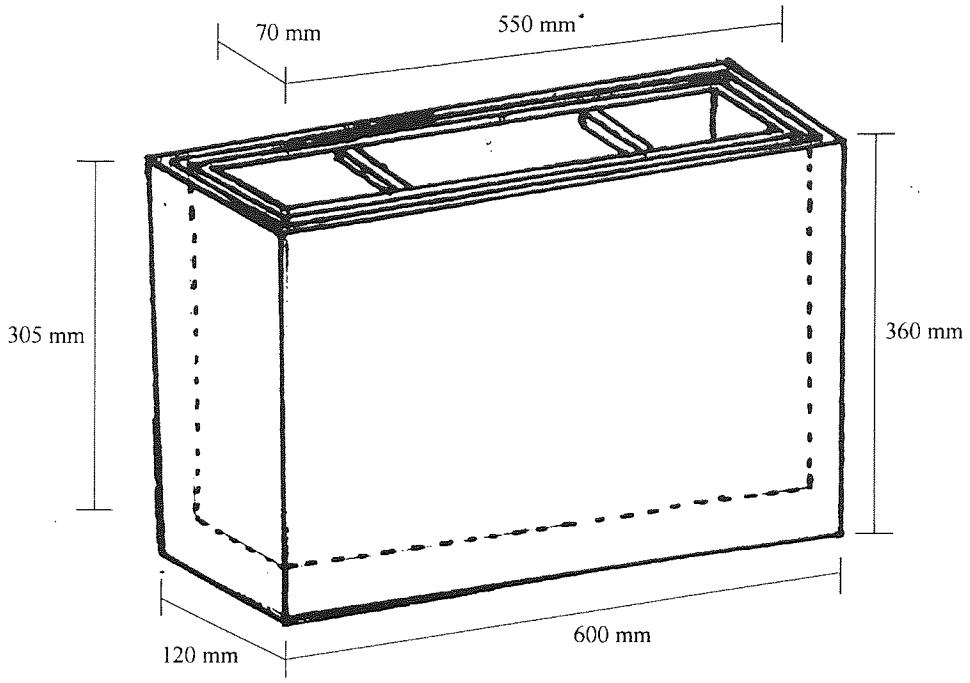

Figure 7.13 Detail of the Bed Load Traps

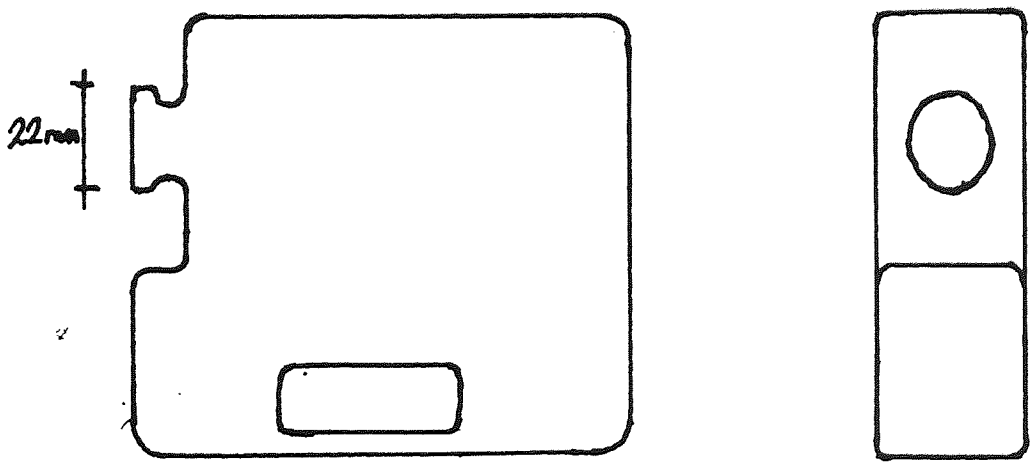

Figure 7.14 Detail of the Suspended Load Traps

However, because of the time restrictions working in the field, instantaneous samplers would be of no use as the time of peak flow and thus maximum sediment concentration was after the end of the working day in the field. It was therefore decided to use the same principle of sediment collection for instantaneous sampling but with a different bottle design and to leave the bottle samplers in the stream for a 24 hr period.

Referring back to figure 7.14, showing the suspended sediment traps, the principle of collection is as follows. Flow enters the bottle through the vertical opening and once inside the bottle the velocity of the flow decreases considerably. Because of this drop in velocity, the particles in suspension will no longer remain in suspension and will fall into the section of the bottle below the level of the neck where it will remain trapped. As more flow enters the bottle, the 'clean water' will be forced back out and thus the cycle will continue.

Pit traps with a grille covering and dug in to the streambed were used for the bed load traps. A pit trap is simply a removal box set into the streambed into which particles that are rolling along the bed will fall, a grille covering over the trap ensures that only transported sediment falls into the trap and prevents unwanted items from falling in and introducing errors into the results if not detected.

7.5.1.3 Stream Gauging

The requirements for setting up the stream gauging location are the same as that of the sediment traps. A minimum amount of disturbance to the flow is required within the section. Therefore, the section of the channel used for the suspended load traps was also used for the gauging equipment. The depth gauging pole was of simple construction, a sturdy approximately 100mm diameter bamboo pole that was firmly

embedded into the stream near the left hand bank. Depth markings were then marked on the side of the pole that had been shaved to a smooth flat surface. Flow measurements were taken using an A-OTT flow meter.

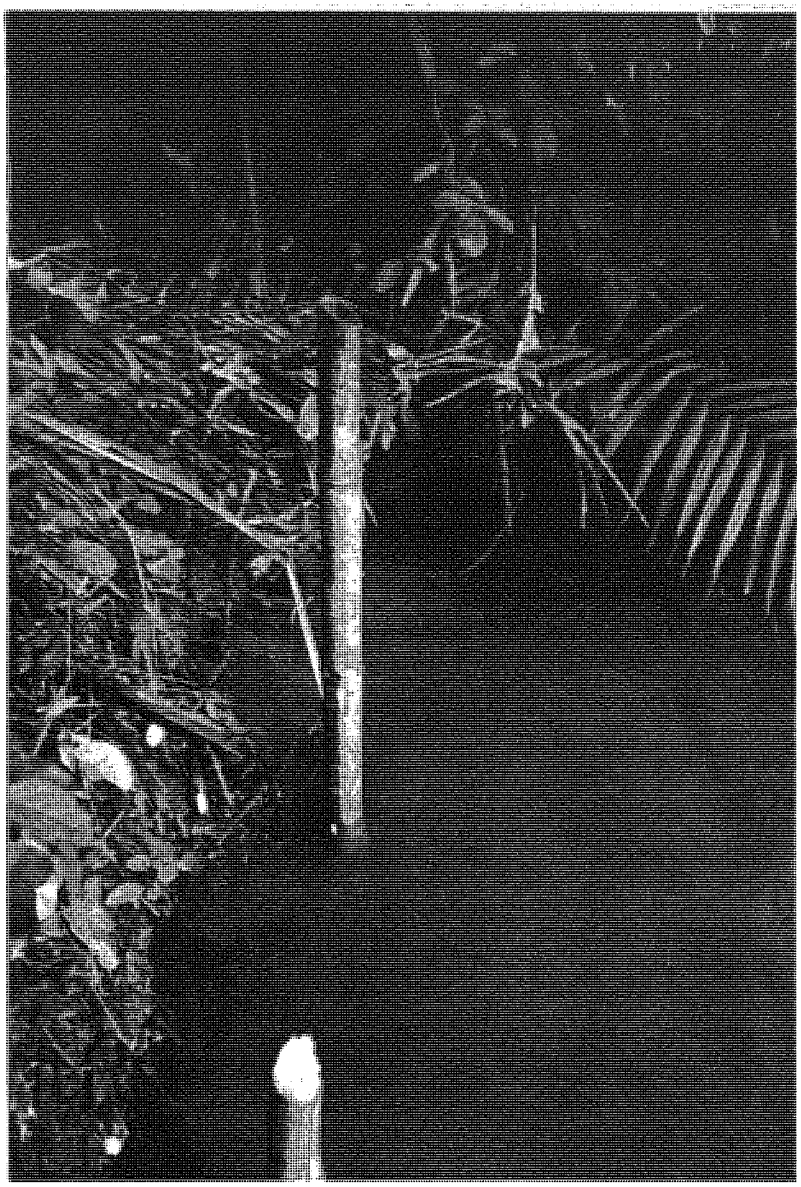

Plate 7.19 The Gauging Pole Positioned Upstream of the Sediment Traps

7.5.1.4 Soil Samples

The soil sampling sites were chosen so as to be representative of the soil types and conditions found within the catchment i.e.: four identified soil types, top of hill

slope and valley bottom. The sites were chosen with the assistance of Mr. Timothy Ayamga and can be seen as locations A to E in figure 7.4.

Soil samples were taken using standardised 60 mm sampling rings.

7.6 Collection of Data

Data was collected in the field using procedures that were designed to ensure practices were consistent. The methodologies adopted are given in Appendix B.

7.7 Summary

The field trip to Ghana provided a useful insight into the processes involved in soil erosion. The formation of gullies, the use of the man made pathways as artificial gullies and the transport of the soil particles were all witnessed given valuable information to support theoretical ideas of the way in which the processes worked.

There were also drawbacks with certain aspects of the field work, due to the long distance travel involved and relatively short period available for field work (due to funding limitations) little equipment could be brought over from England. This meant equipment such as the sediment traps had to be acquired or fabricated once within Ghana, which was either expensive (in the case of the bed load traps) or potentially unreliable (as with the suspended load bottles). However, it was possible to obtain some reasonably good quality data for calibrating the USLE factors from the Soil Research Institute in Kumasi.

To test the value of the experimental data that had been collected a large quantity of analysis was also required that due to time restrictions was left until the return to the UK.

Chapter 8

Results and Data Analysis from Ghana Field Experiments

8.1 Results from experimental catchment

The data and results obtained from the field trip are summarised in this chapter. The main measurements taken from the experimental catchment were the stream gauging at the catchment outlet, rainfall data, soil data, and sediment data. In total nine days storm data were collected; seven days during the field trip to Ghana, and due to sufficient funding, an additional two days of data was collected by the SRI, Accra, after the field trip at the end of October 2000.

8.1.1 Rainfall Data

During the period in which experimental readings were taken, a good range of storm sizes was recorded. The rainfall results are shown in table 8.1. Readings up to the 25th September were taken using the standard calibrated rain gauge measurer, however, this had to be returned to England at the end of field trip, and so for the rainfall readings on the 29th and 30th October an alternative method of calculation was necessary. The rain gauge itself was left in Ghana, so a standardised, calibrated piece of equipment was still available for collecting rainfall.

Date	Rainfall (mm)
14/09/00	0
15/09/00	Trace
19/09/00	71.4
20/09/00	0.8
21/09/00	5.1
22/09/00	0.8
25/09/00	19.7
29/10/00	13.1
30/10/00	10.7

Table 8.1 Daily Rainfall Readings from Experimental Catchment

Instead, rainfall measurements were calculated by weight. The diameter of the rain gauge was known, as is the density of water, enabling the depth of rainfall to be calculated.

The most suitable storms for verification of modelling work are those storms on the 21st and 25th September and 29th and 30th October. The 14th and 15th September readings of no rainfall mean that these days can provide base conditions for comparison with those days when rainfall does occur. Dry day sediment loads and flow rates can be calculated from these two days. The small storms on the 20th and 22nd, as can be seen from the sediment data (section 8.1.3), can provide data for testing low flow rate increases. Such storms can often give relatively high sediment loads by accumulating additional wash load from storage left behind by a previous storm.

The storm on the 19th September being the largest would appear to be the most useful storm for model verification because it could be assumed that the large flows would produce the greatest quantities of erosion giving an idea of the worst-case scenario. However, due to problems with the other measured results (i.e. half the sediment load traps were washed away and no stream level could be recorded), that inclusion of the storm within the study would be counterproductive to gaining meaningful results.

8.1.2 Stream data

Stream data was recorded using an A-OTT flow meter for each of the selected gauging points across the stream cross-section. These readings were converted from revolutions per second, into velocity readings using the calibration chart provided with the gauge.

Table 8.2 shows an example of the readings taken for stream gauging, for ease of calculations on a spreadsheet the equation of the calibration graph was calculated so that readings could be converted automatically in the spreadsheet. The equation of the graph was:

$$v = 0.25(rps) + 0.0375 \qquad \text{Equation 8.1}$$

where v is the velocity and rps the revolutions per second reading. Depth of flow readings were recorded each time gauging measurements was made using the gauging pole embedded in the stream. However, the gauging pole was a distance upstream from the measurement site so a correction factor of +0.09m was used because the bed was at a different depth at the gauging pole. Using the surveys of the cross sections, the area of the stream cross-section was calculated at the gauging point for heights at steps of 5mm, which could then be used with the depth readings to calculate flow rates. Due to the constantly varying water level, all depth readings were taken to the nearest 5mm, giving an accuracy of +/- 2.5mm for these readings. However, if an allowance is taken into consideration for the variable nature of the water level, ripples etc., then the error becomes +/- 5mm.

Flow Meter Results		15/09/00	12:50			
Cross Section at Suspended Sediment Traps						
Position	Dist above bed (mm)	Depth of flow (mm)	Count	Time (s)	RPS	Velocity (ms^{-1})
A	100	345	59	60	0.98	0.28
A	200	345	79	60	1.32	0.37
A	300	345	86	60	1.43	0.40
B	100	210	75	60	1.25	0.35
C	100	160	72	60	1.20	0.34
D	100	160	68	60	1.13	0.32
E	100	155	60	60	1.00	0.29
					Average	0.33
Depth of Flow at Gauging Pole (m)		0.275				
Depth of Flow at point A (m)		0.365				
Area of Flow (m^2)		0.439				
Flow Rate (m^3s^{-1})		0.147				

Table 8.2 Example of Flow Measurements taken at Catchment Outlet in Experimental Catchment

Table 8.3 shows a summary of the flow readings during the field trip. From this, a graph can be constructed for the stage-discharge relationship, which is shown in figure 8.1. From this, it can be seen that over the range of the flow measurements taken the relationship is approximately linear with a correlation coefficient of 0.97.

Depth (m)	Velocity (ms^{-1})	Area (m^2)	Flow Rate (m^3s^{-1})	Date	Time
0.360	0.345	0.425	0.146	15/09/00	15:00
0.365	0.335	0.439	0.147	15/09/00	12:50
0.365	0.377	0.439	0.166	15/09/00	13:10
0.370	0.382	0.453	0.173	14/09/00	15:05
0.370	0.404	0.453	0.183	14/09/00	14:45
0.380	0.418	0.481	0.201	13/09/00	15:00
0.385	0.440	0.496	0.218	14/09/00	11:20
0.390	0.406	0.510	0.207	13/09/00	11:00
0.390	0.435	0.510	0.222	13/09/00	11:30
0.395	0.426	0.524	0.223	13/09/00	10:45
0.400	0.456	0.539	0.246	25/09/00	16:10
0.415	0.476	0.583	0.277	22/09/00	12:20
0.415	0.447	0.583	0.260	25/09/00	11:15
0.420	0.457	0.597	0.273	22/09/00	11:45
0.430	0.449	0.627	0.281	21/09/00	12:05
0.435	0.432	0.642	0.277	20/09/00	12:00

Table 8.3 Summary of Stream Gauging Measurements taken at Experimental Catchment Outlet

The accuracy of the flow rate readings is calculated as follows. The base values for the error calculations are the number of revolutions of the A-OTT propeller, the time over which the revolutions are recorded and the depth of flow.

When taking the initial readings from the A-OTT meter to calculate the flow velocity, the time that the number of revolutions and the number of revolutions both provide systematic errors. Time over which the recording is taken can be assumed to have an error of +/-0.5s and the number of revolutions is subject to an error of +/-0.5 revolutions as the meter only records whole numbers of revolutions. The time over which the readings are taken is consistently 60s giving a percentage error of 0.83%. However, the number of revolutions varies depending upon the reading taken, thus the percentage error will vary accordingly. To avoid this complication and to give an approximation of the error involved the average number of revolutions, 75, is taken giving a percentage error of 0.66%. The maximum and minimum errors can be also be calculated for the range of values of number of revolutions. The maximum revolutions are 125, giving a percentage error of 0.40% and the minimum revolutions are 53, giving a percentage error of 0.93%. The resulting errors in the flow velocity for each of the scenarios are shown in table 8.4.

	Maximum	Minimum	Average
Revolutions	125	53	75
Time (s)	60	60	60
Velocity (ms^{-1})	0.90	0.60	0.69
% Error	0.48	1.13	0.80

Table 8.4 Errors in flow velocity readings calculated from A-OTT flow meter

Calculating the percentage error of the area of flow is also complex. In the same respect that there are variable values of the number of revolutions per minute for the flow meter, the depth also varies. Therefore, the same solution was used for the

area as the velocity, maximum, minimum and average readings were used to give an indication of the errors involved. The assumed error for depth readings is +/- 5mm as stated previously. The results are shown in table 8.5.

	Maximum	Minimum	Average
Depth (m)	0.435	0.360	0.398
Error	1.15	1.39	1.270
Area (m^2)	0.642	0.425	0.532
% Error	2.34	3.290	2.815

Table 8.5 Errors involved in depth calculations

The resulting errors for the calculations of flow rates are shown in table 8.6; errors given are the maximum, minimum and average values of the measured flow rates.

	Maximum	Minimum	Average
Area (m^2)	0.425	0.642	0.532
Velocity (ms^{-1})	0.90	0.60	0.69
Flow (m^3s^{-1})	0.38	0.38	0.37
Total % Error	1.59	3.73	2.64

Table 8.6 Total errors in flow calculations

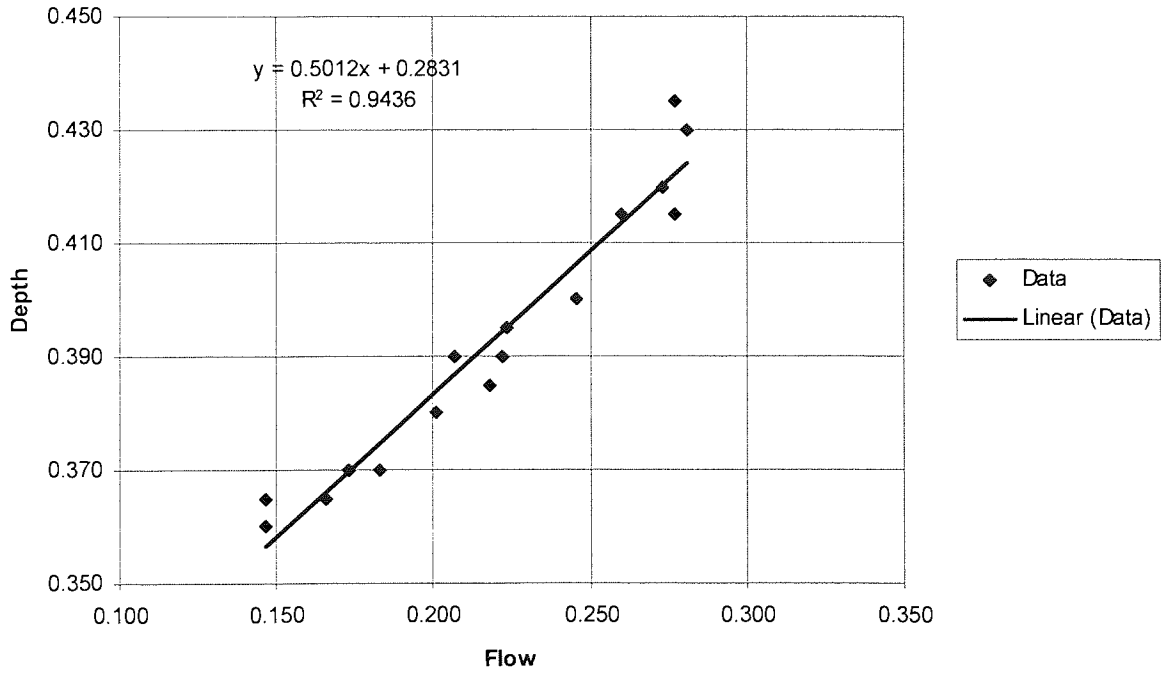

Figure 8.1 Stage Discharge relationship for Stream in Experimental Catchment at Catchment Outlet

8.1.3 Sediment Data

As well as stream gauging information, sediment sampling was also undertaken at the catchment outlet. Readings were taken for both suspended loads and bed loads.

8.1.3.1 Suspended Load Data

Suspended load data was taken as daily readings, sediment bottles were replaced daily at 11am, giving suspended loads for the whole day. According to most literature (e.g. Walling, 1994), suspended loads are taken as instantaneous samples. However, due to the requirements of the data, and the nature of the catchment it was decided that daily loads would be more appropriate. Rainfall in tropical climates, Ghana was no exception, generally occurs once a day in the late afternoon. In the region of the catchment, if there were to be rain for the day, it would start at approximately 4pm and would be the only storm for the day; this was confirmed by local knowledge. The modelling that had been planned was designed to model the sediment delivery resulting from a single storm of x mm of rain, thus the sediment data that was required for verification was the sediment load for the whole storm. Due to logistical problems, it was not possible to remain in the catchment for the duration of the storms as we were advised not to travel outside the Accra (the base) at night. Therefore, the journey needed to start by 4.30pm at the very latest. This did not leave enough time to wait until the storm had finished to collect instantaneous samples throughout the storm and beyond as runoff reached the catchment outlet. However, daily suspended load readings were also taken on dry days, with no rainfall, giving the base sediment load for the stream. Thus, by subtracting the base sediment

load from the daily readings for a storm day the total load for each of the storms could be calculated.

To calculate total suspended loads for the day from the data collected within the sediment bottles, a series of assumptions had to be made. Firstly, due to the unavailability of electronic water level recording equipment and an inability to observe first hand the response of the stream to a rainstorm, the exact water level the stream reached at peak was unknown. However, attempts were made to resolve this. By setting the upper suspended sediment sampling bottles at different heights and by adding extra, small bottles, not needed for sampling purposes, an estimation of the water level reached could be attained. The more of the bottles that had collected water then the higher the water level that had been reached. Once the water level was known, then the cross-sectional area of the flow could be calculated, enabling the total suspended load to be calculated. The exact height of the upper bottles was changed daily depending upon the level of the stream during the day; however, the height above the water level was consistently kept at 10mm, 20mm, up to 50mm.

The basic premise of these calculations was to calculate the ratio of the total collecting area of the openings of the sediment bottles to the total area of the stream and use this to convert the total sediment collected in the bottles to the total sediment passing through the cross-section. However, this method is only applicable to a stream of constant water level. Therefore, a direct relationship between cross-sectional area of the stream and sediment collected could only be used for the area over which the stream level did not fall. This level was given by stream depth data collected each morning and evening at the site. To account for the variable level, an assumption has to be made for the length of time that the stream exceeded the constant level. A correction factor has to be applied to reduce the contribution of total

sediment from the measurements taken from the upper collecting bottles. This correction factor was taken as 0.5 based on calculations of the time of concentration of the storm, compared with the total time over which sediment had been collected.

Originally it was thought that there was one final adjustment to be made to the calculations before the final total sediment load could be calculated. The area of the openings of the collecting bottles is not the total area over which sediment is collected. Referring back to figure 7.15 showing the shape of the collection bottles it was assumed that collection of sediment occurred as follows:

1) Streamflow carrying sediment will enter the bottle.
2) The velocity of the water in the bottle will reduce dramatically and the sediment will fall out of suspension collecting in the lower section of the bottle below the level of the opening.
3) More streamflow will enter the bottle displacing the 'clean' water back out of the opening.

The exact area over which sediment is collected depends upon the change in velocity between the inflow of 'dirty' water and the outflow of 'clean' water. Using standard continuity equations for velocity-area measurements, a correction factor was calculated to be applied depending upon the percentage change of velocity between inflow and outflow (see figure 8.2). For the calculations to determine total sediment loads, it was assumed that the velocity change was 50%, giving a further correction factor of 31.55. The final recorded daily-suspended loads are shown in Table 8.7.

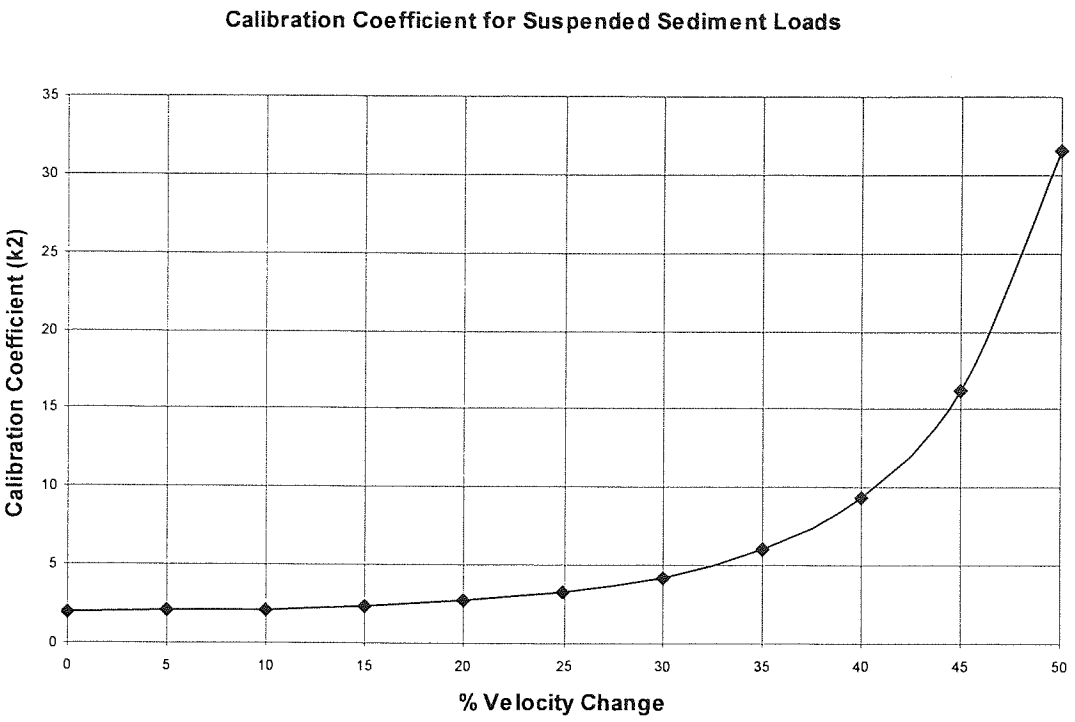

Figure 8.2 Calibration Coefficient for Area Calculations of Suspended Loads

The results for the 19th September have not been included in the table for two main reasons. Firstly, due to the exceptionally high quantity of rainfall experienced on the 19th, the flow rates were very high and the stream became flooded. This made for two complications; firstly, the high flow rates were powerful enough to wash away all of the uppermost sediment bottles, which meant that the water level could not be established. Secondly, due to the large flat flood plain to one side of the stream, area calculations were also virtually impossible, even if the maximum water level had been known. The second reason for neglecting the large storm is based on verification of the model. In extreme cases, conditions exist that may not be the normal steady state conditions, which can affect the validation of the model. Thus, validation is normally carried out using intermediary data values where these extreme conditions do not exist.

Suspended Load Readings									
Diameter of bottle (m)			0.022	Area of Bottle (m^{-2})		0.00038			
Date	Bottle position	Weight of sediment in bottle (g)	Weight in lower bottles (g)	Weight in upper bottles (g)	Day Depth (m)	Max Depth (m)	Day Area (m^2)	Max Area (m^2)	Total Suspended Sediment (kg)
14/09/00	A lower	6.195							
	B lower	9.224							
	C lower	6.191							
	D lower	10.941							
	E lower	4.258	36.809	0.000	0.370	0.370	0.453	0.453	276.761
15/09/00	A lower	6.310							
	B lower	11.821							
	C lower	8.823							
	D lower	8.966							
	E lower	3.883	39.803	0.000	0.370	0.365	0.365	0.453	241.136
20/09/00	A lower	28.428							
	B lower	8.560							
	C lower	9.830							
	D lower	17.528							
	E lower	28.428	92.774	0.000	0.435	0.440	0.627	0.657	965.487
21/09/00	A lower	17.219							
	B lower	34.004							
	C lower	33.032							
	D lower	27.242							
	E lower	15.102							
	A upper	1.241	126.599	0.000	0.430	0.450	0.627	0.687	1317.499
22/09/00	A lower	17.076							
	B lower	28.763							
	C lower	21.367							
	D lower	21.657							
	E lower	14.486	103.349	0.000	0.415	0.420	0.583	0.597	1000.063
25/09/00	A lower	51.352							
	B lower	64.158							
	C lower	97.006							
	D lower	80.231							
	E lower	69.038							
	B upper	2.365							
	C upper	4.566	361.785	6.931	0.415	0.460	0.583	0.718	3510.542
29/10/00	A lower	43.438							
	B lower	52.695							
	C lower	90.367							
	D lower	74.880							
	E lower	52.695							
	A upper	3.112	314.075	3.112	0.410	0.440	0.568	0.657	2965.569
30/10/00	A lower	26.213							
	B lower	43.784							
	C lower	54.538							
	D lower	42.390							
	E lower	38.404							
	B upper	2.848	205.329	2.848	0.400	0.420	0.539	0.597	1839.668

Table 8.7 Suspended Load Readings and Calculations Summary

The bottle positions in table 8.7 refer to the positions highlighted in figure 7.12, although it should be reiterated that the height positions of the upper bottles varies in each case, however, the position along the stream cross section remains the same. The water levels recorded as the maximum water level have an error of +/- 10mm.

8.1.3.2 Bed Load Data

Bed load data was much harder to acquire. As mentioned previously (section 7.3) the streambed (and thus the bed load) was very unstable and constantly moving. This made bed-load measurements awkward to obtain. Due to the exceptionally high bed loads, the traps were unable to be left to record the load during the course of a whole day and thus the bed load sampling was done during the days spent at the experimental catchment for limited time periods. The duration of sampling was largely dictated by how quickly the trap took to fill up, and on the higher flow days after the larger storms usually taken as approximately one hour. This was the length of time required to perform a full set of stream gauging measurements. Table 8.8 shows the bed load readings that were measured.

The data in table 8.8 confirms the original assumptions that the bed was unstable and erratic in nature (see section 7.3). The average loads calculated for the day assuming that the rate of bed load does not increase (which it would in reality but with no means of measurement), vary by as much as 6500kg. This is enough to question the validity and accuracy of the bed load readings, without considering that due to the unstable nature of the bed, the placement of the trap within the bed would be enough to disrupt further the stability of the bed causing scouring of the bed in

front of the trap, thereby introducing further errors into the measured loads. However, the design of the traps was such that this should have been kept to a minimum.

Bed Load Readings								
Date	Position	Total volume of trap (m^{-3})	Empty volume (m^{-3})	Volume of load (m^{-3})	Mass of load (kg)	Average load across bed over time period (kg)	Duration of measurement (min)	Average load for day (kg)
15/09/00	A1	0.0117	0.0067	0.0050	7.027			
	B1	0.0117	0.0108	0.0010	1.351	89.770	210	615
19/09/00	A1	0.0117	0.0000	0.0117	16.487			
	B1	0.0117	0.0019	0.0098	13.784	324.331	205	2278
20/09/00	A1	0.0117	0.0008	0.0110	15.406			
	B1	0.0117	0.0062	0.0056	7.818	248.830	60	5971
21/09/00	A1	0.0117	0.0008	0.0110	15.406			
	B1	0.0117	0.0061	0.0057	7.973	250.488	50	7214
Note: Bed load traps are 0.07m wide, two traps therefore cover 0.14m of the total bed width. Bed is 3m wide, thus, total load across bed is total load in traps multiplied by 3.0/0.14.								
Note: Average load per day is calculated assuming bed load remains constant throughout a 24 hr period.								

Table 8.8 Bed Load Readings taken at Catchment Outlet (positions A and B refer to positions in figure 7.7)

8.1.4 Soil Data

8.1.4.1 Particle Size Analysis

For each of the sol samples that were collected, from each of the sites chosen by Mr. Timothy Ayamga, a particle size analysis was undertaken. Particle size distributions have many uses. They provide information on the soil texture and thus potential infiltration rates, especially in high sand content soils when infiltration rates can be hard to measure using an infiltrometer when more sophisticated modern electronic equipment is unavailable. They can be used to provide measures of erodibility of the soil and can be used for comparative analyses of the sediment loads in the streams to give a picture of how the sediment is transported from the hillslope to the catchment outlet. Taking this into consideration, a particle size analysis was also carried out on samples taken from the bed-load and suspended load traps.

The particle size analyses for each of the soil types identified by Mr Timothy Ayamga are shown in table 8.9. It can be seen from the particle size distributions of each of the soils that they all possess a high proportion of sand. Given that the bed-load sample consists almost entirely of sand, this would suggest that the large majority of sediment is transported as bed-load (see section 8.1.3 and 8.1.5). Table 8.10 shows the average dry and bulk densities for each of the soil samples, the densities were calculated from the samples that were used to calculate moisture content (see section 8.1.4.2).

ID no	Soil Type and Series	Texture	Sands				%Total Sand	%Silt (5μm)	%Clay (0.5μm)
			%Coarse (500μm)	%Medium (355μm)	%Fine (125μm)	%Very fine (63μm)			
3SA1(0-30)	Bejua	Loamy sand	2.68	5.92	25.72	28.69	78.05	15.94	6.01
3SA2(30-100)	Bejua	Sandy loam	2.35	6.83	26.33	28.38	74.43	19.53	6.04
2SB1(0-10)	Bediesi Haplic Nitisol	Sandy loam	4.13	10.21	24.43	25.94	69.77	24.02	6.21
4SB2(0-30)	Fete Lithic Liptosol	Loamy sand	2.29	7.18	29.1	30.31	78.14	18.71	3.15
1SC1(0-30)	Sutawa Gleyic Arenosol	Loamy sand	2.29	6.12	25.44	27.59	72.35	19.75	7.90
1SC1(0-100)	Sutawa Gleyic Arenosol	Loamy sand	2.38	7.66	27.76	29.41	75.2	19.75	5.05
Bed Load	n/a	Sand	5.36	13.85	34.57	36.98	91.9	7.06	1.04
Suspended Load	n/a	Silt	0	0	1.51	2.30	3.81	71.20	24.99

Table 8.9 Particle Size Distribution of Soil Types Found in Experimental Catchment (note: figures in brackets in first column after ID number represent depth over which sample analysed)

Site	Soil	Average Bulk Density (kg m^{-3})	Average Dry Density (kg m^{-3})
1	SA1	1862.838	1490.64
2	SB1	1614.48	1307.617
3	SB2	1764.581	1538.5
4	SC1	1605.175	1324.127

Table 8.10 Average Bulk and Dry Densities for Soil Types in Experimental Catchment

8.1.4.2 Daily Moisture Content

The last data measure to be collected in the field was the daily moisture content readings. Moisture content readings were taken at each of the sites around the catchment. Gravimetric moisture content readings as a percentage are shown in table 8.11. Due to timing constraints within the field and the remote location of site 5, it was not possible to collect data at site 5 every day.

Daily moisture content readings									
Site 1		Site 2		Site 3		Site 4		Site 5	
Date	Moisture Content (%)	Date	Moisture Content (%)	Date	Moisture Content (%)	Date	Moisture Content (%)	Date	Moisture Content (%)
15/09/00	32.232	15/09/00	18.588	15/09/00	8.798	15/09/00	13.301	15/09/00	16.339
19/09/00	17.556	19/09/00	17.161	19/09/00	12.213	19/09/00	18.596	19/09/00	
20/09/00	15.110	20/09/00	20.430	20/09/00	13.328	20/09/00	18.473	20/09/00	
21/09/00	17.475	21/09/00	19.860	21/09/00	15.105	21/09/00	18.202	21/09/00	13.803
22/09/00	15.395	22/09/00	18.840	22/09/00	13.500	22/09/00	18.501	22/09/00	

Table 8.11 Daily Moisture Content Readings (site numbers refer to positions indicated in figure 7.4)

8.1.5 Mass Balance Calculations

As well as collecting the quantities of bed and suspended loads from the stream at the catchment outlet, particle size distribution data was also measured for both suspended and bed loads. Table 8.12 shows the average particles size distributions for the soils and each of the sediment load components.

The principle of the mass balance is that the sediment carried as sediment load to the catchment outlet will have approximately the same characteristics as the soils from which it was originally eroded. This is especially true in a catchment with characteristics like the one that was studied. The soils are not comprised of particles much larger than coarse sand, thus the large majority of the soil that is eroded will be transported out of the catchment even at relatively low flow rates. In addition,

because the particles are all relatively small and transport times are relatively short, sediment is not liable to be broken down into smaller particles during transport. By comparing the particle size distribution data of the two sediment loads with the particle size distribution data of the soils in the catchment, the approximate ratios of transport of bed load to suspended load can be calculated.

	%sand	%silt	%clay
Average Soil	74.66	19.62	5.73
Average Bed Load	91.9	7.06	1.04
Average Suspended Load	3.81	71.20	24.99

Table 8.12 Average Particle Size Distributions for Soil Types, Bed Load and Suspended Loads

Using the particle size distribution data (table 8.9), it was calculated using linear regression that the bed load represented 73.9% of the eroded sediment. However, there is some error in this approximation as the samples used for the suspended load distributions was not as big as would normally be used to determine particle size distributions, and there has to be some consideration for break down of particles during transport even though it is not particularly significant.

8.2 Additional Data from SRI, Kumasi

During the rainy season of 1999, the Soil Research Institute, Ghana, had begun erosion plot experiments at Kumasi. Small experimental plots were set up to measure erosion rates on various different types of farming conditions, including a control plot that was left bare. Data on rainfall amount, runoff and eroded sediment were kept for each plot during the period 24/07/99 to 20/09/99, during which time 595.8 mm of rain fell. Despite being non-standard plots, the bare plot can be used to provide some verification for USLE factors used. Soil types at Kumasi are not the same as those

found in the experimental catchment, however, the plot data can still be used to verify the applicability of the selected USLE parameter equations to Ghanaian soils in general.

Table 8.13 shows the original data collected. The rainfall, despite not being a full year's rainfall, the average rainfall for the station at Kumasi is 892.3mm/yr, is sufficient for calibration of USLE parameters as once rainfall reaches those levels the relationship between rainfall and erosion is approximately linear.

The total collected erosion for the period is 650g. It is interesting to note that the relationship between the collected erosion and rainfall is not linear, but this only reflects the variable nature of soil erosion and shows why the USLE is much better at predicting erosion over the period of a whole year, than for individual rainstorms.

Date	Rainfall Amount(mm)	PLOT 1		
		Bare Plot		
		Soil Loss (g)	Depth of water in tank (mm)	Silt Content (gl^{-1})
24/07/99	1.5	0	0	0
25/07/99	15.4	60	2.1	0
31/07/99	141.2	170	50	30
01/08/99	4	0	0	0
02/08/99	57	40	49.5	40
04/08/99	9.5	0	0	0
05/08/99	19	20	7.9	10
06/08/99	7.6	0	3.7	0
10/08/99	4.5	0	0	0
13/08/99	79.9	120	52	60
17/08/99	20.5	40	4	20
19/08/99	22.7	10	8	20
22/08/99	9.5	0	0	0
02/09/99	26	10	7	0
03/09/99	14	20	4	0
05/09/99	14.3	0	6	0
06/09/99	33.8	10	17	0
09/09/99	35.4	10	6.1	10
11/09/99	1.5	0	0	0
14/09/99	38	60	5.3	20
17/09/99	21.5	70	4	0
20/09/99	19	10	4.4	0
TOTALS	595.8	650	231	210

Table 8.13 Plot Data from Kumasi (Plot 1 is the natural bare earth plot, other plots used combinations of tillage and manure fertilisation)

The changing nature of the micro topography across the plot mimics the behaviour of larger scale fields, in that the same amount of rainfall for one storm will not necessarily produce the same amount of erosion, but averaged out across the period of a year, the total erosion will be much more similar (see also chapter 5).

To verify the USLE factors, certain calculations and assumptions have to be carried out. The erosion rate for the Kumasi plot is 8.02 t/ha/yr. For the purposes of these experiments, the C factor is taken as one, because the plot was bare and thus there was no protection from vegetation. The K factor was derived from the soils data assembled for the Boateng (1998). The soil type found at Kumasi is an Acrisol (Clay Loam) under FAO (1990) classifications. The LS factor for the purposes of the plot analyses was reduced to just the section that calculates the S factor for each of the LS equations. This is because the plot is small in scale, thus the effects of slope length, even if they existed, would be negligible and so have been neglected.

USLE calculations could then be performed using various combinations of the LS and R factors discussed in chapter 3. Table 8.14 shows the results from each of the USLE analyses, and the percentage errors compared with the calculated actual rate of erosion from the plot data.

Total Rainfall	Total erosion (g)	Plot area (m^2)	Land Slope (%)	Erosion (t/ha/yr)	R Factor	R Factor Eq.	LS Factor	LS Factor Eq	K Factor	C Factor	USLE Estimate (t/ha/yr)	% Error
595.80	650.00	0.81	2.00	8.02	200.67	3.6	0.23	3.20	0.18	1.00	8.29	-3.35
595.80	650.00	0.81	2.00	8.02	200.67	3.6	0.60	3.21	0.18	1.00	21.77	-171.34
595.80	650.00	0.81	2.00	8.02	200.67	3.6	0.25	3.16, 3.17	0.18	1.00	8.88	-10.71
595.80	650.00	0.81	2.00	8.02	200.67	3.6	0.16	3.13	0.18	1.00	5.75	28.33
595.80	650.00	0.81	2.00	8.02	200.67	3.6	0.18	3.12	0.18	1.00	6.59	17.93
595.80	650.00	0.81	2.00	8.02	219.76	3.7	0.23	3.20	0.18	1.00	9.08	-13.18
595.80	650.00	0.81	2.00	8.02	219.76	3.7	0.60	3.21	0.18	1.00	23.85	-197.15
595.80	650.00	0.81	2.00	8.02	219.76	3.7	0.25	3.16, 3.17	0.18	1.00	9.73	-21.24
595.80	650.00	0.81	2.00	8.02	219.76	3.7	0.16	3.13	0.18	1.00	6.30	21.51
595.80	650.00	0.81	2.00	8.02	219.76	3.7	0.18	3.12	0.18	1.00	7.21	10.12

Table 8.14 USLE Analysis of Plot Data from Kumasi

It can be seen that the combination of the LS factor equation, equation 3.20 (proposed by Nearing (1997)), and the R factor equation, equation 3.6, used in the CALSITE model (Bradbury et al, 1993), give the best percentage error at –3.35%. These results agree with the theoretical conclusions and decisions made at the end of chapter 3.

Unfortunately, funding has not been available within the SRI to repeat these experiments in subsequent years. If more data were available for other years, the accuracy of parameters could be improved considerably. Correction factors could be calculated for each of the parameter equations so that each of the parameters could be adjusted to reduce the percentage error. However, with only one-year's worth of data this would be unrealistic, as it would not be known which of the parameters needed adjusting. As it stands, one year of data is not sufficient to guarantee that each of the parameter equations is correct, but as it is the only data available for calibrating USLE factors, it is better than nothing at all.

8.3 Summary

In light of the analysis of the data, it was clear that much of the collected data was potentially unreliable and its use in calibration of the intended model would be highly questionable. The many assumptions that had to be made cannot be sufficiently justified to enable other erosion events to be predicted accurately in conjunction with the model. For example, it became clear after consultations later in the project, that the assumptions made regarding the corrections applied to calculate total sediment loads might not be valid. The theories regarding the area over which the sediment bottles collected could not be validated unless the conditions could be replicated in the lab or a return to Ghana was made in order to test experimentally

these assumptions. Furthermore, the theory did not take into account the possibility that the outflowing water could carry sediment back out of the bottle or that turbulence around the opening could also significantly reduce the effective area over which water could flow into the bottle. This rendered the results unusable for calibrating the eventual model.

The results were kept as a record of what was obtained should they become useful in the future following further investigations in the country.

The lack of reliable data is largely attributable to a lack of experience and planning and, as previously stated, a lack of funding and time. The lack of experience and planning led to poor judgement in areas of the fieldwork, the most detrimental of which were in the collection of sediment data from the stream and the stream gauging. The equipment that could be taken to Ghana could only account for part of the required measurements. Since a lack of funding meant that the remaining equipment could not be obtained in Ghana, methods were improvised to enable the remaining measurements to be made; however, the reliability of the substitutes was not fully taken into consideration.

Then a lack of experience meant that the full implications of decisions made in the field in attempting to rectify the situation that presented itself, were not appreciated until the return to the UK, when the data was analysed.

However, the data could at least be used to test the functionality of the developed model in terms of the computer programming and simulations in preparation for further work with better quality data employed to refine the model. Excluding the methods for collection of suspended and bed loads, the methodologies and experiments described here also demonstrate how the field work could be carried out in future exercises.

The next phase of the research was therefore to continue the development of the model, concentrating on creating a model for future use in Ghana. The development of the model would then have two main considerations, firstly, to incorporate those parameters or factors that are most influential to erosion in Ghana, and secondly taking account of lessons learnt about the challenges of data collection in such an environment.

Chapter 9

Model Theory, Development and Programming

9.1 Introduction

The model development was a long and complex process consisting of several stages whilst maintaining an awareness of the restrictions and constraints that applied. At each stage, there were several options available, but most of which were governed by the key constraint, the data that was available. However, the available data is not the only constraint that governs the development of the model; the requirements of the model and what it has to achieve also have to be taken into account.

Due to the lack of available data and the poor quality of data that had been collected, the original emphasis of the thesis, to develop and validate a soil erosion model, had to be reconsidered. The main aim, to develop the model had not been lost, however, instead the direction of the thesis turned to developing a protocol for running the model focussing on what the model should achieve. It was also important to detail how data should be collected in the future to enable the eventual validation of the model to be carried out.

9.2 Modelling Processes

According to Nearing et al (1994), model development may be divided into two phases. The first is the creation of the physical model prototype and the second is model evaluation. This is not just applicable to physically based models, but can be applied to the development of any sort of model in any modelling situation; the logical progression of the modelling process is to a large extent independent of the modelling environment. Figure 9.1 (from Nearing et al, 1994) gives the outline of the procedure for the creation of a physically based model.

This chart is also applicable to other forms of modelling as well as physically based modelling. The general format of analysing the theory, formulating equations, estimating, calibrating and validating parameters also applies to conceptual and empirical modelling as well.

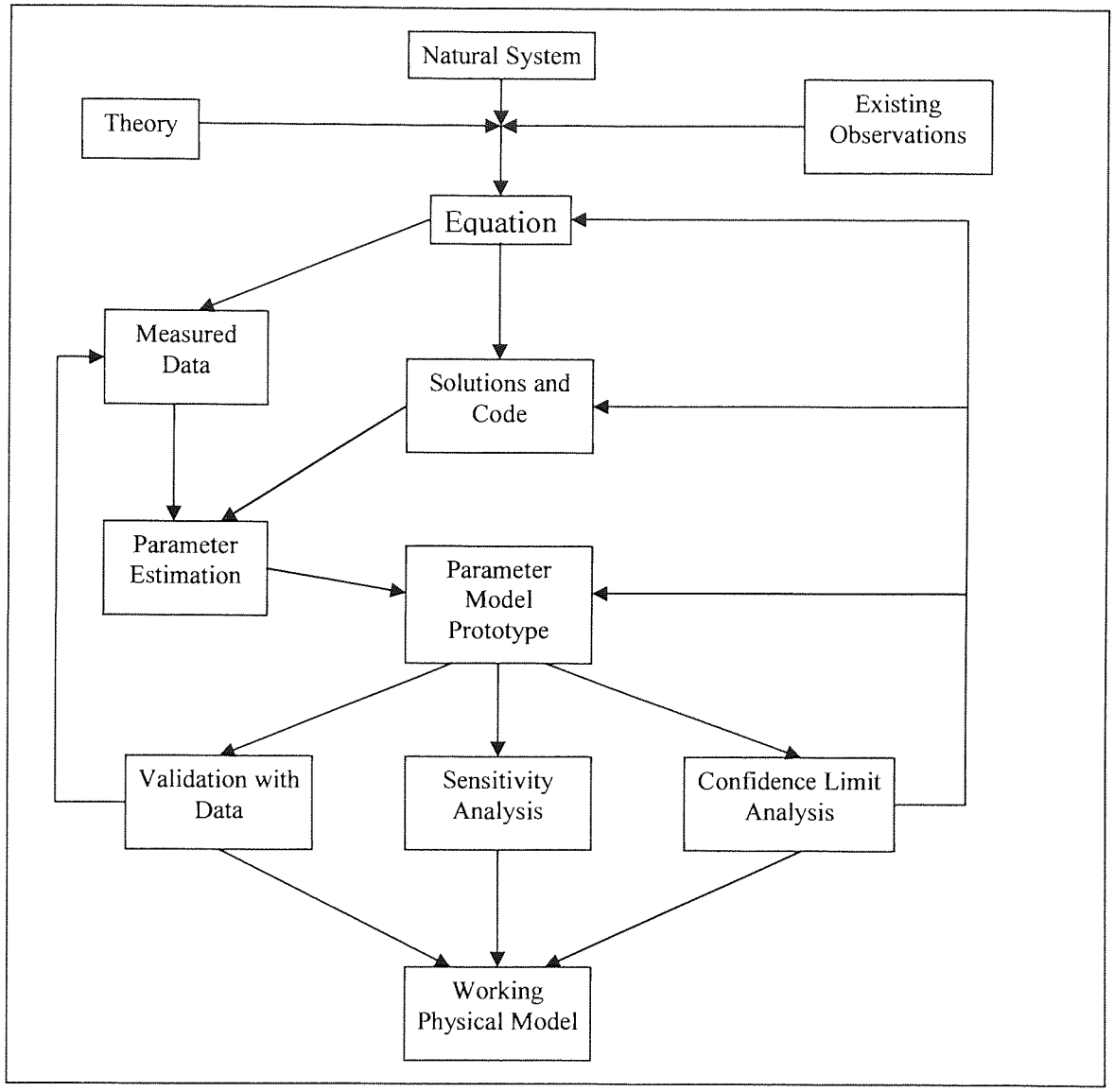

Figure 9.1 Outline for Development of a Physically-Based Erosion Model (from Nearing et al., 1994)

Meyer and Wischmeier (1969) described a simple sediment transport model incorporating the basic processes of soil erosion by water; the flow chart for the model can be seen in figure 9.2.

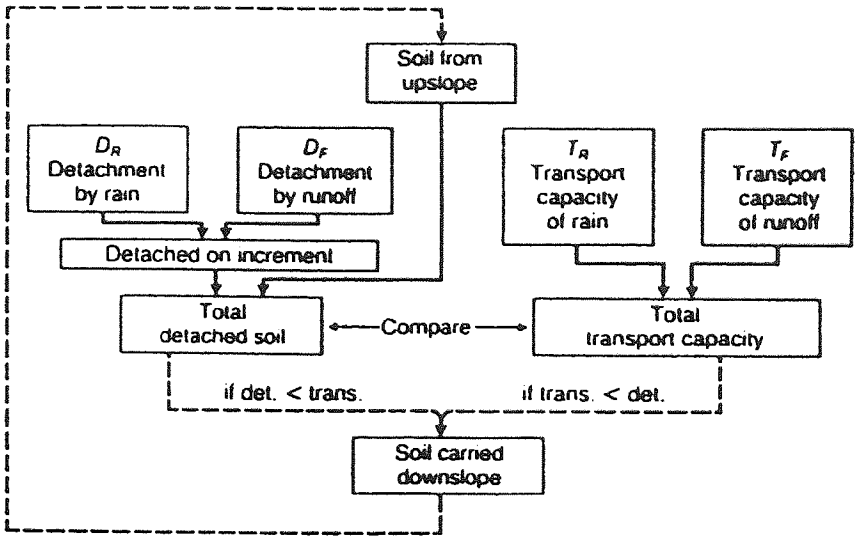

$D_R = k_1 A I^2$

$D_F = k_2 A S^{2/3} Q_w^{2/3}$ Where A = area, I = rainfall intensity,

$T_R = k_3 S I$ S = ground slope ($\sin \theta$),

$T_F = k_4 S^{5/3} Q_w^{5/3}$ Q_w = runoff

Figure 9.2 Flow Chart for Modelling the Processes of Soil Erosion by Water (from Meyer and Wischmeier, 1969)

Kirkby (1980), states that the basic modelling principles can be summarised as efficiency, range of validity and constraints. For a model to be efficient, those processes that have the greatest influence on the behaviour of the model must be simulated in the greatest detail. Quantitatively less important processes can in practise be ignored if never near dominant or dominant. If a minor process is locally dominant, it should be modelled with a minimum of parameters and complexity, and with reasonable accuracy only for its zone of dominance. However, efficiency is often borne out of simplicity providing a model does not progress into over simplification. Kirby (1980), on the subject of practicability says that, no practicable model is valid for all conditions, but a model can also gain efficiency in another sense by maximizing its range of validity for a given number of parameters. It is not, however, always possible to measure the extremes of any given situation. A good

example of which is the exceptionally high flow rates and runoff resulting from an unusually large storm that then cleans out the sediment in storage from within a catchment. The resulting sediment yields at the catchment outlet can vary quite considerably depending upon the previous storms that have occurred and thus, the quantity of sediment in storage. Kirkby (1980) lastly states about constraints that, the main constraints for an erosion model are thought to relate to conservation of mass for sediment and water, and to meeting boundary conditions at plot boundaries, and slope base as relevant. With respect to the balance of quantities, the most important is probably the sediment mass balance. Only the most sophisticated hydrological models complete a full water mass balance, as only they try to recreate the complex nature of the water cycle taking into account, surface, subsurface, inter and groundwater flows in response to a rainfall event. However, with the sediment mass balance sediment that has entered the permanent stream network, especially if the catchment is a small primary catchment, must have the same consistency and properties as the soils of the catchment from which it was eroded.

Returning to the two-phase process described by Nearing et al., (1994), the first phase of model creation involves the following stages:

1) Conceptualisation of the natural system using existing information and the development of mathematical formulae to represent the conceptualisation.
2) Solving the equations and writing the solutions in the form of computer code.
3) Parameter identification from the experimental data.
4) If required, development of methods for predicting model parameters not represented in the data set.

The second phase of model evaluation involves the following steps:

1) Evaluation of model using sensitivity analysis, confidence limit analysis and validation using the data set.

2) Determination of errors.

Nearing et al., (1994) also describe four sources of error in the modelling process:

1) Formulation of basic equations; any mathematical representation of a natural process is approximate, especially when dealing with the range of scales over which soil erosion applies. This is most applicable in an instance when a minor factor is neglected that becomes important in specific conditions.

2) Solution and coding of equations; assuming the elimination of human error, this should be a minor error, except when approximations are made for the sake of computational efficiency.

3) Experimental error and variation in experimental data; experimental data associated with erosion typically has a high degree of variation.

4) Error in the prediction of parameters; any method developed for predicting model parameters for untested situations will have some, and often a large amount of error.

With reference to discussions in sections 2.3 and 3.5, the requirements for a soil erosion model are that it has to identify areas of potentially high soil loss and to calculate the sediment yield from a catchment to study the environmental consequences of those losses. Therefore, it was decided that a sediment yield model, including soil loss output provides the most comprehensive information for conservation planners.

9.3 Modelling Options and Structure

Nearing et al (1994), discuss in some detail modelling on watershed scales; there are several key points that come out of their discussion. Mainly, that the mechanics of detachment, transport, and deposition of soil particles in a watershed are extremely complex to describe in detail. Therefore, abstraction is required to describe those more complex aspects of the erosion and deposition processes at watershed scale. Abstraction is the replacement of the complex system under consideration with a simpler conceptual model that maintains the essence of the structure without the complexity of the original relationships involved.

The first stage to developing the model was to set up a series of flow diagrams detailing the processes involved in soil erosion and its subsequent transport. The flow chart (fig 9.3) contains three key stages; the initial erosion of the sediment at source, the transport of eroded sediment, and the subsequent deposition of the eroded sediment. This three-stage simplification was decided upon as a result of studying work by Schumm (1977) and Lane et al. (1997a), the details of which are discussed in section 5.2. The basic source transport and sink model by Schumm, can be translated to modern soil erosion modelling as detachment, transport and deposition. Each stage is controlled by individual sub-processes and parameters.

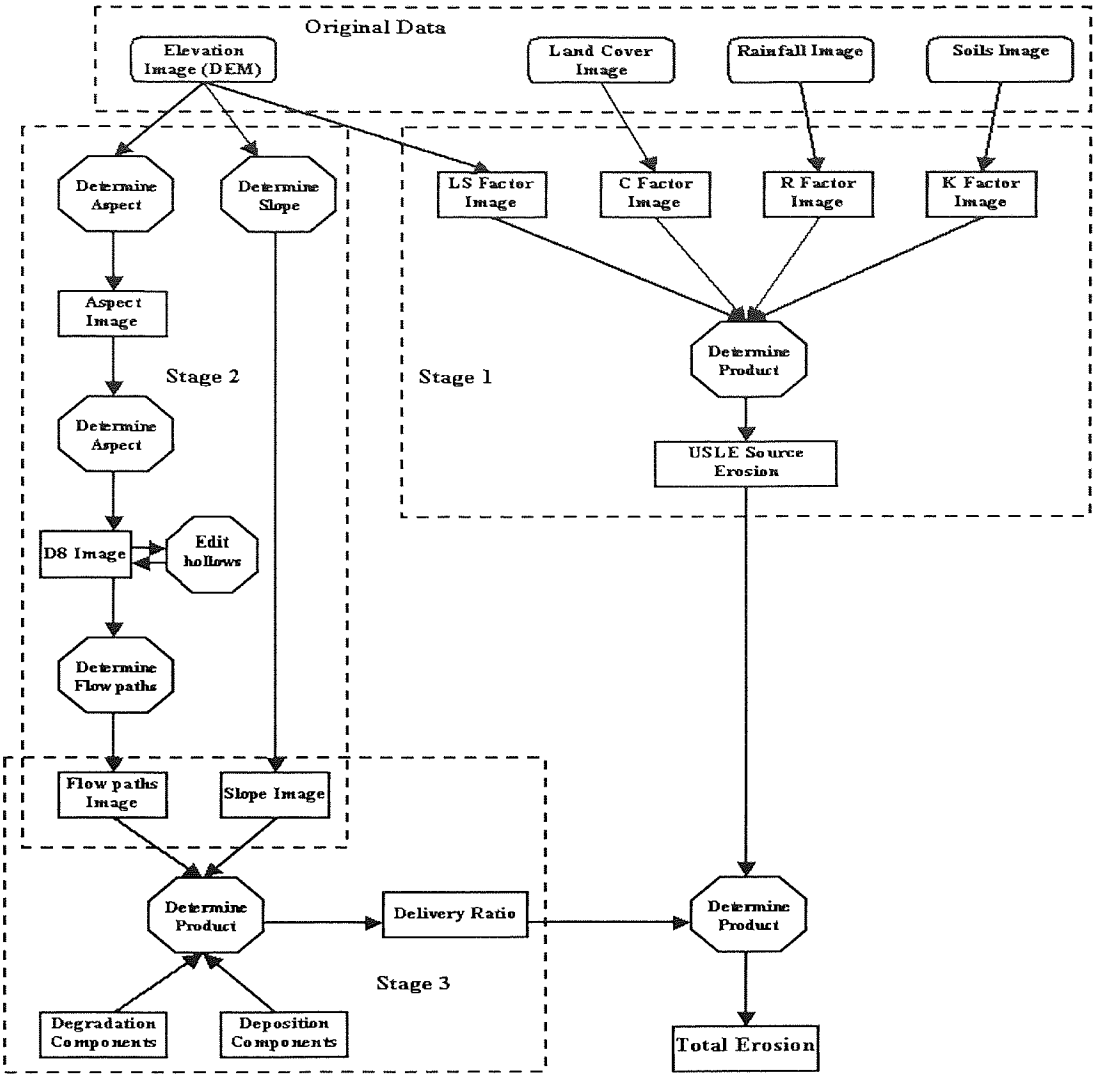

Figure 9.3 Flow Chart of the Model

The first consideration was from what approach was the modelling to be undertaken. The model can be either empirical, conceptual, physically-based or a mixture of two or all three. Bradbury et al (1993) list some useful guidelines for selection of an appropriate model type for soil erosion modelling:

1) Empirical – those which relate sediment yield to morphological characteristics of the catchment as a whole;

2) Conceptual – those which use the USLE as the basis for soil erosion prediction then modify erosion estimates to take into account delivery ratio;

3) Physically-based – those which have separate components for each erosion and sediment transport process.

When considering the flow chart, the available data and the guidelines from Bradbury et al (1993), then an empirical model becomes immediately impractical, the data series is not long enough and the data does not consist of the right sort of information. This leaves either a conceptual model or a physically-based one. Both of which are viable modelling options but both have restrictions that need to be considered.

Conceptual models have the advantage that they are often simple, efficient and easy to apply to many situations provided they can be validated. Conceptual models generally rely on two main concepts; the sediment transport capacity and the sediment delivery ratios. The CALSITE model (Bradbury et al., 1993) is a good example of such a conceptual model that can be applied to ungauged catchments, the only drawback is that the model was developed to provide annual estimates of erosion rather than single storm simulations. Providing the model can be developed to give estimates on a daily basis then it would be suitable for erosion analysis within the experimental catchment.

Physically-based models, especially when considering the complexity involved in sediment yield modelling, often require many input parameters that for Ghana were either impractical or impossible to obtain. Models such as SWAT (Arnold et al., 1993) and SWRRB (Williams et al., 1985; Arnold et al., 1990) are designed for use in ungauged catchments like the study area; however, they are very data intensive and thus they are not suitable for modelling due to the lack of available data and the method of calculating runoff. However, there are other physically-based

models, such as AGNPS, that do not require the some quantity of input parameters and use runoff calculation methods which suit the available data.

9.4 Model Development

After considering the various options available and the data that had been accumulated in Ghana, it was decided that three different version of the CALSITE model would be investigated for their suitability for application in Ghana, by testing on the experimental catchment.

9.5 CALSITE Style Model Components

The CALSITE model currently only calculates erosion on an annual basis, however, single storm modelling is also now considered to have certain advantages over annual predictions. The data that had been gathered was also for individual storms collected on a daily basis; therefore, the model had to be adapted to generate erosion predictions for these storms. This involved different methods to calculate the parameters within the delivery index. Thus, the CALSITE model to be created would incorporate an improved delivery index and delivery ratio with parameters appropriate to single storm modelling. In terms of Schumm's description of a sediment yield model (Schumm, 1977), the transport and sink sections of CALSITE are lumped together in a sediment delivery ratio, which incorporates parameters which control both the transport and deposition phases of sediment yield.

In order to derive a CALSITE style model with an altered sediment delivery ratio it was decided to first program and run the basic CALSITE model in GRASS. The results from this original run would then be analysed, which although will not be very accurate due to a lack of sufficient calibration data, will give an idea of the

potential of the model. It will also enable testing of the functionality of the model within the GRASS environment, ensuring it has been recreated correctly.

The main equations for the CALSITE model are discussed in section 3.6.4 and thus will not be reiterated here. The equations of the model that are altered are discussed in the following sections. Certain aspects of the model are not discussed within the report on CALSITE, for which assumptions were made about the methods used, these are also discussed in the following sections.

Given the complications and problems with programming in GRASS (see section 9.6), the CALSITE program had to be written in several different sections as opposed to one single module. The first section calculates source erosion outputting a source erosion map. The second calculates the flow paths and outputs a text file of the flow paths; the values contained within the flow paths map also represent the effective drainage area. After the flow paths map has been imported into GRASS, the next section calculates the delivery index values from the flow paths map, rainfall map and slope map, and scales the delivery index values from one to a hundred. The fourth section subsequently calculates and outputs as a text file a table of total erosion for each combination of values of s and t (the parameters within the delivery ratio equation 3.42). The final section calculates and produces a map of total erosion using the user selected final values of s and t.

9.5.1 Source

To generate source erosion it was decided to keep with the principles of the CALSITE model and use the USLE equation to predict source erosion. With reference to discussions in section 3.6.4, and in agreement with the assumptions made by Bradbury et al. (1993), the LS factor was reduced to a function of slope steepness

only, as the effects of slope length and thus runoff are dealt with in the transport section of the model.

The various factor equations that were used for the K, S and R parameters were taken from decisions made in chapter 6 and section 8.2 such that:

$$R = \frac{2.5P_a^2}{100(0.073P_a + 0.73)} \qquad \text{Equation 9.1}$$

$$K = \left(0.2 + 0.3e^{(-0.256SAN(1-SIL/100))}\right)\left(\frac{SIL}{CLA + SIL}\right)^{0.3}\left(1 - \frac{0.25C}{C + e^{(3.72-2.95C)}}\right)\left(1 - \frac{0.7SN1}{SN1 + e^{(-5.51+22.9SN1)}}\right) \qquad \text{Equation 9.2}$$

$$S = -1.5 + 17/[1 + (2.3 - 6.1\sin\theta)] \qquad \text{Equation 9.3}$$

C factors are dependent upon land-use type and were resolved in section 6.3.4 and based upon the field studies in chapter 4, such that, figure 9.4 shows a map of the land use types and associated C factors for the various cover conditions found within the experimental catchment.

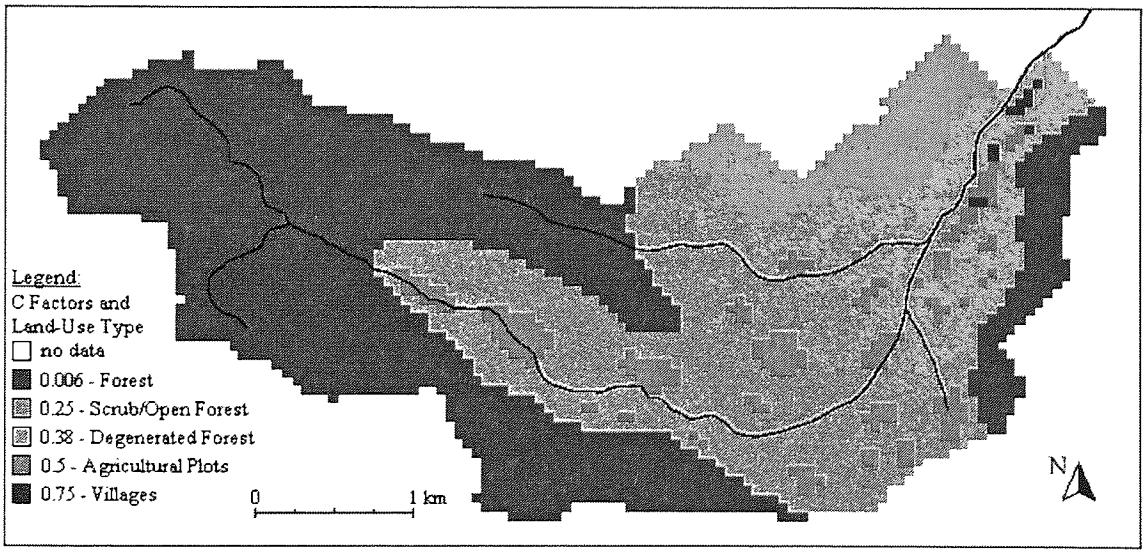

Figure 9.4 C Factors and Associated Land Use Types

The source calculations are virtually identical for both types of the CALSITE model except that for the single storm version the R factor values will vary due to the

decrease in rainfall under analysis. There are two ways to calculate the R factor for a single storm, either the rainfall value for the storm is substituted for the annual rainfall value within the R factor equation, or the R factor is taken as a proportion of the total R factor for the annual rainfall, such that:

$$R_{storm} = \frac{stormrain}{annualrain} R_{annual} \qquad \text{Equation 9.4}$$

where R_{storm} is the R factor for a single storm, *stormrain* is the amount of rainfall for a storm, *annualrain* is the total annual rainfall and R_{annual} is the annual R factor.

Both options were considered when running simulations with the model to see which gave the best results. As the R factor equation is not exactly linear then the two methods will give slightly different results.

The best method is a matter of debate and depends upon the interpretation of the R factor within the USLE. If the R factor is taken to be a direct relationship between rainfall and potential erosion (erosivity), such that x mm of rainfall will produce an erosive potential of y, then the substitution of the rainfall quantity for the storm directly into the R factor equation will be correct. However, if the R factor is considered to be the total effect of the sum of the storms throughout the year then the R factor for an individual storm has to be taken as a proportional value of the total annual R factor. A resolution of the issue is best found within the calibration and validation of the model by using both methods to see which give the best results in predicting erosion.

9.5.2 Transport and Sink

The principles of the two models for the transport and sink are the same. The theoretical amount of erosion that will be transported to the catchment outlet is

determined from a delivery index. However, the delivery index will differ between the two models.

9.5.2.1 Annual Model

The first version of the CALSITE model was written almost identically to the original model. This had two main advantages. Firstly, it enabled testing of the model to be undertaken to check that the model had been coded correctly and was producing realistic results. Secondly, the results gained, although uncalibrated because CALSITE calculates annual estimates of sediment yield that could not be verified with the available data, would give an idea of the range of possible values for sediment yield through the variation of the parameters s and t, from equation 3.42.

The first calculation for the transport and sink section of the model is to create the flow paths map. To calculate flow paths a routing algorithm is used which creates a map of the number of cells that contribute flow to each of the cells throughout the catchment. Although the specific details of the routing algorithm used within the CALSITE model are not given, Bradbury et al. (1993) mention an aspect driven routing structure and thus it is assumed that routing is undertaken using the D8 algorithm. Additional modifications were also made to compare the effects of using the FD8 algorithm to generate the flow paths map instead of the standard D8 algorithm.

The only alteration to the original CALSITE model was within the working of the delivery index equation. The original equation specifies that the delivery index value for a pixel is the minimum value of a function of slope, drainage area and rainfall, along a flow path from source to stream network.

Two main alterations were made that were also maintained in the single storm versions of the model. The first alteration was to the way in which the delivery ratio is calculated. The CALSITE report implies that each flow path is routed from source to stream network and then delivery indices are calculated on this flow paths image. However, for ease of programming, the flow paths were calculated directly to the catchment outlet at first and delivery indices calculated based on this image. Then the delivery ratio was calculated for each cell in the catchment and finally this image was combined with a streams image such that each pixel in the path of the streams network had its delivery ratio changed to one. This method will create the same results but was considered easier to program within the GRASS environment.

The second alteration was to the delivery index itself. The delivery index in CALSITE is expressed as a minimum value of the equation from the point of source to the cell on the flow path under analysis.

The rainfall is considered constant across the catchment rendering the specification of a minimum value irrelevant. For each pixel, the minimum value of the flow path parameter (which is equivalent to the drainage area) is the source pixel itself, if this is taken as a minimum value, then the F parameter within equation 3.41 will be the same for each cell. This will result in a reduction of the runoff generated in the model.

Thus, the only effective parameter in the equation is the slope value, which is more than likely to be at a minimum value at the last cell before the flow path reaches the stream network. This creates a natural sink at the cells before the stream network that the model does not allow to be flushed out, a process that is almost certain to happen with high intensity storms in tropical environments. Therefore, the predicted sediment yield values will be lower than those measured as the model allows sediment

to be dumped within the final cells of each flow path. Instead, for the version of CALSITE programmed in GRASS, when calculating the delivery index for each pixel the values of slope, drainage area and rainfall were used for the pixel. This then treats each pixel as the catchment outlet as flow is progressively routed through the catchment; the amount of sediment passing through that cell is dictated by the attributes of that cell, rather than the cell at the end of the flow path. Sinks are still created at the lower slope value cells near the stream network, but because every slope is taken into account, and not just minimum values, more sediment is allowed to reach these points and thus more sediment will pass through.

9.5.2.2 Single Storm Model

To enable single storm modelling to be simulated the delivery index needed to be changed so that the parameters represented those that influence the movement of sediment under those conditions. The delivery index used in CALSITE is adapted from the sediment transport function proposed by Govers (1990), such that:

$$X = kQ^{a-1}S^{b} \qquad \text{Equation 9.5}$$

where Q is the runoff volume, S is the slope and a and b are parameters dependent upon the D_{50} particle size taken from the work by Govers.

The sediment transport function developed by Govers is independent of time and thus is applicable to both annual and single storm erosion simulations. Therefore the parameters that represent the runoff volume need altering as CALSITE represents annual runoff volume as the drainage area multiplied by the annual rainfall to the power x. This relationship between annual rainfall and runoff is unlikely to be appropriate for single storm modelling. The equation for Q is represented by:

$$Q = FP_a^x \qquad \text{Equation 9.6}$$

where F is the flow path index, P_a is the annual rainfall and x is the parameter that represents the relationship between annual rainfall and runoff. The flow paths index is the effective drainage area and represents the 'catchment' size by the number of flow paths that cross any one particular cell. To calculate the final total transported erosion then the cell size and catchment area is taken into account to convert the readings to t/ha/yr.

To replace the rainfall-runoff relationship a function/method was required that was appropriate to the measured data. There are many rainfall runoff models available, such as; the HEC-1 model, the rational method, the unit hydrograph method and the time-area method.

However, all these models are dependent upon the time of concentration or other such time dependent measures and parameters dictating the response of a catchment, in terms of peak flows etc., to a certain quantity of rainfall. Although all of these models could have been used, without sufficient data available on the nature of the catchment in response to rainfall to calibrate these models, the use of such methods only adds another dimension of irresolvable uncertainty into the model. There are other methods available to calculate runoff that are independent of time. One such model is the SCS (Soil Conservation Service) Curve Number method. Although developed in the US and based upon the soil types of the US, sufficient guidelines are available in the report to adapt the parameters to the situation and environment to which the method is to be applied.

9.5.2.3 Alternative Sediment Transport Function

An alternative sediment transport function was also considered for the single storm model that was proposed by Meyer and Wischmeier (1969). Their function was

very similar to that proposed by Govers but places an equal emphasis on the runoff and slope parameters such that:

$$T_F = S_{TF} S_l^{5/3} Q^{5/3} \qquad \text{Equation 9.7}$$

where T_F is the runoff transport capacity, S_{TF} is a coefficient dependent upon the soils transportability properties, S_l is the slope of the energy grade line of the flow and Q is the flow rate.

Applying the same principles as applied to the Govers sediment transport function and dividing by Q to express the relationship in terms of the concentration of transported sediment then equation 9.7 becomes:

$$X_F = \frac{T_F}{Q} = S_{TF} S_l^{5/3} Q^{2/3} \qquad \text{Equation 9.8}$$

For overland flow then the slope of the energy grade line can be approximated to the land slope S_L and the flow rate Q can be expressed in terms of the effective drainage area multiplied by the runoff volume then the final equation becomes:

$$X_F = S_{TF} S_L^{5/3} Q_R^{2/3} F^{2/3} \qquad \text{Equation 9.9}$$

where Q_R is the runoff volume and F is the flow path index that gives the effective drainage area.

To calculate the runoff volume the curve number method was adopted as before.

9.5.3 Model Variations

Within the model, several variations of parameters could be considered. Three flow routing algorithms were used to calculate the flow path index and thus the effective drainage area. As previously stated, section 9.5.1, two alternative R factor calculations were considered and both of the sediment transport functions. Modules

were also written for both the annual version and the single storm version of the model.

9.6 Modelling Environment and Programming

The model was to be created using the GRASS-GIS software package, chosen for the ease of user-designed module creation. GRASS runs on either the UNIX or LINUX platforms and is coded in the C programming language. GRASS is an open source software package and is written under the GNU GPL (GNU Public License), this enables developers and testers from all around the world to work on code for the package, which is centrally organised, de-bugged and tested at a base, which at the time of writing was set up at the ITC-irst, Trento, Italy. It comes with a complete set of pre-defined C functions specifically designed to enable user programming for the data manipulation side of the GIS.

Documentation on the pre-programmed modules and how to program user-defined modules can be found at the GRASS-GIS website (2003).

The GRASS-GIS programming environment provides a large selection of pre-defined database management functions; in the case of the raster map type the most commonly used functions were for opening and closing maps, reading and writing progressive rows of data and assigning memory buffers for temporary storage of data to perform operations on. Pre-defined storage classes are also provided, that are equivalent to the standard C classes but tailored specifically for raster manipulations (e.g. CELL ≡ integer, FCELL ≡ float, etc.).

However, programming C code for GRASS is not without its difficulties. Because it is open source, bugs can slip through the net, and because LINUX is written under the same license, it has the same problems and this means that machine

dependent bugs can occur. This can result in occasional very unpredictable behaviour when running the software and occurs on a much more regular basis when writing additional, non-standard modules to be attached. Bugs can occur within the program such that a change within one function can result in another function within the module no longer working.

The main programming limitation that had to be overcome in order to perform the required type of modelling was GRASS and C's lack of ability to handle two-dimensional arrays. Although within C a two dimensional array can be set up as a one-dimensional array of pointers each of which, point to a one-dimensional array, this method failed causing a segmentation fault, possibly due to a machine dependent error. However, a segmentation fault error is often very hard to resolve and this may not have been the actual cause, which still remains undetermined.

Instead a parameter declaration of FCELL drainage_area[no_rows][no_cols] was used. This could not be written to a GRASS raster map, and had to be outputted as a text file and re-read into GRASS as an ASCII text file after an appropriate header had been added. Two-dimensional arrays were required for the routing algorithms when in programming terms it was necessary to be able to store the entire DEM within memory at the same time whilst the program was running.

The final code for all the program modules for all the model variations can be found in appendix A. The following sections describe the general principles involved in programming each of the stages of the CALSITE model.

9.6.1 Drainage Area and Flow Path Index Calculations

To calculate the flow path indices two separate approaches can be taken for the flow routing algorithms. Routing can be calculated either by routing flow from

each square within the catchment to the catchment outlet calculating the flow path from every cell one at a time, or by simultaneously routing from all primary squares progressively to the catchment outlet.

The single flow path routing program works by holding open a raster map record of all cells that are part of the catchment, the program then moves progressively column by column, row by row, through the raster map until it finds a cell that is part of the catchment. Then the program enters another loop and using pre-defined D8 routing directions in another map adds one to the drainage area map for each cell that it passes through as it is routed to the catchment outlet.

The progressive routing works by keeping two temporary maps open of the catchment area, one of which contains the cells to which flow has currently been progressed. The second holds a record of all cells to which flow will be passed for the next cycle of the loop. A pair of variables holds the row and column number of the catchment outlet so that once a flow path reaches that point it is terminated.

Both the programming algorithms were used to calculate the D8 and FD8 algorithms. The drainage area for the D8 algorithm was calculated using the one flow path at a time programming algorithm and the FD8 algorithm was calculated using the simultaneous routing of flow from each of the primary squares. The programs were written in this way for ease of programming. Although the second method is much more memory intensive because the FD8 algorithm splits flow from each cell to all downhill cells, the progressive routing algorithm is a much easier program to adapt for the FD8 algorithm. The one flow path at a time program because of its simplicity is adequate for the D8 routing algorithm.

9.6.2 Source Erosion Calculations

Source erosion calculations are relatively simple. The program works by opening all the maps containing the USLE factors and then row by row, it multiplies the values of the four factor maps together for each cell, outputting the result to the corresponding cell of the source erosion map.

9.6.3 Delivery Index Calculations

Delivery index calculations are performed using the same principle as the source erosion calculations, reading in each of the input maps and variables for the delivery index calculations, performing the mathematical functions and then outputting the results to the delivery index map. There is one small difference, on the first instance of calculating the delivery index, the value of the maximum delivery index is held in a variable so that in the second loop, delivery index values can be scaled from 0 to 100.

9.6.4 Delivery Ratio Calculations

The delivery ratio calculations are done in two separate GRASS modules. The first module again using the row by row principle described before, calculates the total transported erosion for all the possibilities of s and t (parameters from equation 3.42) for all occurrences that s is greater than or equal to t. These results are outputted to a text file for user analysis. The second module for delivery ratio calculations allows the user to specify selected values of s and t and calculates the total transported erosion for those values outputting the results in a transported erosion raster map.

9.7 Summary

Due to a lack of accurate and reliable field data collected from Ghana, the model cannot be tested using real data and will therefore not be able to provide estimates of the erosion rates that are currently occurring in areas where forest is being turned over for agricultural use. However, in the next chapter guidelines and procedures for the calibration and use of the model are drawn up; and examples of how to employ the model for prediction purposes are demonstrated using the data that was collected.

Chapter 10

Application of the Model

10.1 Introduction

The application of the model requires two stages: (i) calibration of the parameters – USLE (Wischmeier & Smith, 1978) factors and then the runoff parameters, and (ii) the running of the model.

Of the two modelling options available, either single-storm or annual, it is recommended that the single storm modelling option is utilised. Single storm modelling allows specific conditions to be simulated rather than an average of an entire year. This allows researchers to identify occasions when the environment is most vulnerable to erosion, C factors can reflect the current ground cover conditions and R factors the quantity of rainfall falling during the course of the storm.

10.2 Derivation of Parameters

10.2.1 USLE Factors

The nature of all of the USLE factors has been discussed in detail during earlier chapters and so will not be repeated here. The following sections describe the methodologies that are recommended to derive the factors for use within the model.

These however, are not set in stone. Because the program is written in C code, the source for which is included in the appendices, the model can be tailored and adapted to include revised methodologies for deriving and generating the factor values.

10.2.1.1 R Factors

As discussed in 9.5.1, R factors can be calculated in two ways, either directly or proportionally.

Using the data collected as an example, table 10.1 shows the differences that occur when using the two methods to calculate R factors. Further work needs to be carried out in calibration with accurate datasets in order to assess which more accurately represents the erosive power of a storm.

Storm Date	20/09/00	21/09/00	30/09/00	24/10/00	25/09/00
Rainfall (mm)	0.8	5.1	10.7	13.1	19.7
R Factor (direct)	0.020	0.590	1.894	2.544	4.475
R Factor (proportional)	0.272	1.731	3.632	4.447	6.688

Table 10.1 R Factors for Individual Storms

10.2.1.2 C Factors

There have been many proposed methods for deriving C factors, such as the derivation through measured parameters as used in the RUSLE (Renard et al, 1991), and the use of experimental plots as used in the original USLE. Both of these methods, however, are lengthy processes requiring large amounts of preliminary work to be undertaken. Because many experimental studies have already been carried out using the USLE, there is a large amount of data and calculated C factor values already available. It may often be easier under a restricted budget to utilise these values, which generally are accompanied by good descriptions to match the prevailing conditions found within the study area.

It should be recognised, though, that this is probably the largest cause of systematic errors within the model.

10.2.1.3 S Factors

The equation used to derive the S factors (slope lengths are not included), is discussed in section 9.5.1. However, it is worthwhile reiterating that the program can be adapted if necessary to adopt a different S factor equation, or even an equation for L factors as well.

10.2.1.4 K Factors

Assuming that particle size analysis can be performed then it is recommended that the equation developed for use in the RUSLE is used to derive K factor values. When used in conjunction with the particle size data discussed in section 8.1.4.1, the values that were derived (see section 8.2) were identical (to two decimal places) to those values that had been derived previously by matching the soils to FAO soil types.

However, if particle size data is not available then as with the C factor values, K factors can be derived from other literature, matching the descriptions of soil types to the soils found within the study region and then using the appropriate values.

10.2.2 Model Parameters

10.2.2.1 Govers' Parameters

Bradbury et al (1993) state that Govers (1990) undertook extensive experimental studies of sediment transport under conditions of overland flow in a sloping laboratory channel containing sediment of different sizes. The results of this are shown in table 10.1 according to the D_{50} grain size and laminar or turbulent flow.

D_{50} sediment size (μm)	Laminar Flow			Turbulent Flow		
	a	b	Correlation coefficient (r^2)	a	b	Correlation coefficient (r^2)
58	1.65	1.62	0.98	1.66	1.44	0.87
127	1.55	1.27	0.98	1.80	1.69	0.95
218	1.70	2.50	0.98	1.50	1.96	0.98
414	1.53	1.97	0.96	1.24	1.71	0.99
1098	1.73	1.76	0.98	1.04	1.47	0.97

Table 10.2 Sediment Transport Results from Govers (1990)

Bradbury et al (1993) also state that it may be assumed that, for long flow paths crossing several cells in relatively steep terrain, the main sediment transporting flow is likely to be turbulent. Figure 10.1 shows the graph of the Govers' parameters a and b for turbulent flow.

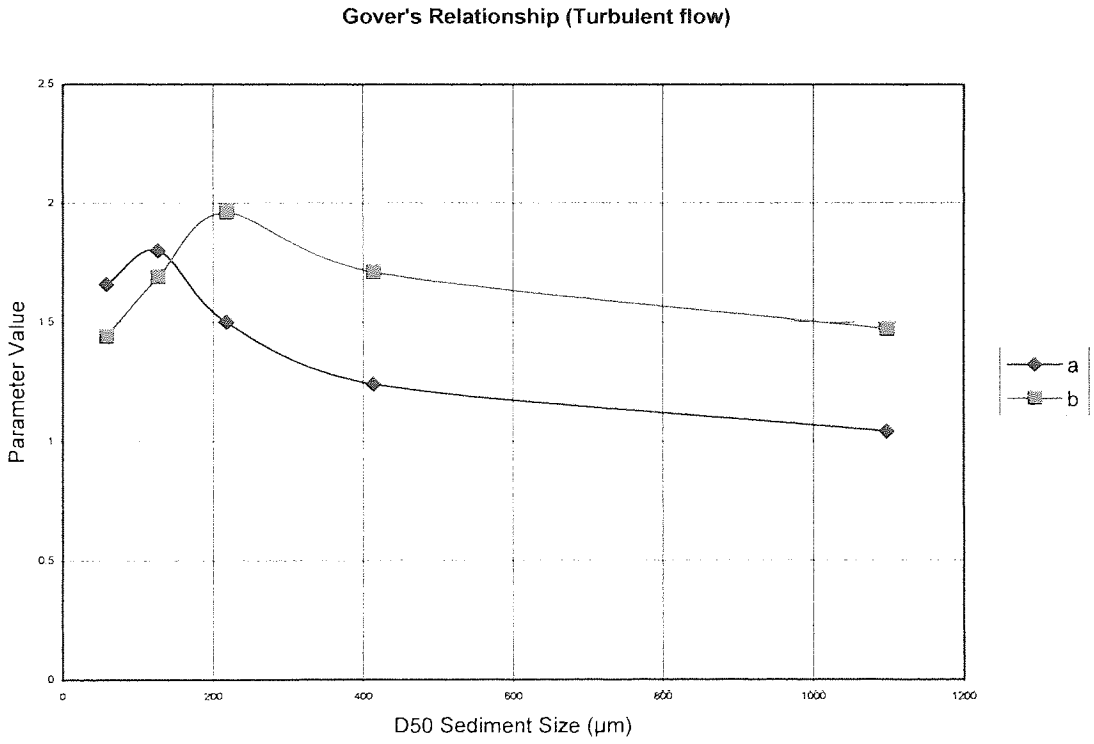

Figure 10.1 Govers' Relationship Parameters for Turbulent Flow

As an example, using the particle size distribution data in section 8.1.4.1 (table 8.9), the D_{50} sediment size can be calculated for each soil type. Each of the soil types has a similar particle size distribution, thus it is reasonable to take an average value of the D_{50} results from all soil types. The resultant D_{50} size is 190μm, therefore from figure 10.1, the resultant Govers' parameters are:

a = 1.56

b = 1.90

Therefore, equation 9.5 becomes:

$$X = kQ^{0.56}S^{1.9} \qquad \text{Equation 10.1}$$

10.2.2.2 s and t Parameters

The s and t within the sediment delivery equation of CALSITE (eq. 3.42) parameters are calibration parameters that represent the catchment characteristics for the routing of flow and transport of erosion, i.e. hypothetical saturation and threshold points for transport across a cell within the catchment. The graph (see figure10.2) on which s and t operate controls the amount of total erosion (TE) that passes through each grid cell. The threshold point is the point at which erosion starts to be transported across a cell and lies between 0 and 50, before which no erosion is transported across the cell. The saturation point, which lies between 1 and 100, is the point at which all the erosion is transported across the cell. The model provides solutions for all values of s and t across the catchment.

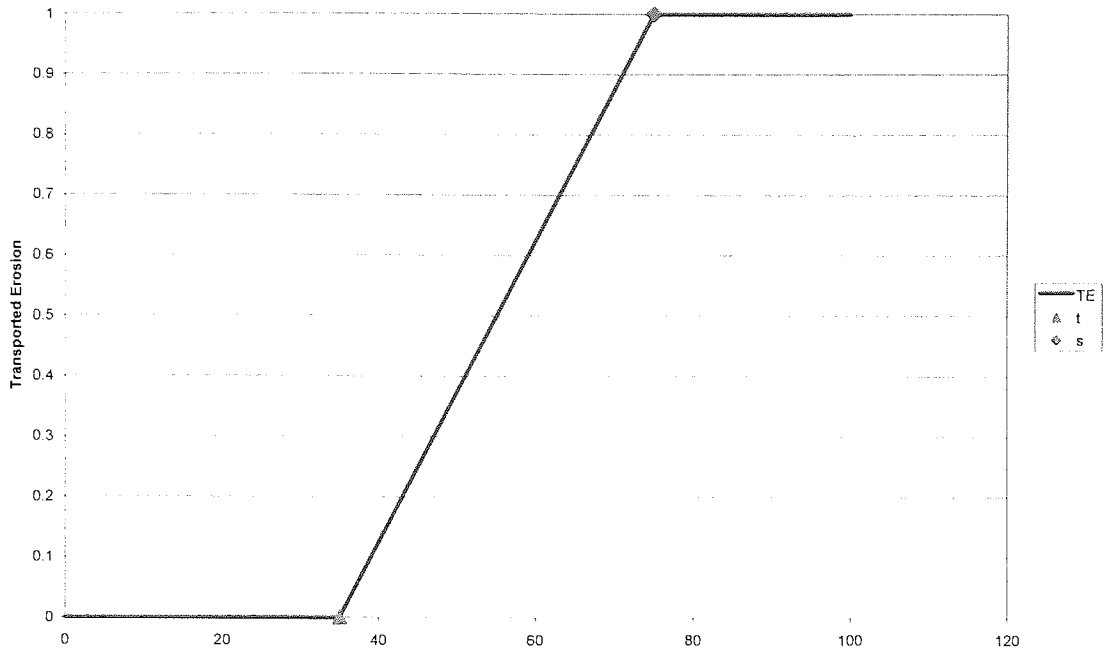

Figure 10.2 The s and t Parameters within the CALSITE model

10.2.2.3 Runoff Parameters

The runoff parameters when calculated by the method used in the CALSITE model (Bradbury et al, 1993) are discussed in sections 9.5.2.1 and 9.5.2.2. The parameters are derived directly from input information into the model, i.e. the DEM (from which is generated a map of flow density) and total rainfall. Whilst testing the principles of model with the unreliable field data, the curve number method was programmed and used, it is described below.

Details of the curve number method for calculation of runoff can be found in ASCE (1996). The principles of the curve number method for calculating runoff are as follows:

1) Soils are assigned to a hydrological group (A-D) based on infiltration rates or soil types and descriptions, from the guidelines provided.

2) Tables are provided to assign a curve number to each land-use type based upon the hydrologic soil group and the hydrologic condition of the land.

3) Curve numbers (CNs) are converted to the correct antecedent moisture condition (AMC I, II or III) using the provided tables. Curve numbers from the land use table are given for AMC II.

4) Runoff is calculated as a function of curve number and rainfall such that:

$$Q = \frac{(P - 0.2S)^2}{P + 0.8S} \qquad \text{Equation 10.2}$$

$$S = \frac{2540}{CN} - 25.4 \qquad \text{Equation 10.3}$$

where Q is the surface runoff (mm), S is the soil retention parameter (mm), P is the rainfall (mm) and CN is the curve number.

Curve numbers that were calculated for each land use type are given in table 10.3. Hydrological soil group A was used, which covers sands, loamy sands and sandy loams. AMC II was used to describe the antecedent moisture condition, which defines the average conditions. This AMC category was selected because although the soils were quite dry (a condition in the guidelines more appropriate to AMC I), observations showed that the infiltration rates were relatively low for a dry soil and thus to compensate AMC II was selected (note: 30 is the minimum CN applicable regardless of land use and AMC).

Land Use Type	C Factor	CN
Forest	0.002	30
Degraded Forest	0.14	31
Open Scrub	0.2	35
Agricultural Land	0.38	72
Villages and Settlements	0.75	77

Table 10.3 Land-use types and associated C Factors and Curve Numbers

10.2.3 Slope and Drainage Area Method

The model also incorporates modules that allow variations in the calculation method for slope and drainage area to be included.

The available methods for calculating the slope are the maximum downward gradient, maximum downhill slope and finite differences. The methods available for calculating drainage area are the D8 and FD8 algorithms.

10.3 Running the Model

As stated in chapter 9 the model can be run on either an annual or a single storm basis. The following two sections will describe briefly how the model is operated for each of these and show examples of output from the model when using some of the data collected from the experimental catchment. Due to the invalidated nature of the data from the catchment the results shown cannot be used to reliably predict erosion from the catchment, but instead should give a user an idea of the results that can be expected when using certain sets of values.

10.3.1 The Annual Model

When the model is run, the user is presented with a series of options to make and required inputs to enter. The model is also split into several modules to simplify the process and to distinguish the outputs of each of the various stages. The first

module calculates the source erosion, the second calculates the range of possible predictions of erosion and the third allows the user to input specific values of the s and t parameters to gain a final map of total predicted erosion for each of the grid squares. Table 10.4 shows the inputs and outputs for each of the three modules.

Modules	Inputs	Outputs
1 - Source Erosion	Maps: K factors, C factors, DEM and rainfall. Parameters: Slope calculation method.	Maps: Source erosion per grid square
2 – Erosion Ranges	Maps: Source erosion, DEM, rainfall.	Maps: Drainage area and flow rates. Tables: Values of erosion for all values of s and t.
3 – Total Erosion	Maps: Source erosion, drainage area and flow rates.	Maps: Total erosion per grid square.

Table 10.4 Program Modules: Inputs and Outputs

The annual model was run with all the possible variations of slope and drainage area methods. Table 10.5 shows the maximum, minimum, average and standard deviations of the transported erosion values for each of the two routing algorithms and each of the three slope calculation methods.

CALSITE annual results						
Simulation	1	2	3	4	5	6
Slope Method	Maximum Downward Gradient	Finite Differences	Maximum Downhill Slope	Maximum Downward Gradient	Finite Differences	Maximum Downhill Slope
Drainage area Method	D8	D8	D8	FD8	FD8	FD8
Transported Erosion (t/yr)						
Maximum	27386.48	28494.27	11701.27	31598.46	31014.91	13003.95
Minimum	25.33	19.50	10.21	44.58	66.36	42.21
Average (mean)	217.02	590.62	101.64	1634.42	1446.56	1238.93
Standard Deviation	1007.77	1940.56	524.48	3652.68	3415.72	1902.97
Median	89.20	67.80	26.59	402.98	371.30	509.72

Table 10.5 Results from Annual CALSITE Simulations

The results from the annual CALSITE simulations in table 10.5 generally reflect the estimations of the effects of slope that were demonstrated in table 5.3. The maximum downhill slope method consistently resulted in considerably lower estimations than the other two methods. However, by using the FD8 algorithm for distributing flow, the maximum downward gradient for calculating slope produced slightly higher results for predicted annual erosion. This may be either an artefact of the specific data used or a direct outcome of the FD8 algorithm, however, as the differences are relatively small, a series of analyses on different catchments would be needed to determine which is the case.

Figures 10.3 to 10.8 show the variation of the total transported erosion values against the values of s and t for each of the six combinations.

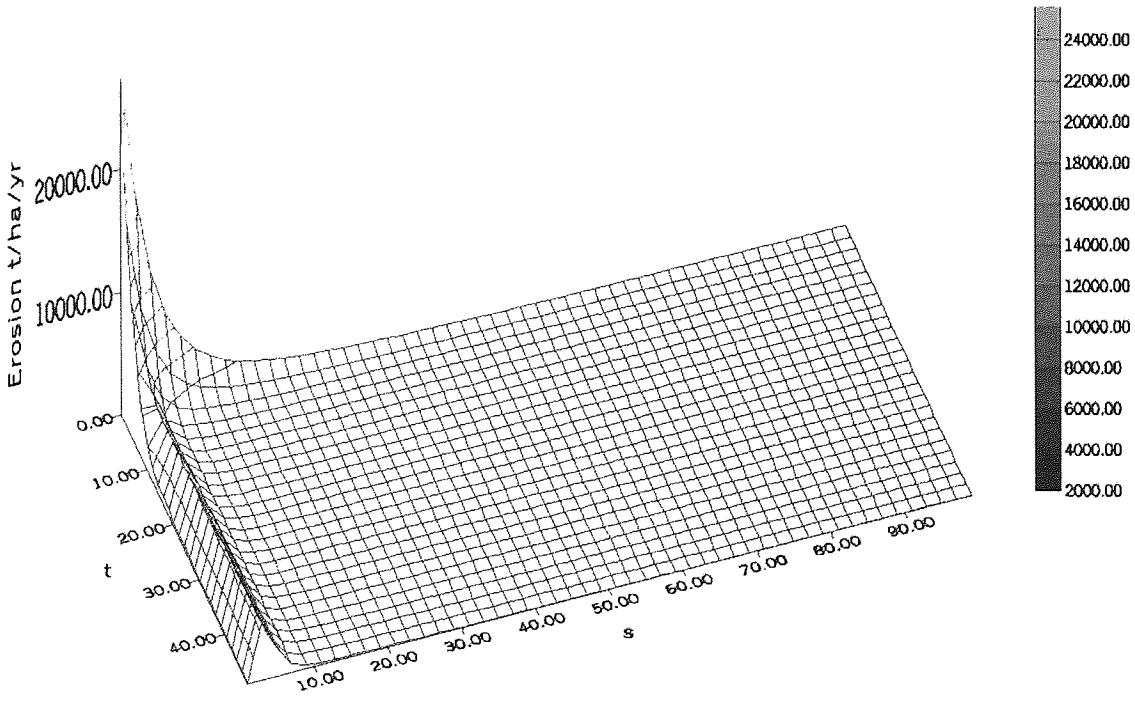

Figure 10.3 Total Transported Erosion for Variations of s and t – Simulation 1

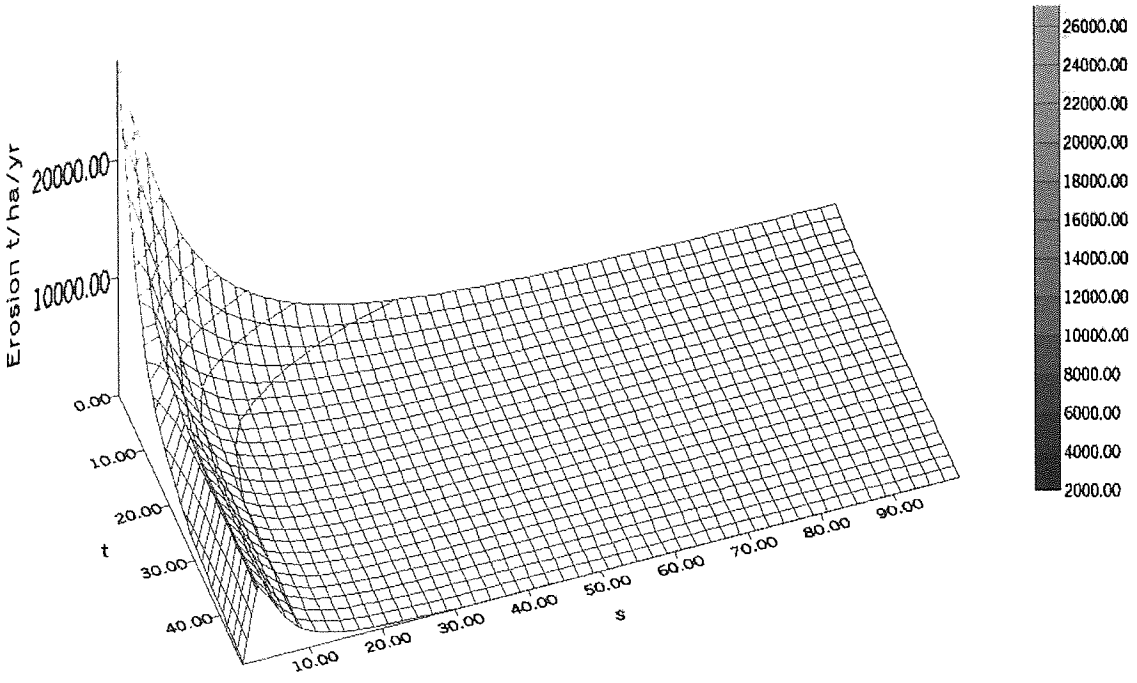

Figure 10.4 Total Transported Erosion for Variations of s and t – Simulation 2

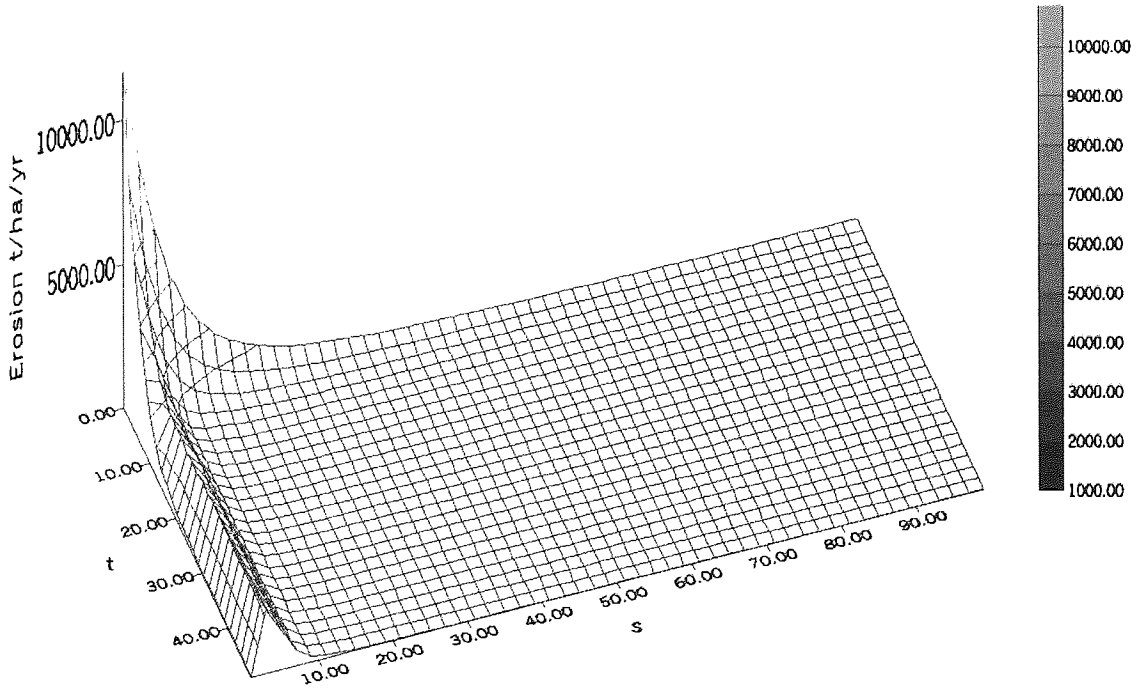

Figure 10.5 Total Transported Erosion for Variations of s and t – Simulation 3

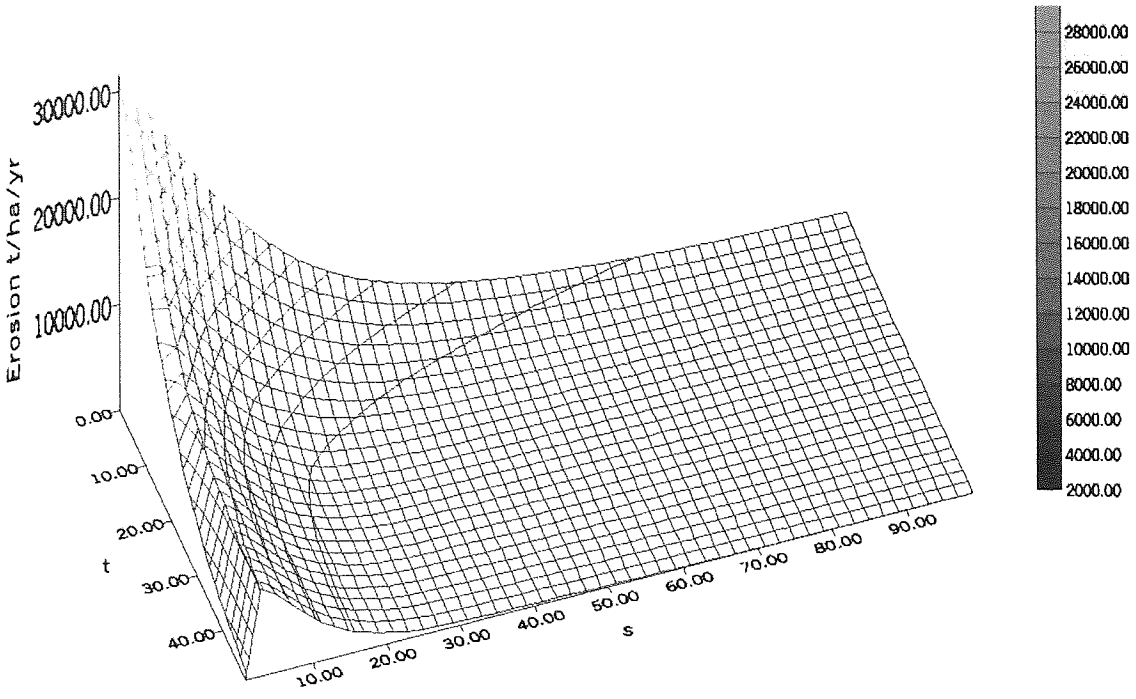

Figure 10.6 Total Transported Erosion for Variations of s and t – Simulation 4

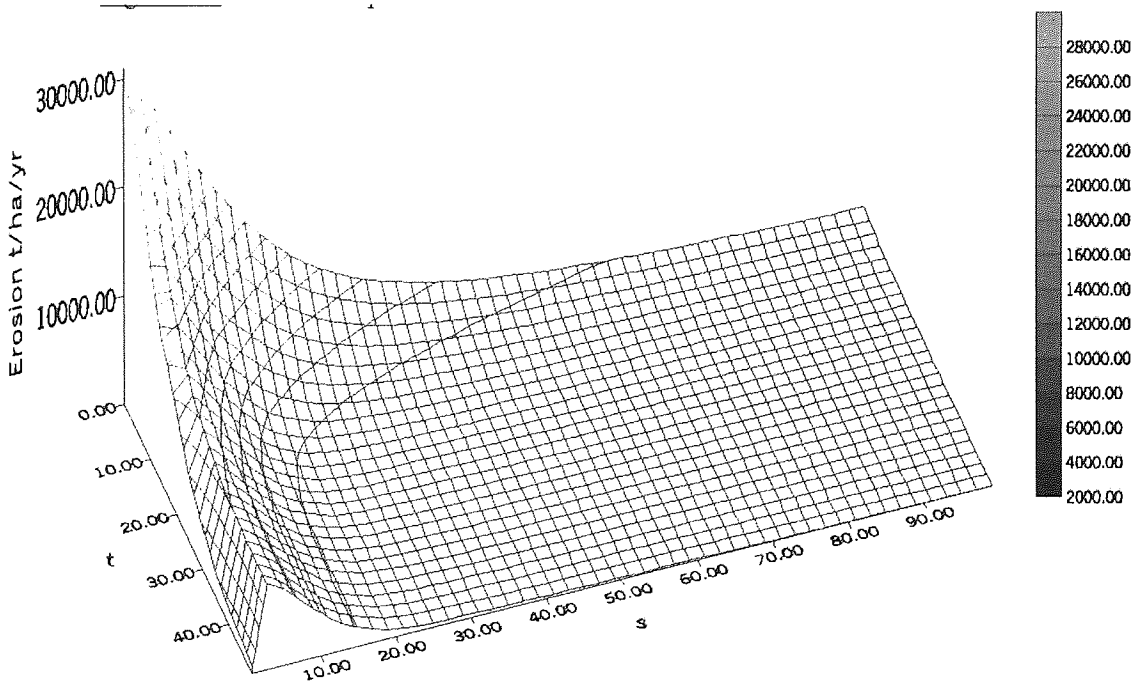

Figure 10.7 Total Transported Erosion for Variations of s and t – Simulation 5

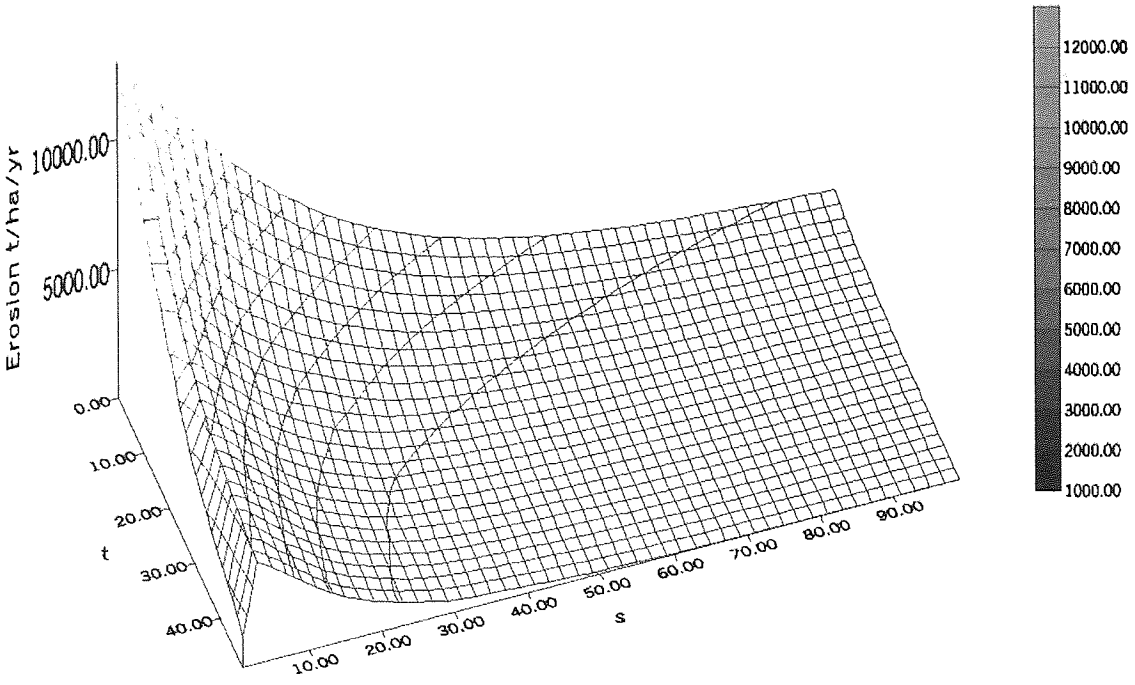

Figure 10.8 Total Transported Erosion for Variations of s and t – Simulation 6

Figures 10.9 to 10.14 show the transported erosion maps associated with the average total erosion values for each combination of the two routing algorithms and three slope calculation methods (table 10.5). Arbitrary values of s and t were looked up from the data that created the erosion surfaces (figures 10.3 to 10.8) and fed into the last section of the annual CALSITE GRASS module to calculate total transported erosion.

In reality, the tables of s and t would be calibrated for several known values of erosion and rainfall to find a best fit, for the values of s and t given in the output tables from the model.

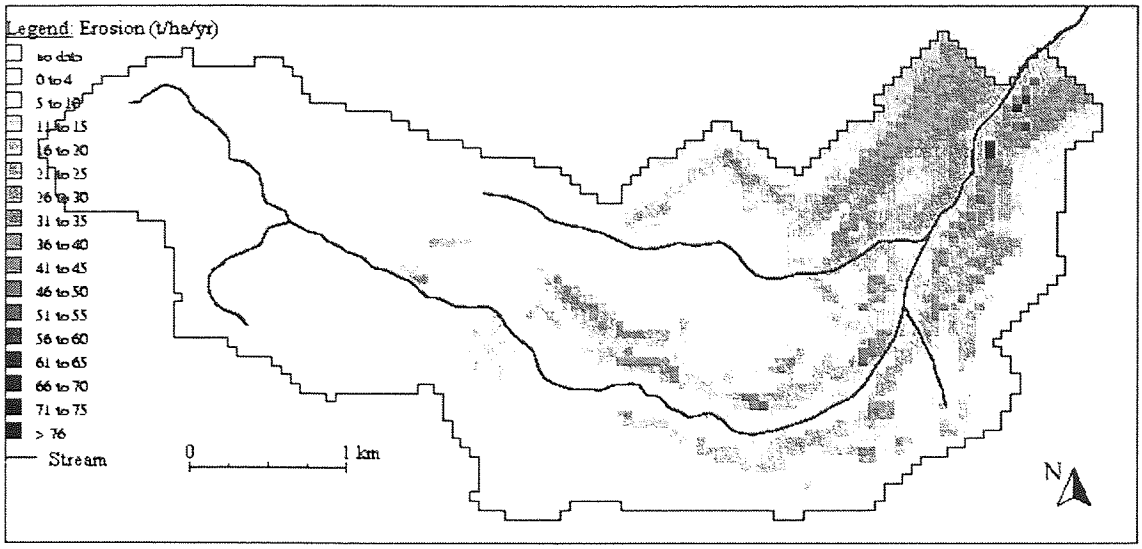

Figure 10.9 Total Transported Erosion per pixel for Simulation 1

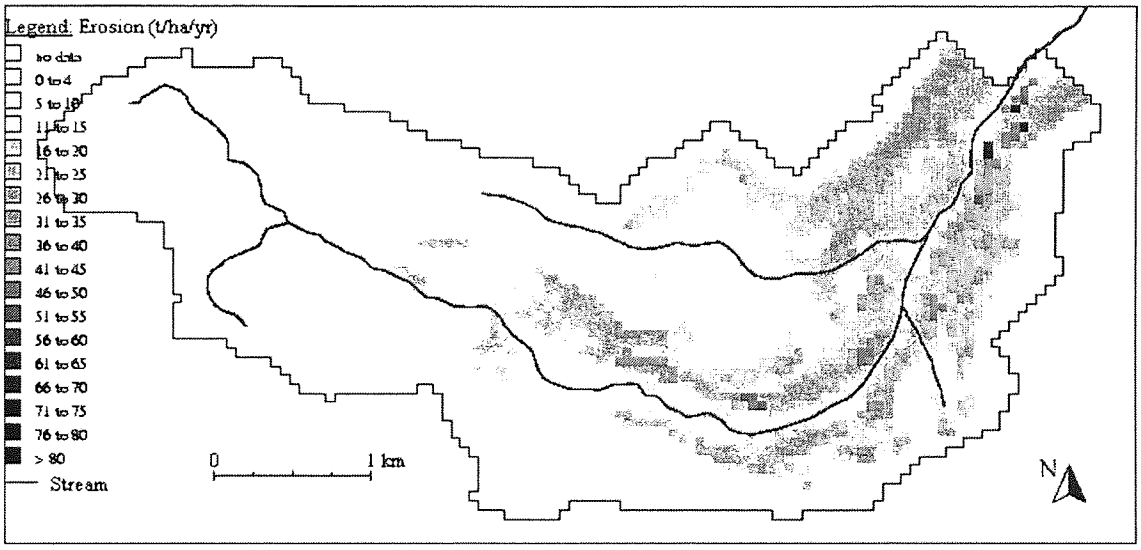

Figure 10.10 Total Transported Erosion per pixel for Simulation 2

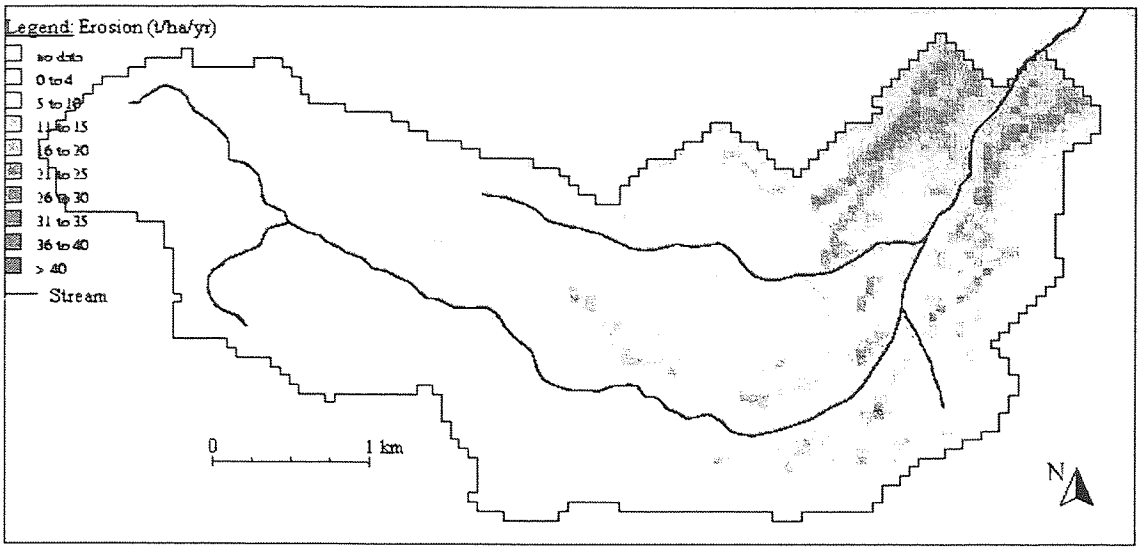

Figure 10.11 Total Transported Erosion per pixel for Simulation 3

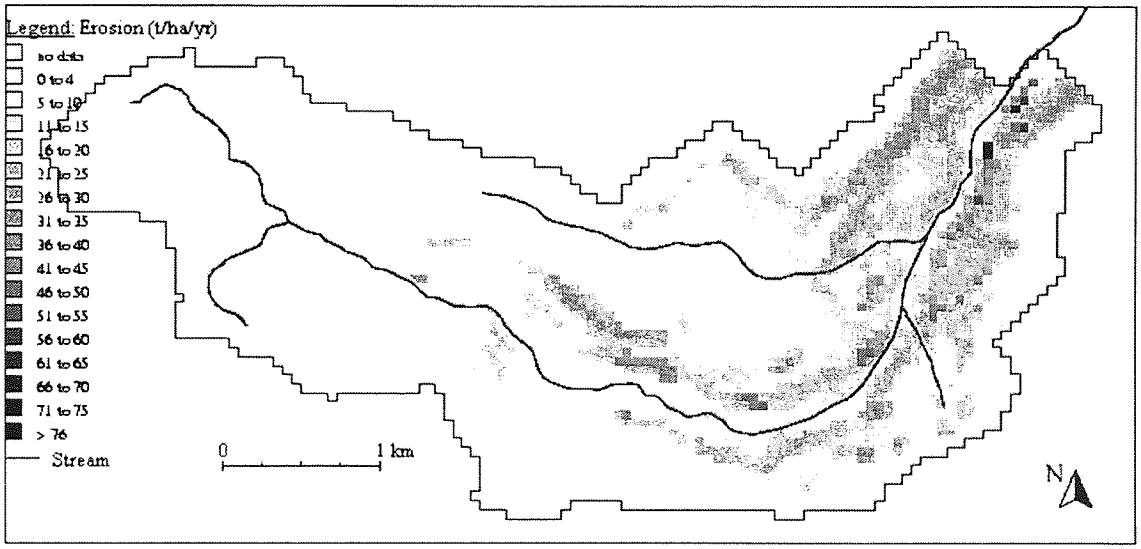

Figure 10.12 Total Transported Erosion per pixel for Simulation 4

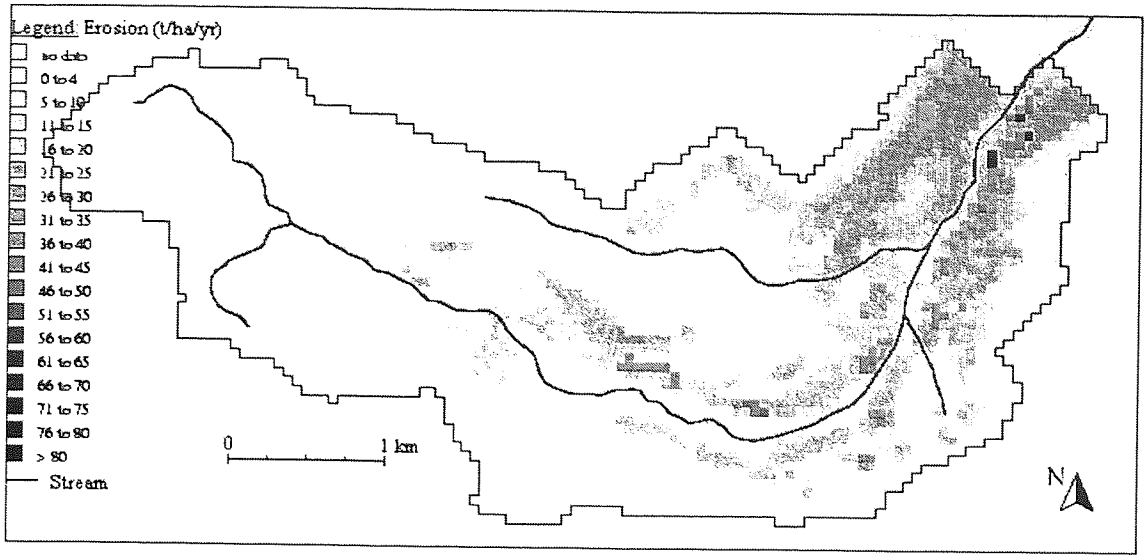

Figure 10.13 Total Transported Erosion per pixel for Simulation 5

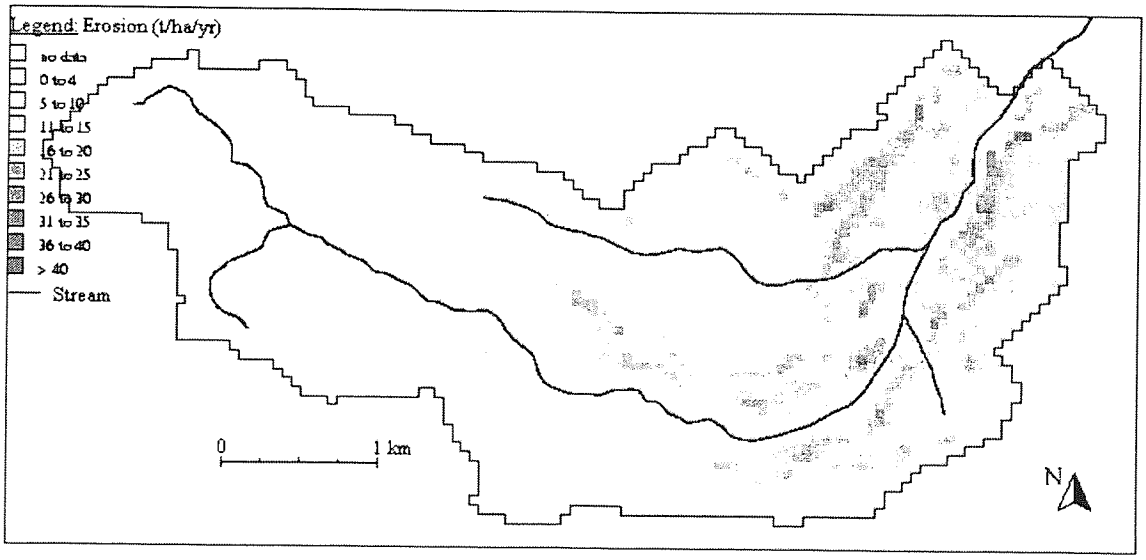

Figure 10.14 Total Transported Erosion per pixel for Simulation 6

Figures 10.9 to10.14, even though for arbitrary values, already show the influence of various factors on the output from the model. Certain areas in all the figures are consistently darker (more susceptible to erosion) than others, which can be attributed to the effects of the natural environment, for example, considering the slope and vegetational cover. The variation in darkness (and thus predicted erosion)

between the figures can be attributed to the different methods for calculating slope and drainage area from the different algorithms.

10.3.2 The Single Storm Model

The principle for running the single storm model is the same as that for the annual model, except that a different set of modules are required to run the flow routing function to deal with single storms. The inputs for this stage of the model differ from those shown in table 10.4 in that curve numbers are also required as an input to run the sediment transport functions.

As with the annual model, once the second module has been run, the outputs containing the tables of the possible erosion from the various values of s and t can be used to establish the calibration of the model. Assuming sufficient reliable data has been collected for daily rainfall and erosion data, these can then be compared with the results from the tables of s and t for each storm to find the best-fit solution for values of s and t. The final values of s and t can then be fed back into the third module of the model to calculate the exact predictions for total storm erosion for each of the events.

Although the data that was collected for individual storms had serious errors in it, the principles of the single storm model can still be tested using that data. The method and results are described as follows.

The single storm model was run several times to model each of the storms that were recorded in Ghana. Eight simulations were run for each storm varying the three methods for calculating R factor, drainage area and sediment transport formula. The combinations for each of the simulations are shown in table 10.6.

Simulation	1	2	3	4
Slope Method	Finite Differences	Maximum Downhill Slope	Finite Differences	Maximum Downhill Slope
Drainage Area Method	D8	FD8	D8	FD8
R Factor type	Proportional	Proportional	Proportional	Proportional
Sediment transport function	Govers	Govers	Meyer & Wischmeier	Meyer & Wischmeier
Simulation	5	6	7	8
Slope Method	Finite Differences	Maximum Downhill Slope	Finite Differences	Maximum Downhill Slope
Drainage Area Method	D8	FD8	D8	FD8
R Factor type	Direct	Direct	Direct	Direct
Sediment transport function	Govers	Govers	Meyer & Wischmeier	Meyer & Wischmeier

Table 10.6 Method Variations in Simulation Numbers

Table 10.7 shows the rainfall amount and observed sediment yields for each of the five storms.

Storm	Date	Rainfall (mm)	Total Observed Sediment (t/day)
1	22/09/00	0.8	2.67
2	21/09/00	5.1	2.87
3	30/10/00	10.7	4.29
4	29/10/00	13.1	7.34
5	25/09/00	19.7	9.52

Table 10.7 Summary of Observed Total Sediment Yield for each Storm

Figures 10.15 to 10.18 show the maximum, minimum, mean and median values for the each of the eight simulation combinations as applied to each of the five storms to be modelled. For comparison figure 10.19 shows the curve for the observed sediment yields for each storm.

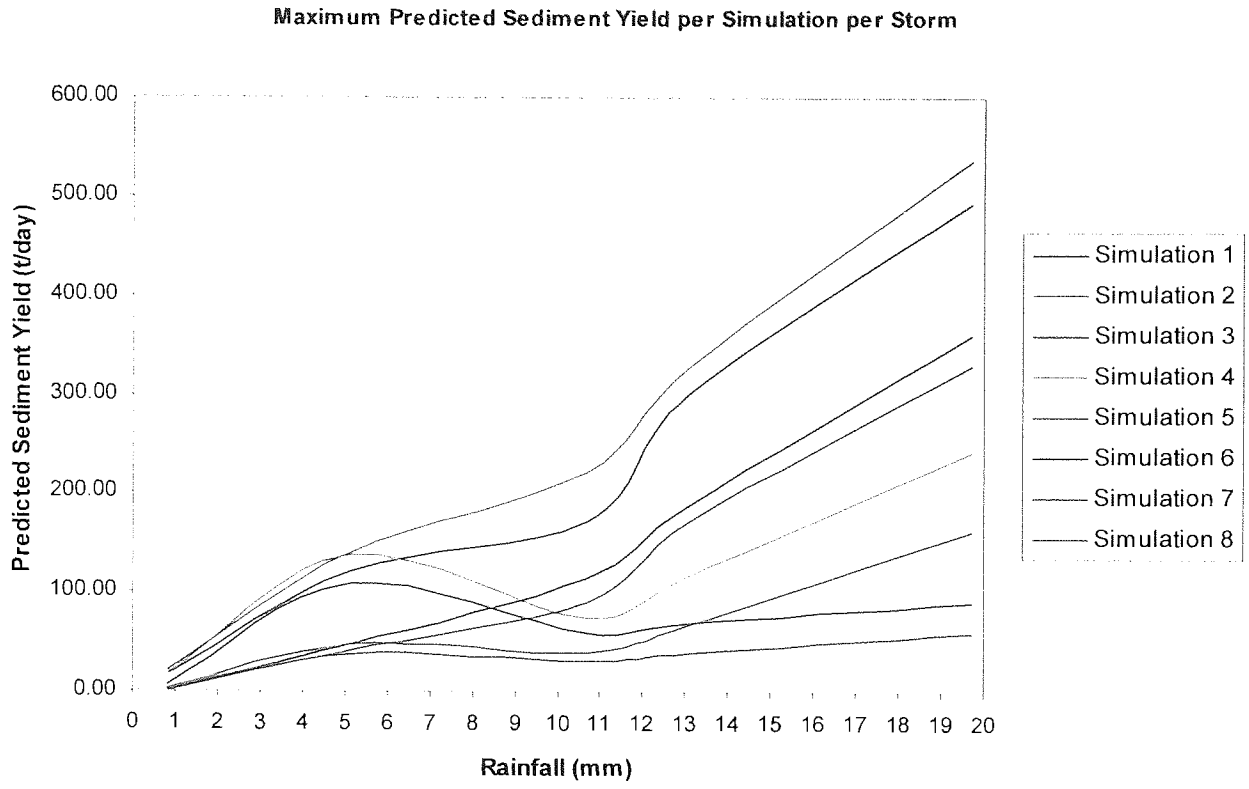

Figure 10.15 Comparison of Maximum Predicted Sediment Yield for each Simulation

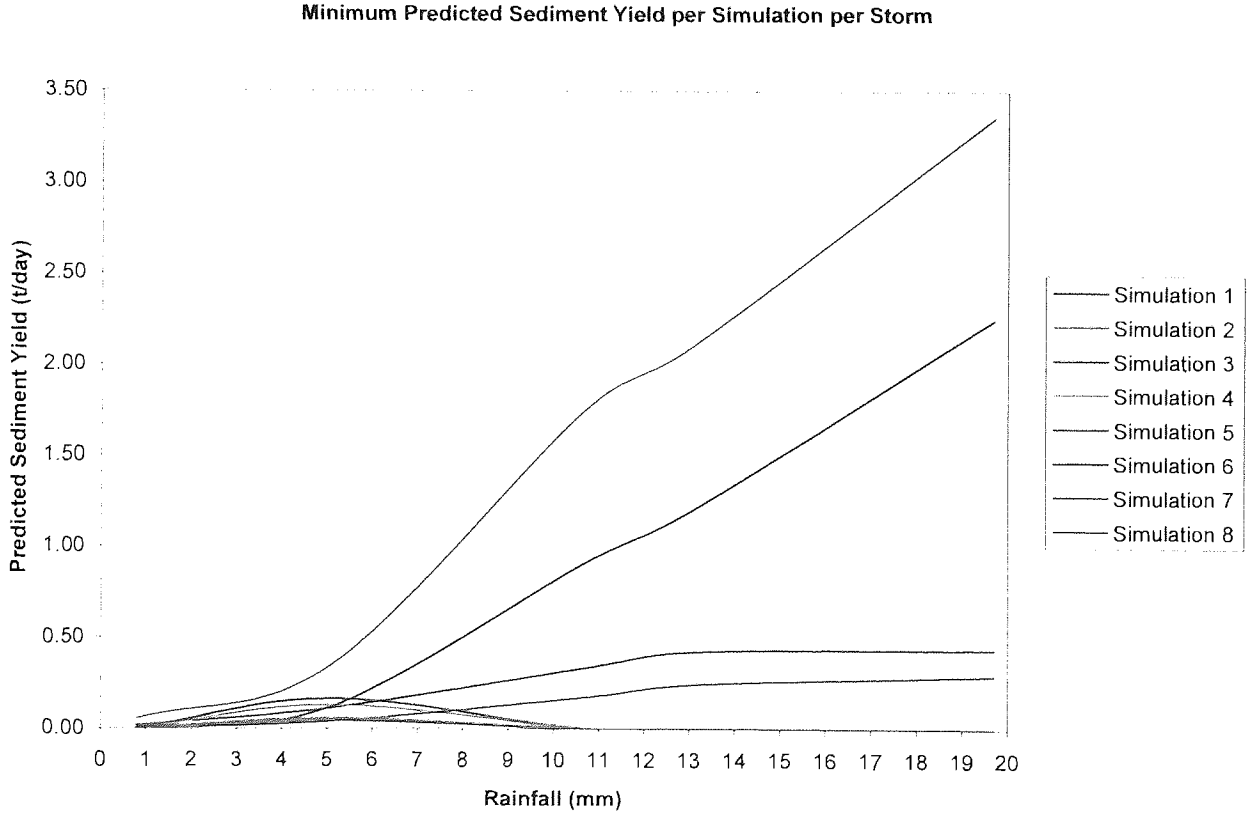

Figure 10.16 Comparison of Minimum Predicted Sediment Yield for each Simulation

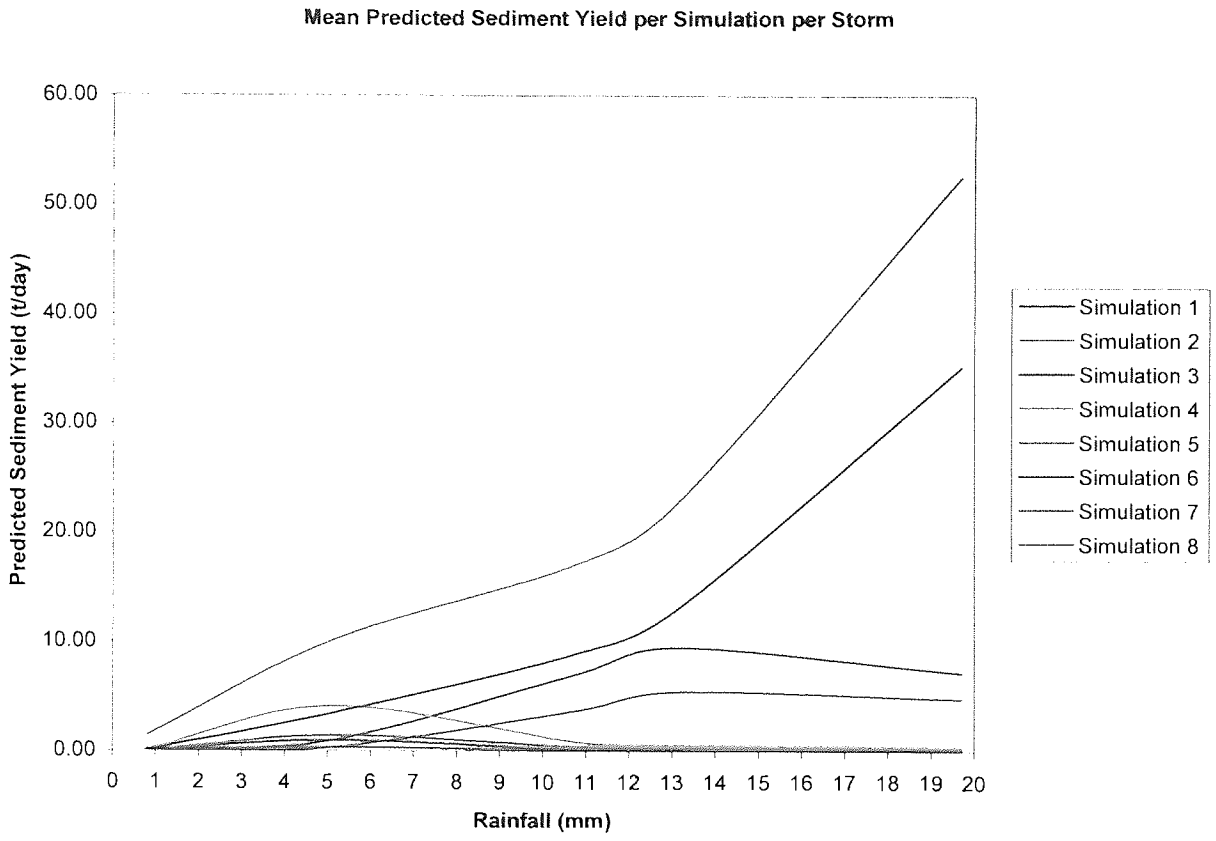

Figure 10.17 Comparison of Mean Predicted Sediment Yield for each Simulation

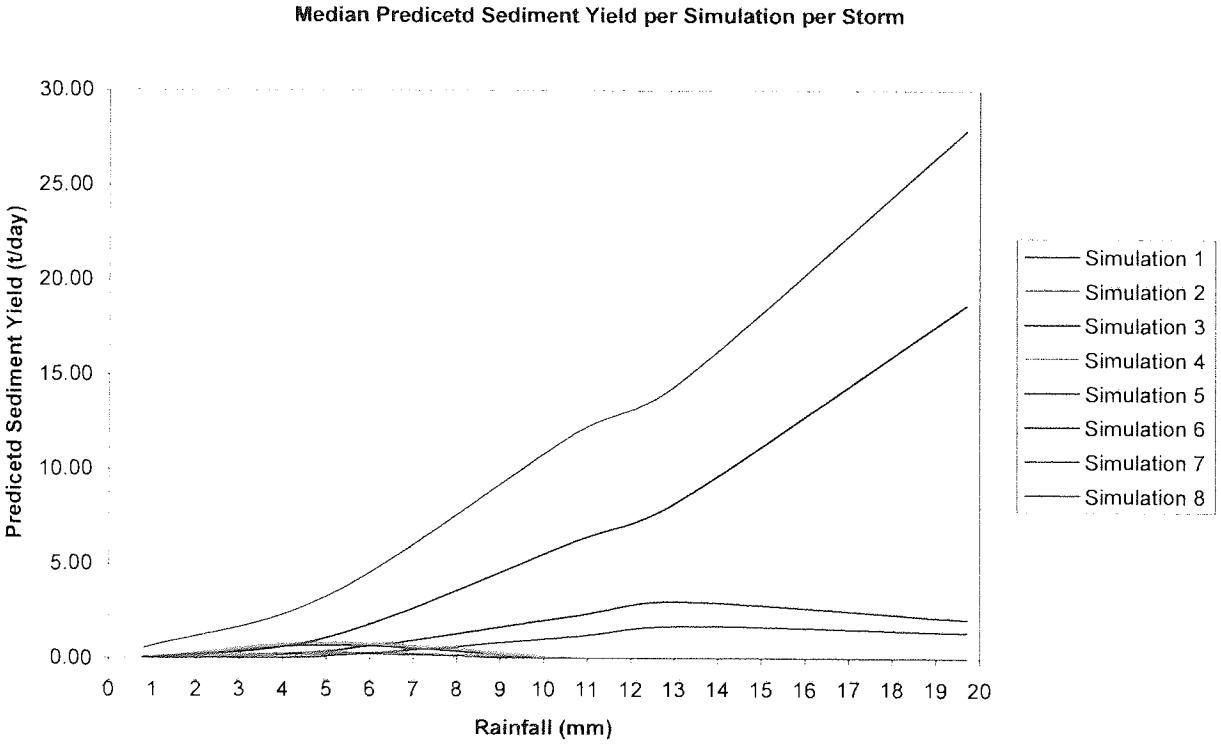

Figure 10.18 Comparison of Median Predicted Sediment Yield for each Simulation

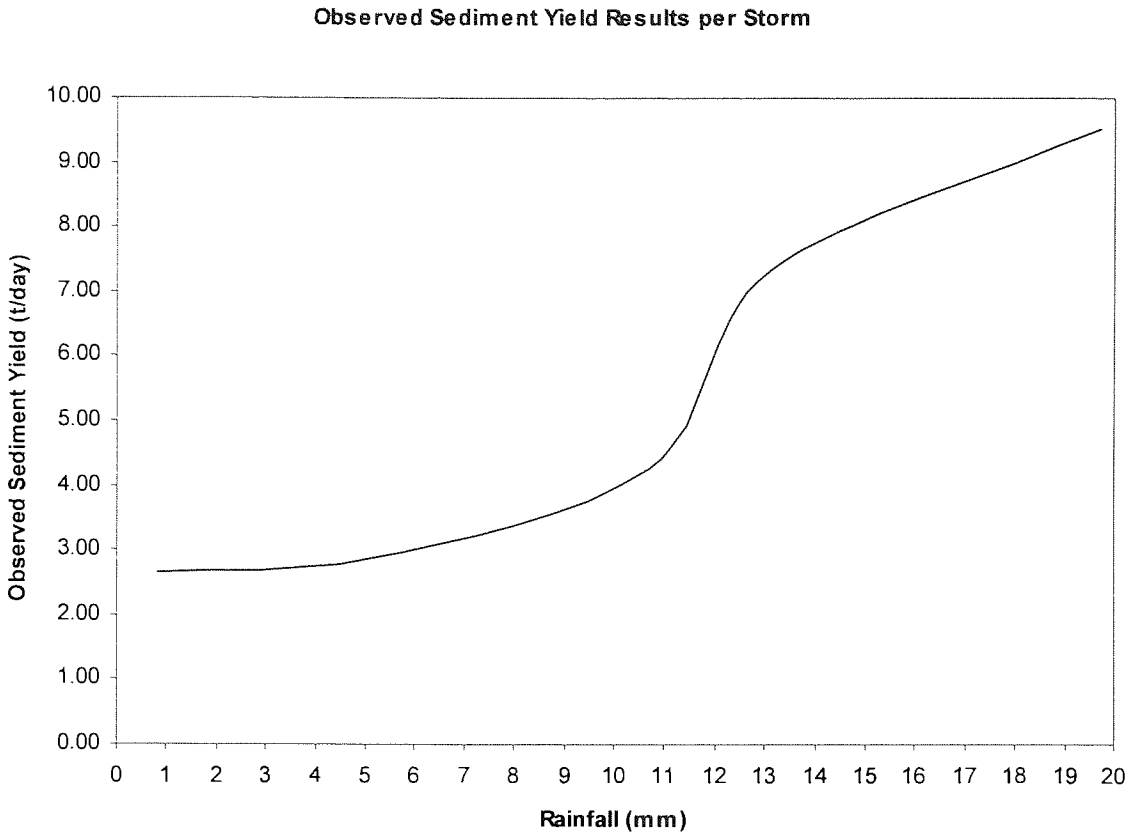

Figure 10.19 Graph of Observed Sediment Yield Results per Storm

Having compared the graphs of predicted and observed erosion rates it was decided that simulation 2 produced a graph for maximum, minimum, median and mean values that best fit the curve produced for the observed sediment yield rates.

Having established simulation 2 using the Govers sediment transport model, the FD8 routing algorithm and the proportional method for calculating the R factor the model needed to be calibrated. The procedure for calibration is as follows:

1) Identify values of parameters s and t within the delivery ratio equation (equation 3.42) that have predicted values of sediment yield that fit with the observed values of each storm.

2) Produce charts of predicted sediment yield for all combinations of storm, s and t.

3) Select values of s and t that best model all storms.

4) Establish calibration coefficient to produce a best fit of predicted sediment yields.

Table 10.8 shows the predicted values of sediment yield for each storm and selection of s and t, and Figure 10.20 the predicted values of sediment yield against the observed values. The combination of s and t that produces the best fit to the graph of observed sediment yield can then be determined. For clarity, the five best fits (using least squares) are shown in figure 10.21.

S	T	Rainfall (mm) / Graph no.	0.8	5.1	10.7	13.1	19.7
2	49	a	2.672	19.332	28.610	37.969	93.961
9	35	b	2.677	18.668	32.525	41.127	98.393
14	82	c	0.446	2.872	10.139	12.391	23.743
21	62	d	0.460	2.878	11.850	14.444	26.640
22	60	e	0.460	2.867	11.922	14.537	26.715
22	93	f	0.020	1.248	6.050	7.351	12.967
23	58	g	0.462	2.870	11.996	14.627	26.799
26	86	h	0.181	1.109	6.024	7.319	12.688
28	99	I	0.125	0.768	4.298	5.218	8.892
29	97	j	0.127	0.750	4.306	5.227	8.882
31	90	k	0.124	0.756	4.636	5.626	9.534
32	44	l	0.496	2.874	12.151	14.829	27.257
32	77	m	0.154	0.922	6.049	7.346	12.538
41	79	n	0.090	0.568	4.284	5.175	8.525
43	73	o	0.091	0.582	4.781	5.769	9.488
47	68	p	0.087	0.557	4.844	5.821	9.510
48	70	q	0.080	0.519	4.294	5.143	8.403
Observed sediment yield			2.670	2.870	4.290	7.340	9.520

Table 10.8 Predicted Sediment Yield for each Combination of s and t and Storm (letters in column 3 refer to graph numbers in figure 10.20)

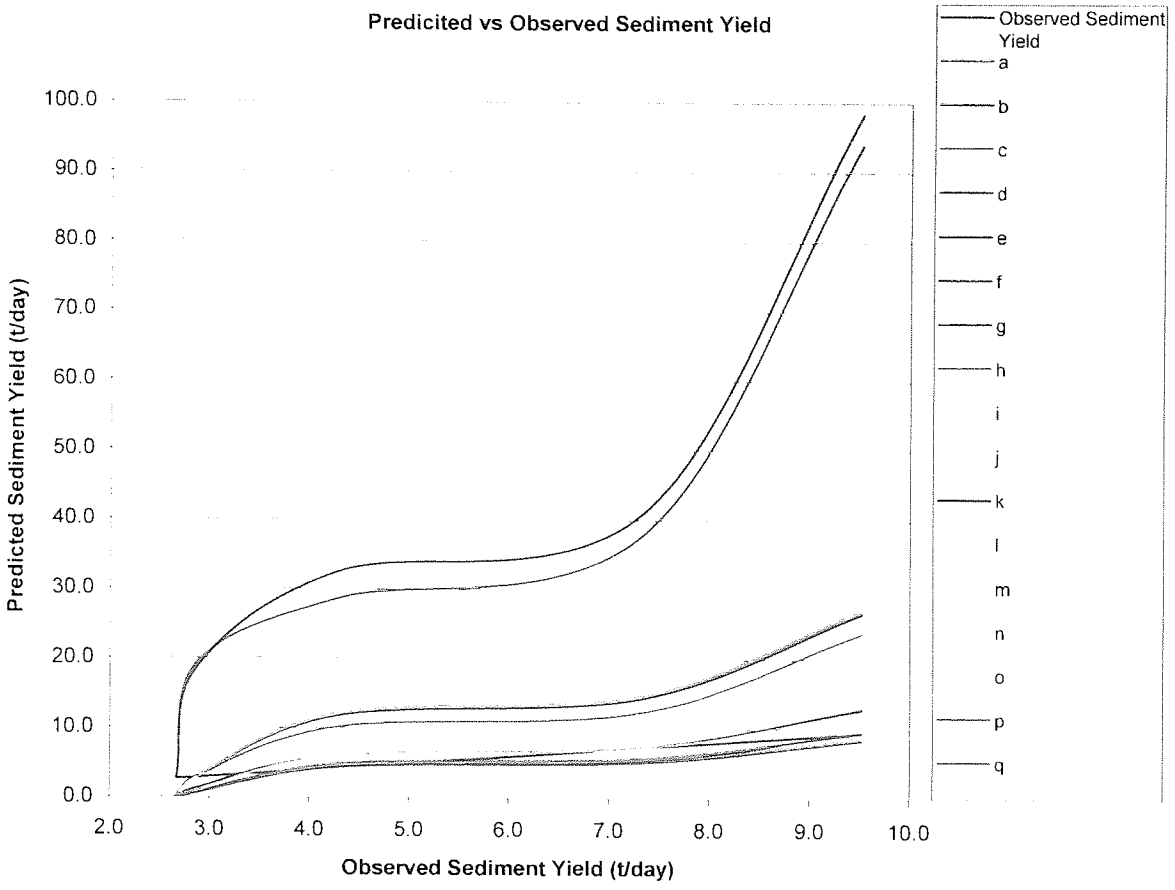

Figure 10.20 Graph of Predicted Sediment Yields and Observed Sediment Yield for each Combination of s and t and Storm (letters refer to s and t combinations in table 10.8)

From the results, the best fit solution using least squares is graph k with parameter values of:

s = 48 and, t = 70.

Figure 10.22 shows the comparison between the observed sediment yield per storm and the predicted sediment yields from simulation k.

Finally, a calibration coefficient has to be established to adjust the predicted values to the observed values. The same calibration coefficient has to be used for each storm but the error between observed and predicted values varies, therefore a compromise value for has to be selected. Table 10.9 shows the difference between the observed and predicted values for each storm and the coefficient required to correct each prediction to the observed value.

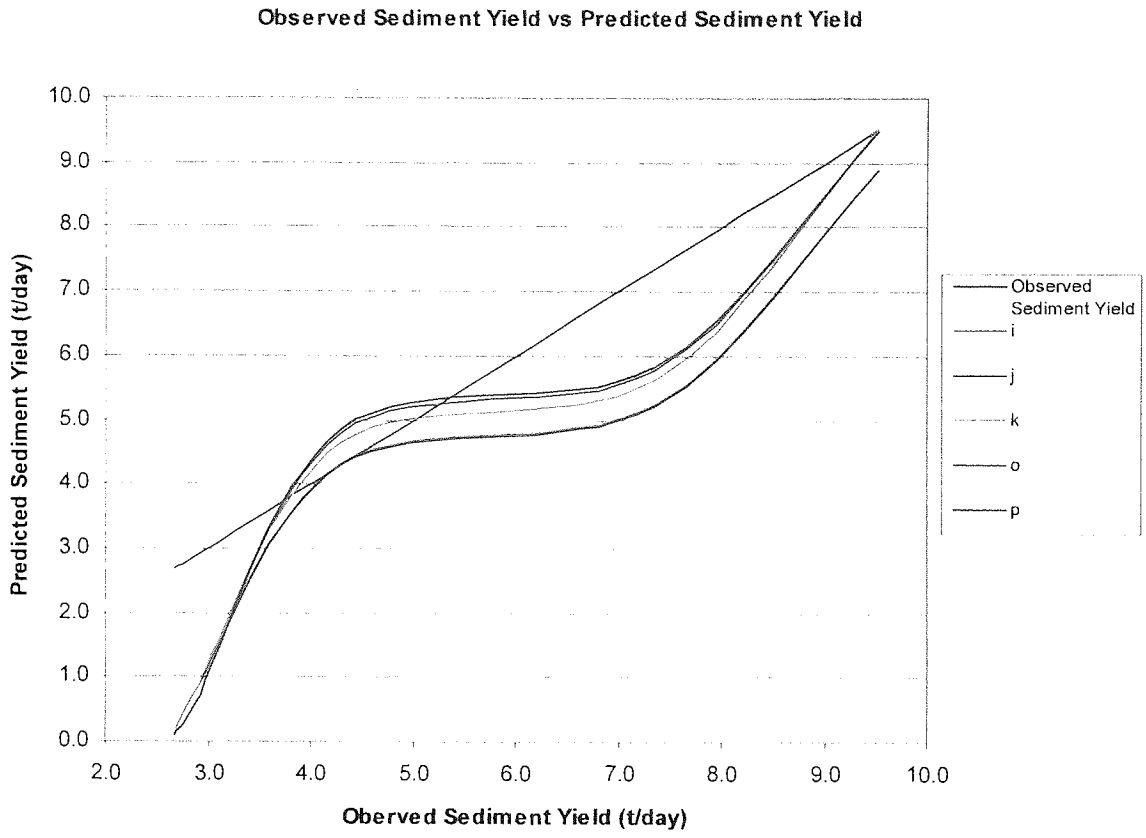

Figure 10.21 Predicted Sediment Yields against Observed Sediment Yields for the five best-fit solutions using least squares

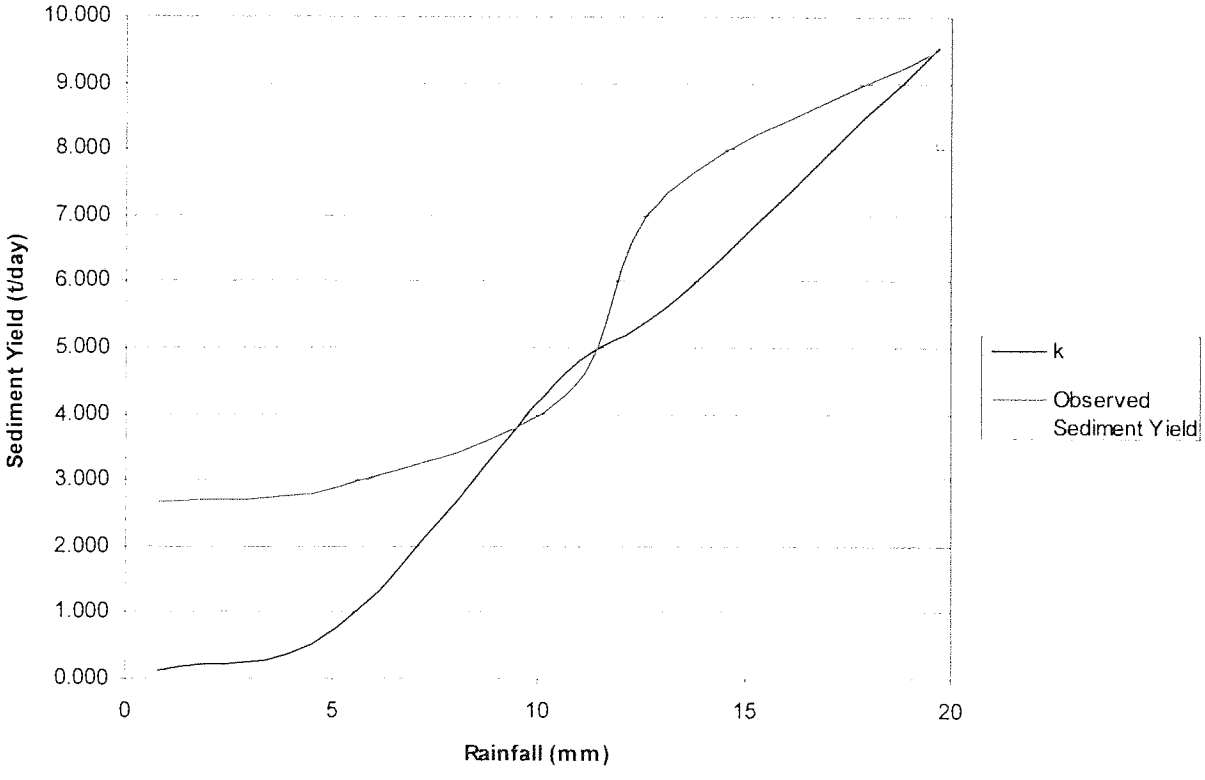

Figure 10.22 Observed Sediment Yield and Predicted Sediment Yield for Solution k

Observed Sediment Yield (t/day)	2.670	2.870	4.290	7.340	9.520
Predicted Sediment Yield (t/day)	0.124	0.756	4.636	5.626	9.534
Correction Coefficient	21.53	3.80	0.93	1.30	1.00

Table 10.9 Observed Values, Predicted Values and Correction Coefficients

From table 10.9, it can be seen that the model is much better at modelling the higher rainfall storms (3-5) than the two low rainfall storms. This was the case for most of the s and t combinations, those that did fit the low rainfall storms only fitted the smallest storm and had a much worse fit for the higher rainfall storms. However, to calibrate the model properly a single correction factor must be established that best-fits the solutions of all the available data. An iterative process was used to get the least squares best fit solution as close to zero as possible. Table 10.10 shows the final predicted values with the percentage error using a correction coefficient of 0.998.

Observed Sediment Yield (t/day)	2.670	2.870	4.290	7.340	9.520
Corrected Predicted Sediment Yield (t/day)	0.124	0.755	4.629	5.618	9.520
% Error	95.36	73.70	-7.91	23.46	0.00

Table 10.10 Observed and Corrected Predicted Sediment Yields with % Errors

10.4 Summary

Although no reliable data results could be utilised to calibrate the model itself, the experimental data that was collected, was still useful for demonstrating and testing the use of the annual and single storm models to see if sensible results could be obtained and to test the process of running and calibrating the model.

Chapter 11

Review and Evaluation of Thesis; Recommendations for Further Work

11.1 Introduction

Radical changes in land use can result in excessive soil erosion. Should the eroded soil be transported overland and into the permanent stream network, then this will increase the sediment yield of the major rivers. The whole process can result in many environmental problems, both at the source, where the soil was eroded and at the sink where the transported material is deposited. This thesis set out to investigate and analyse soil erosion and sediment yield within rural agricultural environments in Southern Ghana, with the aim of establishing and testing a model suitable for predicting sediment yields that could then in the future be used to predict siltation rates for Lake Volta.

The investigation was undertaken in the following main stages:

- Research into soil erosion; what defines soil erosion, the individual processes involved and their interactions, and the point at which soil erosion becomes detrimental to both the environment and to agricultural production. In addition, to establish those circumstances under which the soil is at most risk to erosion by rainfall.
- Predictions of soil loss over large areas of Ghana to identify those areas at the greatest potential risk of extreme soil erosion.
- To measure soil erosion rates, using sediment yields, from a small catchment selected from the at risk areas.

- Development, testing and calibration (using measured data) of a simple sediment yield model, using appropriate techniques, to predict daily sediment yields based upon rainfall, topography, land use and soil type.

11.2 Review and Evaluation

A thorough investigation of the available literature was conducted at the beginning of the research and a field trip to Ghana was planned and undertaken in order to collect data for calibration and validation of a proposed model. However, as the research progressed, it became clear that the original aims of the thesis would not be met and that an alternative strategy had to be pursued. The data collected in the field, was of insufficient quality and was therefore inadequate for the purposes of validating a proposed model. Nevertheless, the data had been collected with the right principles in mind and thus the strategy was revised to define more clearly, how the model would be developed and operated in order to utilise a similar dataset of better quality.

11.2.1 Specific Aims and Objectives

Taking the specific aims and objectives as stated in chapter 1, the following section addresses the evaluation of those aims and objectives of the thesis.

11.2.1.1 Establishment of Basic Data Requirements

The thesis has demonstrated a good understanding of the basic data requirements for producing a sediment yield model for a developing country. That is, the need for a simple model with a small number of parameters for which the data can

be easily collected. The parameters should also reflect the most important of the influencing factors of the processes involved.

However, there was not, as was demonstrated upon return from the field studies, a full appreciation of the methodologies for accurately collecting the data.

11.2.1.2 Use of Basic Data to Create Soil Loss Potential Maps

It has been demonstrated that the use of GIS for modelling soil erosion can provide a very sound base for the effective simulation and visualisation of soil erosion. The GRASS-GIS software package was chosen as a customisable and manipulable program, which enabled various data processing and analysis techniques to be employed. Data sources for these analyses were obtained from previous work in Ghana.

11.2.1.3 Highlighting Areas at Risk to Identify Areas for Study

Again, the combined use of USLE and GIS allowed this to be comprehensively achieved. Techniques such as watershed analysis within the GIS allowed potential catchments to be identified, then by overlaying USLE analyses; those at risk could be highlighted.

11.2.1.4 Collection of Experimental Data

The records obtained from the Soil Research Institute at Kumasi provided useful data for verifying the USLE parameters; however, this was the only data that could meaningfully contribute to the modelling process. Due to a lack of experience and planning, the data collected from the experimental catchment could only be utilised as a sample dataset to test the function rather than accuracy of the model.

Because of the poor experimental data, the direction of the thesis went towards developing the theoretical model and assessing its application.

11.2.1.5 Investigation of Current Models and Creation of the Catchment Model

A full exploration of the currently available models and types of models was undertaken; this enabled an existing model (CALSITE) to be adapted for use in the Ghanaian environment. Building upon existing knowledge, a simple model was created with few input parameters that could be obtained from developing countries.

11.2.1.6 Potential of Model to Predict Sediment Yields

The model's output is designed so that sediment yields are calculated through the catchment and flow routing modules of the program. This enables users to obtain the more useful measures of sediment yield from the catchment. However, soil loss is also given as an output from the model as this can also provide useful information in certain circumstances where the specific affect to an area of land is required rather than an overall detrimental affect on the environment through high sediment loads in the stream network.

11.2.1.7 Potential of Model to Investigate Land-Use Change and Sedimentation

The potential of the model to investigate land use change and sedimentation rates were allowed for in the design of the model. The model can analyse erosion for any input land-use map, and although the process is manual in the current version of the model, it could very easily be programmed to allow automatic comparisons of two or more types of land-use. As the model can estimate sediment yield outputs it could theoretically be used to investigate sedimentation within Lake Volta, however, there

are other issues with this. These issues and the land use change potential are discussed in more detail in section 11.3.

Several other issues also arose from the completed thesis which can be categorised as follows: problems of modelling types, their applicability to developing countries and the associated restrictions due to data availability and quality, and the problems associated with homogeneity of the resulting calibrated model with different parameter sets. These issues are summarised and discussed over the next few sections.

11.2.2 Model Type, Modelling Environment and Scale

The problem of soil erosion is very difficult to quantify accurately in those places where its assessment and rectification is needed most. This applies to both empirical and physically based models, but in different ways. Empirical and conceptual models do not generally require a large variety of different sorts of data but do need long and extensive data sets for those data types to enable the model to be calibrated. Physically based models however, do not require these long datasets but instead (depending upon the level of sophistication) need data for a large variety of data sets. These two different requirements both cause problems when trying to apply such models in developing countries.

In the case of the empirical/conceptual models the long data sets do not generally exist within developing countries and even in those countries where some data is available, the set is often not long or complete enough to get a reliable degree of accuracy. The other problem to arise is the lack of transferability of these models to other environments even if there is sufficient data to enable calibration for the region to be tested. This is especially applicable in countries like Ghana, where

although some plot data is available in the south, due to the size of the country it is not guaranteed that a model developed from that data will give reliable results when applied to areas in the north. The differing weather conditions from north to south are sufficient to question the application of such a model, developed in the south, working in the north as well.

With physically based models, the problem is also due to the lack of availability of data, but for different reasons. Physically based models can often require large quantities of input data. However, the number of different input data types required make these models very hard to run in developing countries where data of this type are not usually available. The data is required on the same basis as the time-step used in the model for whatever period is required to enable calibration/validation of the model to be performed, e.g. flow rates at half hourly intervals, requiring electronic monitoring equipment.

The large majority of work on the study of soil erosion has been carried out in the US where large amounts of funding can be put into projects to produce meaningful and accurate results. It is there that some of the most sophisticated physically-based models have been produced.

However, despite the various issues involved in acquiring sufficient data to model soil erosion within a developing country, it is possible to establish simple and efficient calibrated models that can provide reliable estimates of sediment yield and soil loss.

The issue of data requirements and calibration is summed up very well by Viney and Sivapalan (1999), who state that a large number of sediment models have been developed to describe small-scale or event-based erosional processes (e.g. Knisel (1980) [CREAMS]; Williams, (1980) [SPNM]; Young et al., (1987) [AGNPS]).

Models that are more widely applicable in space and time have been developed by Williams et al., (1985) [SWRRB] and Arnold et al., (1993) [SWAT], are intended for ungauged catchments (i.e. no calibration), but are therefore very data intensive.

However, the term data intensive is somewhat misleading; models can be data intensive on two levels. In the case that Viney and Sivapalan refer to, data intensive refers to the fact that those models require a large number of input parameters to compensate for not being calibrated. However, some calibrated models, (e.g. CALSITE, Bradbury et al., 1993) are very data intensive despite few input parameters, because to calibrate them fully, long data sets are required for those parameters to reduce errors to an acceptable level.

Zhang et al (1996) agree with this, stating that these studies indicate that it is typically difficult, if not impossible, to obtain a unique set of optimal parameters for a physically-based model using parameter estimation methods if more than a few parameters are involved. A major problem of physically-based models is obtaining a 'best fit' parameter set, i.e. the correct balance between number of input parameters and required length of dataset. Because of this, it has been very difficult to apply a physically based model that has been developed for a small area over a much larger area.

11.2.3 Experimental Catchment and Collection of Data

Within the experimental catchment, there are several issues to be resolved regarding the nature of the catchment and the data collected.

Overall, the field trip was relatively unsuccessful for collecting good quality data with which to calibrate the erosion model that was to be developed. This was in part a financial problem, part because of the difficulties associated with research in

developing countries and part, due to a lack of planning and knowledge before going to the field.

Within the field of the data collected, suspended sediment load readings were the biggest disappointment. Whilst the theories of substituting a collection bottle for electronic monitoring equipment seemed at first to be an innovative solution, without the means to calculate the hydraulic nature of the flow in and out of the bottle, the results were meaningless. Instantaneous sampling would not have sufficed, as much of the storm load would pass at times when it was not feasible to take readings. Any readings taken by this method would only give the natural base load of sediment in the stream. In such situations where readings over a long period are required, if electronic monitoring equipment is not available, then collecting over a known area for that period is a reasonable idea, but would require a better experimental solution and better planning.

Bed loads were harder to measure; this however, was at least expected. Although the exact characteristics of the bed load were not known fully until the experiments had begun. Due to the unstable nature and constantly mobile deep sandy bed, which at low flows was transported by saltation of particles, evident from the dune forms on the bed, bed loads formed the large part of sediment movement in the channel. At higher flows, activation of the bed introduced sand particles into the flow increasing the volume of suspended load, implying a large degree of storage of eroded sand particles, distorting the relationship between rainfall events and sediment load at the catchment outlet.

It is possible to suggest that the results indicate that total erosion is directly proportional to rainfall and thus runoff and flow so that sediment yield can be equated to the erosion occurring during that specific rainfall event. In Schumm's (1977)

theory of sinks the higher rainfall events would remove a greater degree of sediment from the sinks increasing sediment yields (higher flow rates produce a larger degree of bed activation). However, they would also erode more sediment which contribute to replenishing the sinks. Alternatively, it could be considered that a very large rainfall event would empty the sinks resulting in a very high sediment load for that storm followed by lower than expected loads for smaller subsequent storms until sinks have been replenished. As the only big rainfall event during the collection of data occurred at the beginning of the field studies, this idea cannot be verified.

Schumm's (1977) theory of the sediment source, transport, sink model fits very well with the observations made in the catchment. However, because of the high sand content of the soil and thus the high degree of bed load, neither of the above theories of the catchment characteristics that describe sediment transport can be proven. For either to be verified, a detailed analysis of the catchment would need to be carried out with sediment monitoring stations at various strategic points around the catchment.

Another issue to be resolved is why the erosion is so severe within the plots in and around the catchment yet they are surrounded by the forest, which itself is a very good protective system against the erosive powers of rainfall and runoff. The trees when acting as a forest do stop erosion by holding the soil together with their extensive root structure; therefore, once the tress are removed, a bare plot will be susceptible to erosion. The trees at the edge of the plot do not act as a barrier to prevent further erosion and stop runoff flowing off the plot, as they are not a continuous line of defence. Over the course of the plot, the surface flow builds into sufficient runoff force to cut its way through the gaps between the trees beyond the plot. Another reason is that often pathways used by the farmers to navigate their way

through the forest that lead up to and along the edges of plots act as pre-defined channels to carry runoff and sediment through to the valley bottom and then out of the watershed in the rivers. Pathways are often found at the downslope end of a plot (see chapter 4) and there is no form of barrier between the field plot and the pathway, thus, runoff from the field carrying sediment has direct access to a flow network and will easily be transported to the catchment outlet.

The topography of the catchment is also a factor that has to be considered. One possible source of error is the large cliff face in the southeast corner of the catchment disrupting slope values. Due to the steep sloped nature of the catchment, it is possible that this will have a considerable effect on the measured values of slope. The artificially enlarged values of slope will give higher estimations of sediment yield for an area that is very unlikely to produce any yield whatsoever. The only counter against this is to assign very low values for the area within the C factor map, which is adapted by ground truthing. This is only a solution for the small-scale catchment on which the model is tested. For larger scale areas, such ground truthing is not feasible due to the expense involved. The aerial images would show the land use type to be consistent with the rest of the area as numerous trees grow from out of the cliff face, making the anomaly virtually impossible to detect.

The plot data from Kumasi was a positive to take away from the field trip. The data enabled an initial calculation of the USLE factors towards Ghanaian conditions and, providing studies there are maintained, this will provide an invaluable resource for furthering the work on the development of the soil erosion model.

11.2.4 Model Application, Data and Parameter Requirements

It was found that the data requirements for modelling the sediment yields was higher than had been estimated during the field exercises. However, this does not mean that the required levels are not achievable given the constraints of working within developing countries.

Due to the nature of the input parameters, an achievable quantity of data is required to run the model. Inputs are restricted to data about the natural environment, the topography, vegetation and soil types, for most of which the information is readily available even within developing countries. In addition, a suitable length of field data from experimental catchments for rainfall and sediment loads on a daily basis is required for experimental catchments

Application of the model then requires a suitable PC, capable of running Linux and GRASS-GIS and analysing the results. Automated analysis of the s and t parameter tables would be relatively easy to program and add to the model for dealing with larger areas and longer datasets.

Providing suitable planning is undertaken before fieldwork has commenced and that appropriate, but not necessarily expensive, equipment can be obtained for the collection of sediment load data, the model should be applicable in many environments.

11.2.5 Socio-economic and Political Factors

Whilst the quantification of soil loss and sediment yield through land degradation lies very much within the bounds of mathematics and science, the resolution of the problems that land degradation causes relies upon consideration of

the socio-economic and political factors that have driven the agricultural workers to misuse the land in the first place.

Mismanagement of land generally takes two forms, either the overuse of current agricultural land or the conversion to agriculture of unsuitable land. The latter problem is the predominant cause of land degradation within the study area, largely due to the steeply sided valleys and the lack of available agricultural land that is not on a slope. The problem of overuse of land is still prevalent within Ghana but is more prevalent in the southernmost regions including the Accra plains and some of the more northern regions.

Despite the problems often having severe consequences, the solutions are often quite simplistic. Although complex soil erosion models provide very useful information about rates of loss, with a lack of data and funding within developing countries are not always practical. In these instances, best practice methods are very reliable in preventing severe soil loss, however, a lot of work still needs to be undertaken to put best practice methods into place and make sure that they are enforced.

The most important factors when adopting best practice methods are support and education from the government, coupled with investment from which the benefits may only be realised after a period of several years.

There has to be prioritisation by the government toward improving agricultural management with the long term aims to provide a base for economic growth and stability. If agricultural self-sufficiency can be achieved then this can be built upon to create export growth, which in turn provides future investment into further growth, enabling more advanced farming methods to be employed, which in turn improves productivity. However, there first has to be a realisation that whilst traditional

farming methods can sustain small village communities, increasing population demands require different approaches to farming methods. As pressure on agricultural land increases, the erosion problem experienced with the current methods only becomes more severe.

Long-term investment from governments must be a main prioritisation and they must not allow themselves to imitate their developed world peers, creating long-term solutions outside of the time frame of their own governance, building for the future. Policies must be constructed that will take agricultural management forward over a period of several years, rather than creating short term 're-election worthy' goals.

Support of the farmers must be undertaken at both national and regional government levels, with additional support from relevant authorities, the EPA (Environmental Protection Agency), SRI (Soil Research Institute), WRRI (Water Resources Research Institute) and other regional and national authorities. Support can also be gained from global authorities, such as FAO (Food and Agriculture Organisation) and other United Nations organisations. The FAO heavily funded investment into the Agro-Ecological Zoning project in Kenya.

Education of the farmers working the land is the final but most important part of the best practice method. Once investment has been secured and a support network established, education of the farmers can begin. However, it must also be realised that methods cannot be changed immediately. New practices will take several seasons to be put in place. New practices can also not be too radical. Old methods are hard to change, and new practices, if too radical may be rejected by farmers used to traditional practices. Solutions must therefore be compromise resolutions that allow farmers to maintain and increase productivity whilst be in keeping with tradition but

reduce environmental impact. The key to developing these solutions is communication at ground level with the farmers upon whose livelihood working of the land depends. As Stocking (1995) discusses it is easy to blame the land-user for the erosion problems. However, they are usually fully aware of the extent of the degradation that is occurring but the farmer is not growing his crops on steep slopes, poor soils and deficient vegetation out of choice. Poor resources, little or no investment and a subsistence to gain leave the farmer with little or no other choice but to persist with methods that they know jeopardise their future well-being.

A degree of realism must also be considered when analysing the potential risks of soil erosion. Although methods of evaluation are very complex, solutions and preventative methods can be very simple. Reduction of rates of soil erosion can be controlled by various factors. The simplest methods involve changing the base factors that affect erosion, i.e. those that make-up the USLE. The soil type and rainfall are unchangeable quantities. However, the vegetational effects can easily be altered by changing the crop types that are grown or employing alternative farming methods such as agroforestry. Although the topographical effects cannot be changed directly, save from moving agricultural plots to other locations (rarely a feasible option), indirect methods such as terrace farming and contour ploughing provide simple and efficient methods of prevention.

As a final note on the socio-economic and political factors, one point has so far been overlooked. When the developed countries were going through the same processes of agricultural improvement, they achieved it at their own pace without external influences of technologies and systems far more superior and advanced than the ones they were employing. The agricultural revolution in Britain lasted for nearly 350 years the period of change can be considered to extend from 1500-1850 AD.

However, in developing countries a degree of change similar to this is being pressed upon them over the course of a matter of decades. This puts increasing pressures on both the land and its users and does not allow agricultural workers to learn from their mistakes and gradually improve the systems they have created to keep a balance as the increasing population puts greater demands on agricultural production.

Chapter 12

Conclusions and Recommendations

12.1 Conclusions

CALSITE sediment yield estimates and suspended sediment data both suggest low erosion rates, yet USLE estimates are much higher. This is even so when using conservative parameter estimates from conservative equation methods, parameters could have been used that would give much higher results. USLE estimates also concur with ground observations; poor farming and conservation practices, and what appeared to be a dry friable soil on fairly steep slopes all add up to suggest high erosion rates. Yet how is this apparent discrepancy between source erosion and sediment yield explained? Considerable bed-load movements were observed and measurements were attempted, but due to the quantity of the loads and the unstable nature of the bed, reliable measurements were difficult to obtain. Most sediment transport studies concentrate on suspended loads as this generally forms the larger part of the load. However, this is often on much larger streams, on small catchments behaviour can be much more uncharacteristic. In smaller catchments, lower flows mean lower transport capacities but no less susceptibility to erosion, just a longer, slower, time-period for transport to occur. Most of the larger sand sized sediment particles remain in storage until large flood storms 'flush' the sediment to the outlet, although a large quantity of sediment is transported as bed load by the process of saltation.

CALSITE and other such models concentrate on suspended loads in their transport formulae and delivery ratios (e.g. fall velocities, and in CALSITE slope acts to slow flow allowing deposition). Whilst this works for high suspended-loads (cohesive silts and clays build up redirecting the courses of streams), high bed loads

(non-cohesive sand) rumble onwards down to the outlet and beyond. Higher flow rates on the larger catchments also allow sand to be carried predominantly as suspended load rather than in the bed load. Deposition acts merely as temporary storage.

This fits well with Schumm's (1977) source/transport/sink model except that in the experimental catchment the outlet corresponds with a major sink. This is also borne out by ground observations. In the smaller shallower upper reaches of the stream, larger rocks and natural earth form the streambed (a much more loamy soil dominates the valley bottom here, also farming is much less prevalent and is restricted to agroforestry, thus erosion rates are much lower). However, as the valley bottom approaches the outlet, farming on the slopes increases (crops such as maize and cassava leave slopes dangerously exposed), thus increasing erosion. Sand is deposited in the beds of all channels (even the pathways that act as a temporary stream network, see section 7.3), waiting to be carried on when the flow rate is sufficient. The effects on the bed profile at the experimental site confirms this, after the big 71.4mm storm the bed profile changed dramatically and rose over 10mm in height from the position of the previous day. As the storm petered out and the flows began to return to normal, the natural sink at the outlet came into force, acting as a dumping ground for the last of the sand particles. The particles would have either fallen out of suspension, or the stream no longer had the power to carry them by saltation, to slowly drift into the section of channel at the outlet and settle on the bed.

However, it must be considered that when observing the source erosion maps most of the erosion is coming from only very small areas of the catchment in proportion to the forested areas remaining. Despite the initial tests, CLASITE calculations suggest that the overall erosion risk to the catchment was quite low,

based upon sediment yield figures; those regions of the catchment exposed to a high erosion risk are suffering environmental consequences as these areas are contributing a large proportion of the erosion towards the sediment yield. Should large sections of the catchment be subject to a land-use change similar to that which the degraded areas had been, then the erosion risk of the catchment as a whole would increase significantly.

Many improvements can be made to this model, not least the inclusion of an integrated, fully calibrated, hydrological model. However, there are obstacles to these improvements. In an ideal world, to calibrate the hydrological model, up-to-date, hi-tech, 24 hr, constant measurement/continuous sampling, stream gauging and sediment monitoring equipment would provide reliable data, vastly improving the accuracy and physical reality of the model. This is not however an ideal world, equipment such as that, especially over the time-scales necessary, is not inexpensive. Other improvements would include the collection of more comprehensive sediment load data, including a way of measuring the actual bed-load contribution to the total load within the stream.

Overall, however, the thesis has set a sound theoretical basis for the continued study of soil erosion and sediment yields within the southern agricultural regions of Ghana. This opens up the potential for the expansion of the work completed within this thesis, as well as offering alternative solutions that can be applied to similar environments elsewhere in the developing world.

12.2 Summary of the Main Limitations of the Thesis

The main limitations of the thesis derive from the scope of work that can be taken from the subject. Soil erosion is a very complex and wide ranging subject to

study. Therefore defining one issue to concentrate on without detracting from the importance of the other factors involved, becomes very difficult at times. This is largely because many of the factors involved in the process of soil erosion share an equal level of significance and involve the study of many different disciplines.

This is exemplified when considering the difficulties faced when researching in developing countries due to the limited availability of funding and data, and the resulting problems in the acquisition of that data.

However, the socio-economic and political issues discussed in section 11.2.5 must not be forgotten. Whilst it is important to evaluate the risks and consequences of soil erosion it is important to consider why the erosion occurs and how it can be prevented. These issues can only be resolved by communicating with the farmers who depend upon the agricultural land for their livelihood, developing compromise solutions that enable productivity levels to be maintained and even increased, whilst protecting the land from further damage due to bad management.

12.3 Recommendations

The main lesson learnt, and thus the recommendations to emerge from the thesis are with respect to the field study and experimental work and the aspects of planning and preparation. With proper planning and application productive results should be able to be produced from the model, enabling erosion within the agricultural areas and eventually sediment yield rates for the whole Volta catchment to be calculated. The progression of this research would likely take the form of some or all of the following stages.

- Validation of the model within one or more rural catchments to establish the correct calibration parameters for the model estimation would be required first.

- Currently the model outputs only include the source erosion per pixel and the total erosion transported from each pixel to the catchment outlet. Outputs of the model could be improved to include data that would enable further investigation of the Schumm (1977) theory of source/transport/sink. The routing algorithms of the model utilise such data but have not as yet been programmed to retain or output the information. This section could be programmed to allow deposition rates in each pixel to be calculated from the differences in the source erosion and the transported erosion.
- The model could also then be adapted to run on a time-series basis to allow multiple storms to be modelled. Data about the erosion and deposition rates within the catchment from previous storms would be retained and added into the equations for subsequent storms. This investigation would determine whether the theory that large storms produce a 'wash-out' effect as described in section 11.2.3 was valid.
- Further application of the model to 'build' networks of catchments, using the sub-basin theories, could then be developed into a large-scale model that can estimate sediment yields within the Volta catchment.
- Translation of those results into estimated sedimentation rates of Lake Volta could then be undertaken. This could possibly include models based on dredging data from Lake Volta to validate the estimated sedimentation. This would only be viable, however, if the hypothesis of mass balance calculations (section 8.1.5) could be proven to work in these circumstances. Stochastic predictions of the particle size distributions of the sediment in the lake would have to be made as contributing catchments would not all have the same characteristics. Both this stage and the previous one also have severe implications on the computer power

required to undertake the modelling, high performance computing techniques may well be needed to complete simulations especially when considering the Volta catchment occupies over 70% of the country.

References

Adler W.F. (1979), 'The mechanics of Liquid Impact', *Treatise on Material Science and Technology*, Preece C. M., Ed., New York: Academic, 1979, **Vol. 16**, 127-183.

Amisigo, B., & Akrasi, S. (2000), 'A suspended sediment yield predictive equation for river basins in the South Western river basin system of Ghana', *Journal of Applied Science and Technology [Online]*, **5(1)**. 108-113

Arnold J.G., Engel B.A. & Srinivasan R. (1993), 'A Continuous Time, Grid Cell Watershed Model' *in* 'Application of Advanced Information Technologies for Management of Natural Resources', Sponsored by ASAE, June 17-19, Spokane, Washington.

Arnold J.G., Williams J.R., Nicks A.D., & Sammons N.B. (1990), *SWRRB – A basin scale simulation model for soil and water resources management*, Texas A&M University Press, College Station, TX.

ASCE, (1996), 'Hydrology Handbook', American Society of Civil Engineering.

Ayamga T, (2000), 'SRI Report – Description of the Geology and Soils of the Study Area for M Bambury's PhD Research', *unpublished.*

Bagnold R.A., (1966), 'An Approach to the Sediment Transport Problem from General Physics', Professional Paper, 422-I, US Geological Survey, Washington DC.

Bambury M.C., (1999) (unpublished), 'Modelling Soil Erosion in Ghana: A Final Year Research Project', Department of Civil Engineering, Aston University.

Beasley D.B., Huggins L.F. & Monke E.J. (1982), 'Modelling Sediment Yields from Agricultural Watersheds', *Journal of Soil and Water Conservation*, **Vol. 37**, No.2, 113-117.

Boateng E., Ayamga T., Chidley T., Elgy J., Savory D. & van Velthuizen H. (1998), ' Ghana Environmental Resource Management Project (GERMP) – Land Suitability Analysis', Soil Research Institute, Accra, Ghana.

Bollinne A., Laurant A., Roseau P., Pauwels J.M., Gabriels D. & Aelterman J. (1980), 'Provisional Rain Erosivity Map of Belgium' *in* de Boodt M. & Gabriels D. (Eds.) 'Assessment of Erosion', Wiley, Chichester.

Bradbury P.A., Lea N.J. & Bolton P. (1993), *Estimating Catchment Sediment Yield: Development of the GIS Based CLASITE Model*, HR Wallingford.

Burrough P.A. & McDonnell R.A. (1998), *Principles of Geographical Information Systems*, Oxford University Press.

Chadwick A. & Morfett J. (1993), *Hydraulics in Civil and Environmental Engineering*, E & FN SPON.

Costa-Cabral M.C. & Burges S.J. (1994), 'Digital Elevation Model Networks (DEMON): a model of flow over hillslopes for computation of contributing and dispersal Areas', *Water Resources Research*, **Vol. 30**. 1681-1692.

Cox C. & Madramootoo C. (1998), 'Application of Geographic Information Systems in Waterhsed management Planning in St. Lucia', *Computers and Electronics in Agriculture*, **Vol. 20**, 229-250.

DoE, (1987), 'Handling Geographic Information' Department of Environment, HMSO, London.

Ellison W. D., (1947), 'Soil erosion studies', *Agricultural Engineering*, **Vol. 28**

Elwell H.A. and Stocking M., (1982), 'Developing a simple yet practical method of soil loss estimation', *Tropical Agriculture*, **Vol. 59**, 43-48

Engelund, F. and E. Hansen, (1967), A Monograph on Sediment Transport in Alluvial Streams, Technisk Vorlag, Copenhagen, Denmark

ESRI, (2004), 'What is ArcGIS? – White Paper', ESRI, (http://downloads.esri.com/support/documentation/ao_/698What_is_ArcGIS.pdf)

Fairfield J. & Leymarie P. (1991), 'Drainage Networks from Digital Elevation Models', *Water Resources Research*, **Vol. 27**, 707-717.

FAO, (2003), 'Ghana', http://www.fao.org/ag/agl/swlwpnr/reports/y_sf/z_gh/gh.htm

FAO, (1990), 'Soil map of the world: revised legend', World Soil Resources Report 60, Food and Agriculture Organization of the United Nations, Rome, 119 pp

Flanagan D.C. & Laflen J.M. (1997), 'The USDA Water Erosion Prediction Project (WEPP)', *Eurasian Soil Science*, **Vol. 30**, No. 5, 524-530.

Folly A. (1995), 'Estimation of Erodibility in the Savanna Ecosystem, Northern Ghana', *Comunications in Soil Science and Plant Analysis*, **Vol. 26**, No. 5, 799-812.

Folly A., Bronsveld M.C. & Clavaux M. (1996), 'A Knowledge-Based Approach for C Factor Mapping in Spain using Landsat TM and GIS', *International Journal of Remote Sensing*, **Vol. 17**, No. 2, 2401-2415.

Foster G. R., (1976) 'Sediments, General: Reporter's Comments' *in* 'Proceedings of the National Symposium on Urban Hydrology, Hydraulics, and Sediment Control' 129-128. University of Kentucky, Lexington, Kentucky, July 26-29, 1976.

Foster G.R., McCool D.K., Renard K.G. & Moldenhauer W.C. (1981), 'Conversion of the Universal Soil Loss Equation to SI Metric Units', *Journal of Soil and Water Conservation*, **Vol. 36**, No. 6, 355-359.

Foster G.R. & Lane L.J. (1987), 'User Requirements: USDA-Water Erosion Prediction Project (WEPP)', NESRL Report No. 1, National Soil Erosion Research Laboratory, USDA-ARS, West Lafayette.

Foster G.R., Lane L.J., Nearing M.A., Finkner S.C. & Flanagan D.C. (1989), 'Erosion Component' *in* 'USDA-Water Erosion Prediction Project: Hillslope Profile Model Documentation', NESRL Report No. 2, National Soil Erosion Research Laboratory, USDA-ARS, West Lafayette.

Freeman G.T. (1991), 'Calculating Catchment Area with Divergent Flow Based on a Regular Grid', *Computers and Geosciences*, **Vol. 17**, 413-422.

Gallant J.C. & Wilson J.P.(2000), 'Primary Topographic Attributes', *in* Wilson J.P. & Gallant J.C. (Eds.), 'Terrain Analysis: Principles and Applications', John Wiley and Sons Inc.

Gordon C.M., (1975), 'Period between Bursts at High Reynold's Number', *The Physics of Fluids*, **Vol. 18**, 141-143.

Govers G., (1990), 'Empirical relationships for the transport capacity of overland flow', *Erosion, Transport and Deposition Processes*, Proceedings of the Jerusalem Workshop, IAHS Publication no. 189, pp. 45-63

Grass A.J., (1970), 'Initial Instability of Fine Bed Sand', *Journal of the Hydraulics Division of the American Society of Civil Engineers*, **Vol. 96**, 619-632.

GRASS Development Team (2003), 'GRASS (Geographical Resources Analysis Support System) – GIS', http://grass.itc.it/

Hens L. & Boon E.K. (1999), 'Institutional, Legal and Economic Instruments in Ghana's Environmental Policy', *Environmental Management*, **Vol. 24**, No. 3, 337-351.

Hickey R., Smith A. & Jankowski P. (1994), 'Slope Length Calculations from a DEM within ARC/INFO Grid', *Computers, Environment and Urban Systems*, **Vol. 18**, No. 5, 365-380.

HMSO, (1961), 'Handbook of Meteorological Instruments: Part I', Great Britain Meteorological Office, Her Majesty's Stationery Office, London.

Holtan H. N., (1961), 'A concept for infiltration estimates in watershed engineering', USDA-ARS Bulletin 41-51, Washington, DC

Hossain, M. M. and Rahman, L., (1998) 'Sediment transport functions and their evaluation using data from large alluvial rivers of Bangladesh,, Modelling soil erosion, sediment transport and closely related hydrological processes, ed. by W. Summer, E. Klagho and W. Zhang, IAHS Publication No. 249.

Huggins L. F. & Monke E.J., (1966), 'The mathematical solution of the hydrology of small watersheds', Technical Report No. 1, Water Resources Research Centre, Purdue University, West Lafayette, IN.

Hutchinson M.F. & Gallant J.C. (2000), 'Digital Elevation Models and Representation of Terrain Shape', *in* Wilson J.P. & Gallant J.C. (Eds.), 'Terrain Analysis: Principles and Applications', John Wiley and Sons Inc.

Jenson S.K. & Domingue J.O. (1988), 'Extracting Topographic Structure from Digital Elevation Model Data for Geographic Information System Analysis', *Photogrammetric Engineering and Remote Sensing*, **Vol. 54**, 1593-1600.

Kassam A.H., Velthuizen van H.T., Fischer G.W. & Shah M.M. (1991), 'Agroecological Land Resources Assessment for Agricultural Development Planning, A Case Study for Kenya', Food and Agriculture Organisation of the United Nations.

Kertesz A (1993), 'Application of GIS Methods in Soil Erosion Modelling', *Computers, Environment and Urban Systems*, **Vol. 17**, 233-238.

Kirkby M.J. (1980), 'The Problem' *in* Kirkby M.J. & Morgan R.P.C., 'Soil Erosion', John Wiley and Sons Ltd.

Knisel W.G. (1980) 'CREAMS: A Field Scale Model for Chemicals, Runoff and Erosion from Agricultural Management Systems', Conversation Research Report No. 26, USDA, Washington.

Kusumandari A. & Mitchell B. (1997), 'Soil Erosion and Sediment Yield in Forest and Agroforestry Areas in West Java, Indonesia', *Journal of Soil and Water Conservation*, **Vol. 52**, No. 4, 376-380.

Laflen J.M., Lane L.J. and Foster G.R. (1991), 'WEPP: A New generation of Erosion Prediction Technology', *Journal of Soil and Water Conservation*, **Vol. 46**, 34-38.

Lal R. & Elliot W. (1994), 'Erodibility and Erosivity' *in* Lal R. Ed. 'Soil Erosion Research Methods', 127-156, Soil and Water Conservation Society and St. Lucie Press.

Lane L.J., Hernandez M. & Nichols M. (1997a), 'Processes Controlling Sediment Yield from Watersheds as Functions of Spatial Scale', *Environmental Modelling & Software*, **Vol. 12**. No. 4, 355-369.

Lane L.J., Renard K.G., Foster G.R. & Laflen J.M. (1997b), 'Development and Application of Modern Soil Erosion Prediction Technology: The USDA Experience', *Eurasian Soil Science*, **Vol. 30**, No. 5, 531-540.

Linsley R.K., Kohler M.A., Paulhus J.L.H., (1982), 'Hydrology for engineers', 3rd ed, McGraw-Hill.

Liu B.Y., Nearing M.A. & Risse L.M. (1994), 'Slope Gradient Effects on Soil Loss for Steep Slopes', *Transactions of the ASAE*, **Vol. 37**, 1835-1840.

MapInfo Corporation, (2006), http://www.mapinfo.com

McCallien W.J. and Burke K., (1957), 'Geology of the Coastal Region near Accra', *Journal West African Scientific Association*, **Vol. 3**, p. 79-90.

McCool D.K., Brown L.C., Foster G.R., Mutchler C.K. & Meyer L.D. (1987), 'Revised Slope Steepness Factor for the Universal Soil Loss Equation', *Transactions of the ASAE*, **Vol. 30**, 1387-1396.

Meyer, L. D., and W. H. Wischmeier W.H., (1969), 'Mathematical simulation of the process of soil erosion by water', *Transactions of the ASAE*, **Vol. 12**, 754-762

Mitasova H. & Hofierka J. (1993), 'Interpolation by Regularized Spline with Tension, II: Application to Terrain Modelling and Surface geometry Analysis', *Mathematical Geology*, **Vol. 25**, 657-669.

Mitasova H., Mitas L., Brown W.M., Gerdes D.P., Kowsinovsky I. & Baker T. (1995), 'Modelling Spatially and Temporally Distributed Phenomena: New Methods and Tools for the GRASS GIS', *International Journal of Geographical Information Systems*, **Vol. 9**, 433-456.

Mitasova H., Hofierka J., Zlocha M. & Iverson L.R. (1996), 'Modelling Topographic Potential for Erosion and Deposition using GIS', *International Journal of Geographical Information Systems*, **Vol. 10**, 629-641.

Mitchell J.K. & Bubenzer G.D. (1980), 'Soil Loss Estimation', *in* Kirkby M.J. & Morgan R.P.C., 'Soil Erosion', John Wiley and Sons Ltd.

Molnar D.K. & Julien P.Y. (1998), 'Estimation of Upland Erosion using GIS', *Computers and Geosciences*, **Vol. 24**, No. 2, 183-192.

Moore I.D. (1992), 'Terrain Analysis Programs for the Environmental Sciences', *Agricultural Systems and Information Technology*, **Vol. 2**, 37-39.

Morgan, R.P.C. (1986), 'Soil Erosion and Conservation', John Wiley and Sons, Inc., New York

Musgrave, G.W., (1947), 'Quantitative Evaluation of Factors in Water Erosion, A First Approximation', *Journal of Soil and Water Conservation*, **Vol. 2**, no. 3, pp. 133-138

Nearing M.A. (1997a), 'The Mechanics of Soil Detachment by Raindrops and Runoff', *Eurasian Soil Science*, **Vol. 30**, No. 5, 552-556.

Nearing M.A. (1997b), 'A Single, Continuous function for slope steepness influence on Soil Loss', *Soil Science Society of America Journal*, **Vol. 61**, 917-919.

Nearing M.A. & Lane L.J. (1989), 'USDA-Water Erosion Prediction Project: Hillslope Profile Model Documentation', NESRL Report No. 2, National Soil Erosion Research Laboratory, USDA-ARS, West Lafayette.

Nearing M.A., Lane L.J. & Lopes V.L. (1994), 'Modelling Soil Erosion' *in* Lal R. Ed. 'Soil Erosion Research Methods', 127-156, Soil and Water Conservation Society and St. Lucie Press.

O'Callaghan J.F., Mark D.M. (1984), 'The Extraction of Drainage Networks from Digital Elevation Data', *Computer Vision and Graphics and Image Processing*, **Vol. 28**, 323-344.

Oduro-Afriyie K. (1996), 'Rainfall Erosivity Map for Ghana', *Geoderma*, **Vol. 74**, No. 1-2, 161-166.

Perrone J. (1997), 'Hyrdologic Modelling of an Agricultural Watershed in Quebec using AGNPS', M.S. Thesis, Department of Agriculture and Biosystems Engineering, McGill University, Montreal, Canada.

Perrone J. & Madramootoo C.A. (1997), 'Use of AGNPS for Watershed Modelling in Quebec', *Transactions of the ASAE*, **Vol. 40**, No.5, 1349-1354.

Perrone J. & Madrammootoo C.A. (1999), 'Sediment Yield Prediction Using AGNPS', *Journal of Soil and Water Conservation*, **Vol. 54**, No. 1, 415-419.

Quinn P.F., Beven K.J., Chevallier P. & Planchon O. (1991), 'The Prediction of Hillslope Flow Paths for Distributed Modelling Using Digital Terrain Models', *Hydrological Processes*, **Vol. 5**, 59-79.

Raudiviki, A.J. & Tan S.K. (1984), 'Erosion of Cohesive Soils', *Journal of Hydraulic Research*, **Vol. 22**, 217-233.

Renard K.D., Foster G.R., Weesies G.A. & Porter J.P. (1991), 'RUSLE: Revised Universal Soil Loss Equation', *Journal of Soil and Water Conservation*, **Vol. 46**, No. 1, 30-33.

Renard K.G., Laflen J.M., Foster G.R. & McCool D.K. (1994), 'The Revised Universal Soil Loss Equation' *in* Lal R. Ed. 'Soil Erosion Research Methods', 127-156, Soil and Water Conservation Society and St. Lucie Press.

Roo, de A.P.J., Hazelhoff L. & Burrough P.A. (1989), 'Soil Erosion Modelling using 'ANSWERS' and Geographical Information Systems', *Earth Surface Processes and Landforms*, **Vol. 14**, No. 6-7, 517-532.

Roslan Z.A. & Tew K.H. (1997), 'Use of Satellite Imagery to Determine the Land Use Management Factors of the USLE', *in* Human Impact on Erosion and Sedimentation (Proceedings of Rabat Symposium 56, April 1997), IAHS Publication No. 245.

SCS, (1986), 'TR55 – Urban Hydrology for Small Watersheds', Soil Conservation Service, Technical Report No. 55.

Schumm S.A. (1977), *The Fluvial System*, John Wiley & Sons Inc., New York.

Shaw E.M. (1994), 'Hydrology in Practice', 3rd ed., Chapman and Hall.

Shields A. (1936), 'Application of Similarity Principles and Turbulence Research to Bed-Load Movement', *Mitteilunger der Preussischen Versuchsanstalt fur Wasserbau und Schiffbau*, **Vol. 26**, 5–24.

Smith D.D. & Whitt D.M. (1948), 'Evaluating Soil Losses from Field Areas', *Agricultural Engineering*, **Vol. 29**, 394-396.

Smith R. E. & Williams J. R. (1980), 'Simulation of the surface water hydrology' *in* Knisel W.G. (1980) 'CREAMS: A Field Scale Model for Chemicals, Runoff and Erosion from Agricultural Management Systems', Conversation Research Report No. 26, USDA, Washington.

Smith D.D. & Wischmeier W.H. (1957), 'Factors Affecting Sheet and Rill Erosion', *American Geophysical Union Transactions*, **Vol. 38**, 889-896.

Smyth R.E. & Young M.D. (1998), 'Costing Soil Erosion: A State-Wide Approach', *Land Degradation and Development*, **Vol. 9**, 513-527.

Springer G.S. (1976), *Erosion by Liquid Impact*, Washington D.C.: Scripta, 1976.

Srinivasan R., Engel B.A., Wright J.R., Lee J.G. & Jones D.D. (1994), 'The Impact of GIS-Derived Topographic Attributes on the Simulation of Erosion Using AGNPS', *Applied Engineering in Agriculture*, **Vol. 10**, No. 4, 561-566.

Stocking M.A., (1995), 'Soil Erosion and Land Degradation' *in* O'Riordan T. Ed. 'Environmental Science for Environmental Management', 287-321, Harlow, Longman.

Survey of Ghana, (First Edition), *Map Sheet No 0601D4*, Scale 1:50000

van Rijn, Leo C., (1984), 'Sediment transport, part III: bed forms and alluvial roughness', *Journal of Hydraulic Engineering*, ASCE, **110(12)**, 1733-1754

Viney N.R. & Sivapalan M., (1999), 'A conceptual model of sediment transport: application to the Avon River Basin in Western Australia', *Hydrological Processes*, **13(5)**, 727-743.

Walling D.E. (1994) 'Measuring Sediment Yield from River Basins' *in* Lal R. Ed. 'Soil Erosion Research Methods', 127-156, Soil and Water Conservation Society and St. Lucie Press.

Weltz M.A., Kidwell M.A. & Fox D.H. (1998), 'Invited Synthesis paper: Influence of Abiotic and Biotic Factors in Measuting and Modelling Soil Erosion on Rangelands: State of Knowledge', *Journal of Range Management*, **Vol. 51**, No. 5, 482-495.

White W.R., (1972), 'Sediment Transport in Channels, a General Function', Internal Report 102, Hydraulics Research, Wallingford.

Williams J.R., (1980), 'SPNM, a model for predicting sediment, phosphorus, and nitrogen yields from agricultural basins', *Water Resources Bulletin*, **Vol 16**, 843-848.

Williams J.R. & Arnold J.G. (1997), 'A system of erosion-sediment yield models', *Soil Technology*, **Vol. 11**, 43–55.

Williams J.R. & Berndt H.D. (1976), (Unseen, Ref taken from Mitchell J.K. & Bubenzer G.D., (1980)), 'Sediment Yield Prediction Based on Watershed Hydrology', Unpublished paper No. 76-2535, *American Society of Agricultural Engineers*, St. Joseph, Michigan.

Williams J.R. & Berndt H.D. (1977), 'Sediment Yield Prediction Based on Watershed Hydrology', *Transactions of the ASAE*, **Vol. 20**, 1100-1104.

Williams J.R., Jones C.A. & Dyke P.T. (1984), 'A Modelling Approach to Determining the Relationship between Erosion and Soil Productivity', *Transactions of the ASAE*, **Vol. 27**, No. 1, 129-144.

Williams J.R., Nicks A.D. & Arnold J.G. (1985), 'SWRRB, a Simulator for Water Resources in Rural Basins', *ASCE Hydrology Journal*, **Vol. 111**, No. 6, 970-986.

Wilson J.P. & Gallant J.C. (1998), 'Terrain-Based Approaches to Environmental Resource Evaluation', *in* Lane S.N., Richards K.S. & Chandler J.H. (Eds.) 'Landfrom Monitoring, Modelling and Analysis. New York: Wiley.

Wischmeier, W.H., & Smith D.D., (1965), 'Predicting rainfall-erosion losses from cropland east of the Rocky Mountains: Guide for selection of practices for soil and water conservation', U.S. Department of Agriculture, Agricultural Handbook No. 282

Wischmeier W.H. & Smith D.D. (1978), 'Predicting Rainfall Erosion Losses – A Guide to Conservation Planning', *Agricultural Handbook 537*, Science and Education Administration, USDA, Washington D.C.

Yalin M.S., (1963), 'An Expression for Bed-load Transportation', *Journal of Hydraulic Division*, **89(HY3)**: 221-250

Yang, C. T., (1973), 'Incipient motion and sediment transport,' *Journal of the Hydraulics Division, ASCE*, **Vol. 99**, No. HY10, Proc. Paper 10067, pp.1679-1704

Yitayew M., Pokrzywka S.J. & Renard K.G. (1999), 'Using GIS for Facilitating Erosion Estimation', *Applied Engineering in Agriculture*, **Vol. 15**, No. 4, 295-301.

Young R.A., Onstad C.A., Bosch D.D. & Anderson W.P. (1987), 'Agricultural Nonpoint Source Pollution Model: A Large Watershed Analysis Tool', *Conservation Research Report No. 35*, USDA-ARS, Washington.

Young R.A., Onstad C.A., Bosch D.D. & Anderson W.P. (1989), 'AGNPS: A Nonpoint-Source Pollution Model for Evaluating Agricultural Watersheds', *Journal of Soil and Water Conservation*, **Vol. 44**, No. 2, 168-173.

Zhang L., O'Neill A.L. & Lacey S. (1996), 'Modelling Approaches to the Prediction of Soil Erosion in Catchments', *Environmental Software*, **Vol. 11**, No. 3-1, 123-133.

Zhang W. & Summer W., (1998), 'Sediment Transport Analysed by Energy Derived Concepts', *in* IAHS publication no. 249, 137-46

Zingg A.W. (1940), 'Degree and Length of Land Slope as it Affects Soil Loss in Runoff', *Agricultural Engineering*, **Vol. 21**, 59-64.

Appendix A – Ghana Field Trip Data

A.1 – Flow Data

Flow Meter Results		15/09/2000	12:50				
Cross Section at Suspended Sediment Traps							
Position	Width*	Dist above bed	Depth of flow	Count	Time (s)	RPS	Velocity
A	4.65	100	345	59	60	0.983333	0.283333
A	4.65	200	345	79	60	1.316667	0.366667
A	4.65	300	345	86	60	1.433333	0.395833
B	5.08	100	210	75	60	1.25	0.35
C	5.56	100	160	72	60	1.2	0.3375
D	5.91	100	160	68	60	1.133333	0.320833
E	6.55	100	155	60	60	1	0.2875
Position of Gauging Pole from A						Average	0.334524
Depth of Flow at Gauging Pole			0.275				
Depth of Flow at point A			0.365				
Area of Flow			0.438673835				
Flow Rate			0.146746842				
* Width is distance from point E, where at far bank measurement is taken at x.x metres from the line EF (See figure 4.x)							

Table A.1 Flow Meter Readings 15/09/2000 12:50pm

Flow Meter Results		15/09/2000	15:00				
Cross Section at Suspended Sediment Traps							
Position	Width*	Dist above bed	Depth of flow	Count	Time (s)	RPS	Velocity
A	4.65	100	340	53	60	0.883333	0.258333
A	4.65	200	340	82	60	1.366667	0.379167
A	4.65	300	340	88	60	1.466667	0.404167
B	5.08	100	210	85	60	1.416667	0.391667
C	5.56	100	160	79	60	1.316667	0.366667
D	5.91	100	165	75	60	1.25	0.35
E	6.55	100	150	54	60	0.9	0.2625
Position of Gauging Pole from A						Average	0.344643
Depth of Flow at Gauging Pole			0.27				
Depth of Flow at point A			0.36				
Area of Flow			0.424655018				
Flow Rate			0.146354319				

Table A.2 Flow Meter Readings 15/09/2000 15:00pm

Flow Meter Results		15/09/2000	13:10				
Cross Section at Suspended Sediment Traps							
Position	Width*	Dist above bed	Depth of flow	Count	Time (s)	RPS	Velocity
A	4.65	100	340	73	60	1.216667	0.341667
A	4.65	200	340	83	60	1.383333	0.383333
A	4.65	300	340	96	60	1.6	0.4375
B	5.08	100	220	87	60	1.45	0.4
C	5.56	100	165	89	60	1.483333	0.408333
D	5.91	100	165	74	60	1.233333	0.345833
E	6.55	100	155	69	60	1.15	0.325
Position of Gauging Pole from A						Average	0.377381
Depth of Flow at Gauging Pole			0.275				
Depth of Flow at point A			0.365				
Area of Flow			0.438673835				
Flow Rate			0.16554715				

Table A.3 Flow Meter Readings 15/09/2000 13:10pm

Flow Meter Results		14/09/2000	15:05				
Cross Section at Suspended Sediment Traps							
Position	Width*	Dist above bed	Depth of flow	Count	Time (s)	RPS	Velocity
A	4.65	100	350	75	60	1.25	0.35
A	4.65	200	350	89	60	1.483333	0.408333
A	4.65	300	350	99	60	1.65	0.45
B	5.08	100	215	90	60	1.5	0.4125
C	5.56	100	160	93	60	1.55	0.425
D	5.91	100	170	86	60	1.433333	0.395833
E	6.55	100	160	84	60	1.4	0.3875
Position of Gauging Pole from A						Average	0.404167
Depth of Flow at Gauging Pole			0.28				
Depth of Flow at point A			0.37				
Area of Flow			0.452782258				
Flow Rate			0.182999496				

Table A.4 Flow Meter Readings 14/09/2000 15:05pm

Flow Meter Results		14/09/2000	14:45				
Cross Section at Suspended Sediment Traps							
Position	Width*	Dist above bed	Depth of flow	Count	Time (s)	RPS	Velocity
A	4.65	100	350	72	60	1.2	0.3375
A	4.65	200	350	83	60	1.383333	0.383333
A	4.65	300	350	89	60	1.483333	0.408333
B	5.08	100	215	92	60	1.533333	0.420833
C	5.56	100	155	85	60	1.416667	0.391667
D	5.91	100	170	79	60	1.316667	0.366667
E	6.55	100	155	79	60	1.316667	0.366667
Position of Gauging Pole from A						Average	0.382143
Depth of Flow at Gauging Pole			0.28				
Depth of Flow at point A			0.37				
Area of Flow			0.452782258				
Flow Rate			0.173027506				

Table A.5 Flow Meter Readings 14/09/2000 14:45pm

Flow Meter Results		13/09/2000	15:00				
Cross Section at Suspended Sediment Traps							
Position	Width*	Dist above bed	Depth of flow	Count	Time (s)	RPS	Velocity
A	4.65	100	345	75	60	1.25	0.35
A	4.65	200	345	83	60	1.383333	0.383333
A	4.65	300	345	101	60	1.683333	0.458333
B	5.08	100	225	82	60	1.366667	0.379167
B	5.08	200	225	105	60	1.75	0.475
C	5.56	100	160	99	60	1.65	0.45
D	5.91	100	175	94	60	1.566667	0.429167
E	6.55	100	160	92	60	1.533333	0.420833
Position of Gauging Pole from A						Average	0.418229
Depth of Flow at Gauging Pole			0.29				
Depth of Flow at point A			0.38				
Area of Flow			0.481212366				
Flow Rate			0.201257047				

Table A.6 Flow Meter Readings 13/09/2000 15:00pm

Flow Meter Results		14/09/2000	11:20				
Cross Section at Suspended Sediment Traps							
Position	Width*	Dist above bed	Depth of flow	Count	Time (s)	RPS	Velocity
A	4.65	100	345	75	60	1.25	0.35
A	4.65	200	345	92	60	1.533333	0.420833
A	4.65	300	345	105	60	1.75	0.475
B	5.08	100	230	82	60	1.366667	0.379167
B	5.08	200	230	106	60	1.766667	0.479167
C	5.56	100	165	110	60	1.833333	0.495833
D	5.91	100	180	105	60	1.75	0.475
E	6.55	100	165	98	60	1.633333	0.445833
Position of Gauging Pole from A						Average	0.440104
Depth of Flow at Gauging Pole			0.295				
Depth of Flow at point A			0.385				
Area of Flow			0.495520161				
Flow Rate			0.218080488				

Table A.7 Flow Meter Readings 14/09/2000 11:20am

Flow Meter Results		13/09/2000	11:00				
Cross Section at Suspended Sediment Traps							
Position	Width*	Dist above bed	Depth of flow	Count	Time (s)	RPS	Velocity
A	4.65	100	340	75	60	1.25	0.35
A	4.65	200	340	89	60	1.483333	0.408333
A	4.65	300	340	99	60	1.65	0.45
B	5.08	100	235	81	60	1.35	0.375
B	5.08	200	235	92	60	1.533333	0.420833
C	5.56	100	160	96	60	1.6	0.4375
D	5.91	100	175	91	60	1.516667	0.416667
E	6.55	100	160	85	60	1.416667	0.391667
Position of Gauging Pole from A						Average	0.40625
Depth of Flow at Gauging Pole			0.3				
Depth of Flow at point A			0.39				
Area of Flow			0.509889785				
Flow Rate			0.207142725				

Table A.8 Flow Meter Readings 13/09/2000 11:00am

Flow Meter Results		13/09/2000	11:30				
Cross Section at Suspended Sediment Traps							
Position	Width*	Dist above bed	Depth of flow	Count	Time (s)	RPS	Velocity
A	4.65	100	350	74	60	1.233333	0.345833
A	4.65	200	350	84	60	1.4	0.3875
A	4.65	300	350	97	60	1.616667	0.441667
B	5.08	100	250	81	60	1.35	0.375
B	5.08	200	250	104	60	1.733333	0.470833
C	5.56	100	165	115	60	1.916667	0.516667
D	5.91	100	180	110	60	1.833333	0.495833
E	6.55	100	165	98	60	1.633333	0.445833
Position of Gauging Pole from A						Average	0.434896
Depth of Flow at Gauging Pole			0.3				
Depth of Flow at point A			0.39				
Area of Flow			0.509889785				
Flow Rate			0.221748943				

Table A.9 Flow Meter Readings 13/09/2000 11:30am

Flow Meter Results		25/09/2000	16:10				
Cross Section at Suspended Sediment Traps							
Position	Width*	Dist above bed	Depth of flow	Count	Time (s)	RPS	Velocity
A	4.65	100	360	81	60	1.35	0.375
A	4.65	200	360	95	60	1.583333	0.433333
A	4.65	300	360	104	60	1.733333	0.470833
A	4.65	350	360	115	60	1.916667	0.516667
B	5.08	100	260	84	60	1.4	0.3875
B	5.08	200	260	102	60	1.7	0.4625
C	5.56	100	175	116	60	1.933333	0.520833
D	5.91	100	185	105	60	1.75	0.475
E	6.55	100	160	102	60	1.7	0.4625
Position of Gauging Pole from A						Average	0.456019
Depth of Flow at Gauging Pole			0.31				
Depth of Flow at point A			0.4				
Area of Flow			0.538814516				
Flow Rate			0.245709397				

Table A.10 Flow Meter Readings 25/09/2000 16:10pm

Flow Meter Results		25/09/2000	11:15				
Cross Section at Suspended Sediment Traps							
Position	Width*	Dist above bed	Depth of flow	Count	Time (s)	RPS	Velocity
A	4.65	100	365	72	60	1.2	0.3375
A	4.65	200	365	94	60	1.566667	0.429167
A	4.65	300	365	105	60	1.75	0.475
B	5.08	100	265	96	60	1.6	0.4375
B	5.08	200	265	111	60	1.85	0.5
C	5.56	100	170	119	60	1.983333	0.533333
D	5.91	100	190	96	60	1.6	0.4375
E	6.55	100	165	93	60	1.55	0.425
Position of Gauging Pole from A						Average	0.446875
Depth of Flow at Gauging Pole			0.325				
Depth of Flow at point A			0.415				
Area of Flow			0.582665323				
Flow Rate			0.260378566				

Table A.11 Flow Meter Readings 25/09/2000 11:15am

Flow Meter Results		22/09/2000	12:20			
Cross Section at Suspended Sediment Traps						
Position	Width*	Dist above bed	Depth of flow	Count	Time (s)	RPS	Velocity
A	4.65	100	370	78	60	1.3	0.3625
A	4.65	200	370	97	60	1.616667	0.441667
A	4.65	300	370	110	60	1.833333	0.495833
B	5.08	100	235	104	60	1.733333	0.470833
B	5.08	200	235	119	60	1.983333	0.533333
C	5.56	100	160	125	60	2.083333	0.558333
D	5.91	100	155	117	60	1.95	0.525
E	6.55	100	160	91	60	1.516667	0.416667
Position of Gauging Pole from A						Average	0.475521
Depth of Flow at Gauging Pole			0.325				
Depth of Flow at point A			0.415				
Area of Flow			0.582665323				
Flow Rate			0.2770695				

Table A.12 Flow Meter Readings 22/09/2000 12:20pm

Flow Meter Results		22/09/2000	11:45				
Cross Section at Suspended Sediment Traps							
Position	Width*	Dist above bed	Depth of flow	Count	Time (s)	RPS	Velocity
A	4.65	100	365	88	60	1.466667	0.404167
A	4.65	200	365	99	60	1.65	0.45
A	4.65	300	365	112	60	1.866667	0.504167
B	5.08	100	250	97	60	1.616667	0.441667
B	5.08	200	250	118	60	1.966667	0.529167
C	5.56	100	160	102	60	1.7	0.4625
D	5.91	100	155	99	60	1.65	0.45
E	6.55	100	170	91	60	1.516667	0.416667
Position of Gauging Pole from A						Average	0.457292
Depth of Flow at Gauging Pole			0.33				
Depth of Flow at point A			0.42				
Area of Flow			0.597405914				
Flow Rate			0.273188746				

Table A.13 Flow Meter Readings 22/09/2000 11:45am

Flow Meter Results		21/09/2000	12:05				
Cross Section at Suspended Sediment Traps							
Position	Width*	Dist above bed	Depth of flow	Count	Time (s)	RPS	Velocity
A	4.65	100	390	68	60	1.133333	0.320833
A	4.65	200	390	88	60	1.466667	0.404167
A	4.65	300	390	103	60	1.716667	0.466667
A	4.65	350	390	110	60	1.833333	0.495833
B	5.08	100	255	78	60	1.3	0.3625
B	5.08	200	255	110	60	1.833333	0.495833
C	5.56	100	190	114	60	1.9	0.5125
C	5.56	100	190	110	60	1.833333	0.495833
D	5.91	100	185	109	60	1.816667	0.491667
E	6.55	100	175	97	60	1.616667	0.441667
Position of Gauging Pole from A						Average	0.44875
Depth of Flow at Gauging Pole			0.34				
Depth of Flow at point A			0.43				
Area of Flow			0.627072581				
Flow Rate			0.281398821				

Table A.14 Flow Meter Readings 21/09/2000 12:05pm

Flow Meter Results		20/09/2000	12:00				
Cross Section at Suspended Sediment Traps							
Position	Width*	Dist above bed	Depth of flow	Count	Time (s)	RPS	Velocity
A	4.65	100	415	68	60	1.133333	0.320833
A	4.65	200	415	74	60	1.233333	0.345833
A	4.65	300	415	99	60	1.65	0.45
A	4.65	350	415	109	60	1.816667	0.491667
B	5.08	100	275	74	60	1.233333	0.345833
B	5.08	200	275	104	60	1.733333	0.470833
C	5.56	100	190	108	60	1.8	0.4875
D	5.91	100	180	116	60	1.933333	0.520833
E	6.55	100	170	100	60	1.666667	0.454167
Position of Gauging Pole from A						Average	0.431944
Depth of Flow at Gauging Pole			0.345				
Depth of Flow at point A			0.435				
Area of Flow			0.627072581				
Flow Rate			0.270860517				

Table A.15 Flow Meter Readings 20/09/2000 12:00pm

Flow Meter Results		22/09/2000	15:45				
Cross Section at Suspended Sediment Traps							
Position	Width*	Dist above bed	Depth of flow	Count	Time (s)	RPS	Velocity
A	4.65	100	350	72	60	1.2	0.3375
A	4.65	200	350	86	60	1.433333	0.395833
A	4.65	300	350	95	60	1.583333	0.433333
B	5.08	100	245	89	60	1.483333	0.408333
B	5.08	200	245	101	60	1.683333	0.458333
C	5.56	100	165	107	60	1.783333	0.483333
D	5.91	100	180	102	60	1.7	0.4625
E	6.55	100	165	94	60	1.566667	0.429167
Position of Gauging Pole from A						Average	0.426042
Depth of Flow at Gauging Pole			0.305				
Depth of Flow at point A			0.395				
Area of Flow			0.524321237				
Flow Rate			0.223382693				

Table A.16 Flow Meter Readings 22/09/2000 15:45pm

A.2 – Soil Data

Date	Sample	1	2	3	4	5
15/09/2000	Site					
	Ring ID	73	115	248	261	99
	Weight of ring	80.473	80.452	80.420	80.651	80.052
	Weight of filter paper	0.000	0.000	0.000	0.000	0.000
	Weight of ring+wet sample	291.714	220.228	224.869	224.360	219.662
	Weight of wet sample	211.241	139.776	144.449	143.709	139.610
	Weight of ring+oven dry sample+filter paper	223.626	194.247	212.160	205.245	196.851
	Weight of oven dry sample	143.153	113.795	131.740	124.594	116.799
	Weight of water	68.088	25.981	12.709	19.115	22.811
	MC %	32.232	18.588	8.798	13.301	16.339
	Bulk density	2.135	1.412	1.460	1.452	1.411
	Dry density g/cm^3	1.447	1.150	1.331	1.259	1.180

Table A.17 Soil Sample Data, 15/09/2000

Date	Sample	1	2	3	4
19/09/2000	Site				
	Ring ID	47	33	63	267
	Weight of ring	80.392	80.278	80.475	80.017
	Weight of filter paper	0.000	0.000	0.000	0.000
	Weight of ring+wet sample	246.644	235.407	233.477	222.630
	Weight of wet sample	166.252	155.129	153.002	142.613
	Weight of ring+oven dry sample+filter paper	217.457	208.785	214.791	196.109
	Weight of oven dry sample	137.065	128.507	134.316	116.092
	Weight of water	29.187	26.622	18.686	26.521
	MC %	17.556	17.161	12.213	18.596
	Bulk density	1.680	1.568	1.546	1.441
	Dry density g/cm^3	1.385	1.299	1.357	1.173

Table A.18 Soil Sample Data, 19/09/2000

Date	Sample	1	2	3	4
20/09/2000	Site				
	Ring ID	111	45	84	88
	Weight of ring	80.474	80.659	80.245	80.511
	Weight of filter paper	0.000	0.000	0.000	0.000
	Weight of ring+wet sample	256.400	243.088	271.537	252.247
	Weight of wet sample	175.926	162.429	191.292	171.736
	Weight of ring+oven dry sample+filter paper	229.817	209.903	246.042	220.522
	Weight of oven dry sample	149.343	129.244	165.797	140.011
	Weight of water	26.583	33.185	25.495	31.725
	MC %	15.110	20.430	13.328	18.473
	Bulk density	1.778	1.641	1.933	1.735
	Dry density g/cm^3	1.509	1.306	1.675	1.415

Table A.19 Soil Sample Data, 20/09/2000

Date	Sample	1	2	3	4	5
21/09/2000	Site					bed-load
	Ring ID	81	70	66	248	261
	Weight of ring	80.213	80.462	80.029	80.396	80.623
	Weight of filter paper	0.000	0.000	0.000	0.000	1.189
	Weight of ring+wet sample	253.508	247.739	272.280	246.056	240.608
	Weight of wet sample	173.295	167.277	192.251	165.660	159.985
	Weight of ring+oven dry sample+filter paper	223.225	214.517	243.241	215.902	219.715
	Weight of oven dry sample	143.012	134.055	163.212	135.506	137.903
	Weight of water	30.283	33.222	29.039	30.154	22.082
	MC %	17.475	19.860	15.105	18.202	13.803
	Bulk density	1.751	1.690	1.943	1.674	1.617
	Dry density g/cm^3	1.445	1.355	1.649	1.369	1.394

Table A.20 Soil Sample Data, 21/09/2000

Date	Sample	1	2	3	4
22/09/2000	Site				
	Ring ID	63	267	33	47
	Weight of ring	80.475	80.017	80.278	80.392
	Weight of filter paper	0.000	0.000	0.000	1.208
	Weight of ring+wet sample	275.495	254.252	272.400	250.916
	Weight of wet sample	195.020	174.235	192.122	170.524
	Weight of ring+oven dry sample+filter paper	245.472	221.426	246.464	220.576
	Weight of oven dry sample	164.997	141.409	166.186	138.976
	Weight of water	30.023	32.826	25.936	31.548
	MC %	15.395	18.840	13.500	18.501
	Bulk density	1.971	1.761	1.941	1.723
	Dry density g/cm^3	1.667	1.429	1.679	1.404

Table A.21 Soil Sample Data, 22/09/2000

ID no	3SA1 (0-30)	3SA2 (30-100)	2SB1 (0-10)	4SB2 (0-30)	1SC1 (0-30)	1SC1 (0-100)	Bed Load Sample
+sand	43.421	44.708	43.586	45.282	41.213	41.386	47.458
No	20	8	79	37	77	120	59
Tare	28.343	29.918	30.11	30.243	27.291	27.072	29.737
Sand	15.078	14.79	14.476	15.039	13.922	14.314	17.691
%sand	78.05	74.43	69.77	78.14	72.35	75.2	91.9
Total	19.318	19.87	19.316	19.239	19.242	19.034	19.251
+fraction	28.273	28.63	28.189	26.753	28.991	27.749	29.483
No	119	86	38	48	33	25	3
Tare	28.14	28.483	28.016	26.621	28.831	27.604	29.483
silt/clay	4.24	5.08	5.84	4.2	5.32	4.72	1.56
Silt	3.08	3.88	4.64	3.6	3.8	3.76	1.36
%silt	15.94	19.53	24.02	18.71	19.75	19.75	7.06
%clay	6.01	6.04	6.21	3.15	7.9	5.05	1.04
+fraction	29.33	29.525	29.354	29.354	29.664	29.665	26.603
No	125	28	7	63	36	116	55
Tare	29.274	29.468	29.297	29.312	29.599	29.614	26.571
Weight(500um)	1.306	1.201	2.251	1.112	1.202	1.253	2.218
Weight(355um)	2.882	3.486	5.561	3.492	3.216	3.873	5.728
Weight(125um)	12.52	13.443	13.306	14.15	13.363	14.63	14.295
Weight(63um)	14.455	14.49	14.13	14.74	14.493	14.86	15.29

Table A.22 Full Particle Size Analysis of Soil Types found within Catchment

ID no	3SA1 (0-30)	3SA2 (30-100)	2SB1 (0-10)	4SB2 (0-30)	1SC1 (0-30)	1SC1 (0-100)	Bed Load Sample
texture	loamy sand	sandy loam	sandy loam	loamy sand	Loamy sand	loamy sand	sand
%coarse	2.68	2.35	4.13	2.29	2.29	2.38	5.36
%medium	5.92	6.83	10.21	7.18	6.12	7.66	13.85
%fine	25.72	26.33	24.43	29.1	25.44	27.76	34.57
%very fine	28.69	28.38	25.94	30.31	27.59	29.41	36.98
%sand	78.05	74.43	69.77	78.14	72.35	75.2	91.9

Table A.23 Particle Size Analysis of Sand Content of Soils within Catchment

Daily moisture content readings					
	Site 1	Site 2	Site 3	Site 4	Site 5
Date	M.C.	M.C.	M.C.	M.C.	M.C.
14/09/2000					
15/09/2000	32.232	18.588	8.798	13.301	16.339
16/09/2000					
19/09/2000	17.556	17.161	12.213	18.596	
20/09/2000	15.110	20.430	13.328	18.473	
21/09/2000	17.475	19.860	15.105	18.202	13.803
22/09/2000	15.395	18.840	13.500	18.501	

Table A.24 Daily Moisture Content Readings at Sample Sites around Catchment

A.3 – Survey Data

Stream Cross Section Data			Bench Mark Datum = 100				
Cross Section One							
Comments	Chainage	BS	IS	FS	Collimation	RL	RL (m)
Bench Mark		2.782			102.782		
	0		2.035			100.747	30.70769
	2		2.63			100.152	30.52633
	4		3			99.782	30.41355
	6		2.845			99.937	30.4608
	8		2.995			99.787	30.41508
	10		2.545			100.237	30.55224
	12		2.36			100.422	30.60863
	14		2.571			100.211	30.54431
	16		4.55			98.232	29.94111
	18		4.35			98.432	30.00207
	20		4.515			98.267	29.95178
Bank	20.68		5.225			97.557	29.73537
Stream bed	21		7.38			95.402	29.07853
Stream bed	22		7.62			95.162	29.00538
Stream bed	23		7.71			95.072	28.97795
Stream bed	24		7.82			94.962	28.94442
Bank	24.4		7.16			95.622	29.14559
	25		7.16			95.622	29.14559
	26		6.84			95.942	29.24312
	28		6.74			96.042	29.2736
	30		6.21			96.572	29.43515
	32		6.545			96.237	29.33304
	34		6.85			95.932	29.24007
	36		6.94			95.842	29.21264
	38		7.18			95.602	29.13949
Bench Mark				2.782		100	30.48

Table A.25 Survey Data for Cross-Section One

Stream Cross Section Data			Bench Mark Datum = 100				
Cross Section Two							
Comments	Chainage	BS	IS	FS	Collimation	RL	RL (m)
Bench Mark		6.49			106.49		
	0		4.295			102.195	31.14904
	2		4.91			101.58	30.96158
	4		5.34			101.15	30.83052
	6		6.335			100.155	30.52724
	8		7.09			99.4	30.29712
	10		8.14			98.35	29.97708
	12		9.36			97.13	29.60522
Bank	13.8	4.985		9.79	101.685	96.7	29.47416
Stream bed	14.1		6.33			95.355	29.0642
Stream bed	15		6.75			94.935	28.93619
Stream bed	16		6.22			95.465	29.09773
Stream bed	16.9		6.14			95.545	29.12212
Bank	17.25		5.07			96.615	29.44825
	18		4.995			96.69	29.47111
	20		5.12			96.565	29.43301
	22		4.79			96.895	29.5336
	24		4.78			96.905	29.53664
	26		4.79			96.895	29.5336
	28		4.56			97.125	29.6037
	29		3.19			98.495	30.02128
	30		1.79			99.895	30.448
	31		0.39			101.295	30.87472
Bench Mark				1.505		100.18	30.53486

Table A.26 Survey Data for Cross-Section Two

Appendix B – Methodologies and Experimental Procedures

B.1 Experimental Procedure for the Collection and Measurement of Sediment Samples

B.1.1 General Rules

1) Whenever working in the water with the bed load or suspended sediment traps, always ensure that there is no disruption of the water in the area directly upstream of the traps. An exclusion zone of at least three metres up stream of the traps should be designated which no one must enter. Although, if possible, a larger area upstream should be maintained, in which the streambed remains undisturbed.
2) If the quantity of bed-load sediment is such that the boxes become overfilled during the collection period then the period should be reduced to an appropriate length of time. Depending upon the quantity of sediment collected one of the two methods followed accordingly.

B.1.2 Position of measuring sites

The rules for the positioning of traps are the same for both bed-load and suspended load traps.

1) The section of stream channel selected for collection of bed-load and suspended load samples should ideally be as straight and long as possible. The section of channel should not contain any significant disruptions (weirs, waterfalls, etc.) to the flow for a significant distance upstream of the measurement site.
2) Sufficient traps should be placed across the stream width (and throughout the depth in the case of suspended load traps) to give a representative sample of the cross section of the flow.

B.2 Bed Load Traps (Pit trap design)

The bed load trap specification is split into two sections after the notes on the removal of water from the trap, depending upon the quantity of bed load that the stream carries and therefore the quantity of sediment that is collected within the allotted period. The pit trap consists of three main elements; the outer casing, which is dug into the streambed, the collecting box, which lies inside the outer casing and the grille covering.

B.2.1 Setting up the trap

1) The trap should be buried in the streambed so that the top of the trap is level with the streambed that originally existed, the level of the bed should not be artificially lowered or raised to meet the top of the trap.
2) The collecting box should be wedged into place within the outer casing so that the upstream face of the collecting box is flush with the upstream edge of the outer casing to secure the collecting box in place and to ensure all sediment is collected.
3) Any sediment should be removed from the bottom of the outer casing so that the collecting box fits in the container with the top of the collecting box slightly lower than the top of the outer casing.
4) The time of placement of the trap shall be recorded.

B.2.2 Removal of the trap

1) The collecting box should be removed slowly and carefully so not to disrupt any of the sediment caught in the trap by creating turbulence, which could then remove sediment from the trap decreasing the results.
2) Any sediment that is not inside the collecting box shall not be included in the results and should be carefully removed – e.g. sediment resting on the rim of the collecting box or outer casing and sediment caught within the grille.
3) Always stand downstream of the trap when removing the collecting box.
4) Care should be taken when removing the grille covering, so that the lid does not spill any sediment into the trap.
5) The time of removal of the trap should be recorded so that the length of time of sediment collection is known.

B.2.3 Removal of water from the box

1) The box should be left to stand for a period to enable the trapped sediment to settle thoroughly. Standing period can be based upon fall velocity, using Stoke's Law and the depth of the box. For example, a box 300mm deep and a standard density of sand, the standing time will be 15minutes.
2) Once left to stand the water should carefully be drained ensuring no sediment is lost until a depth of water of approximately 25mm remains above the collected sediment. If the collected sediment is fairly dense and coarse, then the water may be poured away if not then the water must be removed from the box using a cup or similar object.

If the bed load is small and the quantity of sediment is such that all of it could easily be brought back to the lab then the procedure is as follows:

B.2.4 Removal of sediment from the container

1) The sediment should be scraped/tipped/poured, depending upon its consistency, into an appropriate storage container for subsequent analysis.
2) All sediment should be removed from the collecting box.

B.2.5 Storage of sediment until measurement

1) The sediment should be stored in a suitable sealed container to ensure sediment is not lost in transit.

B.2.6 Labelling of collected sediment

1) The container of the collected sediment should be labelled with the date and time of collection and the stream position of the trap.

B.2.7 Laboratory measurement of collected sediment

1) The collected sediment should be measured to give the dry weight of the sediment and should a sufficient quantity be collected then a particle size analysis should be carried out. Any sediment larger than the largest particle size found in the soils of the catchment should not be included in the results.

Alternatively, if the bed load of the stream is very large and the quantity of sediment collected could not be brought back to the lab then the procedure should run as follows:

B.2.8 On site measurement of sediment

1) After most of the water has been removed then the sediment should be smoothed out so that it is approximately level inside the box.
2) The depth from the top of the box to the sediment should be measured in each of the four corners and halfway down each of the longer sides. As the dimensions of the box are known then the volume of collected sediment can be calculated.

B.2.9 Recording of measurements

1) For each box the date and time of measurement should be recorded, the position of the box in the stream and the depths measured within side the box

B.2.10 Sampling collected sediment

1) A sample of the collected sediment should be taken using a soil sampling tube for the purposes of calculating the dry density.
2) A second sample of sufficient size should also be taken for particle size analysis.

B.2.11 Laboratory measurement of sediment

1) The collected tube sample of sediment should be measured to give the dry weight of the sediment. Any sediment larger than the largest particle size found in the soils of the catchment should not be included in the results.
2) A particle size analysis shall be carried out excluding the larger particles from the results.

B.3 Suspended Sediment Traps

B.3.1 Setting up traps

1) The traps, namely bottles, should be tied firmly in place so that the opening of the bottle is kept facing into the direction of flow and traps should be distributed evenly throughout the cross section of the channel.

B.3.2 Removal of traps

1) The traps should be carefully removed ensuring that at no time does the opening of the bottle point downwards as sediment will be lost. This can be best done by sealing the traps (i.e. putting the lid on) before the trap is removed from the water.
2) The removal of traps should be carried out whilst standing downstream of the traps.
3) Once removed, the seal should be checked and the bottles kept in order until they are dried and labelled.

B.3.3 Labelling of traps

1) The traps should be labelled with date, time and stream position.

B.3.4 Emptying traps

1) The traps should be emptied firstly into a measuring cylinder, very carefully ensuring that all sediment is removed from the trap.
2) Once transferred to the measuring cylinder then the sediment can be removed from the water by pouring the trapped water through filter paper that has been pre-weighed and labelled in a similar manner to that of the bottle.

3) Again, it must be ensured that all the sediment must be drained from the measuring cylinder into the filter paper.

4) However, due to the long period it takes the water to drain through the paper the sample for the bottle is allowed to settle for 24hrs in the measuring cylinder. Then the water is siphoned off until the water is a depth of 10mm above the settled sediment.

5) This sediment is then filtered in the normal way.

6) In the case of more sediment being collected than can be accommodated in the filter paper, then after the settling period the water is drained off until only the sediment remains (some sediment will come out during the draining process so the drained water must be kept). The remaining sediment in the bottom is then transferred to crucibles for drying. Not all the sediment will be removable and so the drained water is then returned to the measuring cylinder and left to settle again and the filtering process is then carried out as before, which collects the remaining sediment.

B.3.5 Measurement of trapped sediment

1) Once the sampled water has been collected then the filter papers must be dried and re-weighed to give the dry weight of sediment collected.

2) The difference between the weights of the two papers will give the quantity of sediment that has been collected.

3) Any crucibles used must be weighed with the dried sediment out cleaned and then re-weighed to give the total dry weight of the sediment collected.

B.4 Experimental Procedure for the Collection and Measurement of Soil Samples for Moisture Content Calculations

B.4.1 General Rules

1) The following procedure should always be kept to so that consistent results are obtained. This is especially important for the more sensitive parameters to reduce any experimental error.
2) The time of day at which the measurements are taken should be kept as consistent as possible. If the same route is used to visit the various sites each day and assuming the visit to the field is approximately the same time each day then this will ensure that soil samples are taken at as consistent a time as possible.

B.4.2 Selection of Soil Sample Sites

1) The sites should be carefully selected so that a representative cross section of the varying moisture contents and soil types in the catchment will be obtained. For example if the same soil type occurred at both the catchment bottom and the top of the hill then a sample would need to be taken in both places as there would likely be a higher moisture content in the soil at the bottom of the catchment than at the top.
2) The selection of the sites is best made by a soil scientist (preferably one who has worked within the area before) with many years of experience in the field.

B.4.3 Collection of Soil Samples

Once sites have been identified, soil samples can be collected on a daily basis on a trip around the working area.

1) The samples are to be collected in a small sampling ring with watertight sealing caps and then stored in plastic bags until returned to the lab.
2) To take the sample both caps of the ring are removed and the ring placed on to a flat area of soil surface. The ring is then gently hammered into the ground by placing a piece of wood over the ring and carefully hammering on the wood using a rubber mallet. Making sure the ring does not sink too deep, thereby compacting the upper layers of soil within the sampling ring, hammer on the wood until the ring is fully in the soil.
3) To remove the ring using a blunt knife dig, away the soil around the ring to a depth greater than the ring itself and then using the knife cut away the soil approximately 20mm beneath the ring. Then with the wood still on top of the ring, carefully invert the ring keeping the wood tight to the top. Carefully trim the excess 20mm of soil, which was left during removal, from the ring and seal that end with one of the caps. Then invert the ring again, remove the wood and place the other cap over the remaining exposed end.
4) Samples should then be labelled with the date, time and position of the sample and placed in the plastic bag to be returned to the laboratory.

B.4.4 Measurement of the Soil Samples for Moisture Content Calculations

Once the sampling rings have been received from the field, the samples can be analysed in the lab using the following procedure.

1) Firstly, the samples need to be weighed in their initial state. To do this remove one of the caps and invert the ring into a pre-weighed and marked/numbered

metal/ceramic crucible and then remove the second cap and carefully empty the entire sample into the crucible. Reweigh the now full crucible, the difference between the two being the wet weight of the soil.

2) The samples are then placed in a drying oven for twenty-four hours at 110°C.
3) Once the samples have been dried, they can be reweighed to find the dry weight of the soil and hence the moisture content of the sample can be calculated.
4) A further measure can also be obtained from the samples, if they are put back in the oven for a further twenty-four hours at the higher temperature of 400 °C the samples can then be reweighed for a further time to calculate the organic matter content, the organic matter is burned off at the higher temperature.

B.5 Experimental Procedure for the Measurement of Flow Rates

B.5.1 General Rules

1) The flow readings, unlike the other measurements, do not have to be taken at a consistent time of day. This is because a wide range of results is required to create a representative stage-discharge diagram.

B.5.2 Selection of a measurement site

1) Flow measurements should be made within the vicinity of the sediment traps so that all the results are kept at a consistent site. Measurements should preferably be made either downstream of the bed load sites so not disturb the bed within the exclusion zone or upstream of the suspended load traps.

2) The site of measurements can ideally be made just in front upstream of the suspended sediment traps. This works well for two reasons. Firstly, there are enough of these traps across the section of the stream so that a representative cross section of flow rates is obtained. Secondly, the suspended sediment traps will then act as marker so that readings can be made in approximately the same place each time.

B.5.3 Recording of flow measurements

The flow meter used during the field trip was a hand held A-OTT flow meter, which should be used according to the following procedure.

1) When taking readings just upstream of the suspended sediment traps the only disturbance is to the bed as the flow meter rests on it. If the meter's stand is close enough to the traps then disturbed material will not flow into the lowest trap set 100mm from the bed, but the meter must not be so close to the trap that it significantly disturbs the flow patterns of the water around the trap.
2) Before measurements begin, the apparatus should be dismantled to check that the oil level is correct within the meter.
3) To take a measurement the apparatus, once reassembled, the meter is positioned at the correct height upon the stand and then lowered into the water so that the base rests upon the bed. The height of the meter on the stand should be set so that when measurements are completed a representative cross section of the stream is given. Considering an example depth of flow varies between 400 and 150mm then readings should be taken at 100, 200 and 300mm from the bed providing that the meter is fully submerged. If the occasion should arise where the meter cannot be fully submerged at the

100mm mark for example, then the reading should be taken at the 50mm mark instead. If the depth of flow was 205mm, there would be insufficient depth to allow the meter to be fully submerged, so a reading should be taken at 150mm.

4) After the apparatus has been submerged, the meter should be aligned into the direction of the flow allowed to run for 30 seconds to ensure it is in the right place and functioning correctly.

5) Once the meter is ready, a stopwatch and the counter on the meter should be started simultaneously and allowed to run for 60 seconds. When the time is up then the counter should be stopped and the number of revolutions that the meter has made should be recorded in a table along with the height and position of the meter and the duration of the measurement period.

6) This procedure should be repeated until the entire cross section has been covered. It should also be repeated as many time as possible so that a representative range of depths is recorded enabling a full stage-discharge relationship to be produced for the stream.

B.6 Experimental Procedure for the Measurement of Daily Rainfall

B.6.1 General Rules

1) The following procedure should always be kept to so that consistent results are obtained. This is especially important for the more sensitive parameters to reduce any experimental error.

2) The time of day at which the measurements are taken should be kept as consistent as possible. If the same route is used to visit the various sites each day and assuming the visit to the filed is approximately the same time each

day then this will ensure that soil samples are taken at as consistent a time as possible.

B.6.2 Selection and preparation of a site

1) The site selected for a rain gauge station in a catchment should be in a position that will be representative of the whole area. Depending upon the size of the area more than one gauge, if available, may be necessary to ensure the rainfall pattern is fully represented.
2) The site must then be cleared of all vegetation both around and over the place where the gauge will be situated. The vegetation is cleared from above so no additional water will fall in from overhanging leaves and branches, but also clearing from the sides to a sufficient distance so that no water splashes into the gauge from surrounding vegetation.

B.6.3 Setting up and specification of instrument

1) The collecting cylinder is buried in the ground to such a depth so that the top of the conical section is at ground level.
2) The gauge should be cordoned off to protect it from disruption.
3) The gauge should be of such and such a specification as detailed in such and such a document.

B.6.4 Collection and measurement of readings

1) The rain gauge should be emptied at the same time every day into a calibrated measuring cylinder, so that the daily rainfall can be recorded.

2) The liquid should be carefully transferred to the measuring cylinder that should then be placed on a level surface and the reading taken at the bottom of the meniscus.

3) Should the situation arise where there is more fluid than a full measuring cylinder, the cylinder should be filled and emptied as many times as necessary until a part cylinder be filled. The daily rainfall is sum total of the full and part cylinders.

Appendix C – GRASS C Scripts

C.1 – CALSITE Emulator

This first set of scripts calculate the source erosion using USLE.

```
/* Grass module for CALSITE style model */
/* calsite 1 calculates the source erosion and creates d8 map*/

#include <stdio.h>
#include <stdlib.h>
#include <stddef.h>
#include "gis.h"
#include <math.h>
#define NAME_LEN 100

int main(int argc, char *argv[])
{

  /* prototypes */

  int getline (char line[], int max);
  void calculate_source_erosion(int no_rows, int no_cols, char
C_map_name[],
                                char k_map_name[], char
ls_map_name[], char
                                r_map_name[], char
source_erosion_name[],
                                char wshed_mask_name[]);
  void set_wshed_mask(int no_rows, int no_cols, char
map_to_mask_name[], char
                      wshed_mask_name[], int map_to_mask_fd);


  void get_c_map_name(char c_map_name[]);
  void get_k_map_name(char k_map_name[]);
  void get_ls_map_name(char ls_map_name[]);
  void get_r_map_name(char r_map_name[]);
  void get_source_erosion_map_name(char source_erosion_name[]);
  void get_wshed_mask_name(char wshed_mask_name[]);

  /* variables */

  char c_map_name[NAME_LEN+1];
  char k_map_name[NAME_LEN+1];
  char ls_map_name[NAME_LEN+1];
  char r_map_name[NAME_LEN+1];
  char source_erosion_name[NAME_LEN+1];
  char wshed_mask_name[NAME_LEN+1];

  int no_rows, no_cols;

  /* initialise the GRASS environment variables */

  G_gisinit (argv[0]);

  /* get map names */
```

```
    get_c_map_name(c_map_name);
    get_k_map_name(k_map_name);
    get_ls_map_name(ls_map_name);
    get_r_map_name(r_map_name);
    get_wshed_mask_name(wshed_mask_name);
    get_source_erosion_map_name(source_erosion_name);

    no_rows = G_window_rows();
    no_cols = G_window_cols();

    /* run CALSITE routines */

    calculate_source_erosion(no_rows, no_cols, c_map_name, k_map_name,
                             ls_map_name, r_map_name,
source_erosion_name,
                             wshed_mask_name);

    return (EXIT_SUCCESS);
}
/* get map names */

#include <stdio.h>
#include <stdlib.h>
#include <stddef.h>
#include "gis.h"
#include <math.h>
#define NAME_LEN 100

int getline(char line[], int max)
{
  int c;
  int i = 0;

  while((c = getchar()) != '\n')
    if(i < max)
      line[i++] = c;
  line[i] = '\0';
  return (c == '\n') ? i : -1;
}

/* input maps */

/* c map */

void get_c_map_name(char c_map_name[])
{
  char *prompt;
  char *mapset;
  char *message;
  struct FPRange *r;
  int check;
  DCELL *min, *max;

  prompt = "please enter c factor raster map file";
  mapset = G_ask_cell_in_mapset(prompt, c_map_name);
  if(mapset == NULL)
  {
    message = "exiting module.... \n";
    G_fatal_error(message);
  }
}
```

```
/* k map */

void get_k_map_name(char k_map_name[])
{
  char *prompt;
  char *mapset;
  char *message;
  struct FPRange *r;
  int check;
  DCELL *min, *max;

  prompt = "please enter k factor raster map file";
  mapset = G_ask_cell_in_mapset(prompt, k_map_name);
  if(mapset == NULL)
  {
    message = "exiting module.... \n";
    G_fatal_error(message);
  }
}

/* ls map */

void get_ls_map_name(char ls_map_name[])
{
  char *prompt;
  char *mapset;
  char *message;
  struct FPRange *r;
  int check;
  DCELL *min, *max;

  prompt = "please enter ls factor raster map file";
  mapset = G_ask_cell_in_mapset(prompt, ls_map_name);
  if(mapset == NULL)
  {
    message = "exiting module.... \n";
    G_fatal_error(message);
  }
}

/* r map */

void get_r_map_name(char r_map_name[])
{
  char *prompt;
  char *mapset;
  char *message;
  struct FPRange *r;
  int check;
  DCELL *min, *max;

  prompt = "please enter r factor raster map file";
  mapset = G_ask_cell_in_mapset(prompt, r_map_name);
  if(mapset == NULL)
  {
    message = "exiting module.... \n";
    G_fatal_error(message);
  }
}
```

```
/* wshed mask */

void get_wshed_mask_name(char wshed_mask_name[])
{
  char *prompt;
  char *mapset;
  char *message;

  prompt = "please enter watershed mask name";
  mapset = G_ask_cell_in_mapset(prompt, wshed_mask_name);
  if(mapset == NULL)
  {
    message = "exiting module.... \n";
    G_fatal_error(message);
  }
}

/* output map, routed erosion is dealt with on separate module run
once values
for s and t have been decided */

/* source erosion map */

void get_source_erosion_map_name(char source_erosion_name[])
{
  int t;
  char *message;

  printf("please enter source erosion map name:\n");
  t = getline(source_erosion_name, NAME_LEN);
  if(t == -1)
  {
    message = "exiting module......\n";
    G_fatal_error(message);
  }
}
/* Set watershed mask */

#include <stdio.h>
#include <stdlib.h>
#include <stddef.h>
#include "gis.h"
#include <math.h>

void set_wshed_mask(int no_rows, int no_cols, char
map_to_mask_name[], char
                    wshed_mask_name[], int map_to_mask_fd)
{
  /* int map_to_mask_fd; */
  int wshed_mask_fd;
  FCELL *map_to_mask_fcell;
  FCELL *wshed_mask_fcell;
  char *message;
  char *mapset;
  int row, col;

  mapset = G_mapset();

  printf("mapset is %s\n", mapset);

  wshed_mask_fd = G_open_cell_old(wshed_mask_name, mapset);
```

```
  if(wshed_mask_fd < 0)
  {
    message = "cannot open watershed mask map, exiting module....";
    G_fatal_error(message);
  }

  printf("map being masked is %s, fd is %i\n", map_to_mask_name,
map_to_mask_fd);

  map_to_mask_fcell = G_allocate_f_raster_buf();
  wshed_mask_fcell = G_allocate_f_raster_buf();

  for(row = 0; row < no_rows; row++)
  {
    G_get_f_raster_row(map_to_mask_fd, map_to_mask_fcell, row);
    G_get_f_raster_row(wshed_mask_fd, wshed_mask_fcell, row);

    for(col = 0; col < no_cols; col++)
    {
      map_to_mask_fcell[col] = map_to_mask_fcell[col] *
wshed_mask_fcell[col];
      printf("%f", map_to_mask_fcell[col]);
    }

    printf("\n");
    G_put_f_raster_row(map_to_mask_fd, map_to_mask_fcell);
  }

  G_free(map_to_mask_fcell);
  G_free(wshed_mask_fcell);

  G_close_cell(map_to_mask_fd);
  G_close_cell(wshed_mask_fd);
}
/* section of module to calculate source erosion */

#include <stdio.h>
#include <stdlib.h>
#include <stddef.h>
#include "gis.h"
#include <math.h>
#define NAME_LEN 100

void calculate_source_erosion(int no_rows, int no_cols, char
c_map_name[],
                              char k_map_name[], char
ls_map_name[], char
                              r_map_name[], char
source_erosion_name[],
                              char wshed_mask_name[])
{
  int c_map_fd;
  int k_map_fd;
  int ls_map_fd;
  int r_map_fd;
  int se_map_fd;
  int wshed_mask_fd;
  int row, col;
  int map_data_type;
  int n;
  DCELL *c_map_fcell;
```

```
DCELL *k_map_fcell;
DCELL *ls_map_fcell;
DCELL *r_map_fcell;
DCELL *se_map_fcell;
DCELL *wshed_mask_fcell;
char *message;
char *mapset;

mapset = G_mapset();

c_map_fd = G_open_cell_old(c_map_name, mapset);
if(c_map_fd < 0)
{
  message = "cannot open c factor map, exiting module\n";
  G_fatal_error(message);
}
k_map_fd = G_open_cell_old(k_map_name, mapset);
if(k_map_fd < 0)
{
  message = "cannot open k factor map, exiting module\n";
  G_fatal_error(message);
}
ls_map_fd = G_open_cell_old(ls_map_name, mapset);
if(ls_map_fd < 0)
{
  message = "cannot open ls factor map, exiting module\n";
  G_fatal_error(message);
}
r_map_fd = G_open_cell_old(r_map_name, mapset);
if(r_map_fd < 0)
{
  message = "cannot open r factor map, exiting module\n";
  G_fatal_error(message);
}

se_map_fd = G_open_raster_new(source_erosion_name, DCELL_TYPE);

wshed_mask_fd = G_open_cell_old(wshed_mask_name, mapset);


c_map_fcell = G_allocate_d_raster_buf();

k_map_fcell = G_allocate_d_raster_buf();

ls_map_fcell = G_allocate_d_raster_buf();

r_map_fcell = G_allocate_d_raster_buf();

se_map_fcell = G_allocate_d_raster_buf();

wshed_mask_fcell = G_allocate_d_raster_buf();

for(row = 0; row < no_rows; row++)
{
  G_get_d_raster_row(c_map_fd, c_map_fcell, row);
  G_get_d_raster_row(r_map_fd, r_map_fcell, row);
  G_get_d_raster_row(k_map_fd, k_map_fcell, row);
  G_get_d_raster_row(ls_map_fd, ls_map_fcell, row);
  G_get_d_raster_row(wshed_mask_fd, wshed_mask_fcell, row);

  for(col = 0; col < no_cols; col++)
```

```
    {
      se_map_fcell[col] = c_map_fcell[col] * r_map_fcell[col] *
k_map_fcell[col] * ls_map_fcell[col] * wshed_mask_fcell[col];
    }

    G_put_d_raster_row(se_map_fd, se_map_fcell);
  }

  G_free(c_map_fcell);
  G_free(k_map_fcell);
  G_free(ls_map_fcell);
  G_free(r_map_fcell);
  G_free(se_map_fcell);
  G_free(wshed_mask_fcell);

  G_close_cell(c_map_fd);
  G_close_cell(k_map_fd);
  G_close_cell(ls_map_fd);
  G_close_cell(r_map_fd);
  G_close_cell(se_map_fd);
  G_close_cell(wshed_mask_fd);
}
```

This next set of scripts shows the programming for the calculation of the drainage area, firstly by the D8 method and secondly by the FD8 method.

```
/* Grass module for CALSITE style model */
/* calsite 1a calculates the source erosion */

#include <stdio.h>
#include <stdlib.h>
#include <stddef.h>
#include "gis.h"
#include <math.h>
#define NAME_LEN 100

int main(int argc, char *argv[])
{

/* prototypes */

  int getline (char line[], int max);
/*  void create_d8_map(int no_rows, int no_cols, char
aspect_map_name[], char d8_map_name[], char wshed_mask_name[]);*/
  void route_stage_one(int no_rows, int no_cols, char
wshed_mask_name[], char d8_map_name[], char contrib_cells_name[]);
/*  void get_aspect_map_name(char aspect_map_name[]);*/
  void get_wshed_mask_name(char wshed_mask_name[]);
  void get_d8_map_name(char d8_map_name[]);
  void get_contrib_cells_map_name(char contrib_cells_name[]);

  /*variables */

  char wshed_mask_name[NAME_LEN+1];
  char d8_map_name[NAME_LEN+1];
  char contrib_cells_name[NAME_LEN+1];
  char aspect_map_name[NAME_LEN+1];
```

```
  int no_rows, no_cols;

  /* initialise the GRASS environment variables */

  G_gisinit (argv[0]);


  /* get map names */

  get_d8_map_name(d8_map_name);
  get_wshed_mask_name(wshed_mask_name);
/*  get_aspect_map_name(aspect_map_name);*/

  no_rows = G_window_rows();
  no_cols = G_window_cols();

/*  create_d8_map(no_rows, no_cols, aspect_map_name, d8_map_name,
wshed_mask_name);*/

  route_stage_one(no_rows, no_cols, wshed_mask_name, d8_map_name,
contrib_cells_name);

  printf("finished route stage one\n");

  return(EXIT_SUCCESS);
}
/* get map names */

#include <stdio.h>
#include <stdlib.h>
#include <stddef.h>
#include "gis.h"
#include <math.h>
#define NAME_LEN 100

int getline(char line[], int max)
{
  int c;
  int i = 0;

  while((c = getchar()) != '\n')
    if(i < max)
      line[i++] = c;
  line[i] = '\0';
  return (c == '\n') ? i : -1;
}

void get_d8_map_name(char d8_map_name[])
{
  char *prompt;
  char *mapset;
  char *message;

  prompt = "please enter d8 map name";
  mapset = G_ask_cell_in_mapset(prompt, d8_map_name);
  if(mapset == NULL)
  {
    message = "exiting module.... \n";
    G_fatal_error(message);
  }
}
```

```
void get_wshed_mask_name(char wshed_mask_name[])
{
  char *prompt;
  char *mapset;
  char *message;

  prompt = "please enter watershed mask name";
  mapset = G_ask_cell_in_mapset(prompt, wshed_mask_name);
  if(mapset == NULL)
  {
    message = "exiting module.... \n";
    G_fatal_error(message);
  }
}

void get_aspect_map_name(char aspect_map_name[])
{
  char *prompt;
  char *mapset;
  char *message;

  prompt = "please enter aspect map name";
  mapset = G_ask_cell_in_mapset(prompt, aspect_map_name);
  if(mapset == NULL)
  {
    message = "exiting module.... \n";
    G_fatal_error(message);
  }
}

/* contributing cells map */

void get_contrib_cells_map_name(char contrib_cells_name[])
{
  int t;
  char *message;

  printf("please enter name of flow paths network map:\n");
  t = getline(contrib_cells_name, NAME_LEN);
  if(t == -1)
  {
    message = "exiting module......\n";
    G_fatal_error(message);
  }
}
/* section to turn aspect map into d8 map */

#include <stdio.h>
#include <stdlib.h>
#include <stddef.h>
#include "gis.h"
#include <math.h>

void create_d8_map(int no_rows, int no_cols, char aspect_map_name[],
char
                   d8_map_name[], char wshed_mask_name[])
{
  FCELL *row_fcell;
  FCELL *d8_map_fcell;
  FCELL *wshed_mask_fcell;
```

```
int d8_map_fd;
int aspect_map_fd;
int wshed_mask_fd;
int row, col;
char *message;
char *mapset;

mapset = G_mapset();

aspect_map_fd = G_open_cell_old(aspect_map_name, mapset);
if(aspect_map_fd < 0)
{
  message = "cannot open aspect map, exiting module\n";
  G_fatal_error(message);
}

d8_map_fd = G_open_raster_new(d8_map_name, FCELL_TYPE);

wshed_mask_fd = G_open_cell_old(wshed_mask_name, mapset);

row_fcell = G_allocate_f_raster_buf();
d8_map_fcell = G_allocate_f_raster_buf();
 wshed_mask_fcell = G_allocate_f_raster_buf();

for(row = 0; row < no_rows; row++)
{
  G_get_f_raster_row(aspect_map_fd, row_fcell, row);
  G_get_f_raster_row(wshed_mask_fd, wshed_mask_fcell, row);

  for(col = 0; col < no_cols; col++)
  {
    if(row_fcell[col] < 22.5)
    d8_map_fcell[col] = 3;
    else if(row_fcell[col] < 67.5)
    d8_map_fcell[col] = 2;
    else if(row_fcell[col] < 112.5)
    d8_map_fcell[col] = 1;
    else if(row_fcell[col] < 157.5)
    d8_map_fcell[col] = 8;
    else if(row_fcell[col] < 202.5)
    d8_map_fcell[col] = 7;
    else if(row_fcell[col] < 247.5)
    d8_map_fcell[col] = 6;
    else if(row_fcell[col] < 292.5)
    d8_map_fcell[col] = 5;
    else if(row_fcell[col] < 337.5)
    d8_map_fcell[col] = 4;
    else
    d8_map_fcell[col] = 3;

    d8_map_fcell[col] = d8_map_fcell[col] * wshed_mask_fcell[col];
  }
  printf("\n");
  G_put_f_raster_row(d8_map_fd, d8_map_fcell);
}

G_free(row_fcell);
G_free(d8_map_fcell);
G_free(wshed_mask_fcell);

G_close_cell(aspect_map_fd);
```

```
  G_close_cell(d8_map_fd);
}
/* first stage of routing */
/* find number of contributing cells and lowest slope value along
flow paths */

#include <stdio.h>
#include <stdlib.h>
#include <stddef.h>
#include "gis.h"
#include <math.h>

void route_stage_one(int no_rows, int no_cols, char
wshed_mask_name[], char d8_map_name[],
                     char contrib_cells_name[])
{
  int row, col, rowa, cola;
  int d8_map_fd;
  int wshed_mask_fd;
  CELL this_square, next_square;
  CELL d8_map_grid[no_rows][no_cols];
  CELL contrib_cells_map[no_rows][no_cols];
  CELL start_flow_path[no_rows][no_cols];
  char *message;
  char *mapset;
  FILE *fpa = fopen("contrib_cells.txt", "w");

  mapset = G_mapset();

  wshed_mask_fd = G_open_cell_old(wshed_mask_name, mapset);
  if(wshed_mask_fd < 0)
  {
    message = "cannot open primary squares map, exiting module\n";
    G_fatal_error(message);
  }

  d8_map_fd = G_open_cell_old(d8_map_name, mapset);
  if(d8_map_fd < 0)
  {
    message = "cannot open d8 map, exiting module\n";
    G_fatal_error(message);
  }

  printf("getting rows\n");

  for(row = 0; row < no_rows; row++)
  {
    G_get_c_raster_row(d8_map_fd, d8_map_grid[row], row);
    G_get_c_raster_row(wshed_mask_fd, start_flow_path[row], row);
  }

  for(row = 0; row < no_rows; row++)
  {
    for(col = 0; col < no_cols; col++)
    {
      contrib_cells_map[row][col] = start_flow_path[row][col];
      printf("row %i col %i ccm %i sfp %i\n", row, col,
contrib_cells_map[row][col], start_flow_path[row][col]);
    }
  }
```

```
  next_square = 1;

  printf("about to analyse\n");

  for(row = 0; row < no_rows; row++)
  {
    for(col = 0; col < no_cols; col++)
    {
      printf("sfp %i\n", start_flow_path[row][col]);
      if(start_flow_path[row][col] == 1)
      {
        this_square = d8_map_grid[row][col];
        rowa = row;
        cola = col;

        while(next_square != 0)
        {
          printf("this_sq %i, next_sq %i, row %i col %i\n",
this_square, next_square, rowa, cola);
          if(this_square == 1)
          {
          contrib_cells_map[rowa-1][cola] = contrib_cells_map[rowa-
1][cola] + 1;
          next_square = d8_map_grid[rowa-1][cola];
          rowa = rowa - 1;
          cola = cola;
          }
          else if(this_square == 2)
          {
          contrib_cells_map[rowa-1][cola+1] = contrib_cells_map[rowa-
1][cola+1] + 1;
          next_square = d8_map_grid[rowa-1][cola+1];
          rowa = rowa - 1;
          cola = cola + 1;
          }
          else if(this_square == 3)
          {
          contrib_cells_map[rowa][cola+1] =
contrib_cells_map[rowa][cola+1] + 1;
          next_square = d8_map_grid[rowa][cola+1];
          rowa = rowa;
          cola = cola + 1;
          }
          else if(this_square == 4)
          {
          contrib_cells_map[rowa+1][cola+1] =
contrib_cells_map[rowa+1][cola+1] + 1;
          next_square = d8_map_grid[rowa+1][cola+1];
          rowa = rowa + 1;
          cola = cola + 1;
          }
          else if(this_square == 5)
          {
          contrib_cells_map[rowa+1][cola] =
contrib_cells_map[rowa+1][cola] + 1;
          next_square = d8_map_grid[rowa+1][cola];
          rowa = rowa + 1;
          cola = cola;
          }
          else if(this_square == 6)
          {
```

```
          contrib_cells_map[rowa+1][cola-1] =
contrib_cells_map[rowa+1][cola-1] + 1;
          next_square = d8_map_grid[rowa+1][cola-1];
          rowa = rowa + 1;
          cola = cola - 1;
          }
          else if(this_square == 7)
          {
          contrib_cells_map[rowa][cola-1] =
contrib_cells_map[rowa][cola-1] + 1;
          next_square = d8_map_grid[rowa][cola-1];
          rowa = rowa;
          cola = cola - 1;
          }
          else if(this_square == 8)
          {
          contrib_cells_map[rowa-1][cola-1] = contrib_cells_map[rowa-
1][cola-1] + 1;
          next_square = d8_map_grid[rowa-1][cola-1];
          rowa = rowa - 1;
          cola = cola - 1;
          }
          else
          printf("oops\n");

          this_square = next_square;
        }
      next_square = 1;
      }
      else
      {
        contrib_cells_map[row][col] = 0;
      }
    }
    printf("analysed number %i row\n", row);
  }

  for(row = 0; row < no_rows; row++)
  {
    for(col =0; col < no_cols; col++)
    {
      contrib_cells_map[row][col] = contrib_cells_map[row][col] *
start_flow_path[row][col];
      fprintf(fpa, "%i ", contrib_cells_map[row][col]);
    }
    fprintf(fpa, "\n");
  }

  G_close_cell(wshed_mask_fd);
  G_close_cell(d8_map_fd);
}
```

For the FD8 routine the first couple of scripts main.c and get_map_names.c are essentially the same, thus to avoid repetition only the two scripts for routing are shown.

```
/* section of module to find primary squares */

#include <stdio.h>
#include <stdlib.h>
#include <stddef.h>
#include "gis.h"
#include <math.h>

void find_primary_squares(int no_rows, int no_cols, char DEM_name[],
char primary_sqs_name[], char wshed_mask_name[])
{
  int primary_sqs_fd;
  int DEM_fd;
  int wshed_fd;
  int row, col;
  int prime_check;
  FCELL *row_one_fcell;
  FCELL *row_two_fcell;
  FCELL *row_three_fcell;
  FCELL *is_primary_square;
  FCELL *wshed_mask;
  char *message;
  char *mapset;

  mapset = G_mapset();

  DEM_fd = G_open_cell_old(DEM_name, mapset);

  if(DEM_fd < 0)
  {
    message = "cannot open dem, exiting module\n";
    G_fatal_error(message);
  }

  wshed_fd = G_open_cell_old(wshed_mask_name, mapset);

  if(wshed_fd < 0)
  {
    message = "cannot open wshed mask, exiting module\n";
    G_fatal_error(message);
  }

  primary_sqs_fd = G_open_raster_new(primary_sqs_name, FCELL_TYPE);

  row_one_fcell = G_allocate_f_raster_buf();
  row_two_fcell = G_allocate_f_raster_buf();
  row_three_fcell = G_allocate_f_raster_buf();
  is_primary_square = G_allocate_f_raster_buf();
  wshed_mask = G_allocate_f_raster_buf();

  printf("analysing dem\n");

  row = 0;

  for(col = 0; col < no_cols; col++)
  {
    is_primary_square[col] = 0;
  }

  G_put_f_raster_row(primary_sqs_fd, is_primary_square);
```

```
 for(row = 1; row < no_rows-1; row++)
 {
   G_get_f_raster_row(DEM_fd, row_one_fcell, row-1);
   G_get_f_raster_row(DEM_fd, row_two_fcell, row);
   G_get_f_raster_row(DEM_fd, row_three_fcell, row+1);
   G_get_f_raster_row(wshed_fd, wshed_mask, row);

   col = 0;

   is_primary_square[col] = 0;

   for(col = 1; col < no_cols-1; col++)
   {

     prime_check = 0;

     if(row_two_fcell[col] >= row_one_fcell[col])
     prime_check = prime_check + 1;
     if(row_two_fcell[col] >= row_one_fcell[col+1])
     prime_check = prime_check + 1;
     if(row_two_fcell[col] >= row_two_fcell[col+1])
     prime_check = prime_check + 1;
     if(row_two_fcell[col] >= row_three_fcell[col+1])
     prime_check = prime_check + 1;
     if(row_two_fcell[col] >= row_three_fcell[col])
     prime_check = prime_check + 1;
     if(row_two_fcell[col] >= row_three_fcell[col-1])
     prime_check = prime_check + 1;
     if(row_two_fcell[col] >= row_two_fcell[col-1])
     prime_check = prime_check + 1;
     if(row_two_fcell[col] >= row_one_fcell[col-1])
     prime_check = prime_check + 1;

     if(prime_check == 8)
     is_primary_square[col] = 1;
     else
     is_primary_square[col] = 0;

     is_primary_square[col] = is_primary_square[col] *
wshed_mask[col];

   }

   col = no_cols;

   is_primary_square[col] = 0;

   G_put_f_raster_row(primary_sqs_fd, is_primary_square);
 }

 row = no_rows;

 for(col = 0; col < no_cols; col++)
 {
   is_primary_square[col] = 0;
 }

 G_put_f_raster_row(primary_sqs_fd, is_primary_square);

 G_free(row_one_fcell);
 G_free(row_two_fcell);
```

```
  G_free(row_three_fcell);
  G_free(is_primary_square);
  G_free(wshed_mask);

  G_close_cell(primary_sqs_fd);
  G_close_cell(DEM_fd);
  G_close_cell(wshed_fd);
}
/* lets try again now have established what exactly i'm trying yo
do!!! */

#include <stdio.h>
#include <stdlib.h>
#include <stddef.h>
#include "gis.h"
#include <math.h>

/* IMPORTANT PLEASE NOTE PG 91 OF GRASS PROGRAMMING MANUAL */

void multiflowpathroutingalgorithm(int no_rows, int no_cols, char
primary_sqs_name[], char DEM_name[], char d8_map_name[], char
wshed_mask_name[])
{

CELL *d8_map_row1, *d8_map_row2, *d8_map_row3, *primary_sqs;
CELL flow_progress[no_rows][no_cols],
flow_progress2[no_rows][no_cols];
FCELL contrib_cells[no_rows][no_cols], DEM[no_rows][no_cols],
temp[no_rows][no_cols];
FCELL cc_now[no_rows][no_cols], cc_next[no_rows][no_cols];
FCELL *wshed_mask;

FCELL s1, s2, s3, s4, s5, s6, s7, s8;
FCELL f1, f2, f3, f4, f5, f6, f7, f8;
FCELL total, cell, cellwidth;

int row, col;
int wshed_out_row, wshed_out_col;
int flow_marker, flow_monitor;
int count, x;

int d8_map_fd, DEM_fd, primary_sqs_fd, wshed_fd;

char *message;
char *mapset;

FILE *fpa = fopen("flowpaths.txt", "w");
FILE *fpb = fopen("routing_output.txt", "w");

/* open raster maps */

mapset = G_mapset();

d8_map_fd = G_open_cell_old(d8_map_name, mapset);
if(d8_map_fd < 0)
{
  message = "cannot open d8 map, exiting module\n";
  G_fatal_error(message);
}

DEM_fd = G_open_cell_old(DEM_name, mapset);
```

```
if(DEM_fd < 0)
{
  message = "cannot open DEM, exiting module\n";
  G_fatal_error(message);
}

primary_sqs_fd = G_open_cell_old(primary_sqs_name, mapset);
if(primary_sqs_fd < 0)
{
  message = "cannot open primary squares map, exiting module\n";
  G_fatal_error(message);
}

wshed_fd = G_open_cell_old(wshed_mask_name, mapset);
if(wshed_fd < 0)
{
  message = "cannot open wshed mask, exiting module\n";
  G_fatal_error(message);
}

cellwidth = (200 * 0.3048);

/* find waterhsed outlet */

d8_map_row1 = G_allocate_c_raster_buf();
d8_map_row2 = G_allocate_c_raster_buf();
d8_map_row3 = G_allocate_c_raster_buf();
wshed_mask = G_allocate_f_raster_buf();

for(row = 1; row < no_rows-1; row++)
{
  G_get_c_raster_row(d8_map_fd, d8_map_row1, row-1);
  G_get_c_raster_row(d8_map_fd, d8_map_row2, row);
  G_get_c_raster_row(d8_map_fd, d8_map_row3, row+1);

  for(col = 0; col < no_cols; col++)
  {
    if(d8_map_row2[col] == 1 && d8_map_row1[col] == 0)
    {
      wshed_out_row = row;
      wshed_out_col = col;
    }
    if(d8_map_row2[col] == 2 && d8_map_row1[col+1] == 0)
    {
      wshed_out_row = row;
      wshed_out_col = col;
    }
    if(d8_map_row2[col] == 3 && d8_map_row2[col+1] == 0)
    {
      wshed_out_row = row;
      wshed_out_col = col;
    }
    if(d8_map_row2[col] == 4 && d8_map_row3[col+1] == 0)
    {
      wshed_out_row = row;
      wshed_out_col = col;
    }
    if(d8_map_row2[col] == 5 && d8_map_row3[col] == 0)
    {
      wshed_out_row = row;
      wshed_out_col = col;
```

```
    }
    if(d8_map_row2[col] == 6 && d8_map_row3[col-1] == 0)
    {
      wshed_out_row = row;
      wshed_out_col = col;
    }
    if(d8_map_row2[col] == 7 && d8_map_row2[col-1] == 0)
    {
      wshed_out_row = row;
      wshed_out_col = col;
    }
    if(d8_map_row2[col] == 8 && d8_map_row1[col-1] == 0)
    {
      wshed_out_row = row;
      wshed_out_col = col;
    }
  }
}

printf("found watershed outlet %i %i \n", wshed_out_row,
wshed_out_col);

/* allocate buffers */

for(row = 0; row < no_rows; row++)
{
  G_get_f_raster_row(DEM_fd, DEM[row], row);
}

printf("read DEM\n");

primary_sqs = G_allocate_c_raster_buf();

/*initialising variables and arrays */

for(row = 0; row < no_rows; row++)
{
  G_get_f_raster_row(wshed_fd, wshed_mask, row);

  for(col = 0; col < no_cols; col++)
  {
    flow_progress[row][col] = 0;
    flow_progress2[row][col] = 0;
    cc_now[row][col] = primary_sqs[col];
    cc_next[row][col] = 0;
    G_get_c_raster_row(primary_sqs_fd, primary_sqs, row);
    flow_progress[row][col] = primary_sqs[col];
    contrib_cells[row][col] = primary_sqs[col];
    temp[row][col] = wshed_mask[col];
  }
}

flow_monitor = 1;

printf("initialised variables\n");

fprintf(fpb, "              s1/f1 s2/f2 s3/f3 s4/f4 s5/f5 s6/f6 s7/f7
s8/f8\n");

/* main analysis routine for flow routing */
```

```
count = 0;

while(flow_monitor != 0)
{

  printf("entered flow routing loop\n");

  for(row = 1; row < no_rows-1; row++)
  {
    for(col = 1; col < no_cols-1; col++)
    {
      flow_marker = flow_progress[row][col];

      if(flow_marker == 1)
      {
        cell = DEM[row][col];

        total = 0;

        if (DEM[row-1][col] > 0)
        s1 = ((cell - DEM[row-1][col])/cellwidth) * 100;
        else
        s1 = 0;
        if (s1 > 0)
          total = total + s1;
        if (DEM[row-1][col+1] > 0)
        s2 = ((cell - DEM[row-1][col+1])/(cellwidth*sqrt(2))) * 100;
        else
        s2 = 0;
        if (s2 > 0)
          total = total + s2;
        if (DEM[row][col+1] > 0)
        s3 = ((cell - DEM[row][col+1])/cellwidth) * 100;
        else
        s3 = 0;
        if (s3 > 0)
          total = total + s3;
        if (DEM[row+1][col+1] > 0)
        s4 = ((cell - DEM[row+1][col+1])/(cellwidth*sqrt(2))) * 100;
        else
        s4 = 0;
        if (s4 > 0)
          total = total + s4;
        if (DEM[row+1][col] > 0)
        s5 = ((cell - DEM[row+1][col])/cellwidth) * 100;
        else
        s5 = 0;
        if (s5 > 0)
          total = total + s5;
        if (DEM[row+1][col-1] > 0)
        s6 = ((cell - DEM[row+1][col-1])/(cellwidth*sqrt(2))) * 100;
        else
        s6 = 0;
        if (s6 > 0)
          total = total + s6;
        if (DEM[row][col-1] > 0)
        s7 = ((cell - DEM[row][col-1])/cellwidth) * 100;
        else
        s7 = 0;
        if (s7 > 0)
          total = total + s7;
```

```
        if (DEM[row-1][col-1] > 0)
        s8 = ((cell - DEM[row-1][col-1])/(cellwidth*sqrt(2))) * 100;
        else
        s8 = 0;
        if (s8 > 0)
          total = total + s8;

        if (s1 > 0)
        {
          f1 = (s1 / total);
          cc_next[row-1][col] = cc_next[row-1][col] +
((cc_now[row][col]) * f1) + temp[row-1][col];
        if(temp[row-1][col] == 1)
          temp[row-1][col] = temp[row-1][col] - 1;
        else
          temp[row-1][col] = 0;
          if((row-1) == wshed_out_row && col == wshed_out_col)
            flow_progress2[row-1][col] = 0;
          else
          {
            flow_progress2[row-1][col] = 1;
          }
        }
        else
          f1 = 0;

        if (s2 > 0)
        {
          f2 = (s2 / total);
          cc_next[row-1][col+1] = cc_next[row-1][col+1] +
((cc_now[row][col]) * f2) + temp[row-1][col+1];
        if(temp[row-1][col+1] == 1)
          temp[row-1][col+1] = temp[row-1][col+1] - 1;
        else
          temp[row-1][col+1] = 0;
          if((row-1) == wshed_out_row && (col+1) == wshed_out_col)
            flow_progress2[row-1][col+1] = 0;
          else
        {
            flow_progress2[row-1][col+1] = 1;
        }
        }
        else
          f2 = 0;

        if (s3 > 0)
        {
          f3 = (s3 / total);
          cc_next[row][col+1] = cc_next[row][col+1] +
((cc_now[row][col]) * f3) + temp[row][col+1];
        if(temp[row][col+1] == 1)
          temp[row][col+1] = temp[row][col+1] - 1;
        else
          temp[row][col+1] = 0;
          if(row == wshed_out_row && (col+1) == wshed_out_col)
            flow_progress2[row][col+1] = 0;
          else
        {
            flow_progress2[row][col+1] = 1;
        }
        }
```

```
        else
          f3 = 0;

        if (s4 > 0)
        {
          f4 = (s4 / total);
          cc_next[row+1][col+1] = cc_next[row+1][col+1] +
((cc_now[row][col]) * f4) + temp[row+1][col+1];
        if(temp[row+1][col+1] == 1)
          temp[row+1][col+1] = temp[row+1][col+1] - 1;
        else
          temp[row+1][col+1] = 0;
          if((row+1) == wshed_out_row && (col+1) == wshed_out_col)
            flow_progress2[row+1][col+1] = 0;
          else
        {
            flow_progress2[row+1][col+1] = 1;
        }
        }
        else
          f4 = 0;

        if (s5 > 0)
        {
          f5 = (s5 / total);
          cc_next[row+1][col] = cc_next[row+1][col] +
((cc_now[row][col]) * f5) + temp[row+1][col];
        if(temp[row+1][col] == 1)
          temp[row+1][col] = temp[row+1][col] - 1;
        else
          temp[row+1][col] = 0;
          if((row+1) == wshed_out_row && col == wshed_out_col)
            flow_progress2[row+1][col] = 0;
          else
        {
            flow_progress2[row+1][col] = 1;
        }
        }
        else
          f5 = 0;

        if (s6 > 0)
        {
          f6 = (s6 / total);
          cc_next[row+1][col-1] = cc_next[row+1][col-1] +
((cc_now[row][col]) * f6) + temp[row+1][col-1];
        if(temp[row+1][col-1] == 1)
          temp[row+1][col-1] = temp[row+1][col-1] - 1;
        else
          temp[row+1][col-1] = 0;
          if((row+1) == wshed_out_row && (col-1) == wshed_out_col)
            flow_progress2[row+1][col-1] = 0;
          else
        {
            flow_progress2[row+1][col-1] = 1;
        }
        }
        else
          f6 = 0;

        if (s7 > 0)
```

```
        {
          f7 = (s7 / total);
          cc_next[row][col-1] = cc_next[row][col-1] +
((cc_now[row][col]) * f7) + temp[row][col-1];
        if(temp[row][col-1] == 1)
          temp[row][col-1] = temp[row][col-1] - 1;
        else
          temp[row][col-1] = 0;
          if(row == wshed_out_row && (col-1) == wshed_out_col)
            flow_progress2[row][col-1] = 0;
          else
        {
            flow_progress2[row][col-1] = 1;
        }
        }
        else
          f7 = 0;

        if (s8 > 0)
        {
          f8 = (s8 / total);
          cc_next[row-1][col-1] = cc_next[row-1][col-1] +
((cc_now[row][col]) * f8) + temp[row-1][col-1];
        if(temp[row-1][col-1] == 1)
          temp[row-1][col-1] = temp[row-1][col-1] - 1;
        else
          temp[row-1][col-1] = 0;
          if((row-1) == wshed_out_row && (col-1) == wshed_out_col)
            flow_progress2[row-1][col-1] = 0;
          else
        {
            flow_progress2[row-1][col-1] = 1;
        }
        }
        else
          f8 = 0;

        if(temp[row][col] == 1)
          temp[row][col] = temp[row][col] - 1;
        else
          temp[row][col] = 0;

      fprintf(fpb, "cell %i, %i: %6.2f %6.2f %6.2f %6.2f %6.2f %6.2f
%6.2f %6.2f\n", row, col, s1, s2, s3, s4, s5, s6, s7, s8);
      fprintf(fpb, "                %6.2f %6.2f %6.2f %6.2f %6.2f %6.2f
%6.2f %6.2f\n", f1, f2, f3, f4, f5, f6, f7, f8);

      }

      else
      {
        x = 0;
      }
    }
  }

  flow_monitor = 0;

  for(row = 0; row < no_rows; row++)
  {
    for(col = 0; col < no_cols; col++)
```

```
    {
      if(flow_progress2[row][col] == 1 || flow_monitor == 1)
         flow_monitor = 1;
      else
        flow_monitor = 0;
    }
  }

  for(row = 0; row < no_rows; row++)
  {
    for(col = 0; col < no_cols; col++)
    {
      contrib_cells[row][col] = contrib_cells[row][col] +
cc_next[row][col];
    }
  }

  for(row = 0; row < no_rows; row++)
  {
    for(col = 0; col < no_cols; col++)
    {
      flow_progress[row][col] = flow_progress2[row][col];
      flow_progress2[row][col] = 0;
      cc_now[row][col] = cc_next[row][col];
      cc_next[row][col] = 0;
    }
  }
  count = count + 1;
  printf("completed %i sweeps of watershed\n", count);
}

for(row = 0; row < no_rows; row++)
{
  G_get_f_raster_row(wshed_fd, wshed_mask, row);

  for(col = 0; col < no_cols; col++)
  {
    contrib_cells[row][col] = contrib_cells[row][col] *
wshed_mask[col];
  }
}

printf("about to start outputting results\n");

for(row = 0; row < no_rows; row++)
{
  for(col =0; col < no_cols; col++)
  {
    fprintf(fpa, "%6.6f  ", contrib_cells[row][col]);
  }
  fprintf(fpa, "\n");
}

G_close_cell(d8_map_fd);
G_close_cell(DEM_fd);
G_close_cell(primary_sqs_fd);
}
```

The following scripts show the three versions of the route_stage_two script, which calculated the delivery index for the CALSITE method. The first is the annual equation, the second is the single storm adaptation for the curve number method for calculating runoff and the third using the Meyer and Wischmeier method for calculating method. Again to avoid repetition the main and get_map_name scripts have been omitted.

```
/* second stage of routing */
/* creates delivery index for each cell */

#include <stdio.h>
#include <stdlib.h>
#include <stddef.h>
#include "gis.h"
#include <math.h>

void route_stage_two(int no_rows, int no_cols, float rainfall, float
x, float a,
                     float b, char DI_map_name[], char
contrib_cells_name[],
                     char lowest_slope_name[])
{

  int row, col;
  int contrib_cells_fd;
  int lowest_slope_fd;
  int DI_fd;
  char *mapset;
  char *message;
  FCELL *contrib_cells_fcell;
  FCELL *lowest_slope_fcell;
  FCELL *DI_fcell;
  float max_DI;

  mapset = G_mapset();

  contrib_cells_fd = G_open_cell_old(contrib_cells_name, mapset);
  if(contrib_cells_fd < 0)
  {
    message = "cannot open contributing cells map, exiting module\n";
    G_fatal_error(message);
  }

  lowest_slope_fd = G_open_cell_old(lowest_slope_name, mapset);
  if(lowest_slope_fd < 0)
  {
    message = "cannot open lowest slope map, exiting module\n";
    G_fatal_error(message);
  }

  DI_fd = G_open_raster_new(DI_map_name, FCELL_TYPE);

  contrib_cells_fcell = G_allocate_f_raster_buf();
```

```
  lowest_slope_fcell = G_allocate_f_raster_buf();
  DI_fcell = G_allocate_f_raster_buf();

  max_DI = 0;

  for(row = 0; row < no_rows; row++)
  {
    G_get_f_raster_row(contrib_cells_fd, contrib_cells_fcell, row);
    G_get_f_raster_row(lowest_slope_fd, lowest_slope_fcell, row);

    for(col = 0; col < no_cols; col++)
    {
      DI_fcell[col] = pow(contrib_cells_fcell[col],(a-1)) *
pow(lowest_slope_fcell[col],b) * pow(rainfall,(x*(a-1)));
      if(DI_fcell[col] > max_DI)
        max_DI = DI_fcell[col];
      else
        max_DI = max_DI;
    }

/* note in above a and b are derived from govers thus need to be
inputted
manually, x is gained from eqn relating rainfall to runoff runoff =
y * (rainfall^x) */
  }

  for(row = 0; row < no_rows; row++)
  {
    G_get_f_raster_row(contrib_cells_fd, contrib_cells_fcell, row);
    G_get_f_raster_row(lowest_slope_fd, lowest_slope_fcell, row);

    for(col = 0; col < no_cols; col++)
    {
      DI_fcell[col] = ((pow(contrib_cells_fcell[col],(a-1)) *
pow(lowest_slope_fcell[col],b) * pow(rainfall,(x*(a-1)))) / max_DI) *
100;
    }

    G_put_f_raster_row(DI_fd, DI_fcell);
  }

  G_free(contrib_cells_fcell);
  G_free(lowest_slope_fcell);
  G_free(DI_fcell);

  G_close_cell(contrib_cells_fd);
  G_close_cell(lowest_slope_fd);
  G_close_cell(DI_fd);
}
/* second stage of routing */
/* creates delivery index for each cell */

#include <stdio.h>
#include <stdlib.h>
#include <stddef.h>
#include "gis.h"
#include <math.h>

void route_stage_two(int no_rows, int no_cols, float rainfall, float
a, float b, char DI_map_name[], char contrib_cells_name[], char
lowest_slope_name[], char CN_map_name[])
```

```
{

  int row, col;
  int contrib_cells_fd;
  int lowest_slope_fd;
  int CN_fd;
  int DI_fd;
  char *mapset;
  char *message;
  DCELL *contrib_cells_fcell;
  DCELL *lowest_slope_fcell;
  DCELL *CN_fcell;
  DCELL *runoff_fcell;
  DCELL *DI_fcell;
  float max_DI;
  float S;

  mapset = G_mapset();

  contrib_cells_fd = G_open_cell_old(contrib_cells_name, mapset);
  if(contrib_cells_fd < 0)
  {
    message = "cannot open contributing cells map, exiting module\n";
    G_fatal_error(message);
  }

  lowest_slope_fd = G_open_cell_old(lowest_slope_name, mapset);
  if(lowest_slope_fd < 0)
  {
    message = "cannot open lowest slope map, exiting module\n";
    G_fatal_error(message);
  }

  CN_fd = G_open_cell_old(CN_map_name, mapset);
  if(CN_fd < 0)
  {
    message = "cannot open curve number map, exiting module\n";
    G_fatal_error(message);
  }

  DI_fd = G_open_raster_new(DI_map_name, DCELL_TYPE);

  contrib_cells_fcell = G_allocate_d_raster_buf();
  lowest_slope_fcell = G_allocate_d_raster_buf();
  CN_fcell = G_allocate_d_raster_buf();
  runoff_fcell = G_allocate_d_raster_buf();
  DI_fcell = G_allocate_d_raster_buf();

  max_DI = 0;

  printf("calculating\n");

  for(row = 0; row < no_rows; row++)
  {
    G_get_d_raster_row(contrib_cells_fd, contrib_cells_fcell, row);
    G_get_d_raster_row(lowest_slope_fd, lowest_slope_fcell, row);
    G_get_d_raster_row(CN_fd, CN_fcell, row);

    for(col = 0; col < no_cols; col++)
    {
      if(CN_fcell[col] > 0)
```

```
      {
        S = (2540 / CN_fcell[col]) - 25.4;
        runoff_fcell[col] = pow((rainfall - (0.2 * S)), 2) /
(rainfall + (0.8 * S));
      }
      else
        runoff_fcell[col] = 0;

      DI_fcell[col] = pow(contrib_cells_fcell[col],(a-1)) *
pow(lowest_slope_fcell[col],b) * pow(runoff_fcell[col],(a-1));

      if(DI_fcell[col] > max_DI)
        max_DI = DI_fcell[col];
      else
        max_DI = max_DI;
    }
  }

  printf("and again\n");

  for(row = 0; row < no_rows; row++)
  {
    G_get_d_raster_row(contrib_cells_fd, contrib_cells_fcell, row);
    G_get_d_raster_row(lowest_slope_fd, lowest_slope_fcell, row);
    G_get_d_raster_row(CN_fd, CN_fcell, row);

    for(col = 0; col < no_cols; col++)
    {
      if(CN_fcell[col] > 0)
      {
        S = (2540 / CN_fcell[col]) - 25.4;
        runoff_fcell[col] = pow((rainfall - (0.2 * S)), 2) /
(rainfall + (0.8 * S));
      }
      else
        runoff_fcell[col]  = 0;

      DI_fcell[col] = ((pow(contrib_cells_fcell[col],(a-1)) *
pow(lowest_slope_fcell[col],b) * pow(runoff_fcell[col],(a-1))) /
max_DI) * 100;
    }

    G_put_d_raster_row(DI_fd, DI_fcell);
  }

  G_free(contrib_cells_fcell);
  G_free(lowest_slope_fcell);
  G_free(CN_fcell);
  G_free(DI_fcell);

  G_close_cell(contrib_cells_fd);
  G_close_cell(lowest_slope_fd);
  G_close_cell(CN_fd);
  G_close_cell(DI_fd);
}
/* second stage of routing */
/* creates delivery index for each cell */

#include <stdio.h>
#include <stdlib.h>
#include <stddef.h>
```

```
#include "gis.h"
#include <math.h>

void route_stage_two(int no_rows, int no_cols, float rainfall, char
DI_map_name[], char contrib_cells_name[], char lowest_slope_name[],
char CN_map_name[])
{

  int row, col;
  int contrib_cells_fd;
  int lowest_slope_fd;
  int CN_fd;
  int DI_fd;
  char *mapset;
  char *message;
  DCELL *contrib_cells_fcell;
  DCELL *lowest_slope_fcell;
  DCELL *CN_fcell;
  DCELL *runoff_fcell;
  DCELL *DI_fcell;
  float max_DI;
  float S;

  mapset = G_mapset();

  contrib_cells_fd = G_open_cell_old(contrib_cells_name, mapset);
  if(contrib_cells_fd < 0)
  {
    message = "cannot open contributing cells map, exiting module\n";
    G_fatal_error(message);
  }

  lowest_slope_fd = G_open_cell_old(lowest_slope_name, mapset);
  if(lowest_slope_fd < 0)
  {
    message = "cannot open lowest slope map, exiting module\n";
    G_fatal_error(message);
  }

  CN_fd = G_open_cell_old(CN_map_name, mapset);
  if(CN_fd < 0)
  {
    message = "cannot open curve number map, exiting module\n";
    G_fatal_error(message);
  }

  DI_fd = G_open_raster_new(DI_map_name, DCELL_TYPE);

  contrib_cells_fcell = G_allocate_d_raster_buf();
  lowest_slope_fcell = G_allocate_d_raster_buf();
  CN_fcell = G_allocate_d_raster_buf();
  runoff_fcell = G_allocate_d_raster_buf();
  DI_fcell = G_allocate_d_raster_buf();

  max_DI = 0;

  printf("calculating\n");

  for(row = 0; row < no_rows; row++)
  {
    G_get_d_raster_row(contrib_cells_fd, contrib_cells_fcell, row);
```

```
    G_get_d_raster_row(lowest_slope_fd, lowest_slope_fcell, row);
    G_get_d_raster_row(CN_fd, CN_fcell, row);

    for(col = 0; col < no_cols; col++)
    {
      if(CN_fcell[col] > 0)
      {
        S = (2540 / CN_fcell[col]) - 25.4;
        runoff_fcell[col] = pow((rainfall - (0.2 * S)), 2) /
(rainfall + (0.8 * S));
      }
      else
        runoff_fcell[col] = 0;

      DI_fcell[col] = pow(contrib_cells_fcell[col],(0.666)) *
pow(lowest_slope_fcell[col],(1.666)) *
pow(runoff_fcell[col],(1.666));

      if(DI_fcell[col] > max_DI)
        max_DI = DI_fcell[col];
      else
        max_DI = max_DI;
    }
  }

  printf("and again\n");

  for(row = 0; row < no_rows; row++)
  {
    G_get_d_raster_row(contrib_cells_fd, contrib_cells_fcell, row);
    G_get_d_raster_row(lowest_slope_fd, lowest_slope_fcell, row);
    G_get_d_raster_row(CN_fd, CN_fcell, row);

    for(col = 0; col < no_cols; col++)
    {
      if(CN_fcell[col] > 0)
      {
        S = (2540 / CN_fcell[col]) - 25.4;
        runoff_fcell[col] = pow((rainfall - (0.2 * S)), 2) /
(rainfall + (0.8 * S));
      }
      else
        runoff_fcell[col] = 0;

      DI_fcell[col] = ((pow(contrib_cells_fcell[col],(0.666)) *
pow(lowest_slope_fcell[col],(1.666)) *
pow(runoff_fcell[col],(0.666))) / max_DI) * 100;
    }

    G_put_d_raster_row(DI_fd, DI_fcell);
  }

  G_free(contrib_cells_fcell);
  G_free(lowest_slope_fcell);
  G_free(CN_fcell);
  G_free(DI_fcell);

  G_close_cell(contrib_cells_fd);
  G_close_cell(lowest_slope_fd);
  G_close_cell(CN_fd);
  G_close_cell(DI_fd);
```

```
}
```

The next scripts show the calculation of the CALSITE delivery ratio per pixel and the script that calculates the stream path index and thus the stream network.

```
/* third stage of routing */
/* creates delivery ratio per pixel */

#include <stdio.h>
#include <stdlib.h>
#include <stddef.h>
#include "gis.h"
#include <math.h>

void route_stage_three(int no_rows, int no_cols, char DI_map_name[],
                       char source_erosion_name[])
{
  DCELL *DI_fcell;
  DCELL *SE_fcell;
  double TEp, TE, DRp;
  int row, col;
  int s, t;
  int SE_map_fd;
  int DI_map_fd;
  char *message;
  char *mapset;
  FILE *fp = fopen("erosion_output", "w");

  mapset = G_mapset();

  if(fp == NULL)
  {
    message = "cannot open erosion output file, exiting module\n";
    G_fatal_error(message);
  }

  SE_map_fd = G_open_cell_old(source_erosion_name, mapset);
  if(SE_map_fd < 0)
  {
    message = "cannot open source erosion map, exiting module\n";
    G_fatal_error(message);
  }

  DI_map_fd = G_open_cell_old(DI_map_name, mapset);
  if(DI_map_fd < 0)
  {
    message = "cannot open delivery index map, exiting module\n";
    G_fatal_error(message);
  }

  DI_fcell = G_allocate_d_raster_buf();
  SE_fcell = G_allocate_d_raster_buf();

  fprintf(fp, "Table of results for transported erosion as s & t
vary\n");
  fprintf(fp, "t\t s\t transported erosion\n");

  for (t = 0; t < 50; t++)
```

```
  {
    for(s = 1; s < 100; s++)
    {
    if(s >= t)
    {
      TE = 0;
      for(row = 0; row < no_rows; row++)
      {
        G_get_d_raster_row(SE_map_fd, SE_fcell, row);
        G_get_d_raster_row(DI_map_fd, DI_fcell, row);

        for(col = 0; col < no_cols; col++)
        {
            DRp = (1 - (cos(((4 * atan(1)) * (DI_fcell[col] - t)) /
(s - t)))) / 2;
/* pi can be taken as 4 * arctan(1) */
            if(DI_fcell[col] < t)
              DRp = 0;
            else
              DRp = DRp;
            if(DI_fcell[col] > s)
              DRp = 1;
            else
              DRp = DRp;

            TEp = SE_fcell[col] * DRp;

            TE = TE + TEp;
        }
      }
      fprintf(fp, "%3i\t %3i\t %6.6f\n", t, s, TE);
    }
    else
    {
      TE = 0;
    }
    }
  }

  G_free(DI_fcell);
  G_free(SE_fcell);

  G_close_cell(SE_map_fd);
  G_close_cell(DI_map_fd);
  fclose(fp);
}
/* function to calculate permanent stream network */

#include <stdio.h>
#include <stdlib.h>
#include <stddef.h>
#include "gis.h"
#include <math.h>
#define NAME_LEN 100

int main(int argc, char *argv[])
{

/* prototypes */

  int getline (char line[], int max);
```

```
  void get_contrib_cells_name(char contrib_cells_name[]);
  void get_streams_name(char streams_name[]);
  void find_streams(int no_rows, int no_cols, char
contrib_cells_name[], char streams_name[]);

  /*variables */

  char streams_name[NAME_LEN+1];
  char contrib_cells_name[NAME_LEN+1];

  int no_rows, no_cols;

  /* initialise the GRASS environment variables */

  G_gisinit (argv[0]);


  /* get map names */

  get_streams_name(streams_name);
  get_contrib_cells_name(contrib_cells_name);

  no_rows = G_window_rows();
  no_cols = G_window_cols();

  find_streams(no_rows, no_cols, contrib_cells_name, streams_name);

  printf("finished route stage one\n");

  return(EXIT_SUCCESS);
}

int getline(char line[], int max)
{
  int c;
  int i = 0;

  while((c = getchar()) != '\n')
    if(i < max)
      line[i++] = c;
  line[i] = '\0';
  return (c == '\n') ? i : -1;
}

void get_contrib_cells_name(char contrib_cells_name[])
{
  char *prompt;
  char *mapset;
  char *message;

  prompt = "please enter contrib cells name";
  mapset = G_ask_cell_in_mapset(prompt, contrib_cells_name);
  if(mapset == NULL)
  {
    message = "exiting module.... \n";
    G_fatal_error(message);
  }
}

/* contributing cells map */
```

```
void get_streams_name(char streams_name[])
{
  int t;
  char *message;

  printf("please enter name of stream network map:\n");
  t = getline(streams_name, NAME_LEN);
  if(t == -1)
  {
    message = "exiting module......\n";
    G_fatal_error(message);
  }
}

void find_streams(int no_rows, int no_cols, char
contrib_cells_name[], char streams_name[])
{

  char *mapset, *message;
  int row, col;
  FCELL *DA, *streams;
  int streams_fd, DA_fd;
  float f;

  mapset = G_mapset();

  DA_fd = G_open_cell_old(contrib_cells_name, mapset);
  if(DA_fd < 0)
  {
    message = "cannot open contirb cells map, exiting module\n";
    G_fatal_error(message);
  }

  streams_fd = G_open_raster_new(streams_name, FCELL_TYPE);

  printf("please enter threshold stream value, f\n");
  scanf("%f", &f);

  streams = G_allocate_f_raster_buf();
  DA = G_allocate_f_raster_buf();

  for(row = 0; row < no_rows; row++)
  {
    G_get_f_raster_row(DA_fd, DA, row);

    for(col = 0; col < no_cols; col++)
    {
      if(DA[col] > f)
        streams[col] = 1;
      else
        streams[col] = 0;
    }

    G_put_f_raster_row(streams_fd, streams);
  }

  G_free(DA);
  G_free(streams);

  G_close_cell(DA_fd);
  G_close_cell(streams_fd);
```

```
}
```

The final section calculates the transported erosion for the catchment giving the total overall erosion.

```
/* Grass module for CALSITE style model */
/* calsite 3 allows a map of finalised total erosion to be produced
based upon chosen values of s and t */

#include <stdio.h>
#include <stdlib.h>
#include <stddef.h>
#include "gis.h"
#include <math.h>
#define NAME_LEN 100

int main(int argc, char *argv[])
{

  /* prototypes */

  int getline (char line[], int max);
  void route_stage_three(int no_rows, int no_cols, char
DI_map_name[],
                         char source_erosion_name[], char
TE_map_name[], float s, float t, char streams_name[]);
  void get_source_erosion_map_name(char source_erosion_name[]);
  void get_DI_map_name(char DI_map_name[]);
  void get_TE_map_name(char TE_map_name[]);
  void get_streams_name(char streams_name[]);


  /* variables */

  char source_erosion_name[NAME_LEN+1];
  char DI_map_name[NAME_LEN+1];
  char TE_map_name[NAME_LEN+1];
  char streams_name[NAME_LEN+1];
  int no_rows, no_cols;
  float s, t;

  /* initialise the GRASS environment variables */

  G_gisinit (argv[0]);

  /* get map names */

  get_source_erosion_name(source_erosion_name);
  get_DI_map_name(DI_map_name);
  get_TE_map_name(TE_map_name);
  get_streams_name(streams_name);

  no_rows = G_window_rows();
  no_cols = G_window_cols();

  printf("please enter values for s, t\n");
  scanf("%f%f", &s, &t);

  /* Calc final TE */
```

```
  route_stage_three(no_rows, no_cols, DI_map_name,
source_erosion_name, TE_map_name, s, t, streams_name);

  return (EXIT_SUCCESS);
}

/* get map names */

#include <stdio.h>
#include <stdlib.h>
#include <stddef.h>
#include "gis.h"
#include <math.h>
#define NAME_LEN 100

int getline(char line[], int max)
{
  int c;
  int i = 0;

  while((c = getchar()) != '\n')
    if(i < max)
      line[i++] = c;
  line[i] = '\0';
  return (c == '\n') ? i : -1;
}

/* input maps */

void get_source_erosion_name(char source_erosion_name[])
{
  char *prompt;
  char *mapset;
  char *message;

  prompt = "please enter source erosion map file";
  mapset = G_ask_cell_in_mapset(prompt, source_erosion_name);
  if(mapset == NULL)
  {
    message = "exiting module.... \n";
    G_fatal_error(message);
  }
}

void get_DI_map_name(char DI_map_name[])
{
  char *prompt;
  char *mapset;
  char *message;

  prompt = "please enter delivery index map file";
  mapset = G_ask_cell_in_mapset(prompt, DI_map_name);
  if(mapset == NULL)
  {
    message = "exiting module.... \n";
    G_fatal_error(message);
  }
}

void get_streams_name(char streams_name[])
{
```

```
  char *prompt;
  char *mapset;
  char *message;

  prompt = "please enter streams map file";
  mapset = G_ask_cell_in_mapset(prompt, streams_name);
  if(mapset == NULL)
  {
    message = "exiting module.... \n";
    G_fatal_error(message);
  }
}

void get_TE_map_name(char TE_map_name[])
{
  int t;
  char *message;

  printf("please enter name of total erosion map:\n");
  t = getline(TE_map_name, NAME_LEN);
  if(t == -1)
  {
    message = "exiting module......\n";
    G_fatal_error(message);
  }
}

/* third stage of routing */
/* creates delivery ratio per pixel */

#include <stdio.h>
#include <stdlib.h>
#include <stddef.h>
#include "gis.h"
#include <math.h>

void route_stage_three(int no_rows, int no_cols, char DI_map_name[],
                       char source_erosion_name[], char
TE_map_name[], float s, float t, char streams_name[])
{
  DCELL *DI_dcell;
  DCELL *SE_dcell;
  DCELL *TE_dcell;
  CELL *streams_cell;
  double DRp;
  int row, col;
  int SE_map_fd;
  int DI_map_fd;
  int TE_map_fd;
  int streams_fd;
  char *message;
  char *mapset;

  mapset = G_mapset();

  TE_map_fd = G_open_raster_new(TE_map_name, DCELL_TYPE);
  if(TE_map_fd < 0)
  {
    message = "cannot open erosion output file, exiting module\n";
    G_fatal_error(message);
  }
```

```
  SE_map_fd = G_open_cell_old(source_erosion_name, mapset);
  if(SE_map_fd < 0)
  {
    message = "cannot open source erosion map, exiting module\n";
    G_fatal_error(message);
  }

  DI_map_fd = G_open_cell_old(DI_map_name, mapset);
  if(DI_map_fd < 0)
  {
    message = "cannot open delivery index map, exiting module\n";
    G_fatal_error(message);
  }

  streams_fd = G_open_cell_old(streams_name, mapset);
  if(streams_fd < 0)
  {
    message = "cannot open streams map, exiting module\n";
    G_fatal_error(message);
  }

  DI_dcell = G_allocate_d_raster_buf();
  SE_dcell = G_allocate_d_raster_buf();
  TE_dcell = G_allocate_d_raster_buf();
  streams_cell = G_allocate_c_raster_buf();

  for(row = 0; row < no_rows; row++)
  {
    G_get_d_raster_row(SE_map_fd, SE_dcell, row);
    G_get_d_raster_row(DI_map_fd, DI_dcell, row);
    G_get_c_raster_row(streams_fd, streams_cell, row);

    for(col = 0; col < no_cols; col++)
    {
      if(streams_cell[col] == 1)
      {
        DRp = 1;
      }
      else
      {
        DRp = (1 - (cos((4 * atan(1)) * (DI_dcell[col] - t)) / (s -
t))) / 2;
/* pi can be taken as 4 * arctan(1) */
      }

      TE_dcell[col] = SE_dcell[col] * DRp;
    }

    G_put_d_raster_row(TE_map_fd, TE_dcell);
  }

  G_free(DI_dcell);
  G_free(SE_dcell);
  G_free(TE_dcell);
  G_free(streams_cell);

  G_close_cell(SE_map_fd);
  G_close_cell(DI_map_fd);
  G_close_cell(TE_map_fd);
  G_close_cell(streams_fd);
```

```
}
```

Each module is compiled using a Gmakefile, an example of which follows:

```
LIBRARIES = $(GISLIB)

OBJ = main.o \
      get_map_names.o \
      route_stage_three.o

PGM = r.calsite_te

$(BIN_INTER)/$(PGM): $(OBJ) $(LIBRARIES)
      $(CC) -o $@ $(LDFLAGS) $(OBJ) $(LIBRARIES) $(XDRLIB) $(MATHLIB)
```

C.2 – Other functions

Next follows some of other functions, first the D8 and DEMON routing scripts both of which share the function to find primary squares.

```
/* section of module to find primary squares */

#include <stdio.h>
#include <stdlib.h>
#include <stddef.h>
#include "gis.h"
#include <math.h>
#define NAME_LEN 100

void find_primary_squares(int no_rows, int no_cols, char
d8_map_name[], char primary_cells_name[])
{
  int primary_cells_fd;
  int d8_map_fd;
  int row, col;
  FCELL *row_one_fcell;
  FCELL *row_two_fcell;
  FCELL *row_three_fcell;
  FCELL *is_primary_square;
  char *message;
  char *mapset;

  mapset = G_mapset();

  d8_map_fd = G_open_cell_old(d8_map_name, mapset);
  if(d8_map_fd < 0)
  {
    message = "cannot open d8 map, exiting module\n";
    G_fatal_error(message);
  }

  primary_cells_fd = G_open_raster_new(primary_cells_name,
FCELL_TYPE);

  row_one_fcell = G_allocate_f_raster_buf();
  row_two_fcell = G_allocate_f_raster_buf();
  row_three_fcell = G_allocate_f_raster_buf();
```

```
  is_primary_square = G_allocate_f_raster_buf();

  row = 0;

  for(col = 0; col < no_cols; col++)
  {
    is_primary_square[col] = 0;
  }

  G_put_f_raster_row(primary_cells_fd, is_primary_square);

  for(row = 1; row < (no_rows-1); row++)
  {
    G_get_f_raster_row(d8_map_fd, row_one_fcell, row-1);
    G_get_f_raster_row(d8_map_fd, row_two_fcell, row);
    G_get_f_raster_row(d8_map_fd, row_three_fcell, row+1);

    for(col = 1; col < (no_cols-1); col++)
    {
      if(row_two_fcell[col] = 0)
      is_primary_square[col] = 0;
      else if(row_two_fcell[col-1] = 3)
      is_primary_square[col] = 0;
      else if(row_two_fcell[col+1] = 7)
      is_primary_square[col] = 0;
      else if(row_one_fcell[col] = 5)
      is_primary_square[col] = 0;
      else if(row_three_fcell[col] = 1)
      is_primary_square[col] = 0;
      else if(row_one_fcell[col-1] = 4)
      is_primary_square[col] = 0;
      else if(row_one_fcell[col+1] = 6)
      is_primary_square[col] = 0;
      else if(row_three_fcell[col-1] = 2)
      is_primary_square[col] = 0;
      else if(row_three_fcell[col+1] = 8)
      is_primary_square[col] = 0;
      else
      is_primary_square[col] = 1;
    }

    G_put_f_raster_row(primary_cells_fd, is_primary_square);
  }

  row = no_rows;

  for(col = 0; col < no_cols; col++)
  {
    is_primary_square[col] = 0;
  }

  G_put_f_raster_row(primary_cells_fd, is_primary_square);

  G_free(row_one_fcell);
  G_free(row_two_fcell);
  G_free(row_three_fcell);
  G_free(is_primary_square);

  G_close_cell(primary_cells_fd);
  G_close_cell(d8_map_fd);
}
```

```
/* alternative routing mechanism for d8 routing (progressive routing)
*/

#include <stdio.h>
#include <stdlib.h>
#include <stddef.h>
#include "gis.h"
#include <math.h>
#define NAME_LEN 100

int main(int argc, char *argv[])
{

/*prototypes */

int getline (char line[], int max);
void get_d8_map_name(char d8_map_name[]);
void get_primary_squares_name(char primary_squares_name[]);
void get_wshed_mask_name(char wshed_mask_name[]);
void routing_function(int no_rows, int no_cols, char
wshed_mask_name[], char d8_map_name[], char primary_squarez_name[]);
void find_primary_squares(int no_rows, int no_cols, char
d8_map_name[], char primary_squares_name[]);

/* variables */

char primary_squares_name[NAME_LEN+1];
char d8_map_name[NAME_LEN+1];
char wshed_mask_name[NAME_LEN+1];
int no_rows, no_cols;

G_gisinit(argv[0]);

no_rows = G_window_rows();
no_cols = G_window_cols();

get_d8_map_name(d8_map_name);
get_primary_squares_name(primary_squares_name);
get_wshed_mask_name(wshed_mask_name);
find_primary_squares(no_rows, no_cols, d8_map_name,
primary_squares_name);
routing_function(no_rows, no_cols, wshed_mask_name, d8_map_name,
primary_squares_name);

return(EXIT_SUCCESS);
}

/* get map names */

int getline(char line[], int max)
{
  int c;
  int i = 0;

  while((c = getchar()) != '\n')
    if(i < max)
      line[i++] = c;
  line[i] = '\0';
  return (c == '\n') ? i : -1;
}
```

```
/* input maps */

void get_d8_map_name(char d8_map_name[])
{
  char *prompt;
  char *mapset;
  char *message;

  prompt = "please enter d8_map raster file";
  mapset = G_ask_cell_in_mapset(prompt, d8_map_name);
  if(mapset == NULL)
  {
    message = "exiting module.... \n";
    G_fatal_error(message);
  }
}

void get_primary_squares_name(char primary_squares_name[])
{
  int t;
  char *message;

  printf("please enter primary squares map name\n");
  t = getline(primary_squares_name, NAME_LEN);
  if(t == -1)
  {
    message = "exiting module......\n";
    G_fatal_error(message);
  }
}

void get_wshed_mask_name(char wshed_mask_name[])
{
  char *prompt;
  char *mapset;
  char *message;

  prompt = "please enter wshed mask raster file";
  mapset = G_ask_cell_in_mapset(prompt, wshed_mask_name);
  if(mapset == NULL)
  {
    message = "exiting module.... \n";
    G_fatal_error(message);
  }
}

void routing_function(int no_rows, int no_cols, char
wshed_mask_name[], char d8_map_name[], char primary_squares_name[])
{

CELL *d8_map_row1, *d8_map_row2, *d8_map_row3, *primary_sqs;
CELL flow_progress[no_rows][no_cols],
flow_progress2[no_rows][no_cols], d8[no_rows][no_cols];
FCELL contrib_cells[no_rows][no_cols], temp[no_rows][no_cols];
FCELL cc_now[no_rows][no_cols], cc_next[no_rows][no_cols];
FCELL *wshed_mask;

int row, col;
int wshed_out_row, wshed_out_col;
int flow_marker, flow_monitor;
int count;
```

```
int x; /* dead variable */

int d8_map_fd, DEM_fd, primary_sqs_fd, wshed_fd;

char *message;
char *mapset;

FILE *fpa = fopen("flowpaths_d8.txt", "w");

mapset = G_mapset();

d8_map_fd = G_open_cell_old(d8_map_name, mapset);
if(d8_map_fd < 0)
{
  message = "cannot open d8 map, exiting module\n";
  G_fatal_error(message);
}

primary_sqs_fd = G_open_cell_old(primary_squares_name, mapset);
if(primary_sqs_fd < 0)
{
  message = "cannot open primary squares map, exiting module\n";
  G_fatal_error(message);
}

wshed_fd = G_open_cell_old(wshed_mask_name, mapset);
if(wshed_fd < 0)
{
  message = "cannot open wshed mask, exiting module\n";
  G_fatal_error(message);
}

d8_map_row1 = G_allocate_c_raster_buf();
d8_map_row2 = G_allocate_c_raster_buf();
d8_map_row3 = G_allocate_c_raster_buf();
wshed_mask = G_allocate_f_raster_buf();

for(row = 0; row < no_rows; row++)
{
  G_get_c_raster_row(d8_map_fd, d8_map_row1, row-1);
  G_get_c_raster_row(d8_map_fd, d8_map_row2, row);
  G_get_c_raster_row(d8_map_fd, d8_map_row3, row+1);

  for(col = 0; col < no_cols; col++)
  {
    if(d8_map_row2[col] == 1 && d8_map_row1[col] == 0)
    {
      wshed_out_row = row;
      wshed_out_col = col;
    }
    if(d8_map_row2[col] == 2 && d8_map_row1[col+1] == 0)
    {
      wshed_out_row = row;
      wshed_out_col = col;
    }
    if(d8_map_row2[col] == 3 && d8_map_row2[col+1] == 0)
    {
      wshed_out_row = row;
      wshed_out_col = col;
    }
    if(d8_map_row2[col] == 4 && d8_map_row3[col+1] == 0)
```

```
    {
      wshed_out_row = row;
      wshed_out_col = col;
    }
    if(d8_map_row2[col] == 5 && d8_map_row3[col] == 0)
    {
      wshed_out_row = row;
      wshed_out_col = col;
    }
    if(d8_map_row2[col] == 6 && d8_map_row3[col-1] == 0)
    {
      wshed_out_row = row;
      wshed_out_col = col;
    }
    if(d8_map_row2[col] == 7 && d8_map_row2[col-1] == 0)
    {
      wshed_out_row = row;
      wshed_out_col = col;
    }
    if(d8_map_row2[col] == 8 && d8_map_row1[col-1] == 0)
    {
      wshed_out_row = row;
      wshed_out_col = col;
    }
  }
}

printf("found watershed outlet %i %i \n", wshed_out_row,
wshed_out_col);

primary_sqs = G_allocate_c_raster_buf();

/*initialising variables and arrays */

for(row = 0; row < no_rows; row++)
{
  G_get_c_raster_row(d8_map_fd, d8[row], row);
}

for(row = 0; row < no_rows; row++)
{
  G_get_f_raster_row(wshed_fd, wshed_mask, row);
  G_get_c_raster_row(primary_sqs_fd, primary_sqs, row);

  for(col = 0; col < no_cols; col++)
  {
    flow_progress2[row][col] = 0;
    cc_now[row][col] = primary_sqs[col];
    cc_next[row][col] = 0;
    flow_progress[row][col] = primary_sqs[col];
    contrib_cells[row][col] = primary_sqs[col];
    temp[row][col] = wshed_mask[col];
  }
}

count = 0;
flow_monitor = 1;

/* main analysis routine for flow routing */

while(flow_monitor != 0)
```

```
{
  printf("entered flow routing loop\n");

  for(row = 0; row < no_rows; row++)
  {
    for(col = 0; col < no_cols; col++)
    {
      flow_marker = flow_progress[row][col];

      if(flow_marker == 1)
      {
        if(d8[row][col] == 1)
        {
          cc_next[row-1][col] = cc_next[row-1][col] +
cc_now[row][col] + temp[row-1][col];
        if(temp[row-1][col] == 1)
          temp[row-1][col] = temp[row-1][col] - 1;
        else
          temp[row-1][col] = 0;
          if((row-1) == wshed_out_row && col == wshed_out_col)
            flow_progress2[row-1][col] = 0;
          else
            flow_progress2[row-1][col] = 1;
        }
       else
          x = 0;
          if(d8[row][col] == 2)
          {
            cc_next[row-1][col+1] = cc_next[row-1][col+1] +
cc_now[row][col] + temp[row-1][col+1];
          if(temp[row-1][col+1] == 1)
            temp[row-1][col+1] = temp[row-1][col+1] - 1;
          else
            temp[row-1][col+1] = 0;
            if((row-1) == wshed_out_row && (col+1) == wshed_out_col)
              flow_progress2[row-1][col+1] = 0;
            else
              flow_progress2[row-1][col+1] = 1;
          }
          if(d8[row][col] == 3)
          {
            cc_next[row][col+1] = cc_next[row][col+1] +
 cc_now[row][col] + temp[row][col+1];
          if(temp[row][col+1] == 1)
            temp[row][col+1] = temp[row][col+1] - 1;
          else
            temp[row][col+1] = 0;
            if(row == wshed_out_row && (col+1) == wshed_out_col)
              flow_progress2[row][col+1] = 0;
            else
              flow_progress2[row][col+1] = 1;
          }
        else
          x = 0;
          if(d8[row][col] == 4)
          {
            cc_next[row+1][col+1] = cc_next[row+1][col+1] +
 cc_now[row][col] + temp[row+1][col+1];
          if(temp[row+1][col+1] == 1)
            temp[row+1][col+1] = temp[row+1][col+1] - 1;
```

```
        else
          temp[row+1][col+1] = 0;
          if((row+1) == wshed_out_row && (col+1) == wshed_out_col)
            flow_progress2[row+1][col+1] = 0;
          else
            flow_progress2[row+1][col+1] = 1;
        }
      else
        x = 0;
        if(d8[row][col] == 5)
        {
          cc_next[row+1][col] = cc_next[row+1][col] +
cc_now[row][col] + temp[row+1][col];
        if(temp[row+1][col] == 1)
          temp[row+1][col] = temp[row+1][col] - 1;
        else
          temp[row+1][col] = 0;
          if((row+1) == wshed_out_row && col == wshed_out_col)
            flow_progress2[row+1][col] = 0;
          else
            flow_progress2[row+1][col] = 1;
        }
      else
        x = 0;
        if(d8[row][col] == 6)
        {
          cc_next[row+1][col-1] = cc_next[row+1][col-1] +
cc_now[row][col] + temp[row+1][col-1];
        if(temp[row+1][col-1] == 1)
          temp[row+1][col-1] = temp[row+1][col-1] - 1;
        else
          temp[row+1][col-1] = 0;
          if((row+1) == wshed_out_row && (col-1) == wshed_out_col)
            flow_progress2[row+1][col-1] = 0;
          else
            flow_progress2[row+1][col-1] = 1;
        }
      else
        x = 0;
        if(d8[row][col] == 7)
        {
          cc_next[row][col-1] = cc_next[row][col-1] +
cc_now[row][col] + temp[row][col-1];
        if(temp[row][col-1] == 1)
          temp[row][col-1] = temp[row][col-1] - 1;
        else
          temp[row][col-1] = 0;
          if(row == wshed_out_row && (col-1) == wshed_out_col)
            flow_progress2[row][col-1] = 0;
          else
            flow_progress2[row][col-1] = 1;
        }
      else
        x = 0;
        if(d8[row][col] == 8)
        {
          cc_next[row-1][col-1] = cc_next[row-1][col-1] +
cc_now[row][col] + temp[row-1][col-1];
        if(temp[row-1][col-1] == 1)
          temp[row-1][col-1] = temp[row-1][col-1] - 1;
        else
```

```
          temp[row-1][col-1] = 0;
          if((row-1) == wshed_out_row && (col-1) == wshed_out_col)
            flow_progress2[row-1][col-1] = 0;
          else
            flow_progress2[row-1][col-1] = 1;
        }
      else
        x = 0;
      }

      else
      x = 0;
    }
  }

  flow_monitor = 0;

  for(row = 0; row < no_rows; row++)
  {
    for(col = 0; col < no_cols; col++)
    {
      if(flow_progress2[row][col] == 1 || flow_monitor == 1)
         flow_monitor = 1;
      else
        flow_monitor = 0;
    }
  }

  for(row = 0; row < no_rows; row++)
  {
    for(col = 0; col < no_cols; col++)
    {
      contrib_cells[row][col] = contrib_cells[row][col] +
cc_next[row][col];
    }
  }
  for(row = 0; row < no_rows; row++)
  {
    for(col = 0; col < no_cols; col++)
    {
      flow_progress[row][col] = flow_progress2[row][col];
      flow_progress2[row][col] = 0;
      cc_now[row][col] = cc_next[row][col];
      cc_next[row][col] = 0;
    }
  }

  count = count + 1;
  printf("completed %i sweeps of watershed\n", count);
}

for(row = 0; row < no_rows; row++)
{
  G_get_f_raster_row(wshed_fd, wshed_mask, row);

  for(col = 0; col < no_cols; col++)
  {
    contrib_cells[row][col] = contrib_cells[row][col] *
wshed_mask[col];
  }
}
```

```
printf("about to start outputting results\n");

for(row = 0; row < no_rows; row++)
{
  for(col =0; col < no_cols; col++)
  {
    fprintf(fpa, "%6.6f  ", contrib_cells[row][col]);
  }
  fprintf(fpa, "\n");
}

G_close_cell(d8_map_fd);
G_close_cell(DEM_fd);
G_close_cell(primary_sqs_fd);
}
/* alternative routing mechanism for d8 routing (progressive routing)
*/

#include <stdio.h>
#include <stdlib.h>
#include <stddef.h>
#include "gis.h"
#include <math.h>
#define NAME_LEN 100

int main(int argc, char *argv[])
{

/*prototypes */

int getline (char line[], int max);
void get_d8_map_name(char d8_map_name[]);
void get_primary_squares_name(char primary_squares_name[]);
void get_wshed_mask_name(char wshed_mask_name[]);
void get_aspect_map_name(char aspect_map_name[]);
void routing_function(int no_rows, int no_cols, char
wshed_mask_name[], char d8_map_name[], char primary_squarez_name[],
char aspect_map_name[]);
void find_primary_squares(int no_rows, int no_cols, char
d8_map_name[], char primary_squares_name[]);

/* variables */

char primary_squares_name[NAME_LEN+1];
char d8_map_name[NAME_LEN+1];
char wshed_mask_name[NAME_LEN+1];
char aspect_map_name[NAME_LEN+1];
int no_rows, no_cols;

G_gisinit(argv[0]);

no_rows = G_window_rows();
no_cols = G_window_cols();

get_d8_map_name(d8_map_name);
get_primary_squares_name(primary_squares_name);
get_wshed_mask_name(wshed_mask_name);
get_aspect_map_name(aspect_map_name);
find_primary_squares(no_rows, no_cols, d8_map_name,
primary_squares_name);
```

```
routing_function(no_rows, no_cols, wshed_mask_name, d8_map_name,
primary_squares_name, aspect_map_name);

return(EXIT_SUCCESS);
}

/* get map names */

int getline(char line[], int max)
{
  int c;
  int i = 0;

  while((c = getchar()) != '\n')
    if(i < max)
      line[i++] = c;
  line[i] = '\0';
  return (c == '\n') ? i : -1;
}

/* input maps */

void get_d8_map_name(char d8_map_name[])
{
  char *prompt;
  char *mapset;
  char *message;

  prompt = "please enter d8_map raster file";
  mapset = G_ask_cell_in_mapset(prompt, d8_map_name);
  if(mapset == NULL)
  {
    message = "exiting module.... \n";
    G_fatal_error(message);
  }
}

void get_primary_squares_name(char primary_squares_name[])
{
  int t;
  char *message;

  printf("please enter primary squares map name\n");
  t = getline(primary_squares_name, NAME_LEN);
  if(t == -1)
  {
    message = "exiting module......\n";
    G_fatal_error(message);
  }
}

void get_wshed_mask_name(char wshed_mask_name[])
{
  char *prompt;
  char *mapset;
  char *message;

  prompt = "please enter wshed mask raster file";
  mapset = G_ask_cell_in_mapset(prompt, wshed_mask_name);
  if(mapset == NULL)
  {
```

```
    message = "exiting module.... \n";
    G_fatal_error(message);
  }
}

void get_aspect_map_name(char aspect_map_name[])
{
  char *prompt;
  char *mapset;
  char *message;

  prompt = "please enter aspect_map raster file";
  mapset = G_ask_cell_in_mapset(prompt, aspect_map_name);
  if(mapset == NULL)
  {
    message = "exiting module.... \n";
    G_fatal_error(message);
  }
}

void routing_function(int no_rows, int no_cols, char
wshed_mask_name[], char d8_map_name[], char primary_squares_name[],
char aspect_map_name[])
{

CELL *d8_map_row1, *d8_map_row2, *d8_map_row3, *primary_sqs;
CELL flow_progress[no_rows][no_cols],
flow_progress2[no_rows][no_cols];
FCELL contrib_cells[no_rows][no_cols], aspect[no_rows][no_cols],
temp[no_rows][no_cols];
FCELL cc_now[no_rows][no_cols], cc_next[no_rows][no_cols];
FCELL *wshed_mask;
FCELL c1, c2;

int row, col;
int wshed_out_row, wshed_out_col;
int flow_marker, flow_monitor;
int count, x;

int d8_map_fd, DEM_fd, primary_sqs_fd, wshed_fd, aspect_fd;

char *message;
char *mapset;

FILE *fpa = fopen("flowpaths(d8).txt", "w");

mapset = G_mapset();

d8_map_fd = G_open_cell_old(d8_map_name, mapset);
if(d8_map_fd < 0)
{
  message = "cannot open d8 map, exiting module\n";
  G_fatal_error(message);
}

primary_sqs_fd = G_open_cell_old(primary_squares_name, mapset);
if(primary_sqs_fd < 0)
{
  message = "cannot open primary squares map, exiting module\n";
  G_fatal_error(message);
}
```

```
wshed_fd = G_open_cell_old(wshed_mask_name, mapset);
if(wshed_fd < 0)
{
  message = "cannot open wshed mask, exiting module\n";
  G_fatal_error(message);
}

aspect_fd = G_open_cell_old(aspect_map_name, mapset);
if(aspect_fd < 0)
{
  message = "cannot open aspect map, exiting module\n";
  G_fatal_error(message);
}

d8_map_row1 = G_allocate_c_raster_buf();
d8_map_row2 = G_allocate_c_raster_buf();
d8_map_row3 = G_allocate_c_raster_buf();
wshed_mask = G_allocate_f_raster_buf();

for(row = 0; row < no_rows; row++)
{
  G_get_c_raster_row(d8_map_fd, d8_map_row1, row-1);
  G_get_c_raster_row(d8_map_fd, d8_map_row2, row);
  G_get_c_raster_row(d8_map_fd, d8_map_row3, row+1);

  for(col = 0; col < no_cols; col++)
  {
    if(d8_map_row2[col] == 1 && d8_map_row1[col] == 0)
    {
      wshed_out_row = row;
      wshed_out_col = col;
    }
    if(d8_map_row2[col] == 2 && d8_map_row1[col+1] == 0)
    {
      wshed_out_row = row;
      wshed_out_col = col;
    }
    if(d8_map_row2[col] == 3 && d8_map_row2[col+1] == 0)
    {
      wshed_out_row = row;
      wshed_out_col = col;
    }
    if(d8_map_row2[col] == 4 && d8_map_row3[col+1] == 0)
    {
      wshed_out_row = row;
      wshed_out_col = col;
    }
    if(d8_map_row2[col] == 5 && d8_map_row3[col] == 0)
    {
      wshed_out_row = row;
      wshed_out_col = col;
    }
    if(d8_map_row2[col] == 6 && d8_map_row3[col-1] == 0)
    {
      wshed_out_row = row;
      wshed_out_col = col;
    }
    if(d8_map_row2[col] == 7 && d8_map_row2[col-1] == 0)
    {
      wshed_out_row = row;
```

```
      wshed_out_col = col;
    }
    if(d8_map_row2[col] == 8 && d8_map_row1[col-1] == 0)
    {
      wshed_out_row = row;
      wshed_out_col = col;
    }
  }
}

printf("found watershed outlet %i %i \n", wshed_out_row,
wshed_out_col);

primary_sqs = G_allocate_c_raster_buf();

/*initialising variables and arrays */

for(row = 0; row < no_rows; row++)
{
  G_get_f_raster_row(aspect_fd, aspect[row], row);
}

for(row = 0; row < no_rows; row++)
{
  G_get_f_raster_row(wshed_fd, wshed_mask, row);
  G_get_c_raster_row(primary_sqs_fd, primary_sqs, row);

  for(col = 0; col < no_cols; col++)
  {
    flow_progress[row][col] = 0;
    flow_progress2[row][col] = 0;
    cc_now[row][col] = primary_sqs[col];
    cc_next[row][col] = 0;
    flow_progress[row][col] = primary_sqs[col];
    contrib_cells[row][col] = primary_sqs[col];
    temp[row][col] = wshed_mask[col];
  }
}

/* main analysis routine for flow routing */

count = 0;

while(flow_monitor != 0)
{

  printf("entered flow routing loop\n");

  for(row = 0; row < no_rows; row++)
  {
    for(col = 0; col < no_cols; col++)
    {
      flow_marker = flow_progress[row][col];

      if(flow_marker == 1)
      {
      if(aspect[row][col] == 0)
      {
        cc_next[row-1][col] = cc_next[row-1][col] + cc_now[row][col]
+ temp[row-1][col];
```

```
        if(temp[row-1][col] == 1)
          temp[row-1][col] = temp[row-1][col] - 1;
        else
          temp[row-1][col] = 0;

        if((row-1) == wshed_out_row && (col+1) == wshed_out_col)
            flow_progress2[row-1][col] = 0;
          else
            flow_progress2[row-1][col] = 1;
      }

        else if(0 < aspect[row][col] < 45)
      {
        c1 = aspect[row][col] / 45;
        c2 = (45 - aspect[row][col]) / 45;

          cc_next[row-1][col] = cc_next[row-1][col] +
(cc_now[row][col] * c1) + temp[row-1][col];
        cc_next[row-1][col+1] = cc_next[row-1][col+1] +
(cc_now[row][col] * c2) + temp[row-1][col+1];

        if(temp[row-1][col] == 1)
          temp[row-1][col] = temp[row-1][col] - 1;
        else
          temp[row-1][col] = 0;
        if(temp[row-1][col+1] == 1)
          temp[row-1][col+1] = temp[row-1][col+1] - 1;
        else
          temp[row-1][col+1] = 0;

          if((row-1) == wshed_out_row && col == wshed_out_col)
            flow_progress2[row-1][col] = 0;
          else
            flow_progress2[row-1][col] = 1;
        if((row-1) == wshed_out_row && (col+1) == wshed_out_col)
            flow_progress2[row-1][col+1] = 0;
          else
            flow_progress2[row-1][col+1] = 1;
        }

      else if(aspect[row][col] == 45)
      {
        cc_next[row-1][col+1] = cc_next[row-1][col+1] +
cc_now[row][col] + temp[row-1][col+1];

        if(temp[row-1][col+1] == 1)
          temp[row-1][col+1] = temp[row-1][col+1] - 1;
        else
          temp[row-1][col+1] = 0;

        if((row-1) == wshed_out_row && (col+1) == wshed_out_col)
            flow_progress2[row-1][col+1] = 0;
          else
            flow_progress2[row-1][col+1] = 1;
      }

      else if(45 < aspect[row][col] < 90)
      {
        c1 = (aspect[row][col] - 45) / 45;
        c2 = (45 - (aspect[row][col] - 45)) / 45;
```

```
          cc_next[row-1][col+1] = cc_next[row-1][col+1] +
(cc_now[row][col] * c1) + temp[row-1][col+1];
        cc_next[row][col+1] = cc_next[row][col+1] + (cc_now[row][col]
* c2) + temp[row][col+1];

        if(temp[row-1][col+1] == 1)
          temp[row-1][col+1] = temp[row-1][col+1] - 1;
        else
          temp[row-1][col+1] = 0;
        if(temp[row][col+1] == 1)
          temp[row][col+1] = temp[row][col+1] - 1;
        else
          temp[row][col+1] = 0;

          if((row-1) == wshed_out_row && (col+1) == wshed_out_col)
            flow_progress2[row-1][col+1] = 0;
          else
            flow_progress2[row-1][col+1] = 1;
        if((row) == wshed_out_row && (col+1) == wshed_out_col)
            flow_progress2[row][col+1] = 0;
          else
            flow_progress2[row][col+1] = 1;
        }

      else if(aspect[row][col] == 90)
      {
        cc_next[row][col+1] = cc_next[row][col+1] + cc_now[row][col]
+ temp[row][col+1];

        if(temp[row][col+1] == 1)
          temp[row][col+1] = temp[row][col+1] - 1;
        else
          temp[row][col+1] = 0;

        if((row) == wshed_out_row && (col+1) == wshed_out_col)
            flow_progress2[row][col+1] = 0;
          else
            flow_progress2[row][col+1] = 1;
      }

      else if(90 < aspect[row][col] < 135)
      {
        c1 = (aspect[row][col] - 90) / 45;
        c2 = (45 - (aspect[row][col] - 90)) / 45;

          cc_next[row][col+1] = cc_next[row][col+1] +
(cc_now[row][col] * c1) + temp[row][col+1];
        cc_next[row+1][col+1] = cc_next[row+1][col+1] +
(cc_now[row][col] * c2) + temp[row+1][col+1];

        if(temp[row][col+1] == 1)
          temp[row][col+1] = temp[row][col+1] - 1;
        else
          temp[row][col+1] = 0;
        if(temp[row+1][col+1] == 1)
          temp[row+1][col+1] = temp[row+1][col+1] - 1;
        else
          temp[row+1][col+1] = 0;

          if((row) == wshed_out_row && (col+1) == wshed_out_col)
            flow_progress2[row][col+1] = 0;
```

```
          else
            flow_progress2[row][col+1] = 1;
        if((row+1) == wshed_out_row && (col+1) == wshed_out_col)
            flow_progress2[row+1][col+1] = 0;
          else
            flow_progress2[row+1][col+1] = 1;
        }

      else if(aspect[row][col] == 135)
      {
        cc_next[row+1][col+1] = cc_next[row+1][col+1] +
cc_now[row][col] + temp[row+1][col+1];

        if(temp[row+1][col+1] == 1)
          temp[row+1][col+1] = temp[row+1][col+1] - 1;
        else
          temp[row+1][col+1] = 0;

        if((row+1) == wshed_out_row && (col+1) == wshed_out_col)
            flow_progress2[row+1][col+1] = 0;
          else
            flow_progress2[row+1][col+1] = 1;
      }

      else if(135 < aspect[row][col] < 180)
      {
        c1 = (aspect[row][col] - 135) / 45;
        c2 = (45 - (aspect[row][col] - 135)) / 45;

          cc_next[row+1][col+1] = cc_next[row+1][col+1] +
(cc_now[row][col] * c1) + temp[row+1][col+1];
        cc_next[row+1][col] = cc_next[row+1][col] + (cc_now[row][col]
* c2) + temp[row+1][col];

        if(temp[row+1][col+1] == 1)
          temp[row+1][col+1] = temp[row+1][col+1] - 1;
        else
          temp[row+1][col+1] = 0;
        if(temp[row+1][col] == 1)
          temp[row+1][col] = temp[row+1][col] - 1;
        else
          temp[row+1][col] = 0;

          if((row+1) == wshed_out_row && (col+1) == wshed_out_col)
            flow_progress2[row+1][col+1] = 0;
          else
            flow_progress2[row+1][col+1] = 1;
        if((row+1) == wshed_out_row && (col) == wshed_out_col)
            flow_progress2[row+1][col] = 0;
          else
            flow_progress2[row+1][col] = 1;
        }

      else if(aspect[row][col] == 180)
      {
        cc_next[row+1][col] = cc_next[row+1][col] + cc_now[row][col]
+ temp[row+1][col];

        if(temp[row+1][col] == 1)
          temp[row+1][col] = temp[row+1][col] - 1;
        else
```

```
          temp[row+1][col] = 0;

        if((row+1) == wshed_out_row && (col) == wshed_out_col)
            flow_progress2[row+1][col] = 0;
          else
            flow_progress2[row+1][col] = 1;
      }

      else if(180 < aspect[row][col] < 225)
      {
        c1 = (aspect[row][col] - 180) / 45;
        c2 = (45 - (aspect[row][col] - 180)) / 45;

          cc_next[row+1][col] = cc_next[row+1][col] +
(cc_now[row][col] * c1) + temp[row+1][col];
        cc_next[row+1][col-1] = cc_next[row+1][col-1] +
(cc_now[row][col] * c2) + temp[row+1][col-1];

        if(temp[row+1][col] == 1)
          temp[row+1][col] = temp[row+1][col] - 1;
        else
          temp[row+1][col] = 0;
        if(temp[row+1][col-1] == 1)
          temp[row+1][col-1] = temp[row+1][col-1] - 1;
        else
          temp[row+1][col-1] = 0;

          if((row+1) == wshed_out_row && (col) == wshed_out_col)
            flow_progress2[row+1][col] = 0;
          else
            flow_progress2[row+1][col] = 1;
        if((row+1) == wshed_out_row && (col-1) == wshed_out_col)
            flow_progress2[row+1][col-1] = 0;
          else
            flow_progress2[row+1][col-1] = 1;
        }

      else if(aspect[row][col] == 225)
      {
        cc_next[row+1][col-1] = cc_next[row+1][col-1] +
cc_now[row][col] + temp[row+1][col-1];

        if(temp[row+1][col-1] == 1)
          temp[row+1][col-1] = temp[row+1][col-1] - 1;
        else
          temp[row+1][col-1] = 0;

        if((row+1) == wshed_out_row && (col-1) == wshed_out_col)
            flow_progress2[row+1][col-1] = 0;
          else
            flow_progress2[row+1][col-1] = 1;
      }

      else if(225 < aspect[row][col] < 270)
      {
        c1 = (aspect[row][col] - 225) / 45;
        c2 = (45 - (aspect[row][col] - 225)) / 45;

          cc_next[row+1][col-1] = cc_next[row+1][col-1] +
(cc_now[row][col] * c1) + temp[row+1][col-1];
```

```
        cc_next[row][col-1] = cc_next[row][col-1] + (cc_now[row][col]
* c2) + temp[row][col-1];

        if(temp[row+1][col-1] == 1)
          temp[row+1][col-1] = temp[row+1][col-1] - 1;
        else
          temp[row+1][col-1] = 0;
        if(temp[row][col-1] == 1)
          temp[row][col-1] = temp[row][col-1] - 1;
        else
          temp[row][col-1] = 0;

          if((row+1) == wshed_out_row && (col-1) == wshed_out_col)
            flow_progress2[row+1][col-1] = 0;
          else
            flow_progress2[row+1][col-1] = 1;
        if((row) == wshed_out_row && (col-1) == wshed_out_col)
            flow_progress2[row][col-1] = 0;
          else
            flow_progress2[row][col-1] = 1;
        }

      else if(aspect[row][col] == 270)
      {
        cc_next[row][col-1] = cc_next[row][col-1] + cc_now[row][col]
+ temp[row][col-1];

        if(temp[row][col-1] == 1)
          temp[row][col-1] = temp[row][col-1] - 1;
        else
          temp[row][col-1] = 0;

        if((row) == wshed_out_row && (col-1) == wshed_out_col)
            flow_progress2[row][col-1] = 0;
          else
            flow_progress2[row][col-1] = 1;
      }

      else if(270 < aspect[row][col] < 315)
      {
        c1 = (aspect[row][col] - 270) / 45;
        c2 = (45 - (aspect[row][col] - 270)) / 45;

          cc_next[row][col-1] = cc_next[row][col-1] +
(cc_now[row][col] * c1) + temp[row][col-1];
        cc_next[row-1][col-1] = cc_next[row-1][col-1] +
(cc_now[row][col] * c2) + temp[row-1][col-1];

        if(temp[row][col-1] == 1)
          temp[row][col-1] = temp[row][col-1] - 1;
        else
          temp[row][col-1] = 0;
        if(temp[row-1][col-1] == 1)
          temp[row-1][col-1] = temp[row-1][col-1] - 1;
        else
          temp[row-1][col-1] = 0;

          if((row) == wshed_out_row && (col-1) == wshed_out_col)
            flow_progress2[row][col-1] = 0;
          else
            flow_progress2[row][col-1] = 1;
```

```
        if((row-1) == wshed_out_row && (col-1) == wshed_out_col)
            flow_progress2[row-1][col-1] = 0;
          else
            flow_progress2[row-1][col-1] = 1;
        }

      else if(aspect[row][col] == 315)
      {
        cc_next[row-1][col-1] = cc_next[row-1][col-1] +
cc_now[row][col] + temp[row-1][col-1];

        if(temp[row-1][col-1] == 1)
          temp[row-1][col-1] = temp[row-1][col-1] - 1;
        else
          temp[row-1][col-1] = 0;

        if((row-1) == wshed_out_row && (col-1) == wshed_out_col)
            flow_progress2[row-1][col-1] = 0;
          else
            flow_progress2[row-1][col-1] = 1;
      }

      else if(315 < aspect[row][col] < 360)
      {
        c1 = (aspect[row][col] - 315) / 45;
        c2 = (45 - (aspect[row][col] - 315)) / 45;

          cc_next[row-1][col-1] = cc_next[row-1][col-1] +
(cc_now[row][col] * c1) + temp[row-1][col-1];
        cc_next[row][col-1] = cc_next[row][col-1] + (cc_now[row][col]
* c2) + temp[row][col-1];

        if(temp[row-1][col-1] == 1)
          temp[row-1][col-1] = temp[row-1][col-1] - 1;
        else
          temp[row-1][col-1] = 0;
        if(temp[row][col-1] == 1)
          temp[row][col-1] = temp[row][col-1] - 1;
        else
          temp[row][col-1] = 0;

          if((row-1) == wshed_out_row && (col-1) == wshed_out_col)
            flow_progress2[row-1][col-1] = 0;
          else
            flow_progress2[row-1][col-1] = 1;
        if((row) == wshed_out_row && (col-1) == wshed_out_col)
            flow_progress2[row][col-1] = 0;
          else
            flow_progress2[row][col-1] = 1;
        }

      else
        printf("severe error\n");
      }

      else
        x = 0;
    }
  }

  flow_monitor = 0;
```

```
  for(row = 0; row < no_rows; row++)
  {
    for(col = 0; col < no_cols; col++)
    {
      if(flow_progress2[row][col] == 1 || flow_monitor == 1)
         flow_monitor = 1;
      else
        flow_monitor = 0;
    }
  }

  for(row = 0; row < no_rows; row++)
  {
    for(col = 0; col < no_cols; col++)
    {
      contrib_cells[row][col] = contrib_cells[row][col] +
cc_next[row][col];
    }
  }
  for(row = 0; row < no_rows; row++)
  {
    for(col = 0; col < no_cols; col++)
    {
      flow_progress[row][col] = flow_progress2[row][col];
      flow_progress2[row][col] = 0;
      cc_now[row][col] = cc_next[row][col];
      cc_next[row][col] = 0;
    }
  }

  count = count + 1;
  printf("completed %i sweeps of watershed\n", count);
}

for(row = 0; row < no_rows; row++)
{
  G_get_f_raster_row(wshed_fd, wshed_mask, row);

  for(col = 0; col < no_cols; col++)
  {
    contrib_cells[row][col] = contrib_cells[row][col] *
wshed_mask[col];
  }
}

printf("about to start outputting results\n");

for(row = 0; row < no_rows; row++)
{
  for(col =0; col < no_cols; col++)
  {
    fprintf(fpa, "%6.6f  ", contrib_cells[row][col]);
  }
  fprintf(fpa, "\n");
}

G_close_cell(d8_map_fd);
G_close_cell(DEM_fd);
G_close_cell(primary_sqs_fd);
G_close_cell(aspect_fd);
```

```
}
```

This next script calculates the LS factor.

```
/* module to calculate LS factor */

#include <stdio.h>
#include <stdlib.h>
#include <stddef.h>
#include "gis.h"
#include <math.h>
#define NAME_LEN 100

int main(int argc, char *argv[])
{

/*prototypes */

int getline (char line[], int max);
void get_slope_map_name(char slope_map_name[]);
void get_ls_name(char ls_name[]);
void calc_ls_factor(int no_rows, int no_cols, char slope_map_name[],
char ls_name[]);

/* variables */

char slope_map_name[NAME_LEN+1];
char ls_name[NAME_LEN+1];
int no_rows, no_cols;

G_gisinit(argv[0]);

no_rows = G_window_rows();
no_cols = G_window_cols();

get_slope_map_name(slope_map_name);
get_ls_name(ls_name);
calc_ls_factor(no_rows, no_cols, slope_map_name, ls_name);

return(EXIT_SUCCESS);
}

/* get map names */

int getline(char line[], int max)
{
  int c;
  int i = 0;

  while((c = getchar()) != '\n')
    if(i < max)
      line[i++] = c;
  line[i] = '\0';
  return (c == '\n') ? i : -1;
}

/* input maps */

void get_slope_map_name(char slope_map_name[])
{
```

```
  char *prompt;
  char *mapset;
  char *message;

  prompt = "please enter  slope map raster file";
  mapset = G_ask_cell_in_mapset(prompt, slope_map_name);
  if(mapset == NULL)
  {
    message = "exiting module.... \n";
    G_fatal_error(message);
  }
}

void get_ls_name(char ls_name[])
{
  int t;
  char *message;

  printf("please enter ls factor map name\n");
  t = getline(ls_name, NAME_LEN);
  if(t == -1)
  {
    message = "exiting module......\n";
    G_fatal_error(message);
  }
}

void calc_ls_factor(int no_rows, int no_cols, char slope_map_name[],
char ls_name[])
{

int row, col;
char *message;
char *mapset;
FCELL *slope, *ls;
int slope_map_fd, ls_fd;
float y;

mapset = G_mapset();

slope_map_fd = G_open_cell_old(slope_map_name, mapset);
if(slope_map_fd < 0)
{
  message = "cannot open slope map, exiting module\n";
  G_fatal_error(message);
}

ls_fd = G_open_raster_new(ls_name, FCELL_TYPE);

slope = G_allocate_f_raster_buf();
ls = G_allocate_f_raster_buf();

for(row = 0; row < no_rows; row++)
{
  G_get_f_raster_row(slope_map_fd, slope, row);

  for(col = 0; col < no_cols; col++)
  {
    y = (slope[col] / 180) * 3.141;
    ls[col] = -1.5 + (17 / (1 + exp(2.3 - 6.1 * sin(y))));
  }
```

```
  G_put_f_raster_row(ls_fd, ls);
}

G_close_cell(ls_fd);
G_close_cell(slope_map_fd);
}
```

And the function written to calculate slope based on the various methods for comparison.

```
#include <stdio.h>
#include <stdlib.h>
#include <stddef.h>
#include "gis.h"
#include <math.h>
#define NAME_LEN 100

/* main */

int main(int argc, char *argv[])
{

/*prototypes */

int getline (char line[], int max);
void get_dem_name(char dem_name[]);
void get_fdslope_p_name(char fdslope_p_name[]);
void get_mdgslope_p_name(char mdgslope_p_name[]);
void get_mdhslope_p_name(char mdhslope_p_name[]);
void get_fdslope_d_name(char fdslope_d_name[]);
void get_mdgslope_d_name(char mdgslope_d_name[]);
void get_mdhslope_d_name(char mdhslope_d_name[]);
void fd_slope(int no_rows, int no_cols, char dem_name[], char
fdslope_p_name[], char fdslope_d_name[]);
void mdg_slope(int no_rows, int no_cols, char dem_name[], char
mdgslope_p_name[], char mdgslope_d_name[]);
void mdh_slope(int no_rows, int no_cols, char dem_name[], char
mdhslope_p_name[], char mdhslope_d_name[]);

/* variables */

char dem_name[NAME_LEN+1];
char fdslope_p_name[NAME_LEN+1];
char mdgslope_p_name[NAME_LEN+1];
char mdhslope_p_name[NAME_LEN+1];
char fdslope_d_name[NAME_LEN+1];
char mdgslope_d_name[NAME_LEN+1];
char mdhslope_d_name[NAME_LEN+1];
int no_rows, no_cols;

/*initialise the grass environment variable */

G_gisinit(argv[0]);

/* run sub-routines*/

get_dem_name(dem_name);
```

```
get_fdslope_p_name(fdslope_p_name);
get_mdgslope_p_name(mdgslope_p_name);
get_mdhslope_p_name(mdhslope_p_name);
get_fdslope_d_name(fdslope_d_name);
get_mdgslope_d_name(mdgslope_d_name);
get_mdhslope_d_name(mdhslope_d_name);
no_rows = G_window_rows();
no_cols = G_window_cols();

fd_slope(no_rows, no_cols, dem_name, fdslope_p_name, fdslope_d_name);
mdg_slope(no_rows, no_cols, dem_name, mdgslope_p_name,
mdgslope_d_name);
mdh_slope(no_rows, no_cols, dem_name, mdhslope_p_name,
mdhslope_d_name);

return(EXIT_SUCCESS);
}

/* get map names */

int getline(char line[], int max)
{
  int c;
  int i = 0;

  while((c = getchar()) != '\n')
    if(i < max)
      line[i++] = c;
  line[i] = '\0';
  return (c == '\n') ? i : -1;
}

/* input name */

void get_dem_name(char dem_name[])
{
  char *prompt;
  char *message;
  char *mapset;

  prompt = "please enter dem name";
  mapset = G_ask_cell_in_mapset(prompt, dem_name);
  if(mapset == NULL)
  {
      message = "exiting module... \n";
      G_fatal_error(message);
  }
}

/*output name */

void get_fdslope_p_name(char fdslope_p_name[])
{
  int t;
  char *message;

  printf("please enter name of finite differences percent slope
map:\n");
  t = getline(fdslope_p_name, NAME_LEN);
  if(t == -1)
  {
```

```
        message = "exiting module....\n";
        G_fatal_error(message);
    }
}

void get_mdgslope_p_name(char mdgslope_p_name[])
{
    int t;
    char *message;

    printf("please enter name of maximum downward gradient percent
slope map:\n");
    t = getline(mdgslope_p_name, NAME_LEN);
    if(t == -1)
    {
        message = "exiting module....\n";
        G_fatal_error(message);
    }
}

void get_mdhslope_p_name(char mdhslope_p_name[])
{
    int t;
    char *message;

    printf("please enter name of maximum downhill percent slope
map:\n");
    t = getline(mdhslope_p_name, NAME_LEN);
    if(t == -1)
    {
        message = "exiting module....\n";
        G_fatal_error(message);
    }
}
void get_fdslope_d_name(char fdslope_d_name[])
{
    int t;
    char *message;

    printf("please enter name of finite differences degrees slope
map:\n");
    t = getline(fdslope_d_name, NAME_LEN);
    if(t == -1)
    {
        message = "exiting module....\n";
        G_fatal_error(message);
    }
}

void get_mdgslope_d_name(char mdgslope_d_name[])
{
    int t;
    char *message;

    printf("please enter name of maximum downward gradient degrees
slope map:\n");
    t = getline(mdgslope_d_name, NAME_LEN);
    if(t == -1)
    {
        message = "exiting module....\n";
        G_fatal_error(message);
```

```
  }
}

void get_mdhslope_d_name(char mdhslope_d_name[])
{
  int t;
  char *message;

  printf("please enter name of maximum downhill degrees slope
map:\n");
  t = getline(mdhslope_d_name, NAME_LEN);
  if(t == -1)
  {
      message = "exiting module....\n";
      G_fatal_error(message);
  }
}

/* finite difference slope function */

void fd_slope(int no_rows, int no_cols, char dem_name[], char
fdslope_p_name[], char fdslope_d_name[])

{
  int row, col;
  FCELL *dem_row_one, *dem_row_two, *dem_row_three;
  FCELL *fdslope_p;
  FCELL *fdslope_d;
  FCELL slope;
  FCELL cell_width;
  char *mapset;
  char *message;
  int dem_fd;
  int fdslope_p_fd;
  int fdslope_d_fd;

  mapset = G_mapset();

  printf("entered fd slope routine\n");


  dem_fd = G_open_cell_old(dem_name, mapset);
  if(dem_fd < 0)
  {
    message = "cannot open DEM, exiting module\n";
    G_fatal_error(message);
  }

  fdslope_p_fd = G_open_raster_new(fdslope_p_name, FCELL_TYPE);

  fdslope_d_fd = G_open_raster_new(fdslope_d_name, FCELL_TYPE);

  cell_width = (200 * 0.3048);

  printf("a\n");

  dem_row_one = G_allocate_f_raster_buf();
  dem_row_two = G_allocate_f_raster_buf();
  dem_row_three = G_allocate_f_raster_buf();
  fdslope_p = G_allocate_f_raster_buf();
  fdslope_d = G_allocate_f_raster_buf();
```

```
  row = 0;

  for(col = 0; col < no_cols; col++)
  {
    fdslope_p[col] = 0;
    fdslope_d[col] = 0;
  }

  G_put_f_raster_row(fdslope_p_fd, fdslope_p);
  G_put_f_raster_row(fdslope_d_fd, fdslope_d);

  for(row = 1; row < no_rows - 1; row++)
  {
      G_get_f_raster_row(dem_fd, dem_row_one, row-1);
      G_get_f_raster_row(dem_fd, dem_row_two, row);
      G_get_f_raster_row(dem_fd, dem_row_three, row+1);

      printf("b\n");

      for(col = 1; col < no_cols - 1; col++)
      {
        slope = pow((pow(((dem_row_one[col] - dem_row_three[col]) /
(2 * cell_width)), 2) + pow(((dem_row_two[col-1] -
dem_row_two[col+1]) / (2 * cell_width)), 2)), 0.5);
        fdslope_p[col] = slope * 100;  /*assuming result of above
calculation is a fraction */
        fdslope_d[col] = ((atan(slope)) / (4 * atan(1))) * 180;
    }

    G_put_f_raster_row(fdslope_p_fd, fdslope_p);
    G_put_f_raster_row(fdslope_d_fd, fdslope_d);
  }

  row = no_rows;

  for(col = 0; col < no_cols; col++)
  {
    fdslope_p[col] = 0;
    fdslope_d[col] = 0;
  }

  G_put_f_raster_row(fdslope_p_fd, fdslope_p);
  G_put_f_raster_row(fdslope_d_fd, fdslope_d);

  G_free(dem_row_one);
  G_free(dem_row_two);
  G_free(dem_row_three);
  G_free(fdslope_p);
  G_free(fdslope_d);

  G_close_cell(fdslope_p_fd);
  G_close_cell(fdslope_d_fd);
  G_close_cell(dem_fd);

}

/* maximum downward gradient slope function */

void mdg_slope(int no_rows, int no_cols, char dem_name[], char
mdgslope_p_name[], char mdgslope_d_name[])
```

```
{
  int row, col;
  FCELL *dem_row_one, *dem_row_two,  *dem_row_three;
  FCELL *mdgslope_p;
  FCELL *mdgslope_d;
  FCELL slope_a, slope_b, slope_c, slope_d, slope;
  FCELL cell_width;
  char *mapset;
  char *message;
  int dem_fd;
  int mdgslope_p_fd;
  int mdgslope_d_fd;

  mapset = G_mapset();


  dem_fd = G_open_cell_old(dem_name, mapset);
  if(dem_fd < 0)
  {
    message = "cannot open DEM, exiting module\n";
    G_fatal_error(message);
  }

  mdgslope_p_fd = G_open_raster_new(mdgslope_p_name, FCELL_TYPE);
  mdgslope_d_fd = G_open_raster_new(mdgslope_d_name, FCELL_TYPE);

  cell_width = (200 * 0.3048);

  dem_row_one = G_allocate_f_raster_buf();
  dem_row_two = G_allocate_f_raster_buf();
  dem_row_three = G_allocate_f_raster_buf();
  mdgslope_p = G_allocate_f_raster_buf();
  mdgslope_d = G_allocate_f_raster_buf();

  row = 0;

  for(col = 0; col < no_cols; col++)
  {
    mdgslope_p[col] = 0;
    mdgslope_d[col] = 0;
  }

  G_put_f_raster_row(mdgslope_p_fd, mdgslope_p);
  G_put_f_raster_row(mdgslope_d_fd, mdgslope_d);

  for(row = 1; row < no_rows - 1; row++)
  {
      G_get_f_raster_row(dem_fd, dem_row_one, row-1);
      G_get_f_raster_row(dem_fd, dem_row_two, row);
      G_get_f_raster_row(dem_fd, dem_row_three, row+1);

      for(col = 1; col < no_cols - 1; col++)
      {
        slope_a = (dem_row_one[col] - dem_row_three[col]) /
(cell_width * 2);    /* need a function to elimiate -ve answer */
        if(slope_a < 0)
          slope_a = (dem_row_three[col] - dem_row_one[col]) /
(cell_width * 2);
        else
          slope_a = slope_a;
```

```
        slope_b = (dem_row_two[col-1] - dem_row_two[col+1]) /
(cell_width * 2);
        if(slope_b < 0)
          slope_b = (dem_row_two[col+1] - dem_row_two[col-1]) /
(cell_width * 2);
        else
          slope_a = slope_a;
        slope_c = (dem_row_one[col-1] - dem_row_three[col+1]) /
(cell_width * (pow(2, 0.5)) * 2);
        if(slope_c < 0)
          slope_c = (dem_row_three[col+1] - dem_row_one[col-1]) /
(cell_width * (pow(2, 0.5)) * 2);
        else
          slope_a = slope_a;
        slope_d = (dem_row_one[col+1] - dem_row_three[col-1]) /
(cell_width * (pow(2, 0.5)) * 2);
        if(slope_d < 0)
          slope_d = (dem_row_three[col-1] - dem_row_one[col+1]) /
(cell_width * (pow(2, 0.5)) * 2);
        else
          slope_d = slope_d;

        if(slope_a > slope_b)
          slope = slope_a;
        else
          slope = slope_b;
        if(slope > slope_c)
          slope = slope;
        else
          slope = slope_c;
        if(slope > slope_d)
          slope = slope;
        else
          slope = slope_d;

        mdgslope_p[col] = slope * 100;  /*assuming result of above
calculation is a fraction */
        mdgslope_d[col] = ((atan(slope)) / (4 * atan(1))) * 180;
    }

    G_put_f_raster_row(mdgslope_p_fd, mdgslope_p);
    G_put_f_raster_row(mdgslope_d_fd, mdgslope_d);
  }

  row = no_rows;

  for(col = 0; col < no_cols; col++)
  {
    mdgslope_p[col] = 0;
    mdgslope_d[col] = 0;
  }

  G_put_f_raster_row(mdgslope_p_fd, mdgslope_p);
  G_put_f_raster_row(mdgslope_d_fd, mdgslope_d);

  G_free(dem_row_one);
  G_free(dem_row_two);
  G_free(dem_row_three);
  G_free(mdgslope_p);
  G_free(mdgslope_d);
```

```
  G_close_cell(mdgslope_p_fd);
  G_close_cell(mdgslope_d_fd);
  G_close_cell(dem_fd);

}

/* maximum downward slope function */

void mdh_slope(int no_rows, int no_cols, char dem_name[], char
mdhslope_p_name[], char mdhslope_d_name[])

{
  int row, col;
  FCELL *dem_row_one, *dem_row_two,  *dem_row_three;
  FCELL *mdhslope_p;
  FCELL *mdhslope_d;
  FCELL slope_a, slope_b, slope_c, slope_d, slope_e, slope_f,
slope_g, slope_h, slope;
  FCELL cell_width;
  char *mapset;
  char *message;
  int dem_fd;
  int mdhslope_p_fd;
  int mdhslope_d_fd;

  mapset = G_mapset();


  dem_fd = G_open_cell_old(dem_name, mapset);
  if(dem_fd < 0)
  {
    message = "cannot open DEM, exiting module\n";
    G_fatal_error(message);
  }

  mdhslope_p_fd = G_open_raster_new(mdhslope_p_name, FCELL_TYPE);
  mdhslope_d_fd = G_open_raster_new(mdhslope_d_name, FCELL_TYPE);

  cell_width = (200 * 0.3048);

  dem_row_one = G_allocate_f_raster_buf();
  dem_row_two = G_allocate_f_raster_buf();
  dem_row_three = G_allocate_f_raster_buf();
  mdhslope_p = G_allocate_f_raster_buf();
  mdhslope_d = G_allocate_f_raster_buf();

  row = 0;

  for(col = 0; col < no_cols; col++)
  {
    mdhslope_p[col] = 0;
    mdhslope_d[col] = 0;
  }

  G_put_f_raster_row(mdhslope_p_fd, mdhslope_p);
  G_put_f_raster_row(mdhslope_d_fd, mdhslope_d);

  for(row = 1; row < no_rows - 1; row++)
  {
      G_get_f_raster_row(dem_fd, dem_row_one, row-1);
      G_get_f_raster_row(dem_fd, dem_row_two, row);
```

```
      G_get_f_raster_row(dem_fd, dem_row_three, row+1);

      for(col = 1; col < no_cols - 1; col++)
      {
        slope = (dem_row_two[col] - dem_row_one[col]) / (cell_width *
2);  /* need a function to elimiate -ve answer */
        if(slope < 0)
          slope_a = 0;
        else
          slope_a = slope;
        slope = (dem_row_two[col] - dem_row_one[col+1]) / (cell_width
* (pow(2, 0.5)) * 2);
        if(slope < 0)
          slope_b = 0;
        else
          slope_b = slope;
        slope = (dem_row_two[col] - dem_row_two[col+1]) / (cell_width
* 2);
        if(slope < 0)
            slope_c = 0;
        else
          slope_c = slope;
        slope = (dem_row_two[col] - dem_row_three[col+1]) /
(cell_width * (pow(2, 0.5)) * 2);
        if(slope < 0)
            slope_d = 0;
        else
          slope_d = slope;
        slope = (dem_row_two[col] - dem_row_three[col]) / (cell_width
* 2);
        if(slope < 0)
            slope_e = 0;
        else
          slope_e = slope;
        slope = (dem_row_two[col] - dem_row_three[col-1]) /
(cell_width * (pow(2, 0.5)) * 2);
        if(slope < 0)
          slope_f = 0;
        else
          slope_f = slope;
        slope = (dem_row_two[col] - dem_row_two[col-1]) / (cell_width
* 2);
        if(slope < 0)
          slope_g = 0;
        else
          slope_g = slope;
        slope = (dem_row_two[col] - dem_row_one[col-1]) / (cell_width
* (pow(2, 0.5)) * 2);
        if(slope < 0)
          slope_h = 0;
        else
          slope_h = slope;

        slope = 0;

        if(slope_a > slope_b)
          slope = slope_a;
        else
          slope = slope_b;
        if(slope > slope_c)
          slope = slope;
```

```
        else
          slope = slope_c;
        if(slope > slope_d)
          slope = slope;
        else
          slope = slope_d;
        if(slope > slope_e)
          slope = slope;
        else
          slope = slope_e;
        if(slope > slope_f)
          slope = slope;
        else
          slope = slope_f;
        if(slope > slope_g)
          slope = slope;
        else
          slope = slope_g;
        if(slope > slope_h)
          slope = slope;
        else
          slope = slope_h;

        mdhslope_p[col] = slope * 100;
        mdhslope_d[col] = ((atan(slope)) / (4 * atan(1))) * 180;
      }

      G_put_f_raster_row(mdhslope_p_fd, mdhslope_p);
      G_put_f_raster_row(mdhslope_d_fd, mdhslope_d);
    }

    row = no_rows;

    for(col = 0; col < no_cols; col++)
    {
      mdhslope_p[col] = 0;
      mdhslope_d[col] = 0;
    }

    G_put_f_raster_row(mdhslope_p_fd, mdhslope_p);
    G_put_f_raster_row(mdhslope_d_fd, mdhslope_d);

    G_free(dem_row_one);
    G_free(dem_row_two);
    G_free(dem_row_three);
    G_free(mdhslope_p);
    G_free(mdhslope_d);

    G_close_cell(mdhslope_p_fd);
    G_close_cell(mdhslope_d_fd);
    G_close_cell(dem_fd);

}
```